Connected and Demountable Hydrogen Fuel Cells System for Electric Vehicles

By

Dongxiao Wu

PhD

May 2024

Acknowledgements

As I stand at the finish line and cast my gaze back, I am struck by a sudden realisation that this research project has been a part of my life for over a thousand days and nights. On the path towards my ultimate academic goal, I have gained academic progress but, more importantly, methodologies and ways of thinking to tackle various challenges. Throughout this academic journey, I could not have reached this point without the treasurable help of those who supported me, their assistance has been indispensable in achieving what I have today.

First and foremost, I must extend my sincere gratitude to my supervisory team: **Dr Huw Davies**, his broader strategic insight enhanced my understanding of the overarching structure of this project and guided me in integrating scientific research theories with real-world policies, economics, and environmental considerations. His professionalism and meticulous academic approach have been with me throughout my research journey and taught me to become a competent academic researcher. **Dr Jinlei Shang**, I appreciate him for introducing me to the realm of academic research. His creativity and expertise in the field of hydrogen and fuel cells have been crucial to my achievements. When I faced challenges, he not only provided professional guidance but also broadened my thinking and helped me develop methodologies for future problem-solving. **Dr Mauro Innocente**, I thank him for his guidance in scientific control logic and his assistance in revising my thesis. **Dr Chongming Wang**, I am grateful for his supervision in the field of lithium batteries and academic thinking, as well as for his innovative approaches in simulation and modelling.

I would like to extend my heartfelt thanks to my dear friends and colleagues at Coventry University: **S.Q. YANG**, **G. QU**, **Dr J. REN**, **Dr M. Apicella**, and **X.Y. LU**. Collaborating and communicating with them throughout my research has enhanced the efficiency of my work while also enriching it with creativity and professionalism.

Lastly, and most importantly, I must convey my deepest gratitude to my parents and all my family members for their unwavering support and steadfast encouragement throughout my life. I also owe a deep debt of appreciation to my wife **T.Y. Wang**, her love and warm companionship were irreplaceable for the completion of this long academic journey.

Abstract

Recognised technology pathways to zero-emission vehicles are Battery Electric Vehicle (BEV) and Fuel Cell Electric Vehicle (FCEV). However, these are underdelivering in terms of achieving a system transition. Combining these two pathways – to leverage advantages and overcome the limitations of these respective technologies – can potentially accelerate a system transition. Hence, a novel powertrain concept of a Demountable Fuel Cell Range Extender (DHFCRE) connected to a BEV is proposed and optimised through the development of an innovative Energy Management System (EMS) that responds to multiple competing challenges including cost reduction; infrastructure provision; vehicle range; etc.

A simulation model based on Matlab/Simulink was developed to evaluate the performance of the proposed powertrain concept and EMS control algorithms. The simulation tests considered different powertrain modes, driving scenarios and control algorithms. The simulation results provide fuel cost, Tank-to-Wheel (TTW) overall energy efficiency and the power distributions between the battery and fuel cell.

There are several key results and findings in this thesis: For the scenarios considered, the combination of Fuel Cell Range Extender (FCRE) + Eco-BEV powertrain, reduced energy cost by 28.4% under long-distance extra-urban cycles, 28.3% in mid-range mixed urban & extra-urban journeys, and 6% in short urban cycles. However, overall efficiency, measured from TTW, was lower. This was due to the higher energy efficiency of the pure BEV powertrain system than the Fuel Cell (FC) powertrain system. Among the four developed control algorithms for the EMS, the Artificial Neuro Network (ANN) algorithm has the best fuel economy while the Energy Consumption Minimisation Strategy (ECMS) provides the highest TTW energy efficiency. The Cost-Benefit Analysis (CBA) of this concept presents that this concept can reduce 79.2% of the Total Cost of Ownership (TCO) for individual BEV users and 29% of the UK national total manufacturing cost in the BEV industry by 2050. The Well-To-Wheel carbon emission in the automotive industry can be decreased by 9.1% per year. Also, Lithium and Cobalt metal raw material consumption will be reduced by 52.4% by 2050.

The simulation results and analysis of these FCRE and EMS optimisation methods could be references for researchers and manufacturers in the field of future range-extended BEV solutions. The quantified CBA results provide data support for individual BEV users and policymakers to make predictions and decisions from both economic and environmental perspectives.

Publications

Dongxiao Wu, Jinlei Shang and Huw Davies. ‘Feasibility of Connected and Demountable Hydrogen Fuel Cell Range Extender for Electric Vehicles’ Fuel Cell & Hydrogen Technical Conference (2018), NEC, Birmingham, UK. (Oral Presentation).

Dongxiao Wu, Jin Ren, Huw Davies, Jinlei Shang and Olivier Haas (2019) Intelligent Hydrogen Fuel Cell Range Extender for Battery Electric Vehicles. World Electr. Veh. J. 2019, 10(2), 29; https://doi.org/10.3390/wevj10020029

Table of Contents

List of Figures

List of Tables

Abbreviations and Nomenclature

The Abbreviations in this thesis are defined as follows:

Abbreviation	Actual
2D	Two-Dimensional
3D	Three-Dimensional
3-DOF	Three-Degree of Freedom
ADVISOR	Advanced Vehicle Simulator
AFC	Alkaline Electrolyte Fuel Cells
AI	Artificial Intelligence
ANN	Artificial Neuro Network
APC	Advanced Propulsion Centre
API	Application Programming Interface
BEV	Battery Electric Vehicle
BMS	Battery Management System
CBA	Cost-Benefit Analysis
DC	Direct Current
DHFCRE	Demountable Hydrogen FC Range Extender
DMFC	Direct Methanol Fuel Cells
DOE	Department of Energy
DP	Dynamic Programming
ECMS	Energy Consumption Minimisation Strategy
Eco-BEV	Economic-Size-BEV
EMS	Energy Management System
EOL	End of Life
ESD	Energy Storage Devices
FASTSim	Future Automotive Systems Technology Simulator
FC	Fuel Cell
FCEV	Fuel Cell Electric Vehicle
GDLs	Gas Diffusion Layers
GHG	Green House Gas

GUI	Graphical User Interface
HEV	Hybrid Electric Vehicles
HSD	Hybrid Synergy Drive
ICE	Internal Combustion Engine
ICEV	Internal Combustion Engine Vehicle
IEA	International Energy Agency
KPI	Key Performance Indicator
LB	Learning-Based
LCV	Low Carbon Vehicle
Li-ion	Lithium-ion
MCFC	Molten Carbonate Fuel Cell
MEA	Membrane Electrode Assembly
ML	Machine Learning
MPGe	Miles per Gallon Equivalent
NEDC	New European Driving Cycle
Ni–MH	Nickel–metal Hydride
NN	Neural Network
NREL	National Renewable Energy Laboratory
OB	Optimisation-Based
OEM	Original Equipment Manufacturer
PAFC	Phosphoric Acid Fuel Cells
PEMFC	Proton Exchange Membrane Fuel Cells
PHEV	Plug-in Hybrid Electric Vehicle
PI	Proportional and Integral
PM	Particulate Matters
RB	Rule-Based
REEV	Range-Extending Electric Vehicle
RL	Reinforcement Learning
SoC	State of Charge
SoH	State of Health

SOFC	Solid Oxide Fuel Cells
SPV	Solar-Powered Vehicle
TCO	Total Cost of Ownership
TTW	Tank-to-Wheel
VCU	Vehicle Control Unit
WTT	Well-to-Tank
WTW	Well to Wheel
ZTE	Zero Tailpipe Emission
ZTEV	Zero Tailpipe Emission Vehicle

The Nomenclatures in this thesis are defined as follows:

Notation	Description	Unit
T_{Cmd}	Output electric motor torque	N·m
$f_{MMTSC}()$	2-D look-up-table function that presents the Motor Max Torque Speed Curve of the electric motor	rad/s
ω	Motor speed	%
S_{Acc}	Acceleration signal from the representative driver model	Pa
P_{Brkrq}	Brake pressure request	
P_{brkMax}	Maximum braking pressure (a model input parameter)	Pa
S_{dec}	Deceleration signal in acceleration signal	%
T_{RG}	Regenerative torque	N·m
P_{BrkRG}	Final brake pressure command signal	Pa
P_{Brkrq}	Brake pressure request	Pa
μ	Coefficient of friction for brake pads	
B_a	Effective radius of the brake disc	m
R_m	Mean radius at which the brake force is applied in	m
N_{pads}	Number of brake pads involved in braking	
N_{diff}	Gear ratio of the differential	
$f_{RGBCO}()$	A look-up-table function which presents a regenerative braking cut-off curve	
v	Vehicle speed	m/s
P_{TR}	Mechanical power from the base shaft	W
P_{TC}	Mechanical power from the follower shaft	W
P_d	Damping power loss	W
P_s	Stored internal torsional energy	W
T_R	Input torque from the electric motor	N·m
T_C	Output torque	N·m
ω	Driveshaft angular velocity	rad/s
b	Rotational viscous damping	N·m·rad
J	Rotational inertia	kg·m^2
T_{brk}	Brake torque	N·m
μ	Disc pad-rotor coefficient of kinetic friction	

P_{BrkRG}	Brake pressure command signal	Pa
B_a	Effective radius of the brake disc	m
R_o	Outer radius of the brake pad	m
R_i	Inner radius of the brake pad	m
N_{pads}	Number of brake pads in disc brake assembly	
μ_{static}	Disc pad-rotor coefficient of static friction	
v	Vehicle speed	m/s
F_x	Longitudinal force of the vehicle in the vehicle fixed	N
F_{wf}	Longitudinal traction force of the front axle	N
F_{wr}	Longitudinal traction force of the rear axle	N
F_d	Aerodynamic resistance in the vehicle fixed x-axis	N
C_d	Aerodynamic coefficient of the vehicle	
A_f	Frontal area of the vehicle	m^2
P_{abs}	Environmental absolute air pressure	Pa
T_a	Environmental air temperature	K
R_a	Atmospheric specific gas constant of the air	J/(kg·K)
v	Vehicle speed	m/s
v_{Wx}	Wind speed in the vehicle fixed x-axis	m/s
ω_w	Wheel angular speed	rad/s
r_w	Wheel radius	m
$r_{t-loaded}$	Loaded radius of the tyre	m
F_g	Longitudinal gravitational force on the vehicle along the vehicle-fixed x-axis	N
M	Vehicle's total mass	kg
g	Gravity acceleration constant	m/s^2
θ	Angle of the road slope	°
I_{Batt}	Required battery current	A
P_M	Mechanical power generated by the motor	W
P_L	Power loss in the motor	W
V_{Batt}	Battery voltage	V
V_T	Voltage per battery module	V

V_O	Battery open-circuit voltage	V
I_{batt}	Current of each battery module	A
R_i	Internal resistance of per battery module	Ω
I_{in}	Combined current flowing from the battery network	A
N_p	Number of battery cells in parallel	
V_{out}	Combined voltage of the battery network	V
N_s	Number of cells in series	
SoC	Battery State of Charge	%
C_{batt}	Battery's maximum capacity	Ah
t	Simulation sample time	s
E_{Batt}	Energy consumption of each battery module	Ah
$P_{charmax}$	Max charge power of the battery pack	W
C_{char}	Charge C-rate of the battery	
V_{nom}	Nominal voltage of the battery pack	V
$P_{discharmax}$	Maximum discharge power of the battery pack	W
$C_{dischar}$	Discharge C-rate of the battery	
V_{FC-out}	Output voltage of the FC stack	V
E_r	Reversible output voltage of the fuel cell	V
V_{act}	Activation loss voltage of the fuel cell	V
V_{ohmic}	Ohmic loss voltage of the fuel cell	V
V_{con}	Concentration loss voltage of the fuel cell	V
N_c	Number of cells in the FC stack	
G_0	Gibbs free energy for the reaction at standard conditions	kJ/mol
n	Number of moles of electrons transferred in the reaction	
F	Faraday constant	C/mol
R	Universal gas constant	J/(mol·K)
T	Absolute temperature	K
α	Charge transfer coefficient	
i	Current density	$\mathrm{A/m^2}$
i_0	Exchange current density	$\mathrm{A/m^2}$

V_{ohmic}	Voltage drop across the fuel cell due to ohmic losses	V
i	Current density in amperes per square meter	$\mathrm{A/m^2}$
A	Activation area of the fuel cell in square meters	$\mathrm{m^2}$
R_{ohmic}	Ohmic resistance	Ω
δ	Thickness of the electrolyte layer	m
σ	Ionic conductivity of the electrolyte	S/m
$i_{\max}$	Maximum current density at which the fuel cell operates in amperes per square meter	$\mathrm{A/m^2}$
C_{H2}	Hydrogen consumption per second	g/s
I_{fc}	Output current of the FC stack	A
N_{fc}	Number of cells in the FC stack	
M_{H2}	Molecular weight constant of hydrogen	g/mol
$N_{V_{H2}}$	Valence number of hydrogen	
C_F	Faraday constant	C/mol
J_{FC}	FC energy consumption	Wh
J_{Batt}	Battery energy consumption	Wh
β	Battery energy penalty coefficient	
P_{FC}	Fuel cell output power	W
P_{Batt}	Battery output power	W
Δt	Sample time of the Matlab/Simulink model	
μ	Constant to reflect the battery charge and discharge characteristics	
SOC	Current battery state of charge	
SOC_{max}	Maximum battery state of charge	
SOC_{min}	Minimum battery state of charge	
C_{r1}	Total running cost of the Eco-BEV + FCRE	£
P_o	Off-Peak electricity price	£/kWh
T_u	Number of annual urban journeys per year based on the published data from the government	
L_u	Average urban journey length	km
η_{u1}	Average urban journey energy efficiency of the Eco-BEV + FCRE	kWh/km
α_E	Proportion of electricity energy used in the extra-urban journey of the Eco-BEV + FCRE	%
P_p	Peak electricity price	£/kWh

T_{ex}	Total annual extra-urban journey times	
L_{ex}	Average extra-urban journey length	km
η_{ex1}	Average extra-urban journey energy efficiency of the Eco-BEV + FCRE	kWh/km
P_{rfc}	Rent price of the FCRE	£ per time
α_{H2}	Proportion of hydrogen energy used in the extra-urban journey of the Eco-BEV + FCRE	%
P_{H2}	Price of the hydrogen gas fuel	£/kg
η_{H2}	Average extra-urban journey hydrogen energy efficiency of the FCRE	kg/km
η_{u2}	The Average urban journey energy efficiency of the Large BEV	kWh/km
η_{ex2}	Average extra-urban journey energy efficiency of the Large BEV	kWh/km
t_L	Lifespan of the BEVs	years
C_{M1}	Manufacturing cost of Eco-BEV + FCRE	£
N_{EV}	Total amount of BEV	
V_{B1}	Battery size in Eco-BEV + FCRE	kWh
C_B	Battery cost	£/kWh
α_{RE}	Coefficient of numbers of DHFCRE required for Eco-BEV	
V_{FC}	Size of the FC system	kW
C_{FC}	Cost of the FC system	£/kW
C_{M2}	Manufacturing cost of Large BEV	£
V_{B2}	Battery size in Large BEV	kWh
M_{c1}	Annual WTW total co_2 Equivalent Emission per year of Eco-BEV + FCRE	kg
N_1	Total amount of the Eco-BEVs in Eco-BEV + FCRE	
T_u	Total annual urban journey times	
L_u	Average urban journey length	km
η_{u1}	Average urban journey energy efficiency of Eco-BEV	kWh/km
α_E	Proportion of electricity energy used in the extra-urban journey of Eco-BEV + FCRE	%
T_{ex}	Total annual extra-urban journey times	
L_{ex}	Average extra-urban journey length	km
η_{ex1}	Average extra-urban journey energy efficiency of Eco-BEV	kWh/km
η_{E-C}	WTT Production/Emission rate - Electricity/co_2 Equivalent	kWh/kg
α_{H2}	Proportion of hydrogen energy used in the extra-urban journey of Eco-BEV + FCRE	%

η_{H2}	Average extra-urban journey hydrogen energy efficiency of the FCRE	kg/km
η_{H2-C}	WTT Production/Emission rate - H_2 Gas/co_2 Equivalent	
N_2	Total amount of the Large BEV	
M_{c2}	Annual WTW total co_2 Equivalent Emission per year of Large BEV	kg
η_{u2}	Average urban journey energy efficiency of the Large BEV	kWh/km
η_{ex2}	Average extra-urban journey energy efficiency of the Large BEV Vehicle	kWh/km
M_1	Total material consumption in Eco-BEV + FCRE	kg
α_1	Market share proportion of Eco-BEV + FCRE	%
N_{EV}	Total amount of BEV	
V_{B1}	Battery size in Eco-BEV	kWh
μ	Production transfer rate of metal material	kg/kWh
M_2	Total material consumption in Large BEV	kg
α_2	Market share proportion of Large BEV	%
V_{B2}	Battery size in Large BEV	kWh
M_{Pt}	Total platinum metal consumption in FCRE	kg
N_{EV}	Total amount of BEV	
V_{FC}	Size of the FC system	kW
α_{RE}	Coefficient of numbers of DHFCRE required for Eco-BEV	

Chapter 1 Introduction

1.1. Background

Since the beginning of the 21st century, an increasing number of countries and regions have regarded the challenges of environmental protection and energy security as strategic issues. Automotive products, particularly the Internal Combustion Engine (ICE) powered passenger road vehicle have been one of the main sources of environmental and energy security issues (Pollet et al., 2012). Considering, the issue of environmental protection, a key issue is Global Green House Gas (GHG) emissions (mainly from fossil fuels) since they have increased nearly tenfold from 1900 to 2023 (Figure 1-1-a) (IEA, 2023). Refer to the report from Environmental Protection Agency (EPA) of US, around 29% of the GHG emissions came from transportation (Figure 1-1-b) (EPA-US, 2023), representing around 10.8 billion tons annually. This makes the removal of GHG emissions from the transportation sector an urgent challenge.

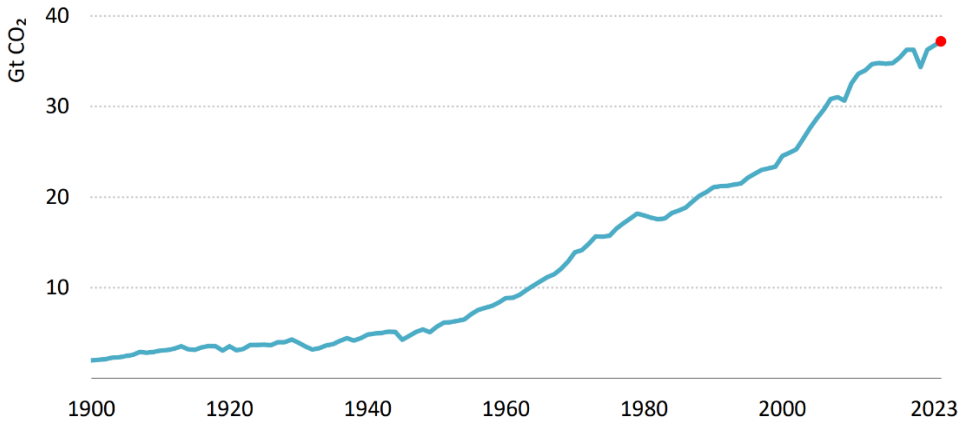

(a)

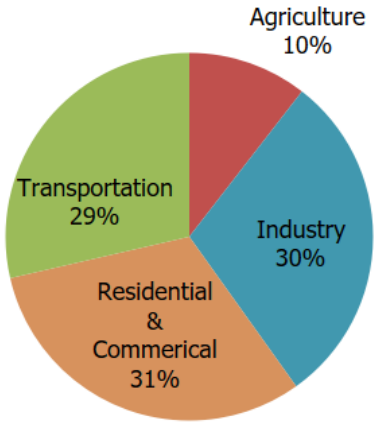

(b)

Figure 1-1 Global GHG emission trends and breakdown sources by sectors. (IEA, 2023; EPA-US, 2023)

In addition to the contribution to GHG, exhaust gas emissions from Internal Combustion Engine Vehicle (ICEV) contain several kinds of harmful gas pollution including nitrogen oxides (NO_X), Carbon monoxide (CO) and Particulate Matters (PM10 and PM2.5). These emissions contribute to air quality degradation, which in turn has a negative impact on human health and well-being. For example, the study by the British RCP suggests that air pollution annually contributes to about 40,000 early deaths per year in the UK (RCP, 2016).

The energy security issue related to the road vehicle includes two aspects with respectively the limited fossil fuel reserves and geopolitics considerations. As per the research result from BP, the year reserves of oil are only enough for 53 years (BP Global, 2017). Since the distribution of fossil fuel reserves is not related to economic development regions, the dependence on fossil fuels is regarded as a strategic problem for some counties and regions. For instance, around 80% of the oil used by EU countries depends on imports and this has an impact on the national energy security considerations and political decisions (EEA, 2009).

In order to deal with these issues, a number of countries have put in place policies supported by appropriate legislation, to direct the future technology development pathways of the automotive industry. For example, within the EU, the current regulatory requirement for a fleet average for GHG emission of all new vehicles is 95 g CO_2 per kilometre by 2021, which is a decrease of more than 40% compared to the 2007 target (European Commission, 2018), however, the actual fleet average GHG emission value of all new vehicles in 2021 was 114 g CO_2 per kilometre (ICCT, 2024), therefore the demand on electrification of new vehicles is mandatory. Further, as Table 1-1 shows, that a number of countries have introduced policies that pledge to remove Internal Combustion Engine Vehicles (ICEV) from the vehicle fleet.

Table 1-1 Planned ban on pure ICEV around the world (CNN, 2019)

Country	Year to ban pure ICEV
Germany	2040 (Tentative)
France	2040
UK	2040
Spain	2040
India	2030
Canada	2040
Netherland	2025

Aside from policy and legalisation, national governments from key regions of the world economy and those contributing significant GHG emissions have incentivised the

purchase of cleaner vehicles and charging infrastructures. For example, the US (IEA, 2018), EU (European Commission, 2017), Japan (Government of Japan, 2016) and China (Ministry of Finance of the People's Republic of China, 2016) have introduced grants for the purchase of Low Carbon Vehicles (LCVs).

The environmental and legislative demands associated with the grants are driving a revolution in the automotive industry to move from ICE propulsion to Zero Tailpipe Emission (ZTE) systems. Among the number of developing LCV technologies, the Battery Electric Vehicle (BEV) and Fuel Cell Electric Vehicle (FCEV) technologies have been recognised as having the most potential for future Zero Tailpipe Emission Vehicle (ZTEV) solutions (Automotive Council UK, 2017).

1.2. Motivation

In the long-term view, current ICEVs will be replaced, via low-carbon vehicles, by ZTEVs. Technology roadmaps have been published by countries around the world to consolidate the role that policy and technology play in the development of the automotive electrification revolution (Wu et al., 2019). The majority of these roadmaps (including those from the EU ETRAC, UK APC and China CEA) regard the BEV and FCEV as future market solutions by 2050 which are ZTE vehicles with zero GHG emission in the Tank-to-Wheel (TTW) stage (ERTRAC, 2018). The roadmaps introduced limitations of technology, infrastructure and associated business models with policy instruments in delivering a product that is competitive to replace the ICEV. Even though the current ZTEVs (BEV and FCEV) have their advantages compared with the current ICEVs, these roadmaps show that the full commercialisation of the BEV and FCEV is still decades away since their challenges are hard to resolve in a short period of time (CEA, 2016; UK Automotive Council, 2017). The main advantages of a transition to a BEV and FCEV vehicle fleet are as follows:

Firstly, compared to current ICEVs, both BEV and FCEV are more environmentally friendly since they have no harmful tailpipe emissions. BEVs only use electricity to power the vehicle thus no tailpipe, FCEV use hydrogen gas to generate electricity and then power the vehicle, the only chemical reaction product is water (Pollet et al., 2012).

Also, ZTEVs have higher TTW overall energy efficiency than the ICEVs, the average overall TTW efficiency of BEV is 60% – 80%, FCEV is around 45% while the diesel and gasoline-powered vehicle average is about 16% – 22% (IEA, 2022).

Meanwhile, the low fuel cost of BEVs is a significant advantage compared to ICEVs and FCEVs. The average electricity cost of the current BEV is approximately from £1.5 to £16 per 100km (depend on different charging method and electricity price), while the average fuel cost of ICEV passenger cars is about £9.25 per 100km (gasoline) and £8.99 per 100km (diesel) (IEA, 2022; Shell UK, 2023). The average fuel cost of FCEVs is around £11.4 per 100km (IEA, 2022; Autotrader, 2023).

The limitations of the current ZTEV include BEV range and charging speed limitation, infrastructure dependency and high cost of core components.

Range anxiety is one of the most significant issues of BEV complaint drivers since the average vehicle range and charging speed of BEV is lower than the ICEV and FCEV (Franke et al., 2016). The range of current BEV significantly relies on the vehicle size due to the battery energy density being incomparable with fossil fuels and hydrogen gas, the energy density of Lithium batteries is about 150 – 260 Wh/kg while gasoline is about 12000 Wh/kg and hydrogen gas is 33300 Wh/kg (Hypertextbook, 2003; IEA, 2022; Tsakiris, 2023). The range of current passenger BEVs varies from 40 to 300 miles while the average passenger ICEV and FCEV range is about 300 – 400 miles (IEA, 2022; Tsakiris, 2023). The charging speed of BEV is also incomparable with ICEV and FCEV, the fastest BEV charging pile can provide about 250 – 300 miles in 20 minutes, while the refuelling speed of ICEV and FCEV is only about 3 – 5 minutes (EvChargingMag, 2023; National Academies of Sciences, Engineering, and Medicine, 2022).

Due to the limited range and charging speed of BEV, it relies more on the charging infrastructure than ICEV and FCEV. Even though the growth speed of the BEV charging infrastructure has been fast in recent years, the density of the BEV charging network is still much lower than the gas stations for ICEVs (ZAP-MAP, 2024). Also, the infrastructure dependency and availability issue is significant for FCEV since there are only 15 hydrogen stations in the UK by 2023 (Hydrogenbatteries.org, 2023), and the growth speed of hydrogen refuelling stations is foreseeable slow due to the high cost and dependency on government support (Waseem et al., 2023).

Moreover, the cost of core components, such as Lithium battery pack for BEV (about £122/kWh), FC stack (about £533/kW) and high-pressure hydrogen gas tank (about £410 to £546 per kg at 700 bar pressure) are very high compared to the ICEV parts (EERE US, 2023; Wanitschke & Hoffmann, 2020; Shin & Ha, 2023).

To deal with the existing issues and leverage the superiorities of current ZTEV technologies, a novel concept is introduced in this thesis – “A demountable hydrogen FC range extender (DHFCRE)” connected with an Economic-Size-BEV (Eco-BEV). Also, by learning from the successful business mode of “sharing E-bike” and “Rent & Drop mobile phone power banks” (Li et al., 2022; Statista, 2023), to increase the cost-effectiveness and functionality of this demountable FC range extender, it can be commercialised under a “Rent & Drop” business mode for Eco-BEV users during their occasional long-distance trips. With the help of this concept, the advantages of BEV including high energy efficiency, low running cost, and the superiorities of FCEV including long range, fast-refuelling speed and environment friendly can be leveraged. Also, the current issues of BEV and FCEV including infrastructure dependency, oversize for range, high cost and raw material consumption could be mitigated. Therefore, it is valuable to scientifically analyse and evaluate the performance of this concept in terms of cost, energy efficiency, functionality, and the macro cost and benefit from both commercial and environmental perspectives as well as provide further optimisations for this concept by using scientific methods. These are the motivations of this project and thesis.

1.3. Aims and Objectives

This project aims to propose an alternative ZTEV powertrain hybridisation concept – A Connected and Demountable Hydrogen Fuel Cell Range Extender (DHFCRE) with Eco-sized Battery Electric Vehicles (Eco-BEV), as well as establish scientific analysis and evaluation for the performance of this concept in terms of cost, energy efficiency, functionality, and the macroscopic cost and benefit from both commercial and environmental perspectives. Also, it will seek to optimise the proposed DHFCRE with the help of scientific energy management strategies and external information including BEV motorist and traffic information, etc.

To accomplish the research aim, this thesis will focus on the following objectives:

Objective One: To identify and particularise the barriers to an effective and efficient transition to the ZTEV fleet. To propose a solution based on leveraging the strengths and mitigating the limitations of existing solutions.

Objective Two: To develop a model for evaluating the performance of a novel drivetrain concept combining battery and fuel cell technologies, and to verify the accuracy of this approach based on experimental data.

Objective Three: To determine appropriate real-world values for the parameters of the system components that can be used to determine the system performance in application.

Objective Four: To identify different Energy Management System (EMS) approaches and to evaluate these with the purpose of linking to system performance.

Objective Five: To evaluate the technical performance of the proposed powertrain concept and optimise system performance through the strategic application of the available EMS based on specific driving requirements.

Objective Six: To evaluate cost considerations of the proposed solution including the derived benefits in order to identify a solution set that would meet stakeholder requirements.

1.4. Methodology

The overview of methodologies implemented in this research are outlined as follows, the detailed methodologies for each chapter are presented in the corresponding sections.

Undertake an extensive review which focuses on the peer research, transportation policies, and strategic roadmaps within the realm of LCV technologies, especially ZTEVs to identify the technological gaps and superiorities of current ZTEV solutions. Explore the potential of the concept of “DHFCRE + BEV” in leveraging the superiorities and bridging the gaps, thereby facilitating a smooth transition from the existing to future ZTEV fleets.

Identify the requirements of the simulation with the consideration of model functionality, simulation efficiency as well as the constraints of project budget and timeline. Then, based on these requirements, evaluate the simulation tools in the field of hybrid power source vehicles by reviewing the relevant literature. After that, select the appropriate simulation tool for this project and establish the simulation model for the proposed “DHFCRE + BEV” powertrain concept.

Address the key parameters and the sizes of the core components of the “DHFCRE + BEV” powertrain based on the analysis of existing scientific research, marketing information and government-published transportation statistics.

Define the functional requirements of the EMS and its control strategies in the hybrid vehicle area, identify the characteristics and application cases of different control

strategies. Develop and test control algorithms for the EMS based on the requirements within the framework of the scientific control strategies. Introduce the methodology of the EMS optimisation by developing a font-end program which allows the internal EMS to be connected with external information and simulation results.

Develop the duty cycle inputs and simulation scenarios based on the published drive cycle data and real-world driving conditions, confirm the Key Performance Indicators (KPI) outputs of the simulation results. Undertake simulations, generate the results of the KPIs under different driving scenarios, powertrain combinations and EMS control algorithms. Analyse the simulation results to quantify the performance of this "DHFCRE + BEV" powertrain concept in terms of fuel cost and vehicle overall energy efficiency compared to the competing powertrain of the full-size Large BEV. Also, through the result analysis, discern the characteristics of different EMS control algorithms. Implement further optimisations for the front-end program of the EMS based on the simulation results of the performance under different driving scenarios.

Conduct a comprehensive Cost-Benefit Analysis (CBA) for this proposed powertrain concept with the comparison to the full-size large BEV based on the simulation results, with both economic and environmental considerations, from individual/household and societal/national perspectives. The individual/household CBA will focus on the Total Cost of Ownership of the vehicle including the additional costs from the range extender. The societal/national CBA involves the analysis of the national total manufacturing cost of the ZTEVs, the Well-to-Wheel (WTW) carbon emissions and the raw material consumption.

1.5. Contributions

The key contributions of this thesis are summarised as follows:

- Quantified evaluation of the proposed novel powertrain concept – A connected and demountable hydrogen fuel cell range extender with eco-sized battery electric vehicles (Eco-BEV + DHFCRE).
- Novel EMS control algorithm pathways development for this DHFCRE + Eco-BEV powertrain, including the State-Machine, the formulated Equivalent Energy Minimisation Strategy (ECMS), Fuzzy Logic and Artificial Neuro Network (ANN) algorithms.
- Based on the simulation results analysis under different driving scenarios, identified the characteristics of each EMS control algorithm and implemented

further optimisations on the EMS front-end control program connected the DHFCRE EMS with the driver's demand and external traffic information.

- An extensive Cost Benefit Analysis (CBA) for this proposed concept from both individual and societal perspectives, with both economic and environmental considerations.

1.6. Thesis Outline

In this thesis, the research background, motivations, research aims and methodology are introduced in **Chapter 1**. The literature review focused on the ZTEV technology and commercialisation gaps associated with the identified potentials for the proposed DHFCRE is presented in **Chapter 2**. Then, the simulation model of the proposed DHFCRE and BEV powertrains including the simulation tool review and evaluation process is discussed in **Chapter 3**. **Chapter 4** presents the simulation parameter setups including the development of the duty cycles and driving scenarios. The literature review of EMS control algorithms for hybrid vehicle applications, the development and optimisation processes of control strategies for this DHFCRE are shown in **Chapter 5**. **Chapter 6** focuses on the simulation result and analysis as well as the further optimisation for the EMS control strategy. The Cost Benefit Analysis (CBA) from individual and societal perspectives with both economic and environmental considerations is presented in **Chapter 7**. At the end of the thesis, the conclusion, limitations and future works will be summarised in **Chapter 8**.

Chapter 2 Literature Review

2.1. Introduction

Though hybrid, electric or fuel cell cars have the potential to lower carbon emissions in transport, they have not yet penetrated the market sufficiently. Reasons for this delayed transition are multiple and relate to technology immaturity, societal expectations, economic considerations, etc. To identify and quantify these limitations a review of the peer assessed literature was undertaken. This chapter reports on that review and through an understanding of the present system limitations, and advantages, puts forwards a proposal for accelerating market penetration of zero emission vehicle technologies and hence support a transition to low carbon mobility systems.

2.2. ZTEV Technology Gaps

Environmental concerns tied to energy security have spurred policy shifts globally (Pollet et al., 2012), incentivising the automotive industry to transition from Internal Combustion Engine Vehicles (ICEVs) to Zero Tailpipe Emission Vehicles (ZTEVs). ZTEV is the term given to a specific type of vehicle that emits no exhaust gases or pollutants from their onboard power sources at the point of operation, thereby avoiding the release of harmful pollutants (such as carbon dioxide, nitrogen oxides, hydrocarbons, and particulate matter) linked with the combustion of fossil fuels (Vehicle Certification Agency UK, 2023). Available ZTEV solutions include Battery Electric Vehicles (BEVs), Hydrogen Fuel Cell Electric Vehicles (FCEVs), Plug-in Hybrid Electric Vehicles (PHEVs) pure electric mode and Solar-Powered Vehicles (SPVs) (EERE US, 2023). In 2017, the UK Automotive Council pinpointed BEVs and FCEVs as the leading future alternatives for ZTEVs, however, there are still challenges and technology gaps that are delaying their commercialisation. The remaining challenges preventing wider commercial adoption of BEV include the insufficient range, dependency on charging infrastructure, limited raw materials and recycling (IEA, 2022) (Tsakiris, 2023). Additionally, the challenges of FCEV include hydrogen fuelling infrastructures, vehicle cost, hydrogen distribution and storage (EERE US, 2023; Wanitschke & Hoffmann, 2020; Shin & Ha, 2023). This section will summarise a review of the literature and discuss the advantages and limitations of BEV and FCEV from various perspectives and identify the technology gaps and potential of a proposed concept of ‘DHFCRE + Eco-BEV’.

2.2.1. Current Status of BEV Technology

BEV is recognized as a ZTEV solution in recent years which exhibits high powertrain energy efficiency and low running cost compared to technologies such as hydrogen fuel cells and petrol hybrid vehicles (Pollet et al., 2012; Ren, 2019). However, current BEV limitations from a societal perspective include range, cost/efficiency with the consideration of the vehicle sizing as well as the dependency on the charging infrastructure. On one hand, the range anxiety caused by BEV range limitation significantly affected BEV’s functionality. On the other hand, limited by current battery energy density, increasing range for BEV will lead higher size which means the increase on vehicle cost and reduction on energy efficiency. The following subsections review the current status of BEVs with regards to identifying and quantifying their advantages and limitations in terms of societal, technical and associated business perspectives compared with conventional ICEVs and other alternative ZTEV technologies.

- **Vehicle range**

One of the perceived limitations of BEV is vehicle range. Range anxiety is one of the most significant issues of BEV complaint drivers since the vehicle's average range and charging speed of BEV are lower than the ICEV and FCEV (Franke et al., 2016). Current battery chemistries have significantly improved the energy storage capability, but these still fall significantly short of that achieved by conventional fossil fuels. Additionally, in meeting societal expectations of increased vehicle range, the lower energy density of the current battery solution requires that additional capacity is added, and this raises the vehicle cost compared with the incumbent fossil fuel equivalent. Further, there is the consideration of refuelling, the typical charging time required for a BEV being multiple times greater than the vehicle technology it is replacing. These complexities, challenge the requirement to transition to a cleaner vehicle fleet. The first significant challenge of current BEV is the limited range as shown in Table 2-1.

dddddddddddddddddddddddddddddddddddddddddddddddddddddddddddddddd
d

Table 2-1The range performance and price of popular BEV models compared to ICEV (Nissan, 2019; Volkswagen, 2023; BMW, 2019; Renault, 2017; Evspecifications, 2023; Volkswagen, 2019)

Vehicles	Official NEDC range	Real-world range	Retail Price	Home charging time (7kW)	Fast charging
NISSAN Leaf 30 kWh (Nissan, 2019)	168 miles	124 miles	£26,190	7.5 hours	1 h (50kW)
Volkswagen e-Golf (Volkswagen, 2023)	186 miles	144 miles	£29,230	5 hours	35-40min (50kW)
BMW i3 120Ah (BMW, 2019)	223 miles	160 miles	£36,935	4.5 hours	35 min (50kW)
Renault Zoe Z.E. 40 (RENAULT, 2017)	250 miles	186 miles	£29,270	7+ hours	1h (43kW)
Tesla Model Y (Evspecifications, 2023)	352 miles	267 miles	£44,990	5.5 hours	22 min (0-80%) (170kW)
Tesla Model 3 (Evspecifications, 2023)	359 miles	272 miles	£39,990	5.5 hours	22 min (0-80%) (170kW)
Tesla Model S 100D (Evspecifications, 2023)	530 miles	402 miles	£93,480	8.5 hours	35 min (0-80%) (150kW)
Volkswagen Golf TSI (Volkswagen, 2019)	613 miles	465 miles	£25,174	-	-

Compared with the ICEV (Golf TSI), the current BEVs have a significantly lower range, especially for similar-size family hatchbacks such as the e-Golf, Nissan Leaf and BMW i3. The ranges of BEV family hatchbacks are from 160 miles to 250 miles while the patrol hatchbacks such as VW Golf TSI is more than 600 miles which is about 3 times of the BEVs. The main reason for this significant range difference is the difference in energy density of the energy sources – Lithium battery and gasoline. The energy density in terms of weight of the current Lithium battery is about 150 – 260 Wh/kg while gasoline is about 12000 Wh/kg and hydrogen gas is 33300 Wh/kg (Hypertextbook, 2003; IEA, 2022; Tsakiris, 2023). The energy density in terms of volume of Lithium battery varies from 250 to 730 Wh/L and about 9500Wh/L for gasoline (IOR Energy, 2022), which is more than 13 times of Lithium battery. (Cao et al., 2020; Zu & Li, 2011; Energy, 2022). For the full-size luxury BEVs such as the Tesla Model S 100D, the range is about 400 miles, close to the conventional ICEVs (such as Golf TSI), however, since it has a 100 kWh battery pack on board with a large saloon-size, the price (more than £93,000) is also much higher than other BEVs and ICEVs (Evspecifications, 2023).

Also, the charging speed of the BEVs is incomparable with the ICEV, even though using the fast-charging method. The most common power of current home chargers of BEV is 7 kW, it will take about a whole night (5 – 11 hours) to fully charge a BEV. For the fast-charging infrastructure, the charging power varies from 40 to 250 kW, and the charging time is from 30 to 60 minutes. However, the refuelling time of a patrol vehicle is about 5 minutes. Meanwhile, the capital cost of the current BEV is higher than the ICEV in a similar class, as the price of the electric version of the VW Golf is 16% higher than the petrol version.

Limited by the characteristics of the batteries of BEV, the current solutions for extending the range of BEVs include increasing battery size and hybridising other propulsions to the BEV, such as Range-Extending Electric Vehicles (REEVs) based on petrol engine (PHEV) or fuel cell systems (FCEV) (Wu et al., 2019).

- **Battery characteristics**

Battery performance is one of the most significant features of the BEV, the main factors to evaluate battery performance include specific energy (Wh/kg), energy density (Wh/L) and specific power (W/kg). In the automotive industry, the consideration of Energy Storage Devices (ESD) also contains life cycle, energy efficiency and production cost (Wu et al., 2019). Table 2-2 presents five alternative battery technologies, lead acid batteries, nickel batteries, and Lithium batteries are current commercial solutions. Lithium-air batteries and Sodium-Sulphur batteries are potential candidates for use in future EVs (Singla, 2024).

Table 2-2 The comparison of energy storage specifications for BEVs. (Battery University, 2023; Mikkelsen, 2010; Singla, 2024).

Characteristics	Lead–Acid	Nickel–metal hydride (Ni–MH)	Lithium-ion (Li-ion)	Sodium–Sulphur	Lithium-air
Specific energy (Wh/kg)	30–50	60–120	150–250	150–240	1,200–2,000
Energy density (Wh/L)	60–110	140–300	250–700	150–300	2,000–3,500
Life cycle	500–1,000 cycles	500–1,000 cycles	500–1,500 cycles	2,500–4,500 cycles	Up to 1,000 cycles
Energy efficiency (%)	70–85%	60–70%	85–95%	85–90%	90–95%
Production cost (£/kWh)	£50–£150	£200–£300	£100–£300	£200–£300	Very high (experimental)

The Ni-MH and Li-ion batteries are widely used in electric vehicles (including BEV and hybrid vehicles) due to their higher performance on energy efficiency and cost compared to other types. The Ni-MH battery is mostly used in Hybrid Electric Vehicles (HEV) such as the Toyota Prius HEV due to battery characteristics and HEV's requirements (Edmondson, 2020; Battery University, 2021):

1) **Durability and reliability:** Ni-MH batteries offer a good balance between cost, durability, and reliability. They can withstand the frequent charging and discharging cycles in HEVs without significant degradation.

2) **Safety and stability:** These batteries are less prone to issues like thermal runaway, making them safer for dual systems in HEVs where batteries are closely integrated with internal combustion engines.

3) **Tolerance to overcharging:** Ni-MH batteries can be overcharged without significant damage, which suits the variable power flow of HEVs.

4) **Established technology:** Ni-MH technology has been well established in the automotive industry for longer, providing a proven track record for HEV applications.

5) **Energy density:** While Ni-MH batteries have a lower energy density than Li-ion, this is less of an issue in HEVs because the gasoline engine can provide additional power.

Li-ion batteries are widely used as the primary Energy Storage Device (ESD) in pure BEVs such as Nissan Leaf and VW e-Golf (Pollet et al., 2012; Battery University, 2021) due to the following characteristics:

1) **Energy density:** Lithium batteries offer high energy density in terms of weight and volume, which means they can store more energy per unit of weight and volume compared to other battery types. This makes them ideal for achieving longer driving ranges without significantly increasing the vehicle's weight.
2) **Lifespan and energy efficiency:** Lithium batteries have a longer lifespan and better performance in terms of charge and discharge efficiency, which are critical for the operational efficiency and sustainability of BEVs.
3) **Charging speed**: Li-ion batteries have a faster charging speed compared with other batteries. This characteristic is important for BEVs, which benefit from the ability to rapidly recharge to minimise downtime during long trips.

The advantages have led to a wide adoption which has driven its cost down and strengthened its market dominance for the current and short-term future. However,

compared to the ICE and Fuel Cell (FC) propulsion, the performance of Li-ion batteries is limited (Wu et al., 2019). Table 2-3 presents the characteristics comparison of ICE, FC and battery propulsions in terms of size and cost, the data of BEV includes battery management and cooling system.

Table 2-3 Characteristics comparison of ICEV, FCEV and BEV (Volkswagen, 2024; Toyota, 2024; Evspecifications, 2024)

Reference vehicle	ICEV (Volkswagen Golf 2024)	FCEV (Toyota Mirai 2024)	BEV (Tesla Model 3 2024)
Fuel weight (kg)	37.5	5	N/A
Energy Storage capacity (kWh)	485	166.5	75
Specific energy – fuel (Wh primary/kg)	12,888	33,300	250
Energy Storage system total weight (kg)	62.5	100	480
Specific energy – fuel + storage (Wh primary/kg)	7,760	1,665	156
Vehicle power (kW)	110-150	128	283
Average energy conversion efficiency	20-30%	40-60%	85-95%

The BEV's main advantage is its high average energy conversion efficiency compared to ICE and FC mainly due to the higher efficiency of electric motors in converting electrical energy into mechanical energy. BEVs avoid the energy losses associated with combustion processes in ICEVs and the energy conversion processes in FCEVs. Electric motors can convert over 85% of electrical energy into propulsion, while ICEs typically achieve 20-30% efficiency. FCEVs are also subject to losses in hydrogen production, storage, and conversion back to electricity. The benefit of lower power plant and auxiliary weight is negated by a higher energy storage system weight. However, the specific energy density are not in the same order of magnitude where the specific energy related to the weight of ICEV and FCEV is about 50 times and 10 times as BEV.

Moreover, the battery performance and BEV range are affected significantly by the temperature as shown in Figure 2-1

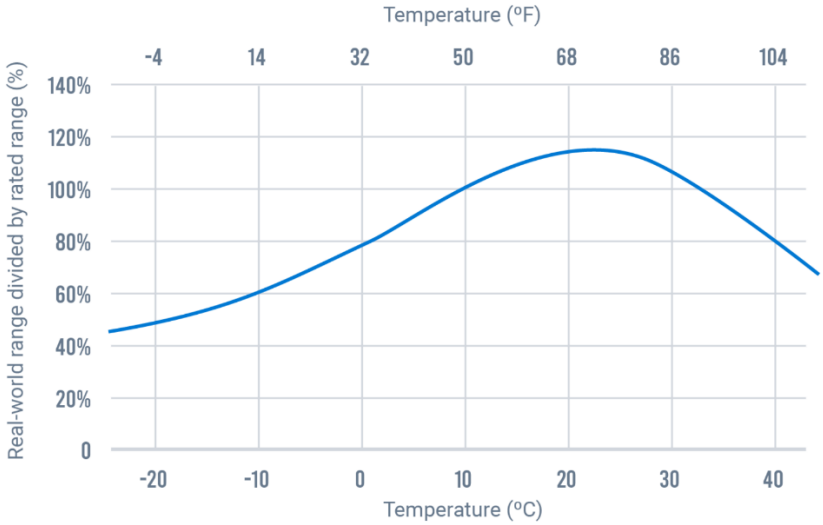

Figure 2-1 Temperature vs real-world BEV range curve (Geotab, 2023)

An analysis conducted by Geotab provides a detailed assessment of the impact of ambient temperature on the range of BEVs, it indicated that BEV performance is highly sensitive to temperature fluctuations, with optimal efficiency occurring at approximately 21.5 $°C$, where vehicles can achieve up to 120% of their rated range. When temperatures deviate from this optimal point, particularly under colder conditions, the range significantly decreases. At -15$°C$, the range drops to around 54% of the vehicle's rated capacity. This reduction is primarily attributed to the additional energy required for cabin heating and maintaining battery temperature. Conversely, in high-temperature conditions above 30$°C$, the range also begins to decline, although the impact is less severe than in cold conditions. The efficiency drop in high temperatures is mainly due to the energy consumed in cooling the battery and cabin. This study underscores the importance of considering environmental conditions when predicting BEV range and highlights the need for efficient battery management systems to mitigate the effects of extreme temperatures on range (Geotab, 2023).

Meanwhile, according to the report from the IEA Global EV Outlook, the top BEV sales countries are presented in Figure 2-2.

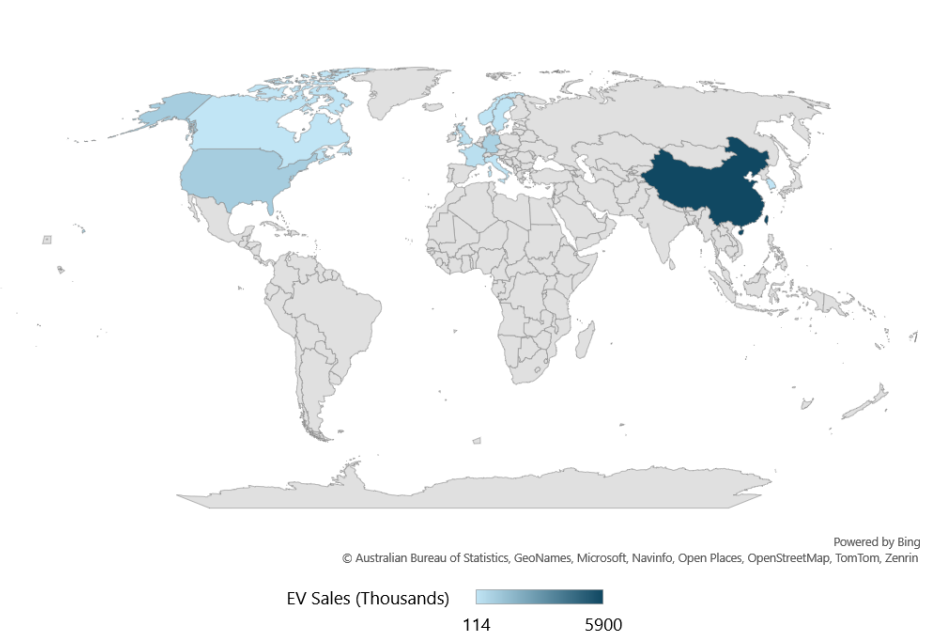

Figure 2-2 Top ten BEV sales (in thousands) by countries (IEA, 2023)

The top ten BEV sales (in thousands) by countries by 2022 are China (5900), USA (990), Germany (830), UK (370), France (340), Norway (166), Sweden (163), South Korea (131), Italy (114) and Canada (114) (IEA, 2023). Most of these countries are located in the mid-high latitudes of the Northern Hemisphere, and the temperature usually drops under 0℃ in the winter which means the BEV range in winter is a significant issue. (Zhang et al., 2017; Bayram, 2021; Delos Reyes et al., 2016). As a result, to increase the range of BEVs, especially for the cold regions, larger-sized battery packs and vehicle bodies are needed, but this will cause another issue related to the energy efficiency and cost of BEVs.

- **BEV efficiency and cost**

Based on the technology roadmaps, BEV is regarded as a replacement solution for the current ICEV, to realise this, it should have a similar range to ICEVs (CEA, 2016; UK Automotive Council, 2017; ERTRAC, 2018). To fulfil the range demand of the BEV, battery packs and vehicle sizes are forced to be grown. However, as Figure 2-3 presents, the oversized batteries (from 250kg to 600kg) to increase vehicle range result in higher energy requirements to move the same vehicle and therefore decrease the vehicle's overall Well to Wheel (WTW) energy efficiency (from 95% to 85%).

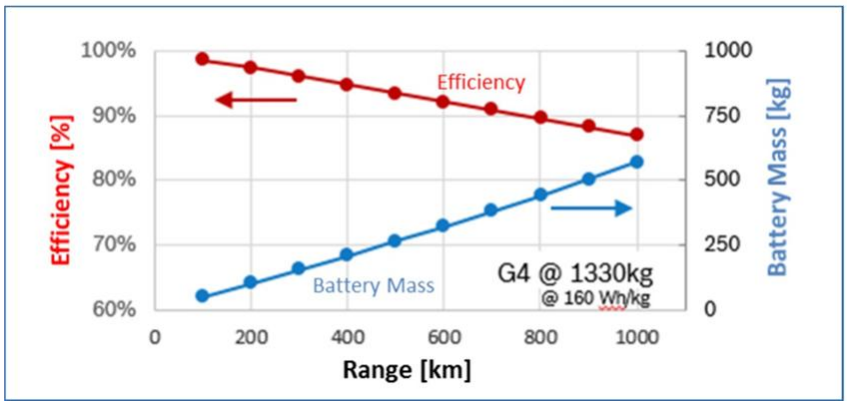

Figure 2-3 Adding battery weight decreases efficiency, which was revealed by an internal analysis based on G4 Vehicles (Golf class). Reproduced from (ETRAC, 2018)

The increase in battery size and reduction in vehicle overall WTW energy efficiency and material consumption leads to increases in both the running cost and manufacturing cost of BEV.

Moreover, as Figure 2-4 shows, that the cost of the drivetrain (especially for the battery pack) in the BEV is higher than the ICEV – 11,630 Euros compared to 3,385 Euros. This makes the proportion of value deriving from the drivetrain higher at 60% for the BEV compared to 33% for the ICEV. To bring price parity between the ICEV and the BEV, and hence facilitate a transition to electric mobility, would require that this disparity be removed. This would require a reduction in the cost of the battery – cost reduction in other parts of the drivetrain would be unable to deliver the required cost reduction, and any reduction in the non-drivetrain part of the vehicle would result in cost reduction for both the ICEV and BEV.

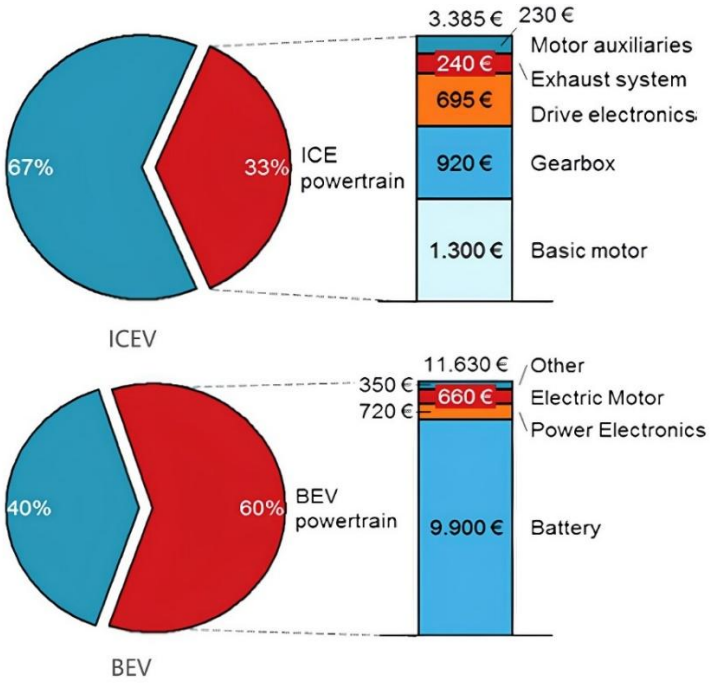

Figure 2-4 Value contributions of the ICEV and BEV (Özel et al., 2013)

Therefore, to bring price parity and enable a transition to BEV would require a reduction in battery cost – either through absolute cost reduction or through the supply of smaller units that would go against consumer pressure for larger units.

Apart from the issue related to the decreasing energy efficiency and increasing vehicle cost due to the range demand of the BEV, the raw material limitation of the battery is also worth to be considered due to the increasingly high demand for the BEV batteries.

- **Battery raw material limitation**

To realise a zero emission road transport system will require an increase in BEV sales. For example, in the UK, at the end of March 2023, there is a fleet of 40.8 million licensed vehicles, evidencing a modest 1.1% expansion relative to the figures from March of the preceding year. Within this aggregate, the contingent of licensed plug-in vehicles surpassed 1.2 million, a substantial uplift of 45% on a year-on-year basis. Notably, the cohort of battery electric vehicles (BEVs) reached 770,000, marking a significant surge of 58% in comparison to the data from March 2022. These statistics underscore the current transition towards electric vehicles in the UK's automotive landscape, reflecting broader environmental policy objectives and consumer adoption trends. (GOV UK, 2023). Further, and based on societal expectation, the autonomy, that is the independent vehicle range, of the present BEV offer will need to increase. Both these factors will place pressure on the supply chain for battery manufacture and the demand for the raw materials to supply the same.

Material involved in battery manufacture includes Manganese and Nickel, Lithium and Cobalt. Manganese and Nickel have large-scale reserves, mature supply chains and only 0.4% of the global nickel demand is for battery use (King & Boxall, 2019). They are therefore not expected to be strongly impacted by demand growth for batteries. Lithium and Cobalt, which are used in Lithium batteries, have a more significant influence on the global BEV market, with batteries representing about 6% of the total demand for Cobalt and 9% of the total demand for Lithium in 2017 (King & Boxall, 2019).

The International Energy Agency predicted that Lithium-ion batteries will remain the market leader for the next twenty years. (IEA, 2018). To fulfil the mass demand for Lithium metal, researchers and engineers around the world are working on the reduction of Lithium metal consumption in the BEV battery (Steward et al., 2019). Even considering that Lithium-air or Sulphur batteries can replace Lithium-ion batteries in the future, raw materials such as Lithium and Cobalt will be still essential.

The resource availability for the manufacture of Lithium-ion cells is an important topic for the continuing development of electric vehicles. Two key elements of material availability are the material market distribution and the industrial structure (Grosjean et al., 2012). According to McKinsey's report, (Figure 2-5), the battery market for Lithium has almost tripled between 2010 and 2017 (McKinsey, 2018). It is expected to represent more than three-quarters of the overall production by 2025. There is a potential discrepancy between the demand and resource for the Lithium required to feed the expansion of BEV. The latter is envisaged to require 1Mt/year Lithium resource after 2026, whilst current resources are estimated to be between 19.2 Mt to 71.3 Mt (Oliveira et al., 2015) which means the available reserves will run out in less than 50 years.

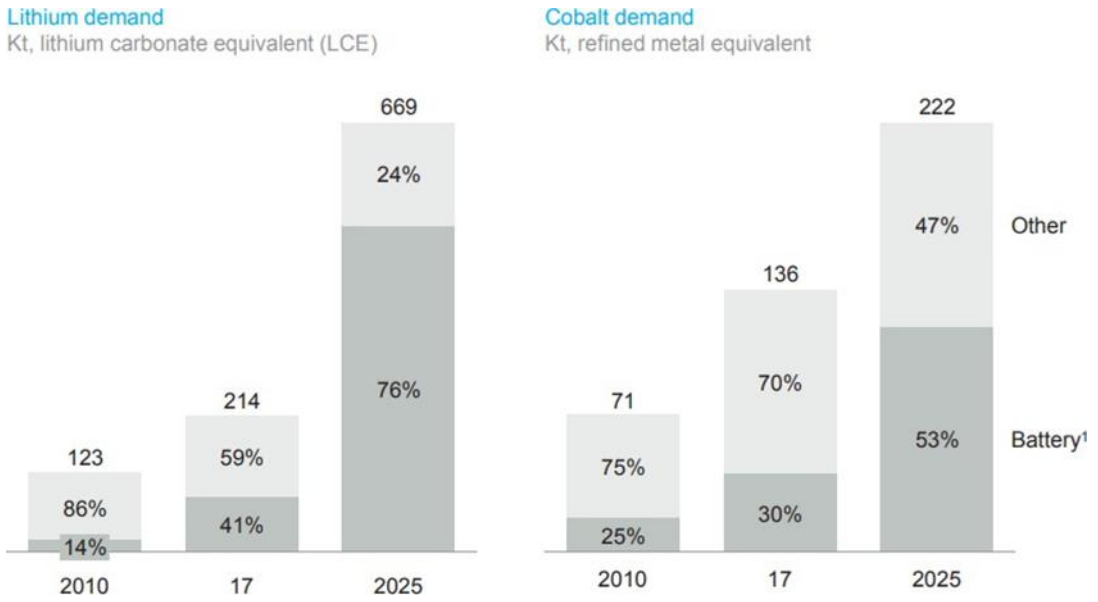

Figure 2-5 Lithium and Cobalt demand the evolution of the whole market. Reproduced from (McKinsey, 2018)

Despite this rapid growth of demand, King & Boxall believe that the increased demand for Lithium should not become an obstacle in the future due to the presence of untapped reserves. However, commercially viable means to exploit oceanic Lithium are yet to be developed and terrestrial stocks have limited extraction capacity. Further, restricted geographic resource distribution has geostrategic implications (King & Boxall, 2019). In particular, the Lithium supply relies on a minority of countries and companies. China, Chile and Australia occupy 85% of the global production market and only four companies Talison, SQM, Albemarle, and FMC supply the majority of mining exports (Oliveira et al., 2015).

Although Lithium is widely used in BEV batteries, Cobalt consumption is more critical due to the geographic distribution and geostrategic implications. Recent analysis indicates that cobalt remains a critical component in lithium-ion batteries, particularly in the field of battery electric vehicles (BEVs). Although the cobalt content has been gradually reduced in new battery chemistries in recent years, it is expected that cobalt will continue to play a significant role in battery manufacturing, with over 50% of cobalt production anticipated to be driven by battery manufacturing by 2025. This aligns with earlier forecasts but reflects a slower-than-expected growth in cobalt usage due to advances in battery design technologies. Additionally, the price of cobalt has experienced significant fluctuations, with a fourfold increase from 2016 to 2018. However, by the end of 2023, the price had substantially decreased to approximately $29,135 per ton (SFA-Oxford,2024; Viernes, 2023; IMARC, 2024). This volatility is attributed to an oversupply in the market and changes in demand as battery electric

vehicle manufacturers explore alternative materials. Cobalt is mostly a by-product of mining Nickel and Copper, the total reserves of Cobalt are about 8.3 million metric tons (Statista, 2023) and the consumption of Cobalt is about 31.6 kt in 2021 (Cobalt Institute, 2022). In 2022, approximately 30% of global Cobalt demand was attributed to the production of BEV batteries. (IEA, 2023).

Lithium battery recycling is a strategy with long-term potential to alleviate the impact of material shortages. However, recent studies indicate that only about 5%-10% of lithium batteries are currently being recycled globally, and the proportion of lithium successfully reused in new products is similarly low. The slow improvement in recycling rates is primarily attributed to the pace of advancements in recycling technologies lagging behind the rapid development of lithium battery technology. Moreover, regulatory frameworks and policies have not yet fully adapted to the growing demand for lithium recycling, leading the industry to focus more on the recycling of cobalt, which has a higher economic value and a more established recycling infrastructure. (Biswal et al., 2024; Zanoletti et al., 2024).

Apart from the raw material limitation issue, the dependency and availability of the charging infrastructure is another challenge of BEV commercialisation speed.

- **BEV infrastructure dependency and availability**

To improve vehicle efficiency, and save cost and raw material consumption, the future BEV requires a reduction of the size of the battery and vehicle body, but this will lead to the range decrease. As a result, the charging frequency of the future BEV will increase, and this will make BEVs depend more on the charging infrastructure, especially for the public charging points. As Table 2-1 above presents, the charging time by using home and fast charging facilities for the popular BEVs, most current BEVs require more than 5 hours when using the home charging due to the limited power available through the domestic supply. For the cases using public fast-charging infrastructures, the charging speed is much higher but still over 30 minutes which is not comparable to the refuelling speed of ICEV and FCEV. Thus, to fully commercialise BEV to replace the current ICEV, the demands of BEV charging infrastructure density, especially for the public rapid charging points, will be much higher than the current petrol stations.

Figure 2-6 presents the amount of total charging connectors changes in the UK from 2020 to 2024.

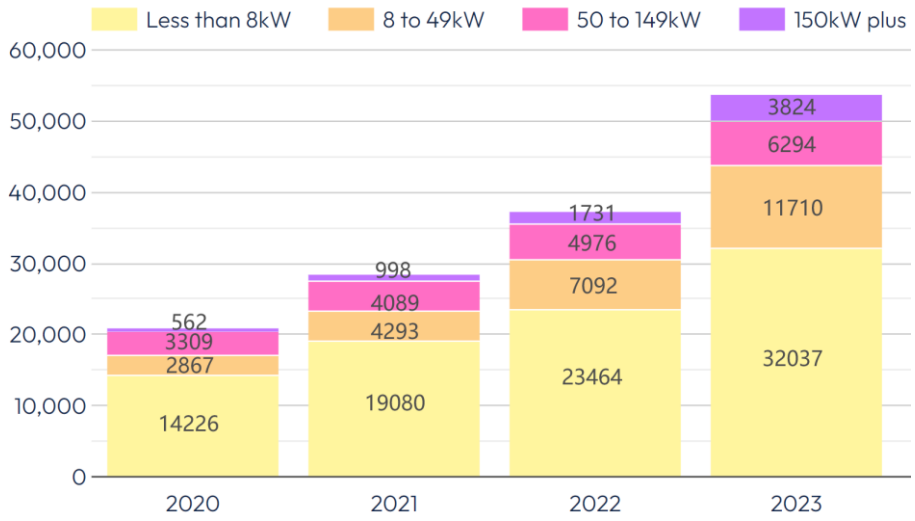

Figure 2-6 Total number of charging connectors in the UK. (ZAP-MAP, 2024)

The 'slow' chargers are most normal home chargers which have power lower than 8 kW, the 'fast' chargers are from 8 to 49 kW including household and public facilities, the rapid chargers are most public specific vehicle charging points whose power is 50-149 kW, the ultra-rapid is defined as more than 150 kW charging points. On one hand, the growth speed of BEV charging infrastructures was not slow in the past few years since the increasing ownership of BEV and governmental efforts, the total amount of charging points has increased by about 157% (from about 21 to 54 thousand) from 2020 to 2023. On the other hand, in the UK, the majority part (about 60%) of the charging points are still 'slow' chargers.

Also, the analysis report published by Statista claimed that in Europe the target ratio of BEV and public charging point is about 10:1 (Statista, 2023). In the UK, the total household passenger vehicles is about 31 million (ZAP-MAP, 2024), if the BEV is targeted to replace all the ICEV, the number of charging points will need to be around 3.1 million, and the current amount of total charging points in 2023 is only about 0.05 million. Therefore, there is still a large gap in the charging infrastructure in the UK. Meanwhile, as National Grid UK indicated in 2017, the rapid growth of BEV charging infrastructure requires investment in the field of both public transport and the power grid domains.

- **BEV safety and risk assessment**

BEVs are gaining popularity due to their potential to reduce greenhouse gas emissions and reliance on fossil fuels. However, there remain certain safety concerns and risks associated with BEVs, particularly those powered by lithium-ion batteries. This section discusses the safety attributes of BEVs by focusing on the risks associated with lithium-ion batteries, their behaviour in post-accident scenarios, challenges in emergency response, implications of long-term use, charging safety, and the environmental impacts related to battery production and disposal.

1) Fuel characteristics and associated risks

The lithium-ion batteries that power most BEVs are renowned for their high energy density and efficiency. However, they may pose significant safety risks, particularly related to a phenomenon known as thermal runaway. Thermal runaway is a chain reaction within the battery that leads to an uncontrolled rise in temperature, potentially resulting in fires or explosions. This condition can be triggered by various factors, including physical damage, overcharging, or exposure to extreme temperatures. For instance, studies have shown that when thermal runaway occurs in a lithium-ion battery, temperatures can soar above 1,000°C, releasing flammable gases such as hydrogen and methane, as well as toxic substances like hydrogen fluoride. (Abada et al., 2016). A study by Sun et al. has further elaborated on the risks associated with thermal runaway, finding that batteries that have been punctured or otherwise physically damaged are particularly susceptible to catastrophic failure. Such failure can result in intense fires that are not only difficult to extinguish but also have the potential to reignite long after initial containment. (Sun et al., 2020). This underscores the critical importance of advanced Battery Management Systems (BMS), which are capable of detecting early signs of failure and taking preventative measures, such as isolating damaged cells to prevent the spread of thermal runaway.

2) Post-accident (crash) safety

The safety of BEVs in post-accident scenarios significantly depends on the structural integrity of the battery pack. Due to the storage of batteries, BEVs tend to be heavier than other types of low-carbon vehicles, which lowers the vehicle's centre of gravity, typically enhancing stability and reducing the likelihood of rollover. However, the presence of large battery packs introduces new risks in the event of a collision. A study by the National Highway Traffic Safety Administration (NHTSA) indicated that while BEVs generally perform well in crash tests, the potential for battery damage increases the risk of fire, particularly in high-impact collisions where the battery pack is compromised. (NHTSA, 2020). Additionally, the location of the battery pack, typically

along the vehicle's floor, makes side impacts particularly hazardous. A study published by the Society of Automobile Engineers (SAE) found that side collisions pose a significant risk to the integrity of the battery pack, potentially leading to short circuits and subsequent fires. The study highlighted the need for reinforced side structures in electric vehicles to better protect the battery pack from such impacts. (CHEN et al., 2022).

3) Emergency response and firefighting

The unique risks posed by lithium-ion batteries necessitate specialised emergency response protocols. Traditional firefighting methods may be inadequate for extinguishing battery fires, as the volatile chemicals involved can cause the fire to reignite. According to the National Fire Protection Association (NFPA), lithium-ion battery fires often require large volumes of water—sometimes exceeding 20,000 litres—to sufficiently cool the battery and prevent reignition. Furthermore, while foam or dry powder extinguishers are effective for gasoline fires, they may be less effective or even hazardous when dealing with battery fires. (NFPA, 2024). The risk of toxic gas release compounds the difficulty of extinguishing battery fires. A study by Larsson et al. found that during thermal runaway, batteries may emit gases such as carbon monoxide, hydrogen fluoride, and other volatile organic compounds, which pose additional risks to the environment and human health. This underscores the importance of firefighters using protective equipment and ensuring that vehicles are stored in well-ventilated areas after the fire has been extinguished to prevent exposure to these harmful substances. (Larsson et al., 2017).

4) Durability and lifespan

Over time, the performance of lithium-ion batteries in electric vehicles may degrade, potentially introducing additional safety risks. As batteries age, their ability to retain charge diminishes, leading to increased stress on the battery cells during charging and discharging cycles. This can heighten the likelihood of thermal runaway, particularly if the battery management system is unable to operate optimally. A study by Keil et al. proved that aged batteries are more prone to internal short circuits, which can cause localized heating and, in some cases, lead to thermal runaway. (Keil et al., 2016). Additionally, the risk of electrolyte leakage increases as batteries age, particularly in those that undergo frequent deep discharges or rapid charging. Such leakage can lead to the corrosion of internal battery components, further heightening the risk of failure. Therefore, regular maintenance and battery health monitoring are crucial for mitigating these risks. (Berecibar et al., 2016).

5) Charging safety

Charging safety is a critical aspect of BEV safety, particularly with the increasing prevalence of fast-charging technology. While slow overnight charging is generally considered safe, fast charging generates a significant amount of heat, which, if not properly managed, can lead to thermal runaway. This risk is especially pronounced in high ambient temperatures or when the battery has underlying internal damage. A study by Tesla indicated that improper use of charging infrastructure, such as damaged connectors or uncertified charging stations, can increase the risk of electrical fires. The study highlighted the importance of using certified charging equipment and regularly inspecting charging ports for signs of wear or damage (Tesla, 2023). Furthermore, as discussed in a report by the National Renewable Energy Laboratory (NREL), fast charging has been shown to accelerate the degradation of lithium-ion batteries, potentially shortening their lifespan and increasing the frequency of required replacements. (NREL, 2019).

6) Environmental and health impacts

The environmental impact of electric vehicles extends beyond their operational phase, particularly concerning the extraction and disposal of materials used in lithium-ion batteries. The mining of lithium, cobalt, and nickel, which are essential for battery production, is associated with significant environmental degradation, including habitat destruction and water pollution. A study by the European Commission emphasized that the extraction of these materials often comes with substantial environmental costs, especially in regions where environmental regulations are less stringent. (European Commission, 2023). Also, the disposal of lithium-ion batteries presents further environmental challenges. Improper disposal can lead to soil and groundwater contamination as toxic chemicals from the batteries leach into the environment. Effective recycling programs are crucial for mitigating these impacts, yet current recycling rates remain low. A report by Harper et al. highlighted the need for improved recycling infrastructure and regulations to ensure that end-of-life batteries are managed in an environmentally responsible manner. (Harper et al., 2019).

7) BEV safety and risk assessment summary

Compared to other emerging ZTEV technologies, the safety risks associated with BEVs, such as thermal runaway, battery degradation, and fire hazards, present significant challenges. However, these risks are being actively mitigated through advancements in battery management systems, emergency response protocols, and

material innovations. While these safety issues are not insignificant, they are unlikely to severely hinder the future development and adoption of BEVs. Ongoing improvements in technology and safety measures are likely to ensure that BEVs remain a viable and competitive option in the evolving automotive sector.

- **Summary of BEV technology current status**

BEV has advantages in energy efficiency and higher environmental performance compared to ICEV and ICE-based HEVs and is recognised as one of the most potential future road vehicle solutions. In order to meet the requirements of people's vehicle demand and reach the target goal of replacing the current ICEV, the BEV will need to increase range and reduce cost. However, limited by the battery performance and main raw material resource, increasing the battery amount for range extension will decrease the vehicle efficiency, and lead the growth in both manufacture and running costs.

According to the 2017 APC Roadmap from the UK Automotive Council, to deal with the issues caused by the increasing demand for BEV batteries for the BEV range extension and market share growth, one of the most effective solutions is to make the future BEV be 'tailored for usage'. This means that the range and size of future BEVs should be adapted to demands and applications. However, the range setting of 'tailored' BEVs should include 3 key consideration points – the vehicle's average daily driving distance, household vehicle ownership status and the driving behaviour related to the percentage of the vehicles used for long-distance journeys. Firstly, for the vehicle average daily driving distance, in the EU countries, the average daily driving distance in the European country varies from 25 miles (UK) to 50 miles (Poland) (European Commission, 2017). This means to meet the demand of the average daily range demand, the BEV can be sized as a small/eco type. Secondly, for the household vehicle ownership status, based on the report published by the Department for Transport of the UK government in 2018, only 35% of families have more than 1 car to meet the demands of all ranges of their trips, this means about 65% the current ICEVs are responsible for fulfilling all kinds of trips for UK families. Thus, if these vehicles need to be replaced by BEVs in the future, the range of the new BEVs should have a large size of battery and body to reach a similar level to the existing ICEVs. Thirdly, for the driving behaviour of how often people take long-distance trips, TNS SOFRES published their survey results from the EU countries and indicated that on one hand, only 19% of vehicles are used frequently to take long-distance trips (longer than 130 km) (TNS SOFRES, 2014). On the other hand, only 19% of household vehicles are never used for long-distance trips. This means most BEV owners have demands for

long-distance trips, but the frequency is very low. This led to a conflict in deciding the BEV size since the long-distance trips are mandatory, but it is also an infrequent demand, increasing the BEV size will offer the additional functionality required for meeting a greater proportion of all vehicle trips, but will lose efficiency and cost-effectiveness.

To conclude, the development of future BEVs and their infrastructure have difficulties and conflicts between vehicle functionality and cost-effectiveness associated with efficiency. Consequently, an alternative or transitional solution will be needed in the future ZTEV market, it should address the limitations of BEV range, cost, raw material consumption, and charging infrastructure dependency as well as maintain the high energy efficiency of BEV.

2.2.2. Current Status of FCEV Technology

Similar to BEV, FCEV is identified as a future option to reduce the dependence on foreign oil significantly and to lower harmful emissions that contribute to climate change. As another future solution, compared with BEV, FCEV has the potential offer of extended range, quicker refuelling speed and less environmental impact but similarly has limitations on cost and infrastructure (Wu et al., 2019). The following sections will look to quantify the current capability of FCEV and will look to establish any critical dependencies that need to be considered when establishing the gap between current capability and what is required of an FCEV fleet – thereby identifying key focus areas.

- **Performance and cost of current FCEV fleet**

FCEV use hydrogen as the energy source for a fuel cell, which, in turn, supplies the appropriate voltage to the vehicle battery and/or drive system. The performance of the FC stack is one of the most important features of the FCEV, and there are some competing FC stack technologies. Table 2-4 shows an overview of the latest situation for the FC stack types and technologies, and characteristics of the various FC stacks including electrochemical, chemical and electric performance are presented.

Table 2-4 Summary of fuel cel technical characteristics. (Mekhilef et al., 2012; Elmer et al., 2015; Sharaf & Orhan, 2014; DoE, 2023)

Fuel Cell Type	Polymer electrolyte membrane (PEM)	Alkaline (AFC)	Phosphoric Acid (PAFC)	Molten Carbonate (MCFC)	Solid Oxide (SOFC)
Anode catalysts	Platinum	Nickel	Platinum	Nickel	Nickel oxide
Cathode catalysts	Platinum	Nickel	Platinum	Nickel oxide	Strontium-doped lanthanum manganite (LSM)
Interconnect material	Carbon-based materials	Steel or nickel-based materials	Graphite	Stainless steel	Ceramic or stainless steel
Electrolyte	Proton-conducting polymer membrane	Potassium hydroxide (KOH)	Phosphoric acid	Molten carbonate salts	Yttria-stabilized zirconia (YSZ)
Fuel	Hydrogen	Hydrogen	Hydrogen	Hydrogen, natural gas, biogas	Hydrogen, natural gas, biogas
Cell voltage	0.7 V	0.85 V	0.7 V	0.7-1.0 V	0.8-1.0 V
Operating Temperature (°C)	<120	<100	150-200	600-700	500-1000
Start-up Speed	<2 mins	<5 mins	30-120 mins	2-10 hours	12-24 hours
Typical Stack Size (kW)	<1 kW – 250 kW	1 – 100 kW	50 – 100 kW	300 kW – 3 MW	1 kW – 2 MW
Electrical Efficiency (LHV)	40-60%	40-60%	35-45%	45-50%	35-65%

The most widely used fuel cell technologies include PEMFC, AFC, PAFC, MCFC, and SOFC. PAFC and SOFC are predominantly utilised in medium to large-scale stationary power generation systems, such as Combined Heat and Power (CHP) systems. In contrast, PEMFC and AFC offer advantages in applications requiring rapid start-up and portability, making them suitable for transport. MCFC, on the other hand, excels in large-scale power generation and distribution, due to its high operational efficiency at industrial scales.

For FCEVs, the key performance indicators, such as start-up speed, operating temperature, and energy efficiency, are critical when assessing the most appropriate fuel cell technology. A detailed comparison of these factors is provided below (DoE, 2023):

1) Start-up Speed:

PEMFC: The start-up speed of PEMFC is extremely fast, typically reaching operational status within two minutes. Its low operating temperature (<120°C) facilitates rapid start-up, making it ideal for automotive applications where quick power supply is essential.

AFC: AFC offers a relatively fast start-up, usually within five minutes. However, AFC's sensitivity to CO_2 and the need to manage its electrolyte composition may slightly reduce its response speed, making it marginally less efficient than PEMFC in this regard.

PAFC: PAFC has a moderate start-up time, generally between 30 and 120 minutes. Its higher operating temperature (150-200°C) accounts for the extended start-up time, making it better suited for stationary power production rather than mobile applications.

MCFC: MCFC requires a significantly longer start-up time, typically taking between 2 to 10 hours due to its high operating temperature (600-700°C). This characteristic limits its feasibility for applications requiring immediate power supply, rendering it more suitable for continuous large-scale power generation.

SOFC: SOFC has the slowest start-up speed, usually taking 12 to 24 hours. Its high operating temperature (500-1000°C) necessitates stringent thermal management, making it unsuitable for applications requiring rapid or frequent start-ups.

2) Operating Temperature:

PEMFC: PEMFC operates at relatively low temperatures, approximately 60-80°C, aiding its rapid start-up and long lifespan, particularly well-suited to applications such as FCEVs.

AFC: AFC operates at moderate temperatures below 100°C, ensuring a relatively quick start-up. However, AFC systems require careful CO_2 management to maintain optimal performance.

PAFC: PAFC operates at 150-200°C, enhancing its tolerance to fuel impurities, making it ideal for stationary power generation. However, the higher temperature extends its start-up time.

MCFC: MCFC operates at temperatures of 600-700°C, allowing flexible fuel usage and offering the potential for internal fuel reforming. However, the high temperature makes it impractical for mobile applications.

SOFC: SOFC operates within a range of 500-1000°C, providing high efficiency and fuel flexibility. Nonetheless, this temperature range limits its application to stationary power systems where effective thermal management is essential.

3) Efficiency:

PEMFC: PEMFC delivers moderate efficiency, typically between 40-60%. Although its efficiency is slightly lower than that of high-temperature fuel cells, its compact design, rapid start-up, and low-temperature operation make it a preferred choice for transport applications such as FCEVs.

AFC: AFC also provides efficiency in the range of 40-60%, but its sensitivity to CO_2 limits its widespread use in environments where CO_2 management poses challenges.

PAFC: PAFC operates with an efficiency of around 35-45%, which is acceptable for stationary applications with high fuel impurity levels. However, this lower efficiency makes it less attractive for mobile applications.

MCFC: MCFC offers relatively high efficiency, usually between 45-50%, with the potential for even higher overall efficiency in CHP applications. This high efficiency makes MCFC suitable for large-scale power production.

SOFC: SOFC provides the highest efficiency among all fuel cell types, often exceeding 60%, and can achieve up to 85% efficiency when integrated into CHP systems. However, its long start-up time and high operating temperature offset this efficiency advantage, making it impractical for mobile applications.

Therefore, among the technologies considered, PEMFC is the most suitable for FCEVs due to its rapid start-up, low operating temperature, and sufficient efficiency. Although SOFC and MCFC offer higher efficiency and greater fuel flexibility, their long start-up times and high operating temperatures make them impractical for automotive applications. AFC may be a viable option for certain transport applications, but its sensitivity to CO_2 restricts its use in broader environments.

However, the costs of the proton exchange membrane and the platinum catalyst are prohibitively high (Wu et al., 2019). Researchers and automotive manufacturers are continuing to optimise fuel cells. For example, the fuel cell stack in the Toyota MIRAI FCEV not only reduced volume by 43% and weight by 48%, but it also improved power delivery by 26% compared with the 2008 model of fuel cell stack (Hunt, 2017). Due to the development potential of fuel cells for portable applications, transportation applications and stationary applications, the fuel cell could become an environmentally friendly, economically competitive energy storage device for the future market (Sharaf & Orhan, 2014). Table 2-5 presents the comparison of FCEV with ICEV, BEV and HEV in different performance perspectives.

Table 2-5 Comparison of vehicle specifications. Adapted from (Pollet et al., 2012; Evspecifications, 2023)

	ICEV (VW GOLF 1.4TSI)	Hybrid (Toyota Prius III)	BEV (Tesla Model 3)	FCEV (Toyota Mirai)
Power supply	IC engine	ICE, electric motor	Battery and electric motor	PEM fuel cells and electric motor
Fuel	Petrol, diesel and alternative fuel	Petrol/diesel as the main fuel	Electricity	Hydrogen
Top speed (mph)	124	112	139	110
Acceleration 0-100 km/h (s)	9.5	10.4	6.1	8.5
Range (miles)	552	716	272	357
Purchasing price	From £22,500	From £25,500	From £39,990	From £49,000
Running fuel price (per mile)	£16.8p	£10.7p	From £2p	From £5p
Fuel economy (mpg or mpg equivalent)	45.6	72.4	138	81
Tailpipe CO_2 Emission (g/km)	144	89	0	0
Charging time (min)	5	5-120	60-660	5

In terms of vehicle range, FCEV has a longer range than BEV and a similar range compared to conventional vehicles. Still, with the development of fuel cell technology and due to the high energy density of hydrogen, it is not hard to increase the range. It will not lead to oversize and significant mass increase (Wu et al., 2019). For example, Toyota has targeted a 620-mile driving range with a fuel cell concept car which can offer more than 50% drive range for the current Mirai FCEV (BLOOMBERG, 2019).

In the customer's view, the purchase price of FCEV is much higher than other vehicles. This is related to the production/sales volume since the current amount of FCEV is incomparable with other types of vehicles. The running costs of FCEV and BEV are currently much lower than ICEVs due to taxes not added to the hydrogen fuel and electricity for charging. However, FCEV operating costs are still expected to remain lower than ICEV, even if taxes were to be added on fuel and electricity charging (Wu et al., 2019).

- **Hydrogen and infrastructure limitation**

The refuelling speed of FCEV is similar to ICEV which only takes about a few minutes. The most significant challenge faced by FCEVs is the limited availability of hydrogen refuelling infrastructure. As of 2023, there are 1,068 hydrogen stations globally, distributed across 35 countries. This number is expected to increase significantly in

the coming years, with projections indicating that more than 6,000 stations will be in operation by 2030. China is currently leading in this sector, with over 350 stations, while Japan and South Korea each operate more than 160 stations. In the UK, the hydrogen refuelling infrastructure remains underdeveloped, with only 11 operational stations as of 2023 (IEA, 2023). This has become a notable barrier to the wider adoption of hydrogen-powered vehicles. To address this issue, the UK government is making significant investments, with plans to establish 200 hydrogen stations by 2030. This plan is part of a broader strategy to promote the hydrogen economy in the UK, including initiatives such as the Tees Valley Hydrogen Hub. Furthermore, efforts in the UK include collaborations with companies such as Element 2 and Exolum, aiming to progressively expand the hydrogen refuelling network across the country, starting from regions such as Northern England. In addition, the government has introduced portable hydrogen refuelling stations as a temporary solution to meet demand during the transition towards a more permanent infrastructure network (Adrian Flux, 2024).

The increase in hydrogen refuelling stations is significantly increasing the demand for hydrogen fuel. The latter requires a significant growth of hydrogen production and a vast distribution network. The remainder of this section addresses both issues.

1) Hydrogen production

Although hydrogen is abundant on the earth, it cannot be obtained directly, unlike oil and gas. There are many ways to produce hydrogen. Natural Gas Reforming is the most common process to produce hydrogen. Steam reforming and partial oxidation methods can produce hydrogen from Methane. Low-cost natural gas reforming can provide hydrogen for FCEVs and other applications such as electric power grids (EERE, 2019). Usually, industries use the natural gas reforming method to produce hydrogen and CO_2. Due to the unwanted release of CO_2 into the air, the hydrogen resulting from this production method is called ‘grey hydrogen’ (GasTerra, 2018). With a long-term view, the usage of oil and gas will be replaced by solar power and wind power to generate hydrogen. This type of hydrogen is often called ‘green hydrogen’. A technology called Carbon Capture and Storage can capture almost 90% of the $CO_2$by-product during the industrial processes, preventing most of the CO_2 from entering the atmosphere (CCSa, 2019). This type of hydrogen is called ‘blue hydrogen’. New techniques to produce hydrogen will be implemented, such as photocatalytic water splitting and high-temperature water electrolysis by nuclear technology. Once these methods become reliable and efficient, the whole production chain will exclude the use of carbon-based energy.

2) Hydrogen storage and distribution

Currently, the most widely used method for hydrogen storage is high-pressure gaseous hydrogen storage, particularly in vehicular applications, due to its relatively low cost and suitability for mobile use. This method enables lightweight storage while maintaining the efficiency required for vehicle applications. Another option is liquid hydrogen storage, which offers a higher volumetric energy density. However, one of the primary challenges associated with this method is the issue of "boil-off losses," where approximately 1-5% of the stored hydrogen evaporates each day, even with advanced insulation technologies (IEA, 2023). This presents a significant obstacle to its widespread adoption in mobile applications. Cryogenic hydrogen storage (at approximately -253°C) provides a potential solution but requires an energy-intensive liquefaction process, which consumes 30-40% of the initial energy content of the hydrogen (IEA, 2023). Compared to other methods, cryogenic storage is less efficient and more costly. Material-based hydrogen storage, including metal hydrides and advanced porous materials such as metal-organic frameworks, is still in the developmental stage and faces challenges related to cost and storage capacity (IEA, 2023). However, as research in these materials progresses, they show promise for future applications. For automotive applications, compressed gaseous hydrogen storage remains the most viable option. Continuous advancements are being made in this technology, with a focus on improving the strength and structure of hydrogen storage tanks and using composite materials to reduce overall weight. In addition, researchers are exploring cryo-compressed hydrogen storage, which combines the benefits of both gaseous and liquid hydrogen storage by compressing hydrogen at lower temperatures to increase density while minimising the energy losses associated with liquefaction (IEA, 2023).

Hydrogen delivery problems are closely linked to hydrogen storage technology. Currently, hydrogen gas is usually stored in a high-pressure tank and delivered by trucks, gaseous tube trailers and railway. Liquid hydrogen is bulk-stored in low-temperature adiabatic tanks and delivered by planes, trucks, ships and railways. It is straightforward to deliver solid hydrogen; however, the efficiency of transportation is less than 1% due to the heavy weight (Jia et al., 2019).

- **FCEV safety and risk assessment**

FCEVs are regarded as a viable alternative to traditional ICEVs and BEVs. However, the safety of FCEVs, particularly those using hydrogen as a fuel source, presents distinct challenges. This paper explores the safety characteristics of FCEVs, with a

focus on the risks associated with hydrogen fuel, post-accident safety, emergency response protocols, long-term durability, hydrogen refuelling safety, and the environmental impacts related to hydrogen production and storage.

1) Fuel characteristics and associated risks

FCEVs are powered by hydrogen, which is stored in high-pressure tanks, typically operating at pressures up to 700 bar. While hydrogen provides a clean energy source, it is highly flammable and can be explosive under certain conditions. The primary risk associated with hydrogen in fuel cell vehicles is leakage, which can lead to the formation of explosive gas mixtures. Unlike conventional fuels, hydrogen is colourless, odourless, and burns with an almost invisible flame, making it difficult to detect leaks without specialized equipment. As highlighted by Toyota, modern hydrogen storage systems in FCEVs are designed to withstand significant impacts and high temperatures, thereby reducing the risk of catastrophic failure. These storage tanks are typically made from carbon fibre-reinforced composites, offering an excellent strength-to-weight ratio and the ability to contain hydrogen even under harsh conditions (Toyota, 2021). However, despite these advancements, the potential for undetected minor leaks remains a concern, particularly in enclosed spaces where hydrogen could accumulate. A study by Song et al. further emphasized the dangers of hydrogen leaks, finding that even a small hydrogen leak could reach explosive concentrations within minutes if not properly ventilated. The study underscored the necessity for continuous monitoring and the integration of leak detection systems in both vehicles and refuelling stations to mitigate this risk (Song et al., 2024).

2) Post-accident (crash) safety

The post-accident safety of FCEVs largely depends on the integrity of the hydrogen storage tank and the vehicle's fuel system. It is crucial to keep these components intact during a collision to prevent hydrogen leaks. Hydrogen tanks in FCEVs undergo rigorous testing, including crash simulations and fire exposure tests, to ensure they can withstand severe impacts. A study found that hydrogen tanks can endure significant forces without rupturing, greatly reducing the likelihood of catastrophic leaks following a collision. However, in the rare event that a hydrogen tank is compromised, the consequences can be severe. The rapid release of hydrogen could create a highly flammable and explosive environment, even a small leak in an enclosed space could reach explosive concentrations within minutes if not properly ventilated. (Wang et al., 2023). This study highlights the importance of using high-quality materials and

adhering to stringent safety protocols to minimize the risk of hydrogen leaks in crash scenarios.

3) Emergency response and firefighting

Emergency response for FCEVs presents unique challenges, particularly because hydrogen fires are difficult to detect. When hydrogen burns, it produces an almost invisible flame, and its rapid dispersion in air can make fires challenging to control. Firefighters require specialized equipment, such as thermal imaging cameras, to detect hydrogen flames. A report by the Redwood Coast Energy Authority emphasized the importance of training emergency responders to handle hydrogen fires, noting that traditional methods used for gasoline or diesel fires are often ineffective against hydrogen. Furthermore, hydrogen can ignite at much lower energy levels compared to conventional fuels, which increases the risks during rescue operations. For instance, even static electricity can trigger a hydrogen leak. Therefore, it is crucial that emergency protocols include procedures for grounding vehicles and using explosion-proof equipment during emergency response activities. (Redwood Coast Energy Authority, 2021).

4) Durability and lifespan

The long-term safety of FCEVs is closely linked to the durability of the hydrogen storage system. Over time, the repeated pressurization and depressurization cycles experienced by hydrogen tanks during refuelling can lead to material fatigue. Research indicates that while carbon fibre-reinforced hydrogen tanks are highly durable, regular inspections are still necessary to detect any signs of wear or damage that could potentially lead to leaks. Hydrogen embrittlement, a process where hydrogen molecules permeate and weaken metal components, poses a risk to the integrity of metal parts within the fuel system. This underscores the importance of continuous monitoring and the development of materials resistant to hydrogen embrittlement to ensure the long-term safety of FCEVs. (Abohamzeh et al., 2021)

5) Refuelling safety

Refuelling an FCEV involves handling hydrogen at extremely high pressures, up to 700 bar. This process necessitates stringent safety measures to prevent leaks or accidental ignition. According to the research by Veres et al., 2021, hydrogen refuelling stations are equipped with multiple safety features, including automatic shut-off valves, pressure sensors, and leak detection systems, to mitigate risks. The study also highlighted that any failure in these systems could lead to significant hazards,

underscoring the importance of regular maintenance and safety inspections. Meanwhile, both the refuelling nozzle and the hydrogen inlet on the vehicle are designed with interlock mechanisms to prevent disconnection while the system is pressurized, thereby reducing the likelihood of accidents. However, as highlighted by an incident reported by H2toos.org, human error during the refuelling process remains a potential risk. In this particular case, improper handling during refuelling led to a hydrogen leak. This incident underscores the necessity of comprehensive training for both operators and users to ensure safe refuelling practices. (H2tools.org, 2020)

6) Environmental and health impacts

While FCEVs emit only water vapour during operation, the production and storage of hydrogen can have significant environmental impacts. Currently, most hydrogen is produced through steam methane reforming, which generates substantial carbon dioxide emissions. A study by the International Energy Agency (IEA) found that without the use of Carbon Capture and Storage (CCS) technology, hydrogen production could offset the environmental benefits of FCEVs. The report suggests that shifting to green hydrogen, produced via electrolysis using renewable energy, is crucial for minimizing the carbon footprint of FCEVs (IEA, 2019).

7) FCEV safety and risk assessment summary

The safety challenges associated with FCEVs, such as hydrogen storage and leak management, are indeed significant, but ongoing technological and infrastructural advancements are effectively addressing these issues. Compared to other ZTEV technologies, FCEVs offer unique advantages, including rapid refuelling and long driving ranges, which continue to drive their development. With improvements in safety protocols and materials, these potential hazards are unlikely to severely impede the future growth of FCEVs, ensuring that they remain strong contenders in the transition to sustainable transportation.

- **Summary of FCEV technology current status**

FCEV advantages include range (compared with BEV), overall efficiency, running cost and zero tailpipe emission compared to other ICEV and HEV. FCEV limitations include the small hydrogen infrastructure and distribution network as well as high purchase costs. FCEV can meet the requirements of daily use and travel demand in the future. FCEV being currently an integral part of the hydrogen economy could supplement it or be restricted by this relation. For now, the high cost of fuel cell systems, the shortage of infrastructures and the immature hydrogen economy all limit the development of

FCEV. Hence, a transition solution is required to bridge the gap between today's and future BEVs and FCEVs. As discussed in Section 1.2, the proposed concept of ' a demountable hydrogen fuel cell range extender (DHFCRE) + an Eco-BEV' has the potential to deal with the current limitations of both BEV and FCEV, as we maintain the advantages.

2.3. Potentials of DHFCRE + Eco-BEV Powertrain Concept

Based on the review of the competing ZTEV technologies presented in sections 2.1.1 and 2.1.2, the advantages of the current BEV and FCEV can be summarised as follows:

- **Environmentally friendly**

Compared to current ICEVs, both BEV and FCEV have no harmful tailpipe emissions. BEVs only use electricity to power the vehicle thus no tailpipe emissions, FCEV use hydrogen gas to generate electricity and then power the vehicle, the only chemical reaction product is water (Pollet et al., 2012).

- **High energy efficiency**

ZTEVs have higher TTW energy efficiency than the ICEVs, the average overall TTW efficiency of BEV is 60% – 80%, FCEV is around 45% while the diesel and gasoline-powered vehicle average is about 16% – 22% (IEA, 2022).

- **Low fuel cost**

The low fuel cost of BEVs is a significant advantage compared to ICEVs and FCEVs. The electricity cost of the current BEV is from £1.5 to £16 per 100km, depend on different charging method, e.g. home charger using off-peak electricity (£0.08-£0.2/kWh) has much lower cost than using public rapid chargers (£0.4-£1.2/kWh) (Zap-Map, 2024), while the average fuel cost of ICEV passenger cars is about £9.25 per 100km (gasoline) and £8.99 per 100km (diesel) (IEA, 2022; Shell UK, 2023). The average fuel cost of FCEVs is around £11.4 per 100km (IEA, 2022; Autotrader, 2023).

The challenges of the current BEV and FCEV can be summarised as follows:

- **BEV range limitation and charging speed**

The vehicle average range and charging speed of BEV are lower than the ICEV and FCEV. The range of current BEV significantly replies to the vehicle size due to the battery energy density being incomparable with fossil fuels and hydrogen gas, the energy density of Lithium batteries is about 150 – 260 Wh/kg while gasoline is about

12000 Wh/kg and hydrogen gas is 33300 Wh/kg (Hypertextbook, 2003; IEA, 2022; Tsakiris, 2023). The range of current passenger BEVs varies from 40 to 300 miles while the average passenger ICEV and FCEV range is about 300 – 400 miles (IEA, 2022) (Tsakiris, 2023). The charging speed of BEV is also incomparable with ICEV and FCEV, the fastest BEV charging pile can provide about 250 – 300 miles in 20 minutes, while the refuelling speed of ICEV and FCEV is only about 3 – 5 minutes (EvChargingMag, 2023; National Academies of Sciences, Engineering, and Medicine, 2022).

- **Infrastructure dependency and availability**

Due to the limited range and charging speed of BEV, it relies more on the charging infrastructure than BEV and FCEV. Even though the growth speed of the BEV charging infrastructure has been fast in recent years, the density of the BEV charging network is still much lower than the gas stations for ICEVs (ZAP-MAP, 2024). The number of hydrogen gas stations for the FCEV is only 15 in the UK (Hydrogenbatteries.org, 2023), and the growth speed of hydrogen refuelling stations is foreseeable slow due to the high cost and dependency on government support (Waseem et al., 2023). The growth of hydrogen stations relies on government policy power. It is a paradoxical “Chicken and Egg’ reality: fewer hydrogen refuelling stations lead to less incentive for people to buy FCEVs; while lower FCEV sales mean that the hydrogen stations have a lower utilization rate in their initial phase of operation, increasing the risk of losses and then companies have less incentive to invest on it. This is a vicious cycle and one of the most significant difficulties for the progress of the commercialisation of FCEVs.

- **High cost of core components**

The cost of core components such as Lithium battery pack for BEV (about £122/kWh), FC stack (about £533/kW) and high-pressure hydrogen gas tank (about £410 to £546 per kg at 700 bar pressure) are very high compared to the ICEV parts (EERE US, 2023; Wanitschke & Hoffmann, 2020; Shin & Ha, 2023).

In summary, the superiorities of current BEVs include zero-emission, high energy efficiency and low fuel cost. However, there are also significant shortcomings including the conflict between the vehicle’s range and its size and cost; the issue of slow charging speed, and the resulting strain it places on public infrastructure; the issue of overconsumption of raw material resources due to low energy density, as well as the future problem of recycling and disposal of the End of Life (EOL) batteries. The advantages of the current FCEV are zero-emission; long range with lightweight and

size due to the high energy and power density of the FC system; and fast charging speed which is similar to the current ICEV. However, the drawbacks of FCEVs are also very evident, such as high purchasing price; lower TTW energy efficiency than BEV and the most important feature of the infrastructure dependency with a foreseeable slow growth speed of hydrogen refuelling stations.

To minimise the impact of the above shortcomings of BEV and FCEV, the UK Advanced Propulsion Centre (APC) reveals the future development direction of BEV and FCEV in the published technology roadmap (Figure 2-7).

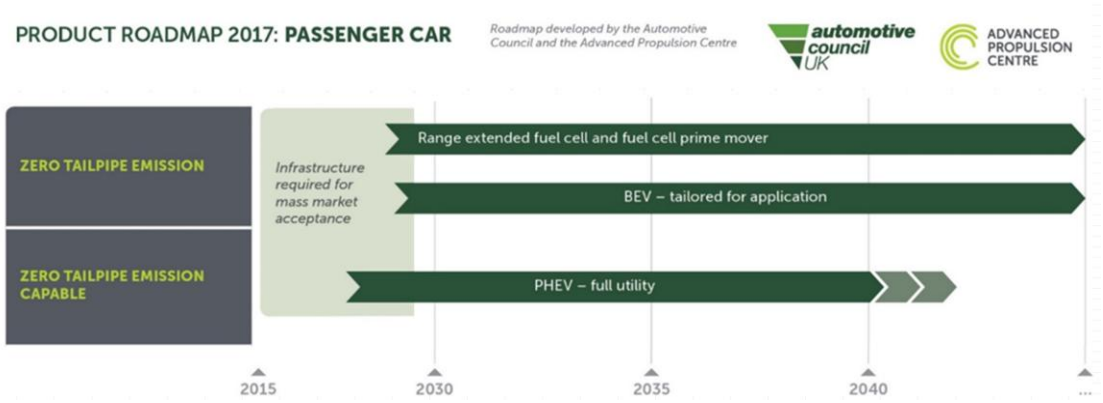

Figure 2-7 UK Passenger Vehicle Roadmap 2017 (UK Automotive Council, 2017)

Guided by this technology roadmap, the future development direction of BEVs will shift from “general-purpose” to being “tailored for specific applications”. This means that future BEVs will have a greater variety of models, sizes, and features to meet diverse needs. However, due to the limitation of the battery energy density, the eco-sized Eco-BEVs will only be tailored for use in urban short-distance journeys. This means that the future BEVs are still not able to fully fulfil the functionalities of existing ICEVs and would need to either lose some functionality or incur some additional costs.

For the FCEVs, the roadmap suggests that the future forms of FC technology will be “range extended FC” and “FC prime mover”. The FC prime mover means that the vehicle primarily relies on the fuel cell to generate electricity, and then powers the electric motor for propulsion. The vehicle can use a small battery pack to only manage peak power demands and recover energy from braking, but the primary energy source is from the hydrogen fuel cell just like a Toyota Mirai (Toyota, 2021). However, this concept will require a qualified infrastructure scale and density, similar to the current gas station network, otherwise, full commercialization cannot be achieved, and this would take decades to realise. The “range extended FC” means that the vehicle will mainly use the power from the battery pack to move the vehicle. Most of the time, the

FC will only be used as an electricity generator like a power bank for mobile phones. It can be designed as either stationary or demountable.

Over the past eight years (2017–2024), significant progress has been made in the fields of BEVs and FCEVs under the guidance of the UK's APC and the UK Automotive Technology Roadmap. This roadmap has emphasised a strategic shift from general-purpose electric vehicles towards specific applications, such as urban transport and short-range travel.

Firstly, for BEVs, there has been an increase in the energy density of batteries; however, limitations remain for long-distance and heavy-duty applications. Due to their lower costs and environmental benefits, BEVs are increasingly being utilised in urban transport. Nonetheless, frequent charging and longer charging times compared to conventional vehicles continue to pose challenges. Research has focused on optimising battery chemistry and efficiency, with the UK government supporting the expansion of charging infrastructure (UK Automotive Council, 2024).

Secondly, FCEVs have seen slower uptake in the passenger car market compared to BEVs, primarily due to infrastructure limitations. However, significant progress has been made in commercial and heavy-duty applications, where hydrogen fuel cells offer advantages in range and refuelling times. The UK's hydrogen strategy outlines plans to expand hydrogen refuelling stations, aiming to accelerate the adoption of FCEVs by addressing infrastructure gaps (UK Automotive Council, 2024).

Thirdly, for the infrastructure development, y 2024, the UK has made substantial investments in both hydrogen refuelling stations and the BEV charging network, with the aim of supporting the widespread adoption of zero-emission vehicles. The development of this infrastructure is crucial to reducing reliance on ICEVs and supporting the UK's broader net-zero emission targets (UK Automotive Council, 2024).

Compared with the "tailored for application BEVs" and "FC prime mover" concepts mentioned in the roadmap, there is a novel concept of "a demountable hydrogen FC range extender (DHFCRE)" connected with an Eco-BEV. As Figure 2-8 Eco-BEV + Shared FCRE concept potentials show, that it could be a transitional solution which has the following potential to bridge the gaps of the existing technical, functional and economic shortcomings of both BEV and FCEV.

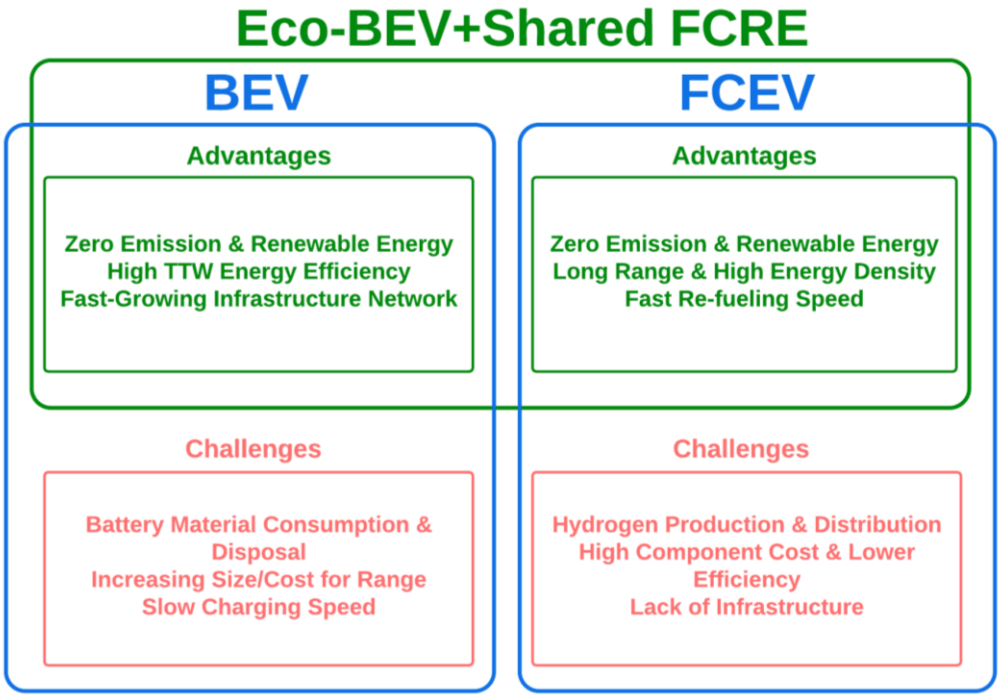

Figure 2-8 Eco-BEV + Shared FCRE concept potentials

This method has the following potential:

- Eco-BEVs have a smaller size and will cost less than the “general purpose BEVs”, as well as being more preferred by British people compared with large vehicles. (Parkers, 2023). It also reduces the running cost due to the lower rolling and aerodynamic resistance.
- Eco-BEVs can fulfil the majority proportion of the daily driving demands since short-distance urban journeys account for more than 98% of the journeys. (Department of Transport UK, 2021)
- A DHFCRE can be connected to the Eco-BEV for the occasional long-distance trips without range anxiety concerns and avoid the long-time waiting for the public charging piles.
- The marketing model for this DHFCRE is not limited to purchasing; it can also offer leasing services. This provides a more flexible and cost-effective choice for the Eco-BEV user which can reach the goal of “tailored for application” as the APC technology roadmap suggests.
- The leasing service chain of the proposed DHFCRE will also provide benefits to the initial stage hydrogen infrastructure. Instead of refuelling each vehicle separately like current FCEVs, this DHFCRE (or its hydrogen tanks) can be centralized for simultaneous distribution and refuelling, similar to the successful business model of the “sharing electric bikes” in China (Li et al., 2022).

- The leasing points of this DHFCRE can be selected in the existing petrol stations and motorway service stations which avoid high upfront costs as well as achieve a proven qualified network density.
- Thanks to the size reduction of BEVs, from a macro perspective, the total raw material consumption, total cost, and overall environmental impact will be significantly reduced.

The listed potentials of this proposed DHFCRE + Eco-BEV concept could minimise the current shortcomings of BEV and FCEV and accelerate both technologies to achieve future goals guided by the technology roadmap. Hence, it is important to conduct a comprehensive analysis and assessment of this concept's performance, considering cost-effectiveness, energy efficiency, functionality, and the broader economic and environmental impacts as well as inform further optimisations to the concept through established scientific energy management strategies.

Chapter 3 Simulation System Modelling

3.1. Introduction

In reviewing of current status of Zero Tailpipe Emission Vehicle (ZTEV) solutions, it can be concluded that limitations are affecting the commercialisation progress of both BEV and FCEV. As a result, the proposed powertrain concept of 'DHFCRE + Eco-BEV' has the potential to overcome the limitations whilst leveraging the benefits of both technologies. To assess the potential of this concept and, at the same time, establish technical and economic comparisons with competing powertrain alternatives, experimental results are crucial. The Demountable Hydrogen Fuel Cell Range Extender (DHFCRE) model, including involved subsystems and components of the simulation model, was developed in the software environment. A further simulation model in this project will be a BEV model to evaluate the technical and economic performance after adding the DHFCRE to the Eco-BEV. The framework and structure of the BEV and FC models will refer to the materials and publications from Coventry University Microcab Laboratory (Microcab, 2017; Apicella, 2019; Ren, 2021) as well as the library blocks and subsystem samples from the Matlab/Simulink opensource materials (MathWorks, 2019). The accuracy and performance of the models will be examined and validated by the existing experimental results generated by Microcab BEV and FCEV real-world experiments (Microcab, 2017). The methodology of the simulation modelling includes:

- Undertake an extensive literature review to identify and evaluate the simulation tools in the field of hybrid energy source vehicle, then select the simulation tool based on the functional requirements of this project.
- Establish the BEV and DHFCRE model refer to the structure from literature and Coventry University Microcab Laboratory (Microcab, 2017; Apicella, 2019; Ren, 2021).
- Validate the models by experimental result from Coventry University Microcab Laboratory (Microcab, 2017; Apicella, 2019).

The following sections will present the modelling process and all the subsystems in the BEV model, the added FC range extender model and the validations of the models based on the experimental data from Coventry University Microcab Laboratory.

3.2. Simulation Tool Evaluation and Selection

This section commenced by outlining the simulation requirements based on the aims and objectives of this project to identify the most focused function and accuracy performance of the simulation tool. Subsequently, it evaluated the current simulation tools available in the automotive sector, with a particular focus on LCV and hybrid vehicle applications. This evaluation will include the strengths and limitations of each tool based on the simulation requirements. Also, the section will select the most appropriate simulation tool for this project and establish a comprehensive analysis of all requirements and the accuracy performance of the simulation tools. Finally, it will introduce the validation method of the simulation model.

3.2.1. Simulation Tool Requirements

Refer to the aims of this thesis in Section 1.3, one of the aims of this project was firstly to evaluate the performance of the proposed powertrain concept 'DHFCRE + Eco-BEV', in terms of cost, energy efficiency, functionality, and the macro cost and benefit from both commercial and environmental perspectives. A further aim was to optimise the DHFCRE energy management strategy using external information including BEV motorist intentions and traffic information, etc.

To accomplish these research aims, the simulation tool was required to fulfil the following functional requirements (Microcab, 2017; Apicella, 2019; Ren, 2021):

1) The simulation model for this novel powertrain concept of "DHFCRE + Eco-BEV" should contain all the vehicle components from the powertrain to the vehicle dynamics (aerodynamic and rolling resistance, etc.), including multiple energy sources (battery and FC).

2) The most significant parameters of inputs in this model include the duty cycle model (vehicle velocity-time data set as input) and external environmental parameters (air temperature, wind speed, road profiles, etc.).

3) The targeted output parameters of this model are vehicle dynamic and aerodynamic responses (such as forces, inertias, power, speeds, accelerations, etc.), electric powertrain and FC system-related electrical responses (such as battery State of Charge (SoC), current, voltage, power, efficiency, energy consumption, etc.), vehicle overall performance factors (including vehicle speed plot, overall energy efficiency, fuel cost, accumulated energy consumptions from both battery and FC system, etc.)

4) Since the main aim of the simulations in this thesis is to establish comparisons between the proposed “DHFCRE + Eco-BEV” concept with the competing powertrains in the vehicle's overall performance level instead of the microscopic technical level. Therefore, the simulation model focused more on the macroscopic vehicle performance indicators including the velocity trace result compared with the given drive cycle, energy consumption and efficiency under a certain drive cycle, battery dynamics such as SoC and current, power, voltage plots, fuel cell dynamics such as FC current, power, voltage plots and FC system efficiency. However, the microscopic technical parameters and their accuracy will not be priorly considered such as comprehensive vehicle aerodynamic performance, rolling resistance related to tyre and suspension profiles, energy loss (mainly heat loss) in vehicle transmission systems (such as brakeing pad, suspension and tyre) and powertrain systems (electric motor, DC-DC converter and fuel cell stack). Because these are not highly related to the key research questions of this project, also the over-complexity of the physical model will have a significant effect on the simulation efficiency. In the simulation of this project, the given duty cycle will need to represent whole journeys of real-world driving conditions which take more than 10 thousand seconds, therefore, the model will be simplified in the above subsystems to ensure realistic simulation speed but will maintain the macroscopic key performance.

5) The simulation model is validated by using experimental data from the Coventry University Microcab Project. In 2004, Microcab Industries Ltd was established and commenced a collaborative venture with Coventry University, effectively functioning as a spinout company. Together, Microcab and Coventry University co-developed a novel design and produced a prototype of a small four-wheeled vehicle, named the Microcab H4 (Figure 3-1), which utilised a 1.2 kW hydrogen fuel cell and a Lithium-ion battery system. A fleet of 5 H4 vehicles was constructed for government-funded trials at the University of Birmingham campus between 2006 and 2008. The data gathered from these trials informed the specifications for a new vehicle design, the FCEV. The experimental data used in this project is from the “New European Driving Cycle (NEDC) Rolling Road Test” of the Microcab FCEV undertaken on the rolling road of MIRA in 2016 (Apicella, 2019).

Figure 3-1 Coventry University Microcab FCEV (Apicella, 2019)

6) The simulation model requires the availability of the development of the Energy Management System (EMS) by using scientific control algorithms to optimise the performance of this DHFCRE.

7) The simulation model should be compatible to generate economic calculations based on the technical simulations by inputting relevant economic parameters to undertake a Cost-Benefit Analysis (CBA) to quantify the cost and benefit of this proposed concept.

3.2.2. Simulation Tool Evaluation

This section reviewed and evaluated the performance of the simulation tools in the field of low-carbon vehicles especially for hybrid powertrain applications and select the simulation tool for this project which can produce results based on the simulation requirements as well as provide the best balance of accuracy and efficiency. The selection of a simulation tool for this project should consider the balance between model fidelity, computational efficiency, and the capacity to integrate various aspects of vehicle design, control, and economic analysis.

To build a comprehensive and quantitative evaluation and comparison of different simulation tools, the following key functional requirements and costs (time and fund) factors will be scored from 0 (worst) to 5 (best). Then, by comparing the total summed score of all the tools to determine the most appropriate simulation tool for this project. The key performance factors include:

- **Accuracy**: The compatible component and overall model level result in accuracy.
- **Complexity**: The complexity of the modelling software and if the model complexity is flexible to be customised.

- **Cost and efficiency**: If requires additional funds to purchase the software licence. If the simulation speed is flexible enough to be customised.
- **Duty cycle availability**: The capacity for different types of duty cycles including 2D and 3D data associated with external environment parameters.
- **Control system availability**: The capacity for the integration with advanced scientific control systems.
- **Economic models integration**: The capacity for establishing economic models and calculations for the proposed CBA.

There are a number of widely used simulation software for automotive and low-carbon vehicle technology applications, the following sections evaluated five popular simulation tools including their advantages, limitations and proven application areas.

3.2.2.1. FASTSim

FASTSim (Future Automotive Systems Technology Simulator) is an automotive simulation tool (especially for low-carbon vehicle technologies) produced by The National Renewable Energy Laboratory (NREL) of the USA (Figure 3-2).

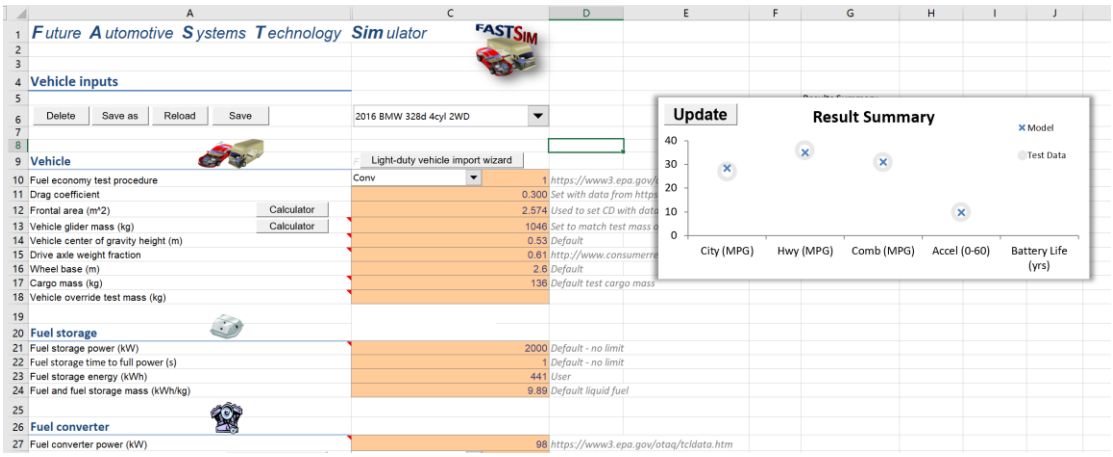

Figure 3-2: FASTSim Simulator

The FASTSim framework offers a streamlined methodology for the comparative analysis of various powertrains, facilitating the evaluation of technological enhancements on vehicular efficiency, performance, cost, and battery longevity. It permits the automatic importation of input data for a wide array of light-duty vehicles, with provisions for user-led modifications to reflect alterations in vehicle architecture or powertrain configurations. After input adjustments, FASTSim executes vehicle simulations across diverse driving cycles, meticulously accounting for factors such as

resistance, acceleration, gradient, rolling resistance, component efficiency, power constraints, and the potential for regenerative braking.

The simulation extends to a multitude of powertrains, encompassing conventional internal combustion engine vehicles, hybrid electric vehicles, plug-in hybrids, purely electric vehicles, those powered by compressed natural gas, and fuel cell variants. Additionally, it offers the capability to simulate electric traction drives within the context of electric road systems, inclusive of dynamic wireless power transfer technologies.

Moreover, FASTSim is equipped with an interface designed to handle a substantial number of real-world driving cycles, delivering a balance between precision and computational rapidity, thus permitting the simulation of extensive travel distances within minutes. The fidelity of FASTSim's outputs is corroborated by benchmarking simulation results against empirical data collated from a broad spectrum of vehicles, thus instilling confidence in the interpretive outcomes.

With its user-friendly graphical interface, FASTSim enhances usability and operational efficiency. The tool relies on a suite of mathematical equations to model interactions between various vehicle components. Compatible with Microsoft Excel and Python environments, the outputs rendered by FASTSim encompass a range of metrics such as efficiency, energy utilisation, distribution patterns, performance benchmarks, state of charge trajectories for batteries, and comprehensive as well as particularised cost analyses (NREL, 2019). The advantages, limitations and ideal applications fields of FASTSim are summarised as follows (Brooker et al., 2015; Torreglosa et al., 2020; De Almeida & Kruczan, 2021):

The **advantages** includes:

1) Easy to use

User-friendly interface and the capability to simulate a wide array of vehicle configurations and driving scenarios without demanding extensive computational resources or specialised technical knowledge.

2) High efficiency

Modular architecture, allowing for easy updates or modifications to components in line with emerging vehicle technologies.

3) Driving cycle availability

Ability to predict vehicle energy consumption and performance metrics over standardised driving cycles or real-world driving cycles, facilitating comparative analysis and optimisation studies.

The **limitations** are:

1) **Limited accuracy**

Predictive accuracy depends on the quality of input data and the assumptions in underlying models, potentially not capturing all nuances of vehicle dynamics or the complex interactions within powertrain components as detailed as more sophisticated simulation tools might.

2) **Limited model functionality**

Focuses predominantly on energy consumption and efficiency, potentially under-addressing other aspects of vehicle performance such as drivability and emissions under transient conditions.

There are several **application areas** including:

1) **Academic and industrial research:** Employed to assess the impacts of novel vehicle technologies, energy storage systems, and powertrains on fuel efficiency and energy consumption.
2) **Policy development:** Assists in the evaluation about how various vehicle technologies can meet environmental targets.
3) **Vehicle design and opimisations:** Supports the optimisation of vehicle designs for improved performance and sustainability, offering a platform for comparing different vehicle configurations under a wide range of scenarios.

The most significant advantage of FASTSim is easy to understand and use which allows one to quickly set vehicle parameters. The main shortage of FASTSim is on the control logic since the simulator is based on mathematics equations, it is hard to install complex control logic in the model.

3.2.2.2. AVL CRUISE

AVL CRUISE (Figure 3-3) is a comprehensive simulation software developed by AVL, widely regarded for its advanced capabilities in modelling and analysing the performance of automotive vehicles, particularly focusing on powertrain systems. As a pivotal tool in the automotive engineering domain, AVL CRUISE supports the

development and optimisation of energy-efficient and low-emission vehicles by facilitating detailed simulations of conventional, hybrid, electric, and fuel-cell vehicles. (AVL, 2019).

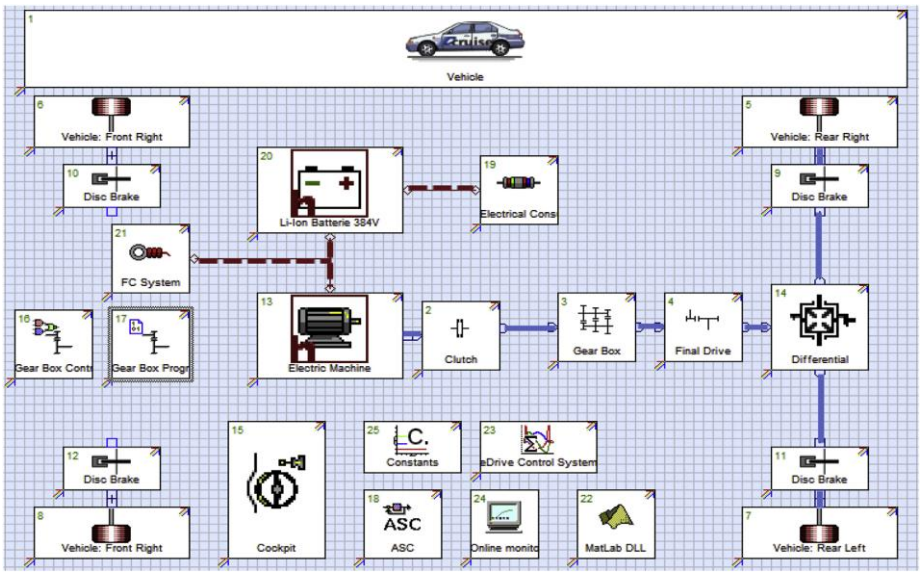

Figure 3-3: Model of electric drive vehicle based on Cruise. (Geng, Jin and Zhang, 2019)

CRUISE serves as a comprehensive tool underpinning the gamut of engine and vehicle development endeavours, catering to standard evaluations such as fuel economy and acceleration under full load. It adeptly handles performance assessments in challenging scenarios like ascents and provides detailed traction maps. Additionally, CRUISE facilitates computational concept studies that span mechanical, electrical, thermal, and control systems. This integrative platform fosters concurrent engineering, a cornerstone for curtailing development durations and associated expenses. CRUISE's versatility renders it suitable for a wide array of Original Equipment Manufacturers (OEMs) within the automotive sector. This includes an array of vehicles from passenger cars to trucks, motorcycles, and specialised vehicles, and extends to component suppliers such as those for engines, gearboxes, and tyres. CRUISE enhances user experience by incorporating an interface compatible with the Simulink Coder MATLAB Application Programming Interface (API), allowing for the execution of Simulink in the Matlab environment. It utilises both fixed and variable time step integration methods for simulation processes, as described by MathWorks in 2019. (MathWorks, 2019). The advantages, limitations and ideal applications fields of AVL CRUISE are summarised as follows (Cioroianu et al., 2017; Cassiano et al., 2016; Yang et al., 2010; Wahono et al., 2016).

The **advantages** includes:

1) **High accuracy:**

Delivers precise modelling of drivetrain components, engine performance, and vehicle dynamics, enabling the development of highly efficient powertrain systems.

2) **Comprehensive analysis ability:**

Offers extensive tools for analysing emissions, fuel consumption, and performance metrics across various driving cycles.

3) **Versatile application range:**

Suitable for a wide array of vehicle types, including conventional, hybrid, electric, and fuel cell vehicles.

4) **3D road and driving scenario simulation:**

Capable of incorporating 3D road profiles and complex driving scenarios, enhancing the realism of simulations.

5) **Integration of control logic:**

Allows for the simulation of vehicle control strategies, providing insights into the interaction between vehicle dynamics and control systems.

The **limitations** are:

1) **Complex user interface:**

The complexity of the software can pose a challenge to new users, requiring a steep learning curve to effectively utilise its full capabilities.

2) **Extended simulation times:**

Detailed and high-fidelity models can lead to longer simulation times, especially for complex scenarios or when analysing multiple vehicle configurations.

3) **Focus on powertrain and drivetrain systems:**

While offering detailed powertrain modelling, it may not cover all aspects of vehicle design and performance with equal depth.

There are several **application areas** including:

1) **Powertrain development and optimisation:**

Designing and analysing conventional and alternative fuel powertrains. Optimising hybrid and electric vehicle energy management strategies.

2) Fuel consumption and emissions analysis:

Evaluating vehicle performance under various driving conditions and cycles. Assessing compliance with emission standards and environmental regulations.

3) Vehicle dynamics studies:

Investigating the impact of drivetrain configurations on vehicle handling and dynamics. Analysing the effect of control strategies on vehicle performance and efficiency.

In conclusion, AVL CRUISE stands as a sophisticated tool in the automotive research and development sector, offering detailed simulations that guide the design and optimisation of energy-efficient vehicles. Despite its complexity and the potential for extended simulation times, its accuracy, comprehensive analysis capabilities, and versatility in application solidify its position as an invaluable asset in the pursuit of advanced automotive engineering solutions. The selection of AVL CRUISE as a simulation tool should be aligned with the specific requirements of the project, taking into consideration the level of detail necessary and the user's proficiency with the software. The key advantages of CRUISE are optimisation on overall/specific energy consumption (efficiency), a comprehensive vehicle powertrain component including new concepts (BEV, FCEV, Hybrid, etc.), thermal management component and evaluation of powertrain effects. These superiorities are mainly focusing on the vehicle powertrain system. It has APIs to connect the model to Matlab/Simulink. For this project, the main disadvantages of CRUISE are the lack of control logic settings for the EMS and the economic evaluation models.

3.2.2.3. Advanced Vehicle Simulator (ADVISOR)

ADVISOR (Figure 3-4) is a simulation tool designed for the analysis and optimisation of vehicles ranging from conventional internal combustion engines to electric and hybrid electric vehicles (HEVs).

ADVISOR was developed in November 1994 by the National Renewable Energy Laboratory (NREL). Its inception was intended as an analytical aid for the United States Department of Energy (DOE) to further the development and comprehension of hybrid electric vehicles (HEVs).

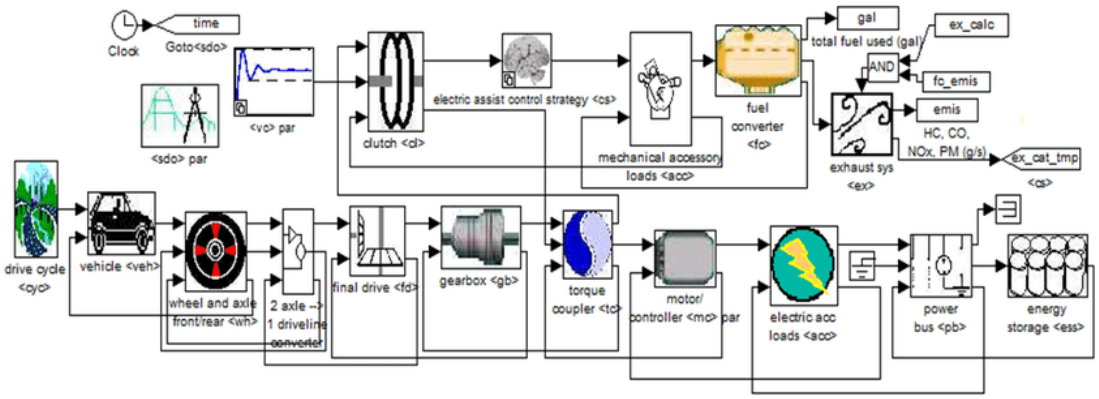

Figure 3-4: Parallel hybrid vehicle simulation model-ADVISOR simulation environment. (Pawełczyk and Szumska, 2018)

The genesis of ADVISOR arose from a collaborative contract involving automotive leaders such as Ford, General Motors, and Chrysler, with the goal of advancing hybrid vehicle propulsion systems (NREL, 2018). As ADVISOR evolved, its enhanced sophistication and adaptability attracted a diverse clientele. It became a resource for many entities to discern system-level interplays among components within hybrid and electric vehicles. (Wipke et al., 2013). The core design of ADVISOR emphasises the analysis of vehicle power systems, with a particular concentration on the dynamics of power flow among components. The advantages, limitations and ideal applications fields of ADVISOR are summarised as follows (Senger et al., 1998; Same et al., 2010; Rezazade et al., 2018; Wahono et al., 2015).

The **advantages** includes:

1) Flexibility in vehicle modelling:

Capable of simulating a wide range of vehicle types, including conventional, hybrid, plug-in hybrid, and electric vehicles, making it a versatile tool for vehicle design and analysis.

2) User-friendly interface:

Offers a Graphical User Interface (GUI) that simplifies the process of vehicle configuration and simulation, making it accessible to users with varying levels of expertise.

3) Integrated energy and emission analysis:

Facilitates comprehensive analyses of energy consumption and emissions, aiding in the design of more environmentally friendly vehicles.

The **limitations** are:

1) **Learning difficulty:**

Despite its user-friendly interface, new users may require time to become proficient in its use due to the complexity of its modelling capabilities.

2) **Computational demand:**

High-fidelity simulations can be computationally intensive, requiring significant processing power for complex analyses.

3) **Model accuracy:**

The accuracy of simulations depends on the quality of input data and the assumptions made in the vehicle models, which may not capture all real-world nuances.

There are several **application areas** including:

1) **Vehicle design and optimisation:**

Evaluating the performance of different powertrain configurations to identify optimal designs for fuel efficiency and emissions reduction.

Simulating the impact of new technologies, such as battery systems and electric motors, on vehicle performance.

2) **Energy consumption and emissions analysis:**

Assessing vehicle energy use and greenhouse gas emissions under various driving cycles to support regulatory compliance and environmental impact studies.

Comparing conventional, hybrid, and electric vehicles to guide policy development and investment in sustainable transportation technologies.

3) **Educational and research applications:**

Serving as a teaching tool in academic institutions for courses related to automotive engineering and environmental science.

Facilitating research into advanced vehicle technologies and their potential to contribute to a more sustainable transportation system.

In conclusion, ADVISOR stands as a significant tool in the field of vehicle simulation, offering extensive capabilities for the analysis and optimisation of a broad spectrum of vehicle types. While it presents certain challenges in terms of computational demand

and the learning curve for new users, its flexibility, user-friendly interface, and open-source nature make it a valuable resource for researchers, engineers, and policymakers focused on advancing sustainable vehicle technologies. The continuous development and enhancement of ADVISOR will undoubtedly contribute to its enduring relevance and utility in addressing the challenges of modern transportation and environmental sustainability. For this project, a significant advantage of using ADVISOR in the Simulink/MATLAB environment is the flexibility and ease of use of the model, such as replacing one control strategy or regenerative braking algorithm with another. (Wipke and Cuddy, 2015). However, similarly to the AVL CRIUSE, it does not have the components of the economic evaluation models.

3.2.2.4. Matlab/Simulink

Simulink, conceived by MathWorks, is a graphical programming environment designed for the modelling, simulation, and analysis of dynamic systems that span various domains. Its chief interface is a graphical block diagram tool accompanied by a suite of customisable block libraries. It offers an integrated experience with the Matlab environment, allowing for its operation and scripting directly from Matlab. (MathWorks, 2019). Simulink is widely used for automatic control and digital signal processing in multi-domain simulation and model-based design (Bodemann, 2004). In the automotive industry, Matlab/Simulink is widely used in control logic programming, duty cycle simulation and economic models. It allows both mathematical and physical components in the simulation with a comprehensive library on the low carbon vehicle components such as Lithium batteries, hydrogen fuel cells and hybrid systems. Figure 3-5 presents a vehicle simulation model based on Matlab/Simulink.

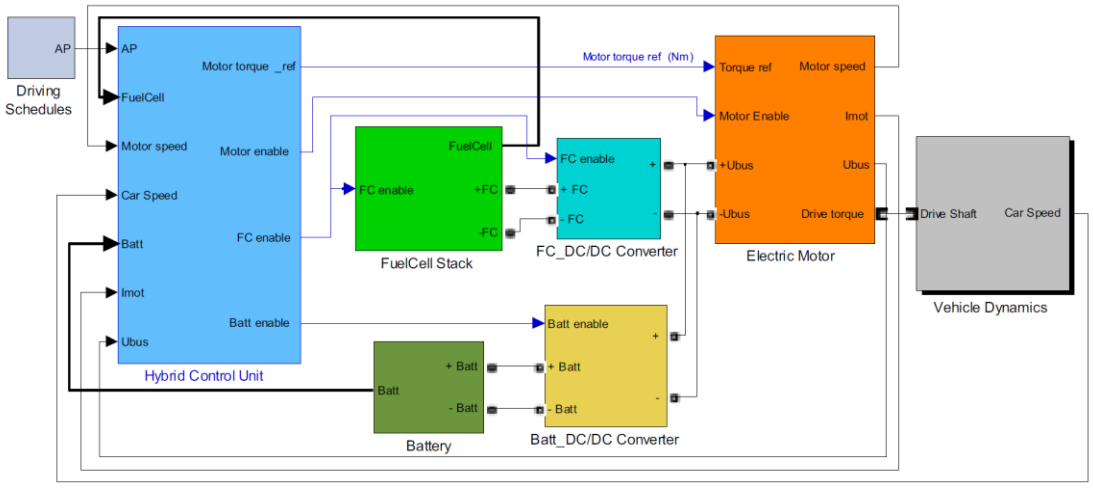

Figure 3-5: Matlab/Simulink FCEV simulation model. (Ning et al., 2009)

The advantages, limitations and ideal applications fields of Matlab/Simulink are summarised as follows:

The **advantages** includes:

1) Control system availability:

Matlab/Simulink offers a powerful platform for control systems including several library blocks related to control algorithms, and energy management strategies and is also available for customised control systems written by Matlab code or other programming languages including C++, Python etc.

2) Economic models:

Matlab/Simulink model provides customised mathematical blocks which allow users to input a wide range of mathematical formulas. Through this, the economic models can be established as well as directly connected with the technical results from the vehicle simulation and output the relevant economic results at the same time.

3) Flexible model complexity:

Matlab/Simulink offer a wide range of vehicle component blocks with different levels of complexity in terms of mathematical and physical performance. Users can choose the required complexity of different components in their model to highlight the main focus of their model and results.

4) Model accuracy:

Matlab/Simulink has both mathematical and physical pathways in the field of vehicle simulation, also, the model accuracy can be easily customised by users based on the simulation requirements through simulation setting functions.

The **limitations** are:

1) Drive cycle availability:

The most common and reliable drive cycle model under the Matlab/Simulink platform is the time-speed plot 2D model which cannot fully simulate the real-world 3D road profiles.

2) Learning difficulty:

Since Matlab/Simulink has both mathematical and physical models, this requires the users to have professional knowledge to use. New users may require time to become proficient in its use due to the complexity of its modelling capabilities.

3) **Computational demand and simulation efficiency:**

High-fidelity simulations can be computationally intensive, requiring significant processing power for complex analyses. Also, some complex physical models require very long simulation time.

There are several **application areas** including:

1) **Education:** Teaching complex engineering concepts through simulation.
2) **Automotive and aerospace:** Designing control systems, and simulating vehicle dynamics and flight systems.
3) **Electrical engineering:** Developing power systems, electronic devices, and signal processing algorithms.
4) **Energy sector:** Analysing renewable energy systems, including solar and wind power integration.

To conclude, for this project, the main advantages of Matlab/Simulink include the availability of control strategies and economic modelling as well as the flexible model complexity which improves the efficiency of the modelling and simulation process. The main limitation of the Matlab/Simulink is operation difficulty and time-consuming the establishment of the model and de-bugging process due to each equation/component containing a large number of blocks, especially for the whole vehicle simulation model.

3.2.2.5. Modelica/Dymola

Modelica/Dymola is a comprehensive and versatile simulation environment widely utilised in the field of engineering for modelling and simulating complex systems that span across multiple domains such as mechanical, electrical, thermal, and control systems. It employs the Modelica modelling language, which is an object-oriented, equation-based language designed to allow component-oriented modelling of complex systems (Modelica, 2018). Modelica consists of several predefined libraries. Therefore, the software can prove to be very useful when investigating areas that are not the operator's expertise, as the basic modelling approach can be established by investigating a given model (Apicella, 2019).

Dymola's unique system engineering capabilities provide a groundbreaking solution for modelling and simulation due to its ability to emulate the dynamic behaviour and complex interactions of systems across numerous engineering disciplines including mechanical, electrical, thermodynamics, hydraulics, pneumatics, thermal, and control

systems. (Dassault Systèmes, 2019). Dymola (Figure 3-6) is built upon the Modelica platform. Consequently, Dymola can encompass all the functionalities of Modelica and potentially even more, as the package provides pre-validated models that users can utilize and build upon.

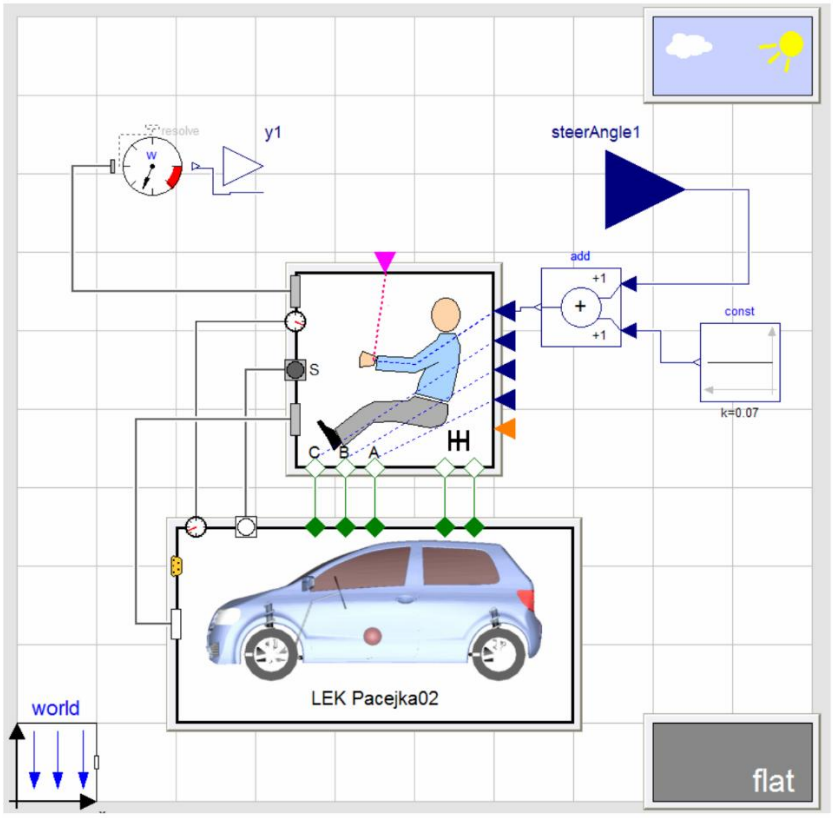

Figure 3-6: Modelica/Dymola vehicle simulation model (Trigell et al., 2009)

One of Dymola's primary advantages over Modelica is its inclusion of a pre-defined and validated library. Moreover, the software supports 3D representation modelling, allowing for a visual depiction of model content when simulating vehicle dynamics. Additionally, the user interface is more user-friendly, permitting more keyboard shortcuts and simpler model replication, which can be quite cumbersome in Modelica. This enables users to create more intricate models and reduce errors more rapidly. The advantages, limitations and ideal application fields of Modelica/Dymola are summarised as follows (Apicella, 2019).

The **advantages** includes:

1) Component-oriented modelling

Facilitates modular and reusable model development, enhancing efficiency and reducing time-to-market for engineering projects.

2) Multi-domain simulation

Capable of simulating systems that span multiple physical domains, enabling comprehensive analysis of integrated systems.

3) Open-source Modelica language

Supports an open and collaborative environment for model development, with a wide range of available libraries covering various domains.

4) Advanced solvers for complex equations

Equipped with robust solvers that can handle highly complex differential and algebraic equations, ensuring accurate simulation results.

5) Graphical User Interface (GUI)

Offers an intuitive GUI for model building and simulation, making it accessible to both experienced engineers and novices.

The **limitations** are:

1) Learning difficulty

The complexity of the Modelica language and the depth of Dymola's simulation capabilities may present a steep learning curve for new users.

2) Lack of economic model

While efficient for a broad range of applications, the economic model is hard to build within the technical simulation model based on Dymola.

3) Cost

While Modelica is open-source, Dymola is a commercial product, and the cost may be prohibitive for some users or small organizations.

There are several **application areas** including:

1) **Automotive industry:** Design and simulation of hybrid and electric vehicle drivetrains. Thermal management systems for batteries and electric powertrain.
2) **Aerospace:** Simulation of aircraft systems, including hydraulic, pneumatic, and environmental control systems.
3) **Renewable energy systems:** Modelling and analysis of wind turbines and solar power systems.

In conclusion, Modelica/Dymola stands out as a powerful and flexible simulation environment capable of addressing the multifaceted challenges in engineering complex systems across various industries. Its comprehensive modelling capabilities, support for multi-domain simulations, and component-oriented approach offer significant advantages. However, the associated costs, computational demands for large-scale simulations, and the learning curve for new users are noteworthy limitations. Despite these challenges, Modelica/Dymola remains a critical tool in the engineering simulation landscape, driving innovation and efficiency in the design and analysis of complex systems. For this project, the key advantages of Modelica/Dymola include the 3D vehicle model representation, 3D road files, and physical components connections which can produce more accurate simulation results. Similar to Matlab/Simulink, the main shortage of Modelica/Dymola is the difficulty and time consuming of the model establishment due to the large number of physical/signal components connections. The most significant limitation includes the cost of purchasing Dymola software and the lack of availability of the economic model for the cost benefit analysis.

3.2.3. Simulation Tool Selection

Through the evaluations of the five simulation tools in the field of low-carbon and hybrid powertrain vehicles, each tool presents a trade-off between accuracy, complexity, and simulation scope. MATLAB/Simulink is highly versatile and accurate but requires substantial expertise and can result in longer simulation times for complex models. ADVISOR offers a balance between user-friendliness and focused simulation capabilities for hybrid and electric vehicles, making it less daunting for new users. AVL CRUISE excels in detailed drivetrain and engine modelling, providing high accuracy at the cost of increased complexity and simulation time. FASTSim, on the one hand, offers the most efficient modelling and simulation process since it is based on Microsoft Excel or Python through mathematical equations, on the other hand, it has the relevant lower accuracy compared to other tools as well as lack of availability for control system and economic models. Modelica/Dymola stands out for its ability to simulate complex, multi-domain systems accurately, though it demands a high level of expertise to navigate its complexity. The choice of simulation tool depends on the specific needs of the project, including the required level of detail, the specific vehicle technologies being modelled, and the expertise of the user. For applications requiring detailed control strategy development or extensive economic analysis, MATLAB/Simulink or Modelica/Dymola might be preferred. In contrast, for projects focusing on vehicle performance and energy consumption with less emphasis on the underlying economic

models, ADVISOR or AVL CRUISE could offer a more straightforward approach. Ultimately, the selection of a simulation tool for this project must consider the balance between model fidelity, computational efficiency, and the capacity to integrate various aspects of vehicle design, control, and economic analysis. The overall comparison of the tools can be summarised as follows:

1) MATLAB/Simulink

- **Accuracy**: High level of accuracy, with extensive libraries and toolboxes that can be used to model complex systems and control strategies accurately.
- **Complexity**: Flexible complexity due to the depth of detail in models, requiring significant expertise to use effectively.
- **Cost and efficiency**: No additional funds are required (License available from Coventry University). Efficiency varies, detailed physical models can lead to longer simulation times.
- **Duty cycle availability**: Limited direct support for 3D duty cycles but can simulate complex vehicle dynamics and control systems.
- **Control system availability**: Strong capabilities in simulating control logic through Simulink.
- **Economic models integration**: Possible through custom development, but not a primary focus of the tool.

2) ADVISOR (Advanced Vehicle Simulator)

- **Accuracy**: Designed specifically for hybrid and electric vehicles, offering reasonable accuracy for vehicle energy consumption and performance.
- **Complexity**: User-friendly interface designed for vehicle simulation, less complex than MATLAB/Simulink.
- **Cost and efficiency**: No additional funds are required (License available from Coventry University). Simulation speed is generally faster due to a more focused scope on vehicle dynamics and energy models.
- **Duty cycle availability**: Does not support 3D duty cycles directly.
- **Control system availability**: Allows for the inclusion of control strategies, though not as extensively as MATLAB/Simulink.

- **Economic models integration**: Limited capabilities for direct economic analysis.

3) AVL CRUISE

- **Accuracy**: High accuracy, especially for driveline components and engine modelling.
- **Complexity**: Complex, aimed at professionals with detailed modelling of powertrain systems.
- **Cost and efficiency**: No additional funds are required (License available from Coventry University). Modelling and simulation time can be lengthy due to the high fidelity of the models.
- **Duty cycle availability**: Supports 3D road profiles and can simulate real-world driving conditions effectively.
- **Control system availability**: Capable of integrating control logic within the simulation environment.
- **Economic models integration**: Primarily focused on physical modelling, with less emphasis on economic analysis.

4) Modelica/Dymola

- **Accuracy**: Highly accurate, with a wide range of domains covered, making it suitable for complex system simulations.
- **Complexity**: High complexity, offering a versatile environment for modelling but requiring in-depth knowledge.
- **Cost and efficiency**: Modelica is open-source with limited functions, Dymola requires additional funds for License (about £5000). Efficiency depends on model detail; complex models can lead to longer simulation times.
- **Duty cycle availability**: Supports 3D models and multi-domain simulations, including vehicle dynamics.
- **Control system availability**: Strong support for control logic through a component-oriented modelling approach.
- **Economic models integration**: Can only incorporate economic models through extensions and custom libraries.

5) FASTSim

- **Accuracy**: Relatively lower accuracy compared with other tools.
- **Complexity**: Low complexity, offering a simple environment for modelling and requiring only general knowledge.
- **Simulation time and efficiency**: No additional funds are required (License available from Coventry University). Short simulation time but this will lead to a lower accuracy and comprehension of modelling.
- **Duty cycle availability**: Supports 2D models.
- **Control system availability**: Lack of support for scientific control logic through a component-oriented modelling approach.
- **Economic models integration**: Can only incorporate economic models through extensions and custom libraries.

To build a comprehensive and quantitative evaluation and comparison of different simulation tools, the following key functional requirements and costs (time and fund) factors will be scored from 0 (worst) to 5 (best).The scoring result of the above five simulation tools is presented in Table 3-1 Simulation tool evaluation scores.

Table 3-1 Simulation tool evaluation scores

	FASTSim	AVL CRUISE	ADVISOR	Matlab/ Simulink	Modelica/ Dymola
Accuracy	3	4	4	5	5
Complexity	5	5	5	5	4
Cost and Efficiency	5	5	5	5	2
Duty Cycle Availability	3	5	5	4	5
Control System Availability	1	4	4	5	4
Economic Models Integration	3	1	3	5	1
Total Score	20	24	26	*29*	21

Based on the comparisons of the five simulation tools above, with the consideration of the balance in different requirements of this project. The MATLAB/Simulink achieved the highest total score of 29, thus it is selected in this project to develop a simulation model for this novel powertrain concept of DHFCRE + Eco-BEV, which contains all the vehicle components from the powertrain to the vehicle dynamics (aerodynamic and rolling resistance, etc.), including multiple energy sources (battery and FC). Also, the simulation model will focus on the development of the EMS by using scientific control

algorithms to optimise the performance of this DHFCRE. This model will generate the simulation results of the KPI outputs to evaluate the performance of this DHFCRE and different control algorithms under different driving scenarios as well as generate economic calculations based on the technical simulations by inputting relevant economic parameters to undertake a Cost-Benefit Analysis (CBA) to quantify the cost and benefit of this proposed concept.

3.3. BEV Modelling

Through the literature review and discussion based on the aims and objectives of this project, the simulation model for evaluating the performance of the proposed DHFCRE + Eco-BEV powertrain concept and the EMS control strategies will be established on the Matlab/Simulink platform. Matlab/Simulink has a powerful modelling capability with a large number of library blocks and subsystems for the HEV, BEV and FCEV applications, with various levels of model complexity for different demands and scenarios. It also provides customised mathematical functions for the calculations apart from physical models such as fuel economy calculations with adaptive inputs of fluctuating prices and enables the cost-benefit equations directly linked to the technical simulation results. The simulation system modelling process of the proposed BEV model is undertaken on the Matlab/Simulink platform. A standardised BEV model based on Matlab/Simulink generally includes several key subsystems (MathWorks, 2019; Apicella, 2019; Ren, 2021):

- Drive cycle input model
- Environmental parameters input model
- Representative driver model
- Vehicle dynamics subsystem
- Vehicle electric powertrain subsystem
- Vehicle Control Unit (VCU) subsystem
- Simulation result output channel

The workflow logic of the subsystems and channels in the BEV model is shown in Figure 3-7 and the layout of the Simulink model is shown in the Figure 3-8.

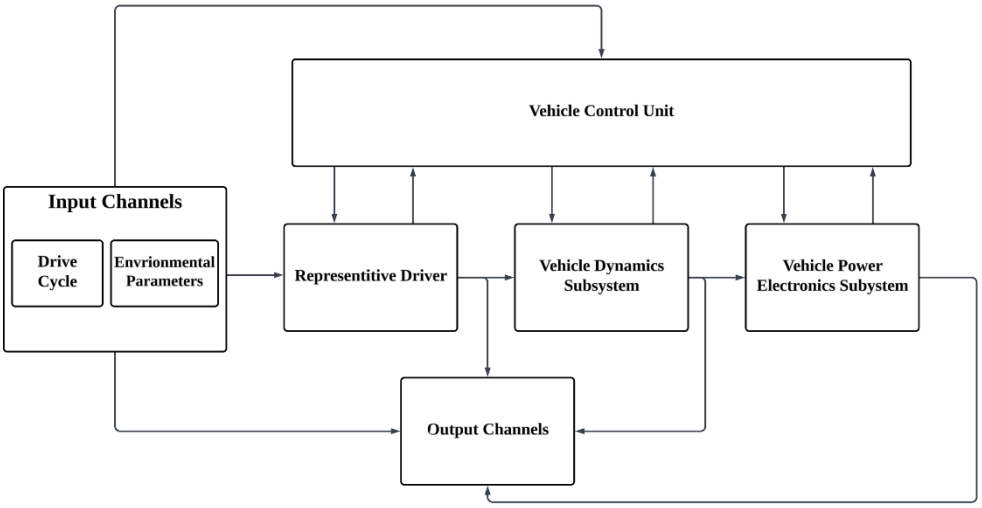

Figure 3-7 BEV model workflow logic diagram

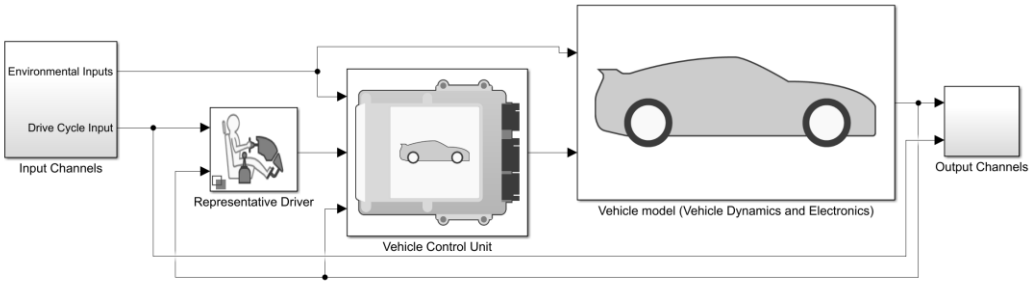

Figure 3-8 BEV model overview (MathWorks, 2019)

Starting from the input channels subsystem including the drive cycle model and environmental parameters, it provides the primary signals to the whole model including vehicle speeds under different simulation time and environmental parameters to the representative drive model, the VCU subsystem and as the reference speed for the output channel. Then, the representative driver model will transfer the reference speed signal to the acceleration/deceleration signals to the vehicle dynamics subsystem and vehicle control unit. The calculations in the vehicle dynamics subsystem will transfer the received acceleration and deceleration signals to the required power and send it to the VCU and electric powertrain subsystem to calculate the required power from batteries. Finally, all the output signals will be sent to the output channels and will be presented as either curve plots or numbers through a set of calculations. In the following sections, the detailed theories and equations of each model and subsystem will be presented and discussed.

3.3.1. Input Channels Subsystem

The input channels subsystem contains two models, the drive cycle model and environmental parameters model which provide the primary information for the whole system.

3.3.1.1. Drive Cycle Input Model

The drive cycles (also known as driving cycles, duty cycles or test cycles) are standardised routes or series of conditions under which a vehicle is operated for the purpose of assessing its performance, emissions, fuel consumption, and other parameters. The cycles are meticulously designed to simulate a variety of driving conditions, ranging from urban stop-and-go traffic to highway driving, in order to provide a comprehensive evaluation of a vehicle's behaviour under different environments (Transport Policy, 2022; EPA.GOV, 2022).

On the Matlab/Simulink platform, a standardised block is available in the library which has a set of installed popular drive cycle resources such as NEDC, FPT72/75, Japanese 10-15, etc (MathWorks, 2019). It can also accept user's customised duty cycle inputs through text or CSV files, Figure 3-9 shows the custom drive cycle plot from this block.

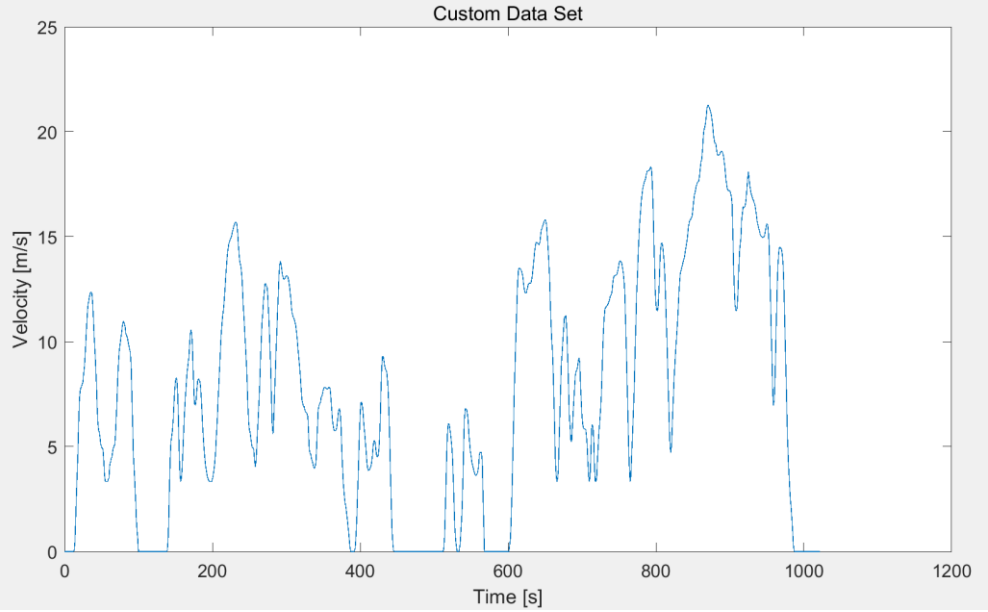

Figure 3-9 Simulink drive cycle plot

3.3.1.2. Environmental Parameters Input Model

The second model in the input subsystem is the environmental parameters model as shown in Figure 3-10.

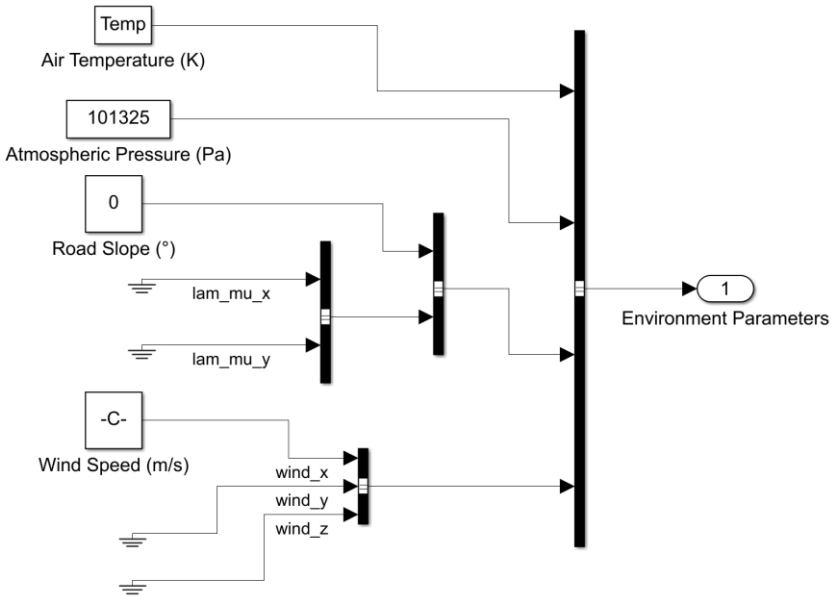

Figure 3-10 Environmental parameters model

The environmental parameters input model includes 4 parameters: the air temperature, the atmospheric pressure, the road slope and the wind speed in the x-axis (the same direction as the vehicle movements). These output parameters will be used in the VCU subsystem and vehicle dynamics subsystems for the calculations of the aerodynamic and rolling resistance of the vehicle under certain drive conditions.

3.3.2. Representative Driver Model

The second subsystem is the representative driver model (Figure 3-11).

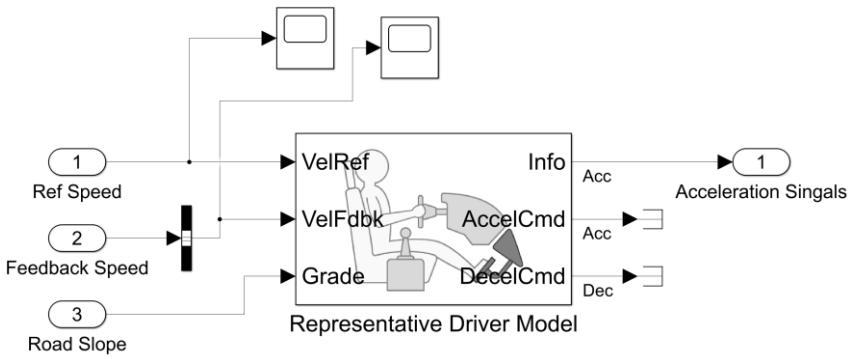

Figure 3-11 Representative driver model

The main part of the representative driver model is the Longitudinal Driver block, it functions as a longitudinal speed-tracking controller. Utilising both reference and feedback vehicle speeds, this block outputs normalised acceleration and braking signals, which range from 0 to 1 (MathWorks, 2019).

3.3.3. VCU Subsystem

The VCU subsystem is one of the most important models in the BEV model since it controls all the components of the vehicles including the vehicle dynamics system, and the electric powertrain components. The structure of this BEV VCU model refers to the EV Reference Application structure of the Powertrain Blockset toolbox on the Matlab platform (MathWorks, 2021) and Coventry University Microcab BEV structure (Microcab, 2017; Apicella, 2019), the overview structure of the VCU system is shown in Figure 3-12.

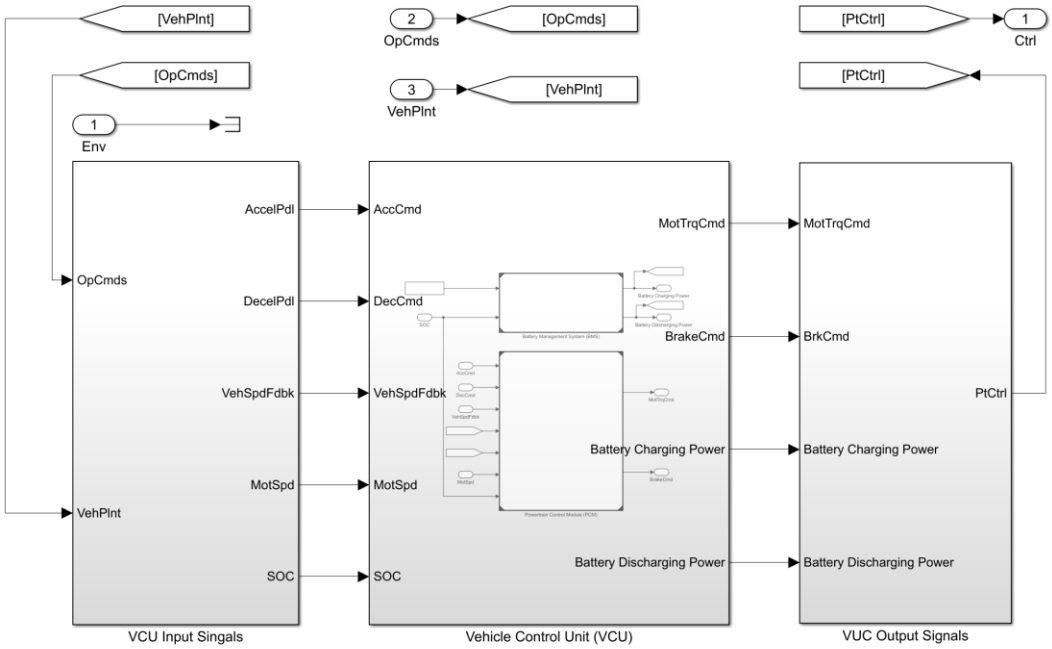

Figure 3-12 VCU subsystem structure overview

The input signals of the VCU subsystem include acceleration/deceleration commands, battery SoC, vehicle actual speed (feedback from the vehicle dynamics subsystem) and motor speed (feedback signal from the vehicle electric powertrain subsystem). Through the calculations of the VCU, the output signals are the required torque from the electric motor, the battery charging/discharging power signals and the braking command signal. To process these conversions and calculations, the VCU system has

been divided into three modules, the battery management module, the motor torque conversion module and the regenerative braking module.

3.3.3.1. BMS Module

Battery Management System (BMS) is an important subsystem in BEVs to oversee and regulate the operation of batteries, particularly in applications where battery performance, longevity, and safety are of paramount importance. It is crucial for managing rechargeable batteries, ensuring optimal performance, extending their lifespan, and preventing situations that could lead to battery damage or failure. BMS are extensively used in various sectors, including Electric Vehicles (EVs), renewable energy storage, portable electronic devices, and more (Xiong & Shen, 2018). The BMS system in this model (Figure 3-13) is developed as a simplified functional BMS referring to the Coventry University Microcab BEV version (Microcab, 2017) and sample models from Matlab official examples (MathWorks, 2019).

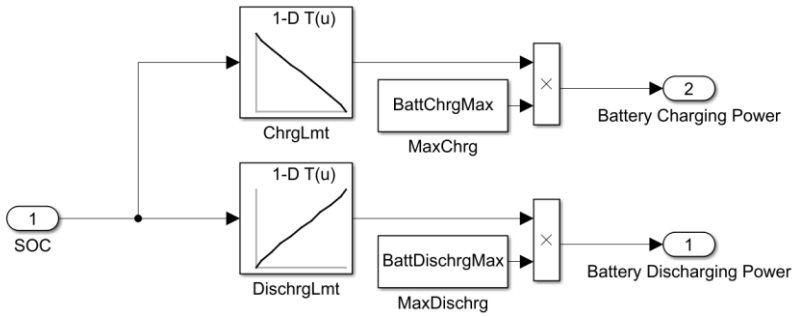

Figure 3-13 Simplified BMS system

The input signal of this BMS is the battery State of Charge (SoC), and the output signals are the battery charging/discharging powers. The main function of this BMS is to regulate charging/discharging powers values of the battery pack within the battery charging/discharging limit powers based on the battery SoC signal and transmit them to the power electronic systems. The higher SoC is, the charging power for the battery is lower and the discharging power is higher. It used 2-D look-up-table functions in the Simulink library, the table values can be modified to adapt to different battery and motor sizes (MathWorks, 2019).

3.3.3.2. Motor Torque Conversion Module

The second module in the VCU is the motor torque conversion module, it has the main function of converting the acceleration signals into motor torque signals for the power electronic subsystem. The input signals of this module are the acceleration signal and the motor speed signal (feedback signal from the electric powertrain subsystem).

The first step is to transfer the acceleration signal to the motor torque signal by using mathematical blocks shown in Figure 3-14 to realise the conversion.

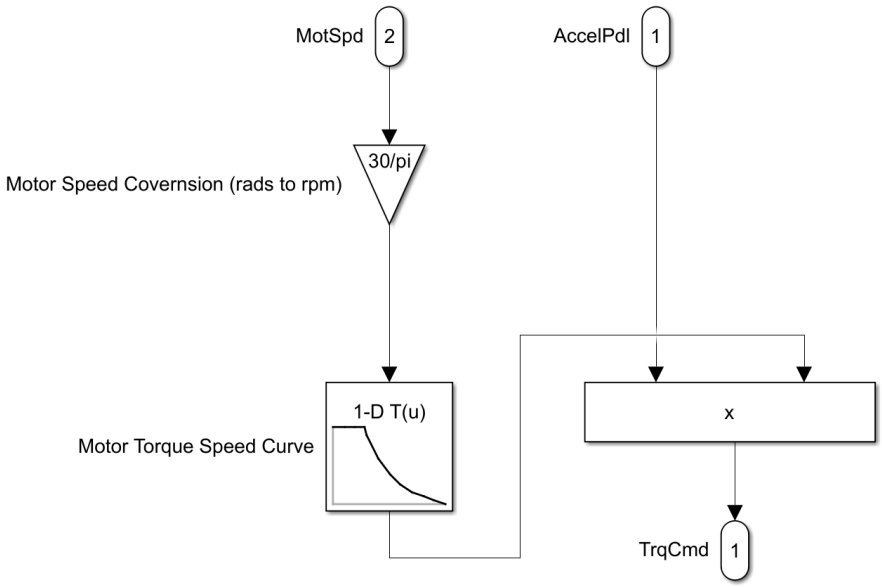

Figure 3-14 Singal conversion calculation – Acceleration to motor torque

The equation used in this conversion is shown in 3-1

$$T_{Cmd} = f_{MMTSC}(\frac{60\omega}{2\pi}) \cdot S_{Acc} \quad (3\text{-}1)$$

Where

T_{Cmd} is the output electric motor torque in (N·m).

$f_{MMTSC}( )$ is a 2-D look-up-table function that presents the Motor Max Torque Speed Curve of the electric motor, (the detailed table data and diagrams are presented in the Appendix 1.1).

ω is the motor speed feedback signal from the power electronic system in (rad/s).

S_{Acc} is the acceleration signal from the representative driver model in (%).

The 2nd step is to validate if the value of T_{Cmd} is within the limited torque, and also confirm the battery SoC is < 1 to avoid the overcharge. This process is shown in Figure 3-15.

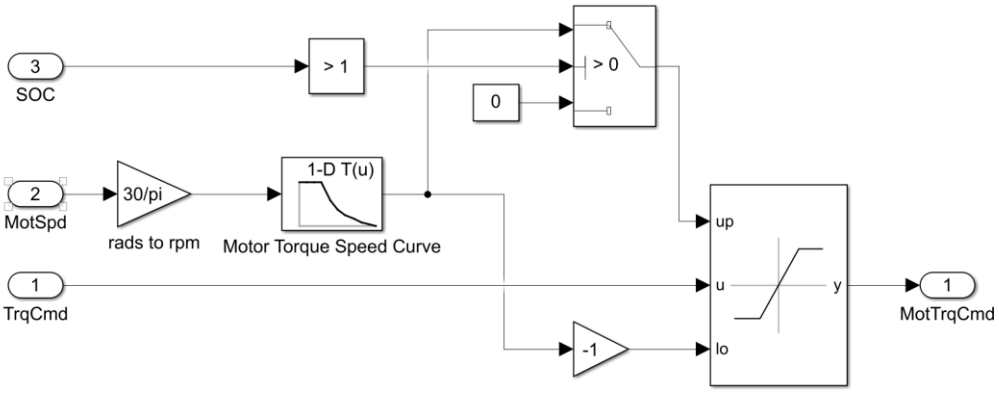

Figure 3-15 Torque command signal validation path

The input signals are battery SoC, motor torque from the first step and the motor speed (feedback from the electric powertrain subsystem), the output signal is the final motor torque. It first converts the motor speed to the referenced torque using 3-1. Then checks if the input T_{Cmd} is within the given limit, if it is within the specified range, it passes through; otherwise, the output will be the limit values (the limit values are reference torque and -1 multiplying the reference torque). And if the SoC is ≥ 1, this means that if the battery is overcharged, then it will need to shut down the system and the output of motor torque will be 0.

3.3.3.3. Regenerative Braking Module

The regenerative braking system is a significant innovation in the automotive industry, particularly within the context of electric and hybrid electric vehicles. This system embodies the principle of energy conservation and efficiency by capturing the vehicle's kinetic energy during deceleration, which would otherwise be dissipated as heat through traditional braking methods and converting it into electrical energy. This electrical energy is then stored in the vehicle's battery, thus augmenting its range and improving overall energy efficiency. The functionality of the regenerative braking system hinges on the dynamic conversion of the vehicle's kinetic energy into electrical energy. This process is facilitated through the use of the electric motor as a generator during the braking phase. When the driver applies the brake, instead of utilizing conventional friction brakes to slow the vehicle, the system reverses the motor's operation, thereby generating electricity. This electricity is subsequently directed to the battery for storage and future use (Islameka et al., 2023).

The third module in the VCU subsystem is the regenerative braking module (Figure 3-16), the structure of this module is based on the sample application published by

Simulink officials and the BEV version of Coventry University Microcab (MathWorks, 2019; Ren, 2021; Apicella, 2019).

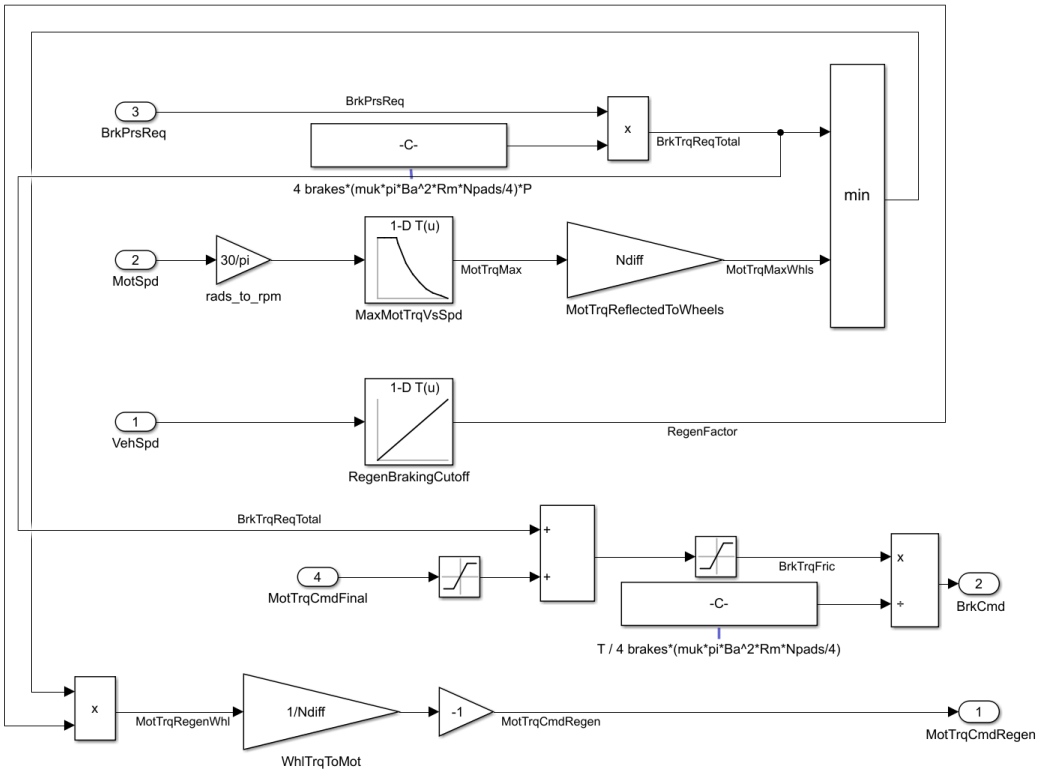

Figure 3-16 Regenerative braking module

The input signals of this module include the vehicle speed signal (feedback signal from the vehicle dynamics subsystem), the motor speed signal (feedback signal from the electric powertrain subsystem) and the brake pressure request signal calculated through 3-2 based on the deceleration signal from the representative driver model.

$$P_{Brkrq} = P_{brkMax} \cdot S_{dec} \quad (3\text{-}2)$$

Where

P_{Brkrq} is the brake pressure request in (Pa).

P_{brkMax} is the maximum braking pressure (a model input parameter) in (Pa).

S_{dec} is the deceleration signal in acceleration signal from the representative driver model in (%).

The output signals of this module are the regenerative torque in (N·m) and the final brake pressure command signal in (Pa). The calculation process of the regenerative torque output signal is shown in the following steps and equations:

- **Regenerative torque path**

$$T_{RG} = min\left\{\left[P_{Brkrq}\cdot\left(4\times\mu\times\pi\times {B_a}^2\times R_m\times\frac{N_{pads}}{4}\right)\right], \left[f_{MMTSC}\left(\frac{60\omega}{2\pi}\right)\times N_{diff}\right]\right\}\times \frac{-f_{RGBCO}(v)}{N_{diff}}$$

(3-3)

- **Final brake pressure command path**

$$P_{BrkRG} = \frac{P_{Brkrq}\cdot\left(4\times\mu\times\pi\times {B_a}^2\times R_m\times\frac{N_{pads}}{4}\right) + T_{Cmd}}{4\times\mu\times\pi\times {B_a}^2\times R_m\times\frac{N_{pads}}{4}}$$

(3-4)

Where

T_{RG} is the first target output signal – regenerative torque in (N·m).

P_{BrkRG} is the 2nd target output signal – final brake pressure command signal in (Pa).

P_{Brkrq} is the brake pressure request in (Pa), calculated from 3-2.

μ is the coefficient of friction for brake pads.

B_a is the effective radius of the brake disc in (m).

R_m is the mean radius at which the brake force is applied in (m), calculated by R_m = (outer radius of the brake pad + inner radius of the brake pad) / 2.

N_{pads} is the number of brake pads involved in braking.

$f_{MMTSC}()$ is a 2-D look-up-table function which presents the Motor Max Torque Speed Curve of the electric motor, the detailed diagrams are presented in the Appendix 1.

ω is the motor speed feedback signal from the power electronic system in (rad/s).

N_{diff} is the gear ratio of the differential in the vehicle power dynamics subsystem.

$f_{RGBCO}()$ is a look-up-table function which presents a regenerative braking cut-off curve.

v is the vehicle speed in (m/s)

T_{Cmd} is the electric motor torque in (N·m), (output from motor torque conversion module).

The fundamental function and logic of this module is to firstly calculate the regenerative torque based on brake pressure and parameters of disc brakes. Then, maximise the regenerative torque which comes from the motor to increase the energy recycling percentage. Finally, the input signal T_{Cmd} decides the amount of regenerative torque permitted, any request for braking torque that the motor cannot fulfil will be provided by the P_{BrkRG} final brake pressure command.

3.3.4. Vehicle Dynamics Subsystem

The fourth subsystem of this BEV model is the vehicle dynamics subsystem, as Figure 3-17 shows (MathWorks, 2019), the input signals of this system include the motor torque in (N·m), the brake pressure signal in (Pa) from the VCU subsystem, the road slope in (°) and wind speed in (m/s) signals from the environmental parameters. The output signals of this model are the feedback signals of the vehicle speed in (m/s) and the motor speed in (rad/s), these signals will be sent to the VCU, the electric powertrain and the simulation output subsystems.

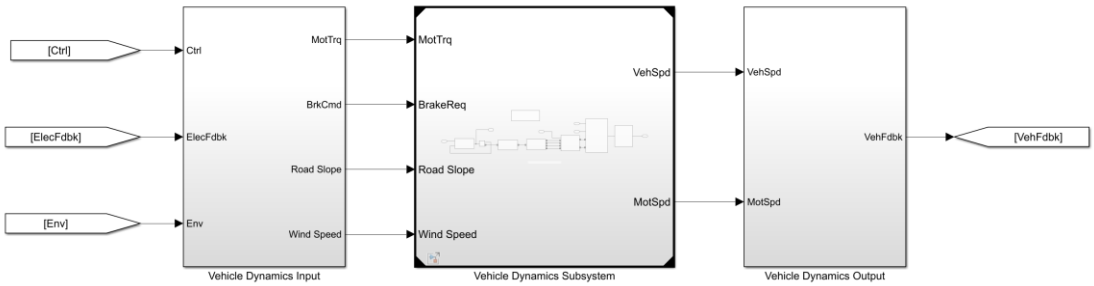

Figure 3-17 Vehicle dynamics subsystem overview

The main function of this subsystem is to calculate the actual speed of the vehicle and electric motor after the effects of various internal/external forces, resistances and energy losses, such as friction and heat loss from mechanical components including drive shafts, braking pads and differential; the aerodynamic resistance related to the vehicle aerodynamic parameters and external information. There are three main components in this subsystem connected by both signal and physical paths based on the Matlab/Simulink rules: the differential (with relevant drive shafts), wheels & brake and the vehicle body.

The first component is the differential and drive shafts shown in Figure 3-18. The main functions of this component are to calculate the motor speed reference signal for the VCU and electric powertrain subsystem as well as to transfer the signals from Simulink Analog signals to Simulink physical signals for the wheels & brakes and the vehicle body.

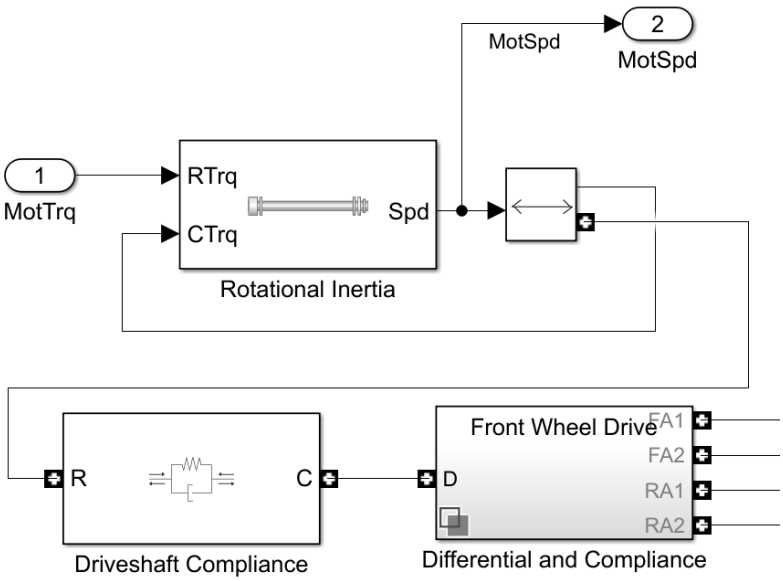

Figure 3-18 Differential and driveshaft components structure

The output signal of motor speed is calculated through the 3-5 (MathWorks, 2019).

$$\begin{cases} P_{TR} = P_{TC} + P_d + P_s \\ P_{TR} = T_R \cdot \omega \\ P_{TC} = T_C \cdot \omega \\ P_d = -b \cdot \omega^2 \\ P_s = \omega \cdot \frac{d\omega}{dt} \cdot J \end{cases} \quad (3\text{-}5)$$

Where:

P_{TR} is the mechanical power from the base shaft in (W).

P_{TC} is the mechanical power from the follower shaft in (W).

P_d is the damping power loss in (W).

P_s is the stored internal torsional energy in (W).

T_R is the input torque from the electric motor in (N·m).

T_C is the output torque in (N·m).

ω is the driveshaft angular velocity in (rad/s).

b is the rotational viscous damping in (N·m·rad), using Matlab/Simulink default value 0.001.

J is the rotational inertia in (kg·m^2), using Matlab/Simulink default value 0.1.

The 2nd component is the wheels & brakes shown in Figure 3-19 using the Matlab/Simulink library block Longitudinal Wheel (MathWorks, 2019).

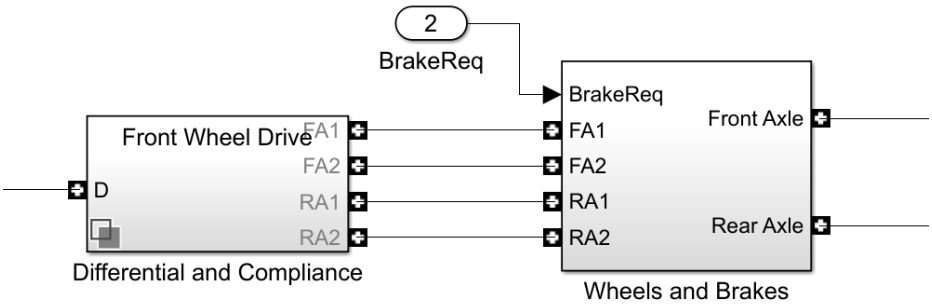

Figure 3-19 Wheels & brakes model

The main function of this model is to calculate the braking forces on the front and rear axle based on the input signal of brake pressure, through the (3-6.

$$T_{brk} = \begin{cases} \dfrac{\mu \times P_{BrkRG} \times \pi \times {B_a}^2 \times (R_o + R_i) \times N_{pads}}{8} & when\, v \neq 0 \\ \dfrac{\mu_{static} \times \pi \times {B_a}^2 \times (R_o + R_i) \times N_{pads}}{8} & when\, v = 0 \end{cases}$$

(3-6)

Where

T_{brk} is the brake torque in (N·m).

μ is the disc pad-rotor coefficient of kinetic friction.

P_{BrkRG} is the brake pressure command signal in (Pa).

B_a is the effective radius of the brake disc in (m).

R_o is the outer radius of the brake pad in (m).

R_i is the inner radius of the brake pad in (m).

N_{pads} is the number of brake pads in disc brake assembly.

μ_{static} is the disc pad-rotor coefficient of static friction.

v is the vehicle speed in (m/s).

The last component is the vehicle body model based on the simplified Three-Degree of Freedom (3-DOF) Longitudinal Vehicle Body library block (shown in Figure 3-20), it did not account for the longitudinal suspension forces on the front and rear axles to

reduce the complexity of the vehicle suspension system which is not the key consideration for this project and increased simulation speed (MathWorks, 2019). The input signals are physical signals from the wheels & brakes model of forces on 2 axles and the output signal is mainly the vehicle speed feedback signal in (m/s).

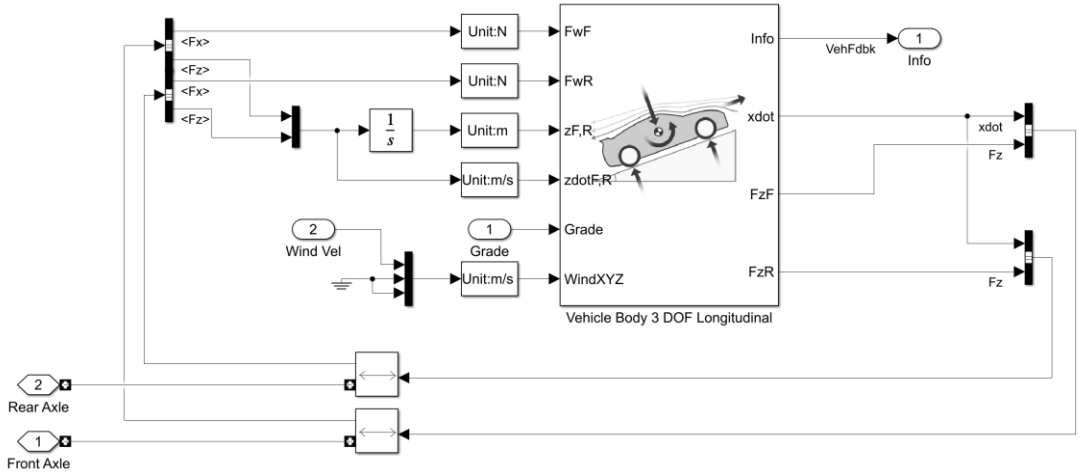

Figure 3-20 Vehicle body model structure

The main function of the vehicle body model is to calculate the vehicle's actual speed after resistance forces deductions through 3-7.

$$\begin{cases} F_x = F_{wf} + F_{wr} - F_d - F_g \\ F_d = \frac{1}{2} \times C_d \times A_f \times \frac{P_{abs}}{T_a R_a} \cdot (v - v_{Wx})^2 \\ v = \omega_w \times (r_w + r_{t-loaded}) \\ F_g = M \cdot g \cdot \sin\theta \end{cases} \quad (3\text{-}7)$$

Where

F_x is the longitudinal force of the vehicle in the vehicle fixed in (N).

F_{wf} is the longitudinal traction force of the front axle in (N).

F_{wr} is the longitudinal traction force of the rear axle in (N).

F_d is the aerodynamic resistance in the vehicle fixed x-axis in (N).

C_d is the aerodynamic coefficient of the vehicle.

A_f is the frontal area of the vehicle in (m^2).

P_{abs} is the environmental absolute air pressure in (Pa).

T_a is the environmental air temperature in (K).

R_a is the atmospheric specific gas constant of the air in [J/(kg·K)].

v is the vehicle speed in (m/s).

v_{Wx} is the wind speed in the vehicle fixed x-axis in (m/s).

ω_w is the wheel angular speed in (rad/s).

r_w is the wheel radius in (m).

$r_{t-loaded}$ is the loaded radius of the tyre in (m).

F_g is the longitudinal gravitational force on the vehicle along the vehicle-fixed x-axis in (N).

M is the vehicle's total mass in (kg).

g is the gravity acceleration constant in (m/s^2).

θ is the angle of the road slope in (°).

The output motor speed signal is sent to the VCU and the electric powertrain subsystems, and the vehicle feedback speed signal is sent to the VCU and the simulation result subsystems.

3.3.5. Vehicle Electric Powertrain Subsystem

The vehicle's electric powertrain subsystem (Figure 3-21) represents the energy and power source of this BEV model which includes two main components – an electric motor model and a battery pack model both based on the blocks from Matlab/Simulink library (MathWorks, 2019).

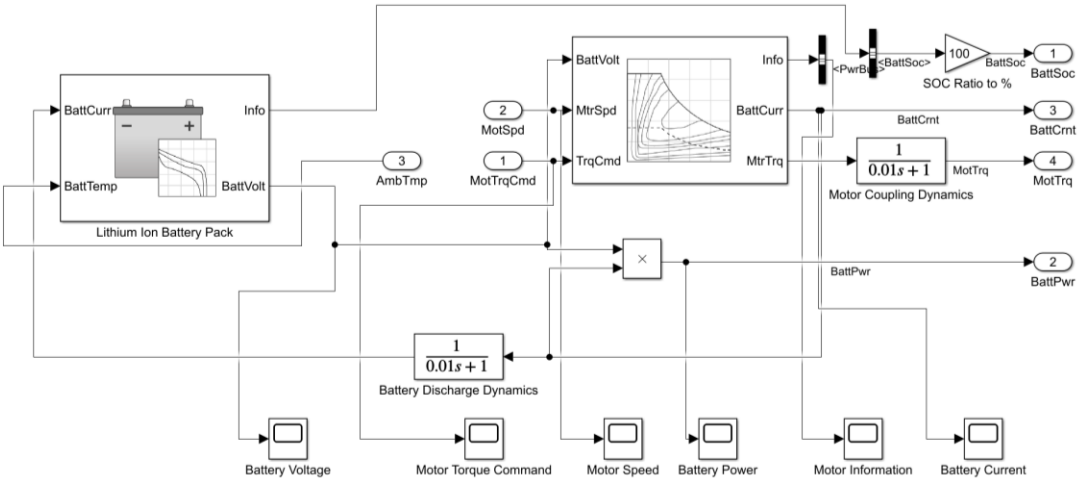

Figure 3-21 Vehicle electric powertrain subsystem

The input signals of this subsystem are the required motor torque and speed from the VCU the vehicle dynamics subsystems and the environment temperature from the

environmental parameters model. The output signals from this subsystem include the battery SoC, the battery power in (W), the battery current in (A) and the actual motor torque in (N·m). The main function of this subsystem is to calculate the actual motor torque, the required battery current and power, as well as the feedback signal of the battery SoC for the VCU subsystem.

- **Electric motor model**

There are various different electric motor models available in the Matlab/Simulink library, such as physical models in Matlab/Simscape Toolbox including DC brushed motors, stepper motors, brushless motors, etc. These physical models can provide a higher accuracy of the motor simulation results but will also require a more complex model and increase the simulation time. There are also some mathematical formulas and look-up-table function-based simplified motor models in the Powertrain Blockset Toolbox including mapped motor, induction motor, surface mount PMSM motor, etc (MathWorks, 2019). According to the discussions in the simulation tool selection, due to this project requires a relevant high simulation speed, thus, the mapped motor model (right side of Figure 3-21) which mainly uses the look-up-table function is selected. The simulation accuracy can be ensured as long as the input table data is accurate enough (such as based on the official data from the motor manufacturer), at the same time increasing the simulation speed.

The "Mapped Motor" model within the MATLAB library is a computational framework designed to simulate the dynamics of a motor and its associated drive electronics in a torque-control mode. Functionally, the Mapped Motor model serves to replicate the motor's performance by utilizing empirical data which maps the relationships between key operational parameters such as battery voltage, motor torque, and motor speed. This data-driven approach enables the simulation of motor behaviour under various loading conditions and control inputs, making it an invaluable tool in the design and analysis of electric vehicle propulsion systems. The working principle of the Mapped Motor model is fundamentally based on the use of lookup tables or multidimensional maps that contain pre-calculated values of motor torque and speed for given inputs of battery voltage (BattVolt) and torque commands (TrqCmd). These maps are generated from experimental data or from detailed motor simulations that consider the physical and electrical properties of the motor (MathWorks, 2019). There are two input databased diagrams used in the look-up-table functions in this model – the 2D max torque-speed curve and the 3D motor efficiency map (these table data, plots and surface maps are presented in the Appendix 1.1). Through these look-up-table

functions, the output signal of actual motor torque can be calculated by deducing all energy losses and the required battery current can be calculated through 3-8.

$I_{Batt} = \frac{P_M + P_L}{V_{Batt}}$ (3-8)

Where

I_{Batt} is the required battery current in (A).

P_M is the mechanical power generated by the motor in (W).

P_L is the power loss in the motor in (W).

V_{Batt} is the battery voltage in (V).

- **Battery pack model**

There are a number of battery models available in the Matlab/Simulink and Simscape Toolbox, such as physical models including the Simscape physical battery model while others are mathematical data-based models such as datasheet battery model and equivalent circuit battery model (MathWorks, 2019). Similar to the electric motor model selection, to ensure the simulation speed, the datasheet battery model is selected (shown on the left side of Figure 3-21).

The Datasheet Battery block in MATLAB/Simulink provides an efficient and accurate means to simulate the performance of various types of batteries, such as Lithium-ion, Lithium-polymer, and lead-acid, using manufacturer data. This block is essential for predicting battery behaviour under different operating conditions, which is vital for the design and implementation of battery management systems. It facilitates simulations by leveraging empirical data and utilises lookup tables that correlate the SoC and temperature with the battery's open-circuit voltage and internal resistance which are the key parameters to define the battery's state and efficiency (MathWorks, 2019).

The input signals of this battery model are the required battery current and the air temperature from the environmental inputs and the output signals are battery voltage and SoC which are calculated through the following steps:

The first step is to calculate the battery open-circuit voltage (V_O) of the battery by utilising the look-up-table function for the open-circuit voltage and internal resistance (R_i) of the batteries and this is influenced by the SoC and the temperature of the battery, thereby providing a detailed depiction of the battery’s efficiency across a spectrum of operational scenarios.

The second step is to calculate the SoC, battery module voltage, battery pack SoC, energy consumption, max charging and discharging power of the battery pack through 3-9.

$$\begin{cases} V_T = V_O + I_{Batt} \cdot R_i \\ I_{batt} = \frac{I_{in}}{N_p} \\ V_{out} = N_s \cdot V_T \\ SoC = \frac{1}{C_{batt}} \int_0^t I_{Batt} dt \\ E_{Batt} = V_{out} \cdot \int_0^t I_{Batt} dt \\ P_{charmax} = C_{batt} \cdot C_{char} \cdot V_{nom} \\ P_{discharmax} = C_{batt} \cdot C_{dischar} \cdot V_{nom} \end{cases} \quad (3\text{-}9)$$

Where

V_T is the voltage per battery module in (V).

V_O is the battery open-circuit voltage in (V).

I_{batt} is the current of each battery module in (A).

R_i is the internal resistance of per battery module in (Ω).

I_{in} is the combined current flowing from the battery network in (A).

N_p is the number of battery cells in parallel.

V_{out} is the combined voltage of the battery network in (V).

N_s is the number of cells in series.

SoC is the battery State of Charge.

C_{batt} is the battery's maximum capacity in (Ah).

t is the simulation sample time in (h).

E_{Batt} is the energy consumption of each battery module in (Ah).

$P_{charmax}$ is the max charge power of the battery pack in (W).

C_{char} is the charge C-rate of the battery.

V_{nom} is the nominal voltage of the battery pack in (V).

$P_{discharmax}$ is the maximum discharge power of the battery pack in (W).

$C_{dischar}$ is the discharge C-rate of the battery.

3.3.6. Simulation Result Output Channel

The last subsystem of this BEV model is the simulation result output channel (Figure 3-22) which generates and presents the simulation results of the main monitored output factors.

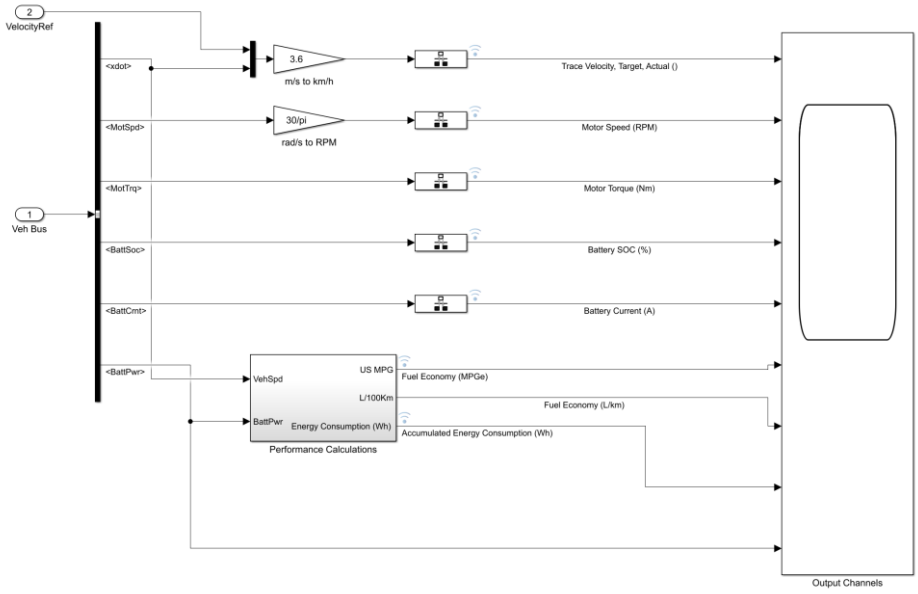

Figure 3-22 Simulation result output channel structure

The monitored output factors of this BEV model include the vehicle speed in (m/s and km/h), the motor speed in (rad/s and RPM), the motor torque in (N·m), the battery SoC in (%), the battery current in (A), the vehicle fuel economy in (MPGe and L/100km) the accumulated energy consumption in Wh and the battery power in (W).

3.4. FC Range Extender System Modelling

According to the discussions in Section 1.3, the purpose of this DHFCRE is to extend the range for BEVs at the same time increasing the vehicle functionality and efficiency. Through the literature review of the current FCEV technology, as one of the core energy supply devices, the PEMFC is the most appropriate type of FC used in automotive applications. In this project, the proposed DHFCRE was developed based on a PEMFC system with relevant subsystems. The range extender was expected to be demountable which allows the user to install and return the whole system of this range extender. Thus, the physical connection methods of this FCRE were proposed by three styles, the trailer style which is based on a small trailer connected in the rear of the vehicle (EP Tender, 2019), the roof-rack style which is located on the roof rack of the vehicle like the roof language box and the boot style which is stored in the boot

storage. In this project, the main research question is to evaluate and optimise the performance of this proposed powertrain concept of “DHFCRE + Eco-BEV”, therefore, the simulation modelling of the FCRE used the boot style connection method which minimised the influence from the confounding variables such as the errors from the extra rolling resistance on the wheels & axle of the trailer style connection method and the aerodynamic resistance due to changes on the vehicle frontal area and aerodynamic coefficient of the roof-rack style connection method, detailed discussions about the future works for the physical connection methods are presented in Section 8.2. The boot style connection method only changed parameters of the vehicle mass and the centre of mass bias which are easily parameterised in the vehicle dynamics subsystem. This could increase the accuracy of the simulation as well as increase the simulation speed, the simulation and experimental tests of the effects due to different connection methods can be done in future works which focus on the industrial and user-friendly levels of considerations.

3.4.1. PEMFC System Chemical and Physical Principles

The PEMFC is regarded as a cornerstone of modern clean energy technology, leveraging the electrochemical potential of hydrogen to generate electricity (Ren, 2019; (Li et al., 2019). The intricate processes within PEMFCs encompass multifaceted electrochemical reactions (shown in Figure 3-23) that are influenced by polarization effects, internal resistances, and reactant consumption rates.

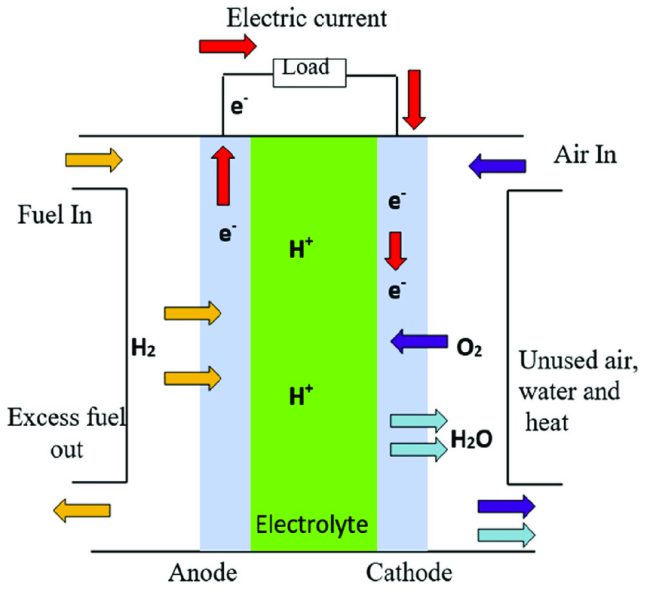

Figure 3-23 PEMFC working principle overview (Li et al., 2019)

A PEMFC power supply system is constituted by several components including the Membrane Electrode Assembly (MEA), catalyst layers, Gas Diffusion Layers (GDLs), flow plates, end plates, cooling systems and humidifiers (Li et al., 2019). In an FCEV, the PEMFC system is the core energy source which provides electricity for both the vehicle dynamic system and the battery pack to move the vehicle (Du et al., 2022), the physical structure of the FCEV is shown in Figure 3-24.

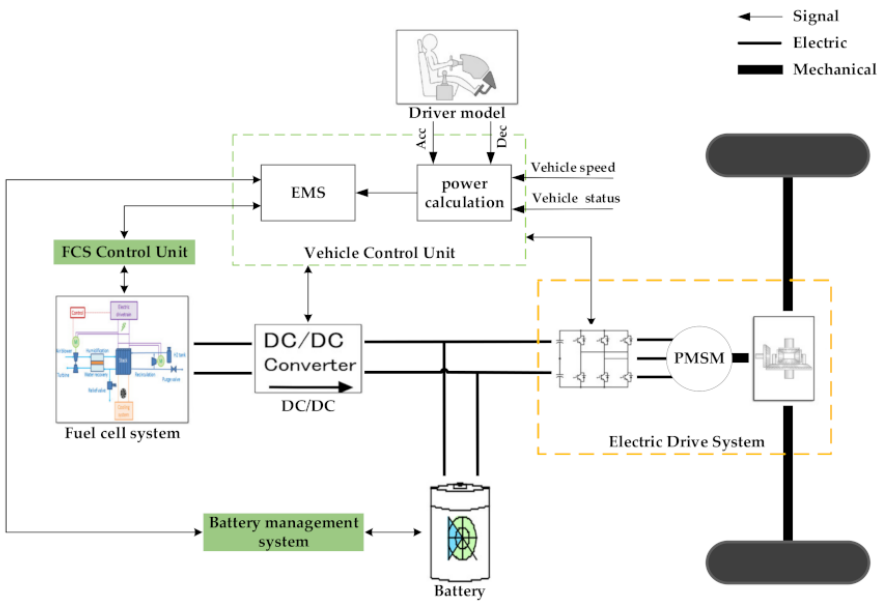

Figure 3-24 FCEV model structure overview (Du et al., 2022)

The PEMFC operates on the principle of electrochemical conversion of hydrogen fuel and oxygen from the air into electricity, heat, and water. At the heart of its operation lies the MEA, which facilitates the electrochemical reactions. The anodic reaction splits hydrogen molecules into protons and electrons, while the cathodic reaction combines these protons with oxygen and electrons to form water. The chemical reactions of the PEMFC are shown in the following equations (Ballard, 2014).

Anode reaction:

$$\mathrm{H_2} \xrightarrow{Catalyst} 2\mathrm{H^+} + 2e^- \quad (3\text{-}10)$$

Cathode reaction:

$$2\mathrm{H^+} + 2e^- + \frac{1}{2}\mathrm{O_2} \xrightarrow{Catalyst} \mathrm{H_2O} + \mathrm{Heat} \quad (3\text{-}11)$$

Overall reaction:

$$\mathrm{H_2} + \frac{1}{2}\mathrm{O_2} \xrightarrow{Catalyst} \mathrm{H_2O} + \mathrm{Heat} + \mathrm{Electricity} \quad (3\text{-}12)$$

3.4.2. FC Range Extender System Mathematical Model

In the real world, the PEMFC system is a device using chemical reactions to generate electricity with hydrogen and oxygen gas. In the simulation modelling based on the Matlab/Simulink platform, the chemical and physical reactions need to be transferred into mathematical formulas. As Figure 3-24 presents, in the FCEV model, the PEMFC stack is connected with a DC-DC converter and then connected to the vehicle's electric bus with the battery pack and electric motor. Similarly, for the proposed DHFCRE, the PEMFC will also be connected with the DC-DC converter, battery pack and electric motor as Figure 3-25 shows.

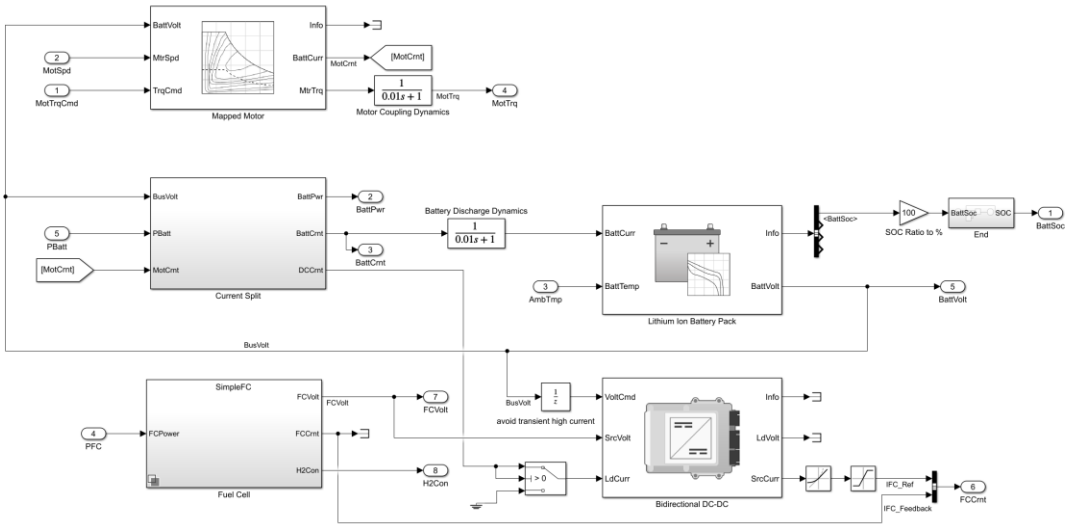

Figure 3-25 FC-Battery-powered electric vehicle powertrain model

The most important input and output signals of the DHFCRE subsystem include: the required FC power and FC stack characteristics as input signals, the FC stack output current, voltage and hydrogen gas consumption are output signals, these outputs can be calculated by the following equations.

$$V_{FC-out} = (E_r - V_{act} - V_{ohmic} - V_{con}) \times N_c \quad (3\text{-}13)$$

Where

V_{FC-out} is the output voltage of the FC stack in (V).

E_r is the reversible output voltage of the fuel cell in (V).

V_{act} is the activation loss voltage of the fuel cell in (V).

V_{ohmic} is the ohmic loss voltage of the fuel cell in (V).

V_{con} is the concentration loss voltage of the fuel cell in (V).

N_c is the number of cells in the FC stack.

Reversible output voltage (E_r), also known as the thermodynamic voltage, is the maximum potential difference between the anode and cathode under ideal conditions (no current flow, 100% efficiency). It is determined by the Gibbs free energy change of the electrochemical reaction. For a hydrogen fuel cell operating at standard conditions (25 ℃, 1 atm), the reversible voltage can be calculated using the following equation (Ballard, 2014):

$$E_r = -\frac{\Delta G_0}{n \times F} = \frac{-273.3\left(\frac{kJ}{mol}\right)}{2\,(mol) \times 96485\left(\frac{C}{mol}\right)} = 1.229\,(V) \quad (3\text{-}14)$$

Where

G_0 is the Gibbs free energy for the reaction at standard conditions in (kJ/mol).

n is the number of moles of electrons transferred in the reaction.

F is the Faraday Constant 96 485.3329 (C/mol).

The activation loss voltage (V_{act}), also known as activation polarization, occurs due to the kinetics of the electrochemical reactions at the electrodes. It is more significant at lower currents and can be estimated using the Butler-Volmer equation for the anode and cathode. However, a simplified expression in the linear region near the open-circuit voltage is widely used in FC system modelling (Li et al., 2019; Ren, 2019):

$$V_{\text{act}} = \frac{RT}{\alpha F} \ln\left(\frac{i}{i_0}\right) \quad (3\text{-}15)$$

Where

R is the universal gas constant, which is 8.314 J/(mol·K).

T is the absolute temperature in (K).

α is the charge transfer coefficient.

i is the current density in ($\mathrm{A/m^2}$).

i_0 is the exchange current density in ($\mathrm{A/m^2}$), indicative of the intrinsic rate of the electrochemical reaction.

The ohmic loss voltage (V_{ohmic}) also known as ohmic overpotential refers to the voltage loss within the fuel cell caused by the resistance within the electrolyte, electrodes, and the connectors of an electrochemical cell. This resistance hinders the flow of ions in the electrolyte and the transport of electrons in the electrodes, leading to the

dissipation of energy in the form of heat. Contact resistance between components, such as between the electrodes and current collectors, further exacerbates this loss. 3-16 (Li et al., 2019; Ren, 2019).

$$\begin{cases} V_{ohmic} = i(A \times R_{ohmic}) \\ i = \frac{I}{A} \\ R_{ohmic} = \frac{\delta}{\sigma} \end{cases} \quad (3\text{-}16)$$

Where

V_{ohmic} is the voltage drop across the fuel cell due to ohmic losses in (V).

i is the current density in amperes per square meter in ($\mathrm{A/m^2}$).

A is the activation area of the fuel cell in square meters ($\mathrm{m^2}$).

R_{ohmic} is the ohmic resistance in (Ω).

δ is the thickness of the electrolyte layer (m).

σ is the ionic conductivity of the electrolyte (S/m).

The concentration loss voltage V_{con}, also known as mass transport overpotential, occurs when the rate of electrochemical reaction at the electrode surface is limited by the rate at which reactants are transported to the electrode. At high current densities, this can become significant, leading to a noticeable drop in voltage as the cell is unable to sustain the reaction due to depleted reactants at the electrode interface. This limitation can be a result of insufficient reactant flow, poor diffusion in the electrode, or inadequate water management in the cell (Li et al., 2019; Ren, 2019). The ohmic loss voltage can be calculated through 3-17.

$$V_{\text{con}} = \frac{RT}{nF} \ln\left(\frac{i_{\max}}{i_{\max} - i}\right) \quad (3\text{-}17)$$

Where

$i_{\max}$ is the maximum current density at which the fuel cell operates in amperes per square meter ($\mathrm{A/m^2}$).

There are three types of PEMFC models available in the Matlab library. The first model is the complex physical PEMFC model (Figure 3-26) in the Matlab/Simscape Toolbox which provides the most accurate and comprehensive results of FC electric and heat responses, but the simulation speed is very low (MathWorks, 2019).

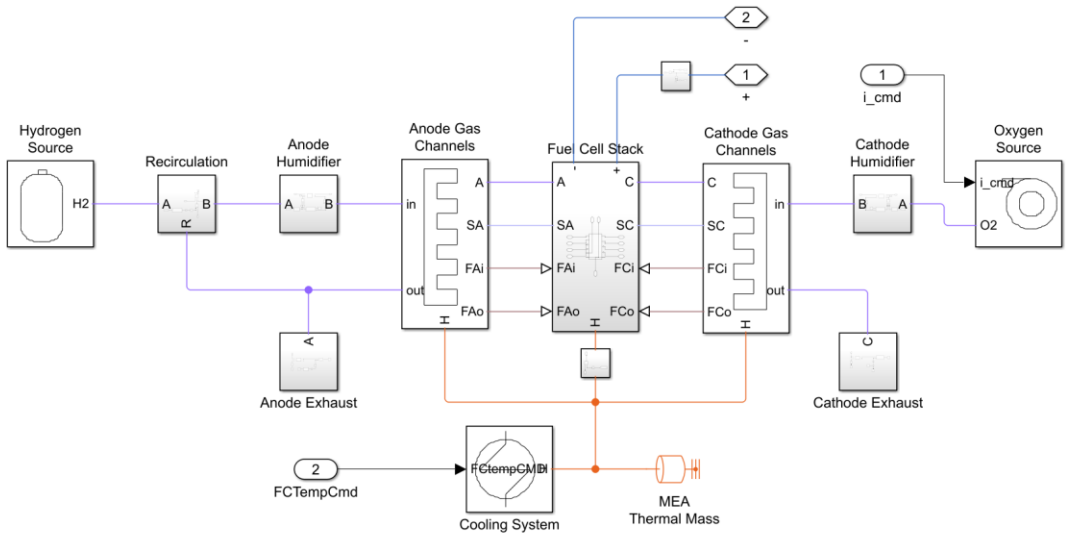

Figure 3-26 Matlab/Simscape PEMFC model

The second model is a mathematical formula-base model which calculates the output signals based on the above equations, the simulation accuracy and speed are medium. The last model is the look-up-table function-based simplified model by reading the target data from the input PEMFC polarisation curve (Figure 3-27), the accuracy depends on the polarisation data and the simulation speed is the fastest.

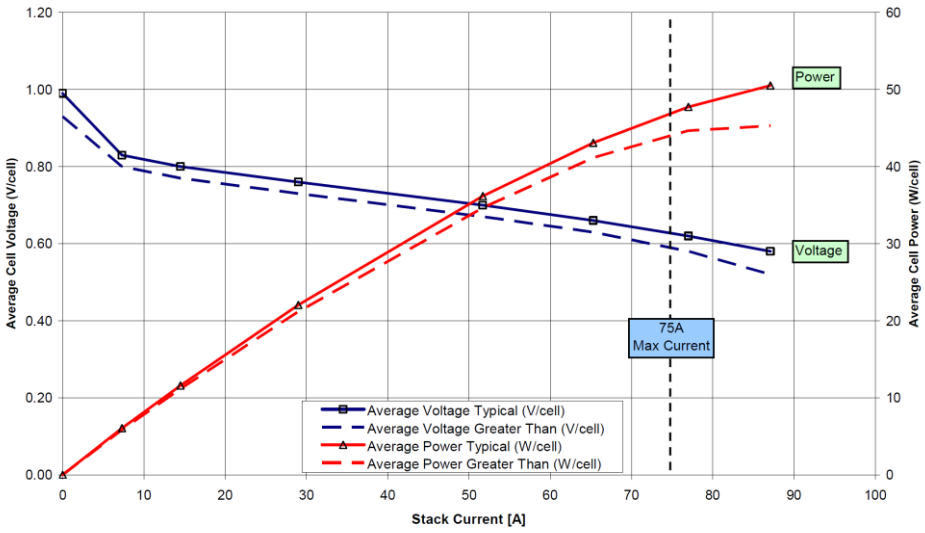

Figure 3-27 Polarisation curve of Ballard 1020ACS PEMFC (Ballard, 2014)

Similar to the model type selection methods of electric motor and battery pack, since this project requires a high simulation speed for repeating long-time driving cycles, the third option of look-up-table-based PEMFC is selected in this model due to its highest simulation speed and ensured accuracy level relies on the quality of table data (come from fuel cell manufacture data). The hydrogen gas consumption of the look-up-table-

based PEMFC model can be calculated by 3-18, this equation neglects the hydrogen fuel consumption caused by purging and gas leakage during the operation of the fuel cell since the typically estimated hydrogen consumption for purging and leakage accounts for only approximately 1% to 2% of the total hydrogen usage. Also, this proportion is relatively small in well-designed fuel cell systems, as most of the hydrogen is consumed in the electrochemical reaction. (Ballard, 2014).

$C_{H2} = I_{fc} \cdot N_{fc} \cdot \frac{M_{H2}}{N_{V_{H2}} \times C_F}$ (Ballard, 2014) (3-18)

Where

C_{H2} is the hydrogen consumption per second in (g/s).

I_{fc} is the output current of the FC stack in (A).

N_{fc} is the number of cells in the FC stack.

M_{H2} is the molecular weight constant (2.016) of hydrogen in (g/mol)

$N_{V_{H2}}$ is the valence number (2) of hydrogen.

C_F is the Faraday Constant (96485) in (C/mol).

In the proposed powertrain concept of the “DHFCRE + Eco-BEV” model, a DC-DC converter model is connected to the PEMFC stack, and an Energy Management System (EMS) is added into the VCU system which controls the energy flow of the FC stack and battery pack (Figure 3-28). The DC-DC converter model is the Bidirectional DC-DC block from the Matlab/Simulink library with input parameters of the overall efficiency and power limits.

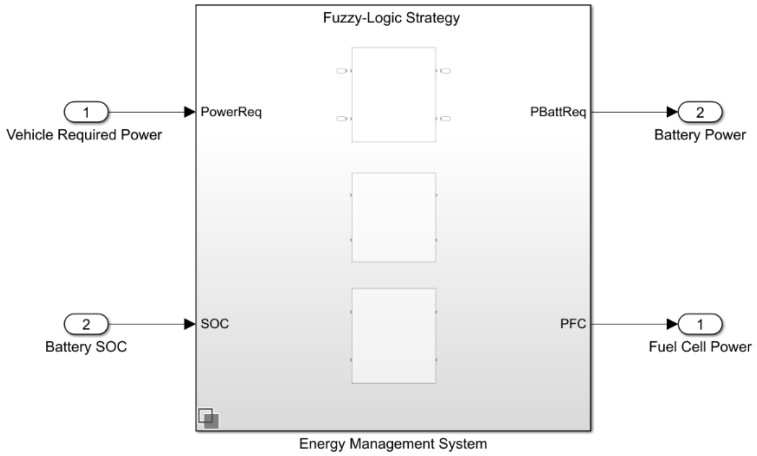

Figure 3-28 Energy management system model structure

The input signals of the EMS model are the required power and the battery SoC signals from the vehicle's electric powertrain subsystem, the output signals are the output power of the battery pack and FC stack.

3.5. Model Validations

The purpose of establishing this Matlab/Simulink-based simulation model is to quantify the technical performance of the given BEV and FC range extender. To ensure the reliability and accuracy of the output technical results from this vehicle model, the model validations focused on the overall vehicle level outputs under given duty cycles and environmental conditions. The experimental results from Coventry University Microcab's real-world tests were used as the reference values to examine the accuracy of this vehicle model. The methodology of this validation is to input all the parameter values used in Microcab's real-world test including the duty cycle, internal vehicle powertrain parameters and environmental parameters, and examine the selected simulation output results with the experimental results from Microcab. The errors are presented and analysed with consideration of the potential sources of errors, the tolerance of the errors were set as $\pm 3\%$ since the simulation of this DHFCRE + Eco-BEV concept focused on the vehicle overall performance level which analysis the comparison with other competing powertrains.

3.5.1. Microcab ECE-15 BEV Test

The Microcab ECE-15 BEV test was undertaken by using their BEV version vehicle under the ECE-15 duty cycle (Figure 3-29), which is the urban part of the NEDC drive cycle. This duty cycle was devised to represent city driving conditions such as in Paris or Rome. It is characterised by low vehicle speed, low engine load, and low exhaust gas temperature. (DieselNet, 2022). The total time of the ECE-15 cycle is 195s and the total driving distance is 0.9941 km. The NEDC duty cycle was established in the 1980s and was last updated in 1997, in recent years, NEDC is regarded as an idealised duty cycle and has gradually been replaced by other cycles such as the Worldwide Harmonised Light Vehicle Test Procedure (WLTP) and Environmental Protection Agency (EPA) cycles. (J.D. Power, 2022).

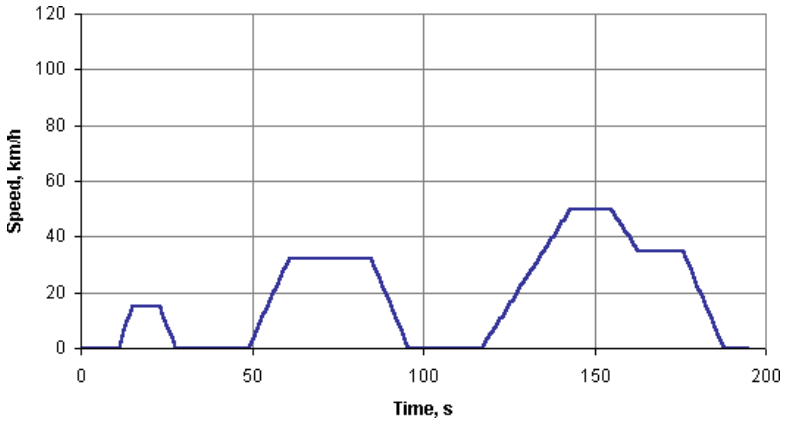

Figure 3-29 ECE-15 duty cycle plot (Speed - Time)

This physical test was undertaken by MIRA at their testing facility in Nuneaton, West Midlands, UK. The author was absent for the duration of the test and due to security reasons, no photos are allowed whilst on the MIRA premises, thus, a written description of the test procedure is provided here. (Apicella, 2019). The Microcab team selected this cycle since the maximum speed of Microcab is 55 mph and they needed to test their systems under the designed workload. In the test of Microcab, it used 8 times the ECE-15 cycle with a total driving time of 1630s which includes a 70s warm-up and 1560s of driving 8 times under the ECE-15 cycle, the total journey distance is about 8 km.

The velocity profile of the Microcab ECE-15 BEV test is presented in Figure 3-30.

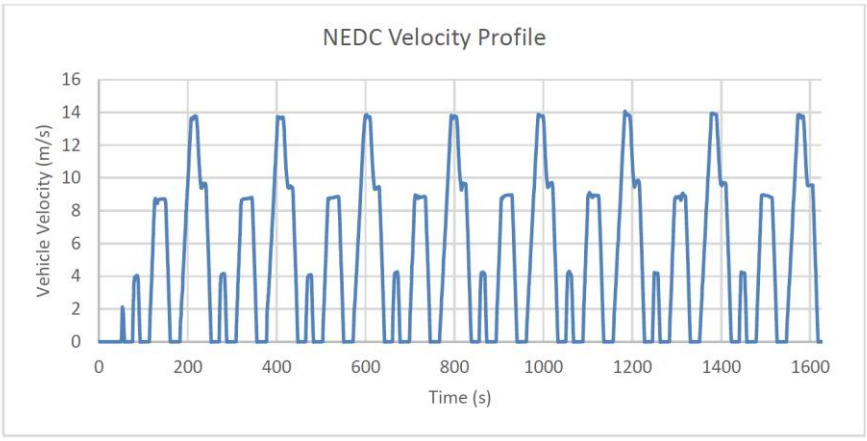

Figure 3-30 Microcab ECE-15 BEV test result – Velocity Profile (Apicella, 2019)

The velocity profiles show that the driver can closely match the speed of the values requested by the duty cycle. However, there are slight over and undershoots on high accelerations stop or start parts. This shows that the driver can closely represent a typical driver's responses to speed change requests (Apicella, 2019).

The performance benchmark monitored in this experiment is the accumulated battery energy consumption. Figure 3-31 presents the test result plot of the accumulated battery energy consumption in Microcab's ECE-15 BEV test (red) (Apicella, 2019).

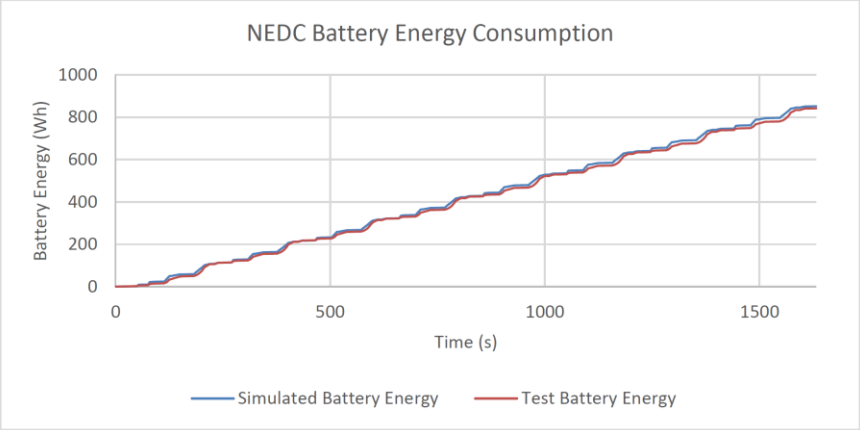

Figure 3-31 Microcab ECE-15 BEV test result accumulated battery energy consumption (Battery Energy – Time) (Apicella, 2019)

The total energy consumption result of this Microcab BEV ECE-15 experiment is 841.5 Wh. (Apicella, 2019).

3.5.2. BEV Model Validation

3.5.2.1. Validation Simulation Setup

The simulation for validation used the same parameters as Microcab's test mentioned in Section 3.5.1. Firstly, the duty cycle used in this simulation is 8 times of ECE-15, but due to the limitations of Microcab's report and confidential regulations of MIRA testing, the vehicle velocity profile of the 70s warm-up in advance of the ECE-15 cycles could not be read. However, as Figure 3-30 shows, that the missing part of this 70s warm-up would only impact the result of accumulated energy consumption, the value in the first 70s is close to 0 Wh. Secondly, the parameters of the vehicle were collected from Microcab and inputted into the simulation model as Table 3-2 shows. Thirdly, the environment parameters including the absolute air pressure, air temperature values on the day of the experiment and the gravitational acceleration of the location of the MIRA testing centre were not mentioned in Microcab's report, the values of these parameters are used in the nominal values and the air temperature is 20 ℃ (293.15 K). Finally, the weight of the testing staff in Microcab's test was not mentioned.

Table 3-2 Parameters in the simulation of Microcab BEV for model validations

Parameter Field	Parameter Name	Model Name	Microcab Value	Unit
Environment	Absolute Air Pressure	Pabs	101325	Pa
	Air Temperature	T	293.15	K
	Gravitational acceleration	g	9.81	m/s^2
Vehicle Body	Vehicle Mass	Mass	800	kg
	Drag Coefficient	Cd	0.35	
	Frontal Area	Af	2.94	m^2
	Horizontal distance from CG to front axle	a_CG	1.18	m
	Horizontal distance from CG to rear axle	b_CG	1	m
	CG height above axles	h	0.37	m
	Lift coefficient	Cl	0	
	*Initial vertical position	z_o	0.37	m
	Inertia	Iyy	378	kg·m^2
	Pitch drag moment coefficient	Cpm	0.89	
	Number of wheels on the front axle	NF	2	
	Number of wheels on rear axle	NR	2	
	Carrier to driveshaft ratio	Ndiff	3.94	
Wheel and Axle	Wheel inertia	Iyy_Whl	0.679	kg·m^2
	Relaxation length	Lrel	0.12	m
	Loaded radius	Re	0.2805	m
Battery and BMS	Battery Capacity Max	BattChargeMax	55.6	Ah
	Battery Capacity Initial	BattCapInit	55.6	Ah
	Number of Cells in Series	Ns	24	
	Number of Cells in Parallel	Np	4	
	Open Circuit Voltage Table	Em	3.5	V
Electric Motor	Maximum torque	Torque_max	35.5	Nm
	Maximum power	Power_max	11700	W
	*Motor speeds	MotSpd	<1x15> matrix	
	Motor torques	MotTrq	<1x15> matrix	

*Initial vertical position: Initial vertical CG position, along the vehicle-fixed z-axis.

*Motor speeds and motor torques are <1x15> matrix. The motor curve plots and efficiency map are presented in Appendix 1.1.

In Table 3-2, the first row is the ‘parameter field’ which locates the subsystems of the listed parameters. The ‘parameter name’ row presents the names of the parameters and the ‘model names’ are the parameter codes used in the simulation model. The last two rows present the values of the parameters and their units.

3.5.2.2. Validation Results

Similar to the Microcab ECE-15 BEV test, the focus of the simulation results was the vehicle velocity profile and accumulated energy consumption. Figure 3-32 shows the vehicle velocity trace profile including the target (red solid line) and actual speed (black dotted line).

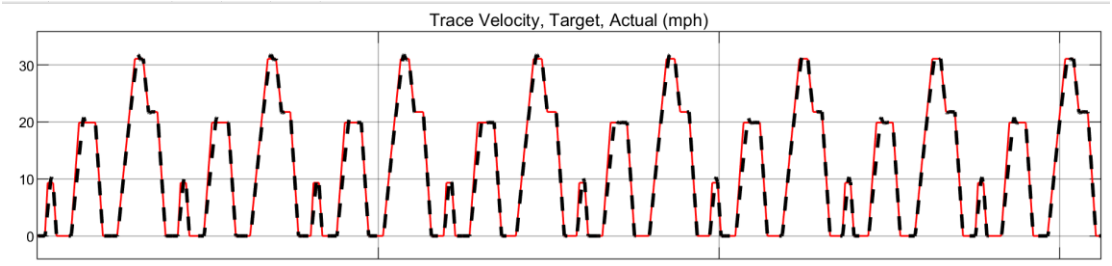

Figure 3-32 Simulation result – Microcab BEV velocity profile under ECE-15 cycle - target and actual (mph) (Apicella, 2019)

Similar to Microcab's testing result of the vehicle velocity profile presented in Figure 3-30, the velocity trace plot of the simulation results showed some under and overshoots on the start/end parts of the accelerations, this means that the driver model from the Matlab/Simulink database could represent actions close to the real driver's behaviours. The vehicle in the simulation model could provide enough speed to match the requirements of the ECE-15 duty cycle.

The most important result was BEV's accumulated energy consumption, Figure 3-33 presents the plot of the comparison between the simulation (blue) and experimental (red) results of the accumulated energy consumption in Wh.

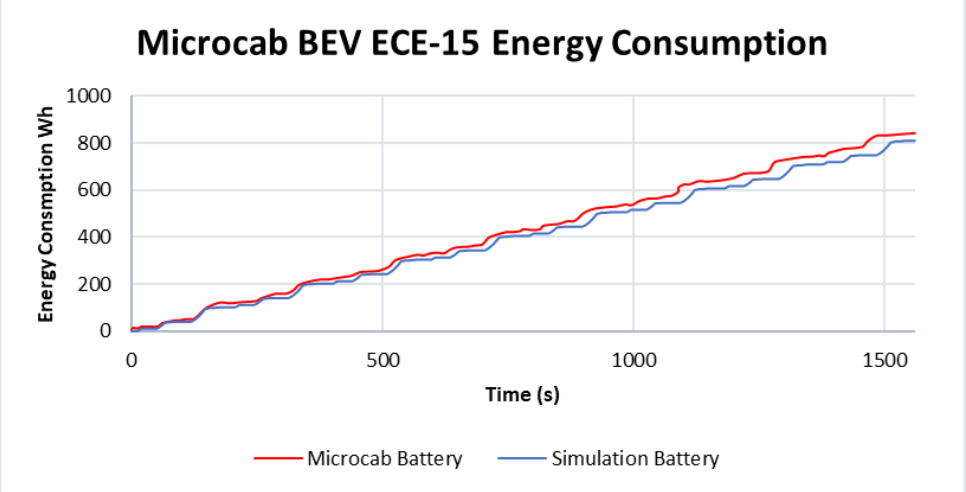

Figure 3-33 Result comparison – Accumulated BEV Energy Consumption under ECE-15 cycle (Wh) - Microcab vs Simulation

The total accumulated energy consumption from the simulation Microcab BEV under 8 times ECE-15 driving was 809.2 Wh. Compared with the result from Microcab's testing data, there is an error rate of around 3.88%.

3.5.2.3. Validation Result Analysis and Discussion

Firstly, the most significant potential error source is the missed weight of testing staff (driver). Since Microcab is a compact car which has a curb weight of only 800 kg, adding the weight of the driver to the vehicle's total mass will increase rolling resistance. To test the impact of this, an assumed weight of 70 kg was added to the total vehicle mass while all other parameters were fixed, and then the total accumulated energy consumption increased to 830.5 Wh which means the error rate is 1.35%.

Secondly, the previous discussions in Section 3.3 stated that the environmental parameters of Microcab's test were missing. While in the Midlands, UK the air pressure and gravitational acceleration vary by a very small order of magnitude, while the average temperature of a year is around 13 ℃ (286.15 K). By changing the air temperature to 286.15 K, the result of total accumulated energy consumption dropped from 830.5 Wh to 827.2 Wh which means that the air temperature contributes only a small part of the total errors.

Finally, as Figure 3-33 shows, that the difference between the simulation battery energy consumption and the Microcab experimental data gradually grows with time since the measured energy consumption is accumulated over time. Also, as stated in the Simulation set-up part, Microcab's test has a warm-up around 70s in advance of the ECE-15 cycles, the turning points of the curve in the red line (Microcab data) appear earlier than those points in the blue one (simulation) result. However, as the discussion above in the Simulation set-up part, the speed is 0 the most of time during the warm-up period and did not consume a large proportion of energy. Therefore, the difference in the vehicle speed profile is one of the sources of error, but its proportion is relatively low.

3.5.3. Fuel Cell System Model Validation

The procedure of Microcab's FCEV test was the same as the BEV test, the only difference was that a fuel cell stack was turned on as the power supply for the battery pack, and all the other parameters are the same. (Apicella, 2019). The fuel cell stack in Microcab FCEV is a 3 kW Ballard low-temperature air-cooled fuel cell stack with a 350 bar 1.65 kg hydrogen tank. In this test, the fuel cell was set to produce a fixed

power of 1935.5 W to charge the battery with an efficiency of 97% on charging and ignored the efficiency of the DC-DC inverter. From their result, the vehicle was under the same velocity profile as the BEV test, and the total accumulated energy consumption of the FC system was 866.1 Wh.

The validation simulation of the fuel cell range extender used the same set-up as Microcab's test, apart from the FC system being turned on for a fixed output power of 1935.5 W, all the other parameters were the same with the values shown in Table 3-2. The plot of the accumulated energy consumption comparison between the simulation and Microcab's result is presented in Figure 3-34.

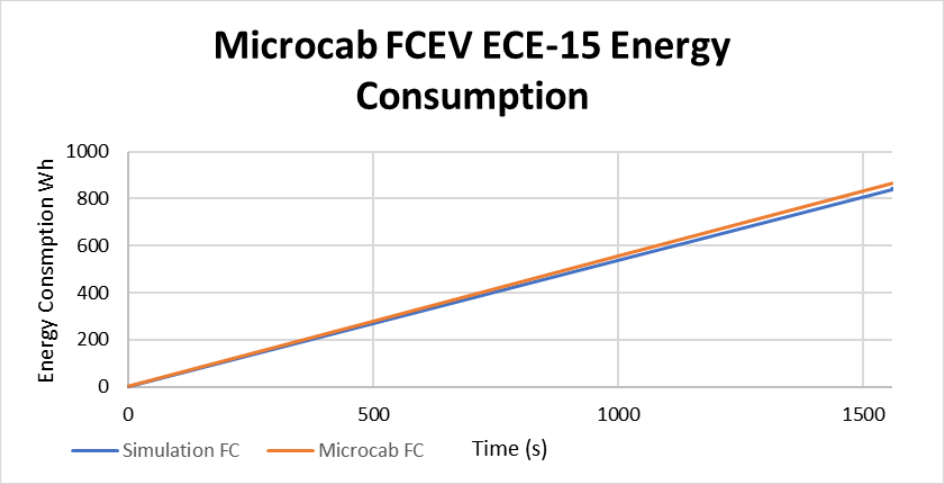

Figure 3-34 Result comparison – Accumulated FCEV Energy Consumption under ECE-15 cycle (Wh) - Microcab vs Simulation

As Figure 3-34 shows, that the curve of total accumulated FC energy consumption of both Microcab's and simulation result are straight lines since the FC system was set as a fixed power supply, the fluctuations of the power demand from the duty cycle only drive the changes on the power of the battery, the FC system always charges the battery in the same power 1935.5 W.

The total accumulated energy consumption from the FCEV in the simulation model was 844.8 Wh, where the error rate is 2.46%. Apart from the discussed main error sources in Section 3.5.2, the errors in this FCEV simulation also include the ignored energy loss from the DC-DC inverter.

To conclude, the main error source of validation in the Matlab/Simulink vehicle model is the driver's weight which related to the total mass of the vehicle in the simulation, the environmental parameters and the difference between vehicle speed profiles contribute small proportions to the total error rate. Also, as Microcab's report stated, the NEDC testing is a highly stylised and outdated testing method, they found that

there is an approximate difference rate of 37% compared with their real-world driving tests. The ECE-15 test was only for testing their vehicle and components from a comparative perspective. Similar to Microcab's NEDC testing purpose, the validation here is only to validate the vehicle outputs by inputting the same parameters as Microcab's test to examine the performance of this simulation model. The simulations of the following chapters will use some latest duty cycles.

3.6. Summary of Simulation System Modelling

This chapter evaluated the simulation tools based on the requirements of this project which considered the model functionality, simulation efficiency and the constraints of the project budget and timeline. Based on the selected software – Matlab/Simulink, a simulation model for the proposed novel powertrain concept of "DHFCRE + Eco-BEV" was established to evaluate the performance of this concept. The process of developing the framework and components of this model referred to the published research, the resources from Coventry University Microcab Laboratory as well as the internal toolboxes and library blocks of Matlab. The simulation model was validated by the experimental data from the Microcab BEV and FCEV physical tests undertaken by MIRA at their testing facility in Nuneaton, West Midlands. The validation result showed that the error rates of the BEV and FCEV powertrain models were respectively 1.35% and 2.46% which are within the given error tolerance of $\pm 3\%$. The main error sources were identified including the driver's weight, environmental parameters, warm-up energy consumption and the energy loss from the DC-DC converter.

The limitations of the modelling and validation process are summarised as follows:

- **Modelling limitations**

According to the modelling requirement and process discussions in Section 3.3, limited by the real-world experimental resources and project time constraints, the simulation model in this project used some look-up-table-based and simplified mathematical formula-based model components (such as electric motor, battery pack and FC system) to realise a fast simulation speed to avoid over-long simulation time consumptions. The accuracy of these components highly relied on the accuracy of the given table database which in theory is lower than the physical models.

- **Model validation limitations**

At the beginning of the project, the original plan for the simulation model validation is to use the BEV and FC system laboratory resources of Coventry University Microcab

to validate the model by each main component as well as the whole vehicle. Firstly, use the testing facilities in Microcab FCEV Lab including battery testing, fuel cell testing and electric motor testing systems to validate the accuracy of each main powertrain component. Then, use the Microcab BEV version and FCEV version vehicle to test the accuracy in the vehicle's overall performance level under given drive cycles (Apicella, 2019). However, referring to the validation methodology in Section 3.5, due to the termination of the collaboration between Coventry University and Microcab Ltd, the laboratory testing facilities were no longer available for this project. The validation method was forced to be modified and simplified by using the existing vehicle dyno test results of the Microcab BEV and FCEV vehicles in the vehicle's overall performance level.

- **DHFCRE physical connection method limitation and considerations**

Referring to the physical connection method of the proposed DHFCRE for BEV in Section 3.4, the physical connection styles of the FC range extender are boot-based, roof-luggage-rack-based and trailer-based. In this project, the physical connection of boot-based is used for the simulation parameterisations. However, the physical connection method should depend on the demand of the users since different connection style has various costs and benefits. For the boot style, the advantage is that adding the range extender will only increase the total weight of the vehicle and the weight contribution on the front and rear axles. This will increase the rolling resistance of the vehicle but will not change the aerodynamic drag force. However, this will affect the vehicle functionality since it reduces the vehicle boot luggage space. For the roof-luggage-rack-based connection style, the advantage is that it will not affect the boot luggage space but it will increase the frontal area and aerodynamic drag coefficient. This will lead not only to a higher rolling resistance but also a higher aerodynamic resistance which will affect the overall vehicle energy efficiency and increase the fuel cost. The trailer-based connection style will not affect the vehicle functionality and the aerodynamic resistance, but it will increase driving difficulties for the driver since towing a trailer will have a different driving experience which may require a higher level of driving technique (Monticello, 2019). Also, with the consideration of the modelling complexity, the boot style used in this thesis requires minor changes in the vehicle structure and parameters.

Chapter 4 Simulation Model Parameterisation

4.1. Introduction

Following the modelling and validation processes, the simulation model of the proposed powertrain concept "DHFCRE + Eco-BEV" has been established based on the Matlab/Simulink platform. This model integrates both external information including environmental conditions, duty cycles, driver preferences and internal parameters pertinent to the vehicle and fuel cell system. According to the aims and objectives discussed in Section 1.3, the purpose of the simulation in this project is to quantify and evaluate the performance of the proposed powertrain concept compared with the full-sized BEV, under different driving scenarios including different duty cycles, energy management strategies and driver preferences. Consequently, prior to commencing the simulations, it is imperative that the parameters, encompassing both external information and internal vehicle specifications, be configured in advance.

In this chapter, the duty cycles, encompassing environmental parameters, along with the parameterisations of principal components within the proposed powertrain concept (comprising vehicle powertrains and dynamics, battery electric systems, and fuel cell range extender systems) are analysed and presented.

4.2. Duty Cycle and Environmental Parameters

Duty cycles used in the simulation of this project were classified into 2 types – the urban cycles (for normal urban journeys) and the extra-urban cycles (for long-distance journeys). According to the discussions in Section 3.5.2, the NEDC cycle was the most popular vehicle fuel economy and emission test duty cycle in the last century. However, in recent years, the NEDC cycle has been regarded as an outdated and stylised duty cycle and has gradually been replaced by new cycles including the EPA Federal Test Procedure (American), Worldwide Harmonised Light Vehicle Test Procedure (WLTP) (EU) and JC08 (Japanese) cycles (Apicella, 2019; Ren, 2021). Since this DHFCRE is proposed for UK and EU BEVs, in this project, the EU WLTP duty cycle is selected as the input of the simulation model to evaluate the performance of the proposed powertrain concept and EMS control algorithms developments. The US EPA will be used for partly of the EMS optimisation process.

4.2.1. WLTP Duty Cycle

In this project, the range extender is developed for the UK & EU light-duty passenger vehicles, thus, the latest WLTP cycle – class 3, version 5 (Figure 4-1) is selected in the simulation model used for the component parameterisations and technical result-generating (Transport Policy, 2022).

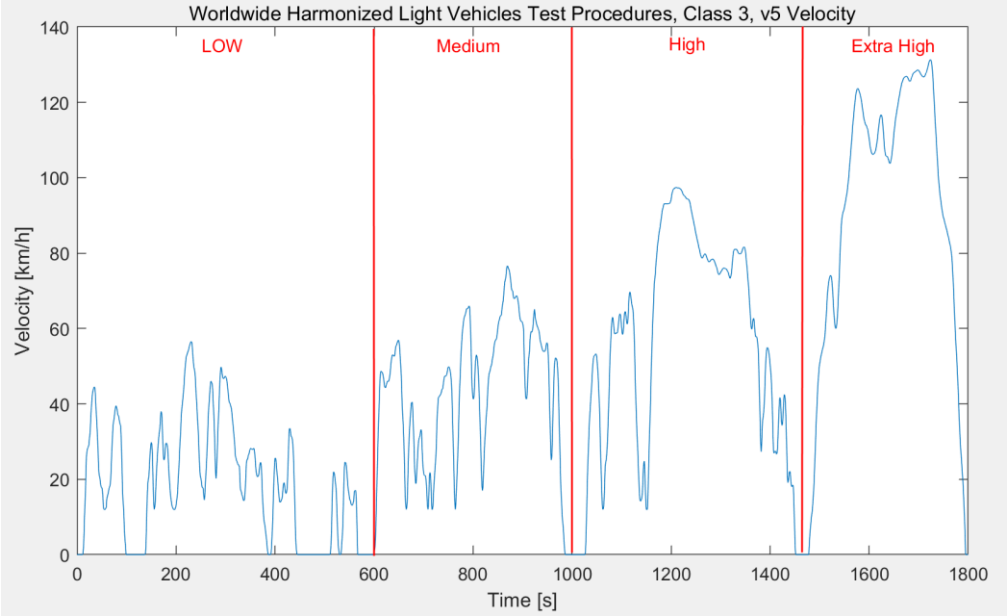

Figure 4-1 WLTP cycle class3, version 5 (Transport Policy, 2022)

This WLTP cycle contains 4 phases classified by vehicle speed which are Low (0 – 60 km/h), Medium (0 – 80 km/h), High (0 – 100 km/h) and Extra-high (0 – 130 km/h). The total time is 1800s and the total driving distance is 23.262 km. In this chapter, the WLTP cycle is split into 2 parts to represent the urban (Low and Medium phases) and extra-urban (High and Extra-high phases) duty cycles. The total time of the urban cycle the extra-urban cycle are 1022s and 778s. By inputting the simulation time into the Matlab/Simulink model, the total distance of the two cycles can be calculated, which are respectively 7.85 km and 15.412 km.

4.2.2. EPA Duty Cycle

The EPA Federal Test Procedure includes a series of driving cycles published by the US Environmental Protection Agency (EPA) to measure the emissions and fuel economy of passenger vehicles. The latest EPA duty cycles were updated in 2008 and include four test scenarios: The urban dynamometer driving schedule (UDDS) (also known as FTP-72), highway driving (HWFET), aggressive driving (SFTP US06), and optional air conditioning test (SFTP SC03). (EPA.GOV, 2022).

The FTP-72 duty cycle (Figure 4-2) and the HWFET cycle (Figure 4-3) will be implemented as urban and extra-urban driving cycles to develop and test the technical performance of different EMS control algorithms.

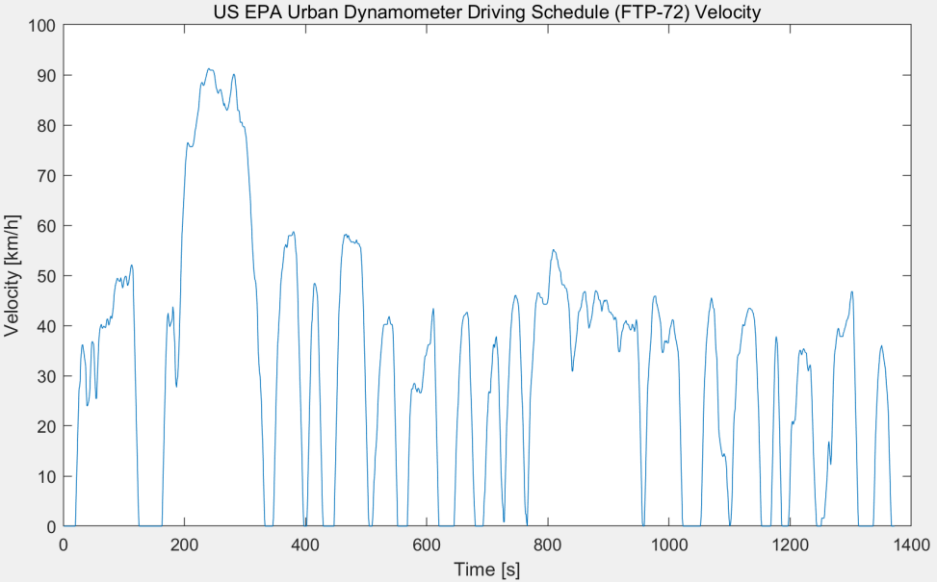

Figure 4-2 FPT-72 duty cycle plot - Speed vs Time

The FTP-72 cycle simulates an urban route of 12.07 km with frequent stops. The maximum speed is 91.25 km/h and the average speed is 31.5 km/h. The duration of this cycle is 1372s.

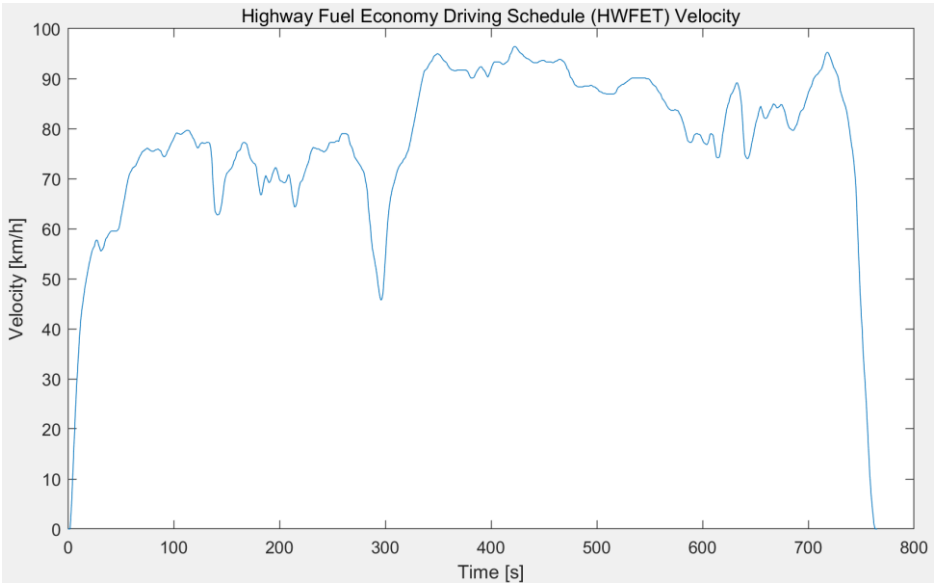

Figure 4-3 HWFET duty cycle plot - Speed vs Time

The HWFET cycle simulates an extra-urban driving route of 16.75 km with an average speed of 77.7 km/h and the duration is 765s.

4.2.3. Environmental Parameters

The environmental parameters can have an impact on vehicle performance and hence the result of the vehicle dynamometer tests (EPA, 2022). The significant environmental parameters include the aerodynamic parameters (air pressure, wind profile and air temperature) and rolling resistance parameters (acceleration of gravity, road grade angle, and tyre friction model). In this simulation, the air pressure value used was 101325 Pa (nominal air pressure), and the air temperature was 293.15 K (20 ℃), the wind in x, y and z axis were all 0 m/s, the acceleration of gravity is 9.81 m/s^2, the road grade angle was 0° and tyre friction model used the Magic Formula Model based on the Matlab/Simulink Library. (Matlab, 2019).

4.3. Vehicle and Main Component Parameters

4.3.1. Target Vehicle Parameterisation – Eco-BEV

The parameterisation process of the Eco-BEV used in this project focused on two areas: the key vehicle powertrain & dynamics parameters, and the battery electric system parameters. The methodology for parameterising the key vehicle powertrain was to review and refer to the parameters from commercially available BEV solutions. The methodology for defining the battery electric system parameters was to consider government-published data of UK public travelling behaviours to confirm the daily urban driving range demand for the light-duty family vehicle, then input the range (transformed into repeated urban cycles) into the model to simulate the total required electric energy. The total energy required for the combined drive cycle was set as 80% of the total battery capacity to ensure the battery State of Health (SoH) of the Eco-BEV. This method of battery capacity can ensure the Eco-BEV fulfils the daily urban driving range as well as avoid deep-discharge and maintain battery SoH.

The parameters of the Eco-BEV vehicle powertrain & dynamics parameters referred to the data from the best-selling urban BEV (family hatchbacks) in the UK. The detailed parameters are listed in Table 4-1. (EVspecifications, 2022; Moveelectric, 2022; Mathworks, 2022; Tiresize.com, 2022).

Table 4-1 Eco-BEV powertrain & dynamics parameters

Parameter Field	Parameter Name	Model Name	ECO-BEV_Value	Unit
Vehicle Body	Vehicle Mass	Mass	1200	kg
	Drag Coefficient	Cd	0.28	
	Frontal Area	Af	2.276	m/s^2
	Horizontal distance from CG to front axle	a_CG	1.323	m
	Horizontal distance from CG to rear axle	b_CG	1.377	m
	CG height above axles	h	0.5	m
	Lift coefficient	Cl	0.1	-
	Initial vertical position	z_o	-0.5	m
	Inertia	Iyy	3000	kg· m^2
	Pitch drag moment coefficient	Cpm	0.1	-
	Number of wheels on the front axle	NF	2	-
	Number of wheels on rear axle	NR	2	-
	Carrier to driveshaft ratio	Ndiff	7.94	-
Wheel and Axle	Wheel inertia	Iyy_Whl	0.8	kg· m^2
	Relaxation length	Lrel	0.15	m
	Loaded radius	Re	0.327	m
Electric Motor*	Maximum torque	torque_max	280	Nm
	Maximum power	power_max	80000	W

*The motor curve plots and efficiency map are present in Appendix 1.1

The battery capacity for the Eco-BEV came from the simulation result of inputting the above vehicle parameters and the daily urban range demand based on the national travel behaviour data published by the UK government, the range demand is transferred to the repeat WLTP cycles as input of the simulation model. The Department for Transport published the statistical data set of UK family vehicles' mode of travel in the perspective of numbers of travel and journey length from 2002 to 2022 (Figure 4-4). (GOV.UK, 2020).

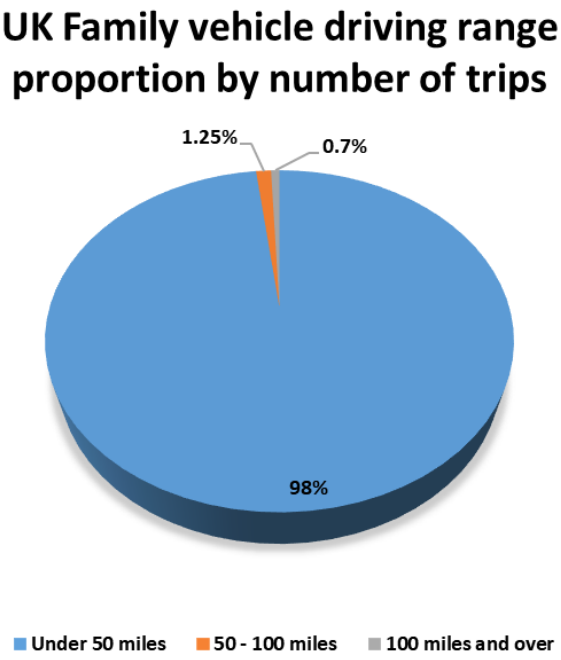

Figure 4-4 UK family vehicle driving range proportion by number of trips and journey length

The travelling statistical data used in this section is the average value from 2009 to 2019 since the national travelling behaviour between 2020 and 2022 was significantly changed due to the COVID-19 pandemic and cannot represent the driving behaviour in the UK. (GOV.UK, 2022). Through the data analysis based on the government-published driving behaviour data, approximately 98.05% of journeys are less than 50 miles in length, while journeys spanning 50 to 100 miles account for about 1.25% and journeys exceeding 100 miles constitute a mere 0.7% of the total. Considering the driving behaviour in the UK, the hypothesis on the Eco-BEV range is 50 miles, it fulfils the demand of more than 98% of trips in the UK.

As section 4.2 mentioned, the driving distance of the WLTP urban cycle is 7.85 km and the total time is 1022s, the 80 km range can be transformed into 10.2 times repeating of the WLTP urban cycle and the total simulation time is 10450s. Thus, the duty cycle input of simulation for Eco-BEV battery capacity setup was set as repeating WLTP urban cycle for 10450s, since the driving distance of this duty cycle is not averaged over time, the total length is calculated as 79.82 km. The input vehicle parameters are listed in Table 4-1 above and the target output parameter is the total battery energy consumption which represents 80% of the Eco-BEV battery capacity to avoid the deep-discharge for the battery pack (10% and 90% are set as the min & max battery SoC to protect the battery) (Du et al., 2022; Ferahtia et al., 2023). The total accumulated battery energy consumption plot results from the Eco-BEV in the given 10450s simulation are shown in Figure 4-5.

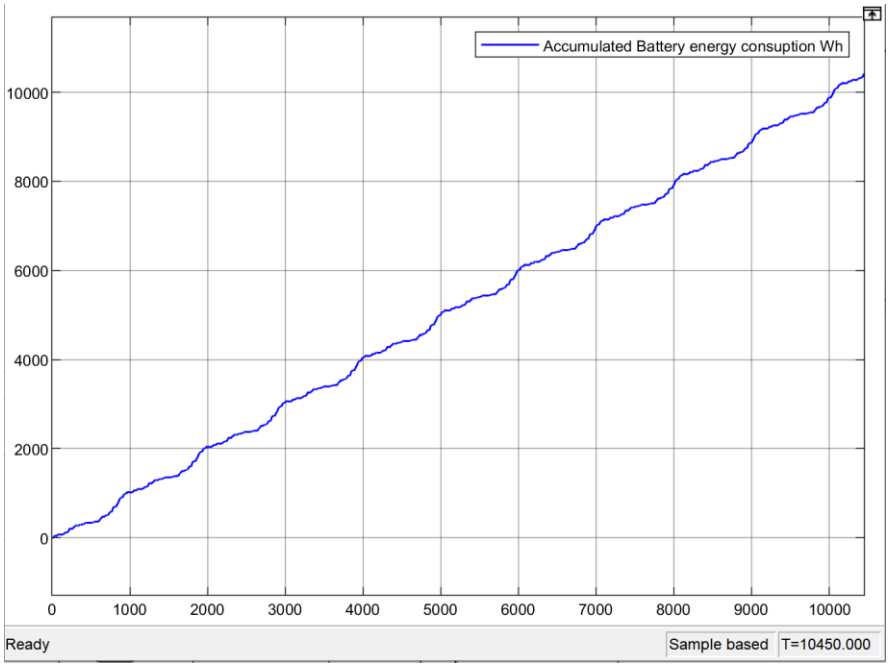

Figure 4-5 Total accumulated battery energy consumption result - Eco-BEV

The total battery consumption result from this simulation was 10.37 kWh under the repeating WLTC urban cycle with a total driving distance of 79.82 km. Therefore, the battery capacity of the Eco-BEV was calculated as 12.96 kWh.

The hypothesis of the battery pack parameter was developed as Table 4-2 shows.

Table 4-2 Parameter of the battery pack in the Eco-BEV

Open_Circuit_Cell_Voltage	3.75	V
Battery_Cell_Capacity_Max	3	Ah
Nubmer_of_Cells_in_Parallel_per_Module	6	-
Nubmer_of_Cells_in_Series_per_Module	1	-
Nubmer_of_Modules_in_Series	96	-
Nubmer_of_Modules_in_Parallel	2	-

The nominal voltage of the battery cell referred to the 18650 Lithium battery which was set as 3.75 V, and the battery cell capacity was set as 3 Ah (Tycorun Batteries, 2022). There were 1152 pieces of 18650 battery cells in the battery pack, each battery module has 6 cells in parallel, 96 modules were connected in series and 2 modules in parallel. Thus, the battery pack's total voltage was 360 V and the capacity was 36 Ah (12.96 kWh).

The maximum power demand from the vehicle under a given duty cycle should be considered to examine if the battery pack has a peak discharge power higher than the peak power demand. Figure 4-6 and Figure 4-7 present the battery power curve plot

under WLTP urban and extra-urban duty cycles, the power demand was in the range from (-) 33 kW to (+) 46 kW (during regenerative braking scenarios, the power demand is a negative value).

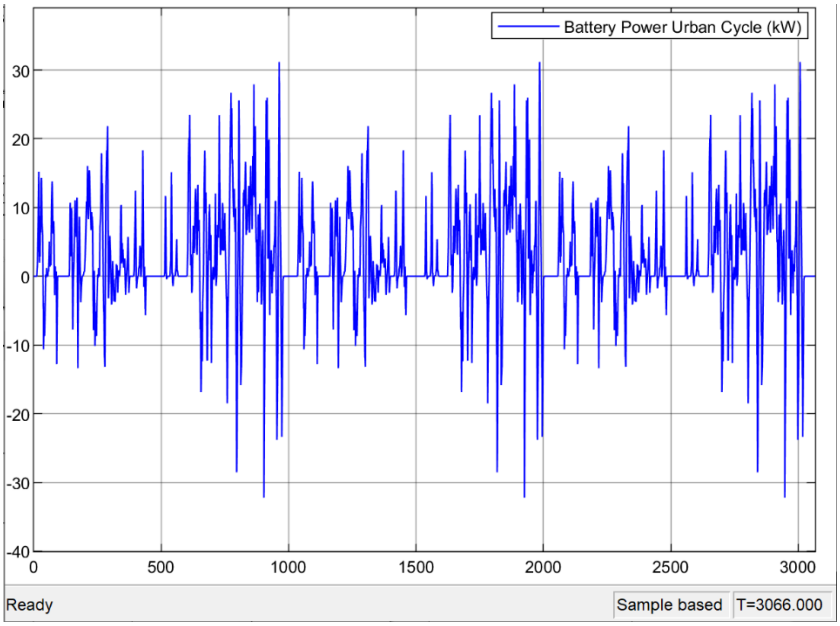

Figure 4-6 Eco-BEV power demand under urban duty cycle

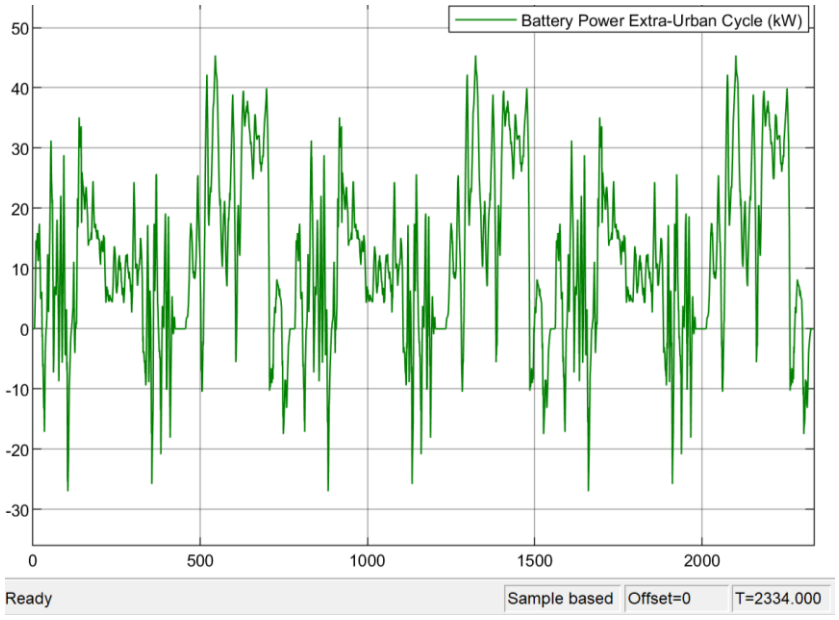

Figure 4-7 Eco-BEV power demand under extra-urban duty cycle

Referred to the characteristics of the Lithium batteries, the charge C-rate and discharge C-rate of this battery pack were set as 0.8 C and 5 C (Battery University, 2022), thus, through the calculations by 3-9, the maximum charge and discharge power of this battery pack is about (-) 10 kW and (+) 65 kW. Therefore, the maximum discharge power of the battery pack is higher than the peak power demand, but the

absolute value of maximum charge power is lower than the absolute value of the peak regenerative power, this will be regulated by the EMS system to ensure the charging power for the battery pack always lower than 10 kW to avoid deep-discharge.

In summary, the vehicle powertrain & dynamics parameters referred to the current market-ready popular BEV data in the UK and the battery pack parametrisations considered vehicle range demand refers to the travel behaviour data published by the UK Department of Transport. The vehicle and battery parameters of the Eco-BEV are listed in Table 4-1 and Table 4-2.

4.3.2. Target Vehicle Parameterisation – Large BEV

Similar to the parameterisation methodology of the Eco-BEV, the parameters of the Large BEV used in this project include 2 main parts: the main vehicle powertrain & dynamics parameters and the battery electric system parameters. The method of parameterisation of the vehicle powertrain components was to review and refer to the parameters from best-selling full-size (large saloon and SUV) BEVs in the current BEV market. The method of confirming the battery pack parameters included the literature review, analysis of marketing data of UK best-selling full-size BEVs and considerations of the length of the cross-city journeys in the UK to confirm the extra-urban (long-distance trips) range the demand for the light-duty family vehicle, then input the range (transformed into the repeat extra-urban cycles) into the model to simulate the total electric energy consumed as 80% of the total battery capacity (assuming the battery SoC from 90% to 10%) of the Large BEV. This method of defining battery capacity ensured that the Large BEV can fulfil most of the long-distance journey driving ranges as well as avoid deep-discharging to maintain battery SoH.

Referred to the best-selling full-size BEV data, the parameters of the Large BEV vehicle powertrain & dynamics parameters are listed in Table 4-3. (CarEngineer, 2020; Tiresize.com, 2022; EVspecifications, 2022; Moveelectric, 2022; Mathworks, 2022).

Table 4-3 Large-BEV powertrain & dynamics parameters

Parameter_Field	Parameter_Name	Model_Name	EVLarge_Value	Unit
Vehicle Body	Vehicle_Mass	Mass	1900	kg
	Drag_Coefficient	Cd	0.24	
	Frontal_Area	Af	2.341	m/s^2
	Horizontal distance from CG to front axle	a_CG	1.5688	m
	Horizontal distance from CG to rear axle	b_CG	1.3912	m
	CG height above axles	h	0.5	m
	Lift coefficient	Cl	0.1	-
	Initial vertical position	z_o	-0.5	m
	Inertia	Iyy	1500	kg· m^2
	Pitch drag moment coefficient	Cpm	0.1	-
	Number of wheels on the front axle	NF	2	-
	Number of wheels on rear axle	NR	2	-
	Carrier to driveshaft ratio	Ndiff	9	-
Wheel and Axle	Wheel inertia	Iyy_Whl	0.8	kg· m^2
	Relaxation length	Lrel	0.15	m
	Loaded radius	Re	0.35	m
Electric Motor*	Maximum torque	torque_max	335	Nm
	Maximum power	power_max	114000	W

*The motor curve plots and efficiency map are present in Appendix 1.1.

The determination of the BEV battery capacity referred to the range demand for the Large (full-size) BEV with the considerations of various factors including literature review, marketing data and real-world conditions.

Firstly, through the literature review, a study discussed the requirements for lithium-ion batteries in electric vehicles to achieve a driving range of 200 to 300 miles (Deng et al., 2020). Another research on the BEV range demand based on driving requirements and charging infrastructure conditions indicated that more than 77% of private vehicles required less than 300 miles (Shi et al., 2019). A UK BEV leasing specialist suggested that current BEVs could usually travel between 150-300 miles on a charge, which was determined to fulfil the demands of driving to finish long-distance commutes every day for work (DriveElectric, 2023). A report from the largest used car retailer in the USA discussed that the sufficient range for BEV customers should cover the daily commute three times, and add an extra 30% if the temperature regularly drops below freezing (CarMax, 2023). For UK drivers, the average commute distance was about 19.5 miles

for a single occupancy car journey (Mobilityways, 2022), thus the daily commute length was about 39 miles and the range of household BEV was about 152 miles.

Secondly, the top ten best-selling BEVs in the UK (2023) had ranges from 145 to 374 miles, however, for the large saloon and SUV models, the ranges were mostly higher than 200 miles (EV Magazine, 2023; Evspecifications, 2023).

Apart from the literature review and best-selling full-size BEV data, the range of the Large BEV also considered the real-world long-distance trip demands in the UK. Since the full-size BEV was regarded as the replacement solution for the conventional ICEVs, its ideal range should fulfil most of the single cross-city journeys. For the Large BEV here, the range setup also considered the distance between London and the main cities in England which meant that the Large BEV could fulfil most of the single cross-city trips in England. Shows the distance between London and the main cities in England. (Google, 2022).

Table 4-4 Cross-city trip distances in England

Cross-city Trips	Distance (mile)	Distance (km)
London to Birmingham	117	187.2
London to Manchester	200	320
London to Newcastle	287	459.2
London to Liverpool	212	339.2
London to Leeds	198	316.8
Average distance	202.8	324.48

Thus, the average single cross-city trip distance is 202.8 miles (324.48 km), the hypothesis on the battery capacity is 80% of the total capacity to provide enough electric energy for this range and the total range should be 405.6 km (253.5 miles). Cross-validated by the above literature review and marketing data, the range of Large BEV is representative for a normal full-size BEV.

To calculate the battery capacity, this range was transformed into the repeating extra-urban part of the WLTP cycles which has a simulation time of 778s and a total distance is 15.412 km. The simulation time of this parameterisation simulation was 20525 s and the total driving distance is 405.7 km.

The plot of accumulated battery energy consumption is shown in Figure 4-6

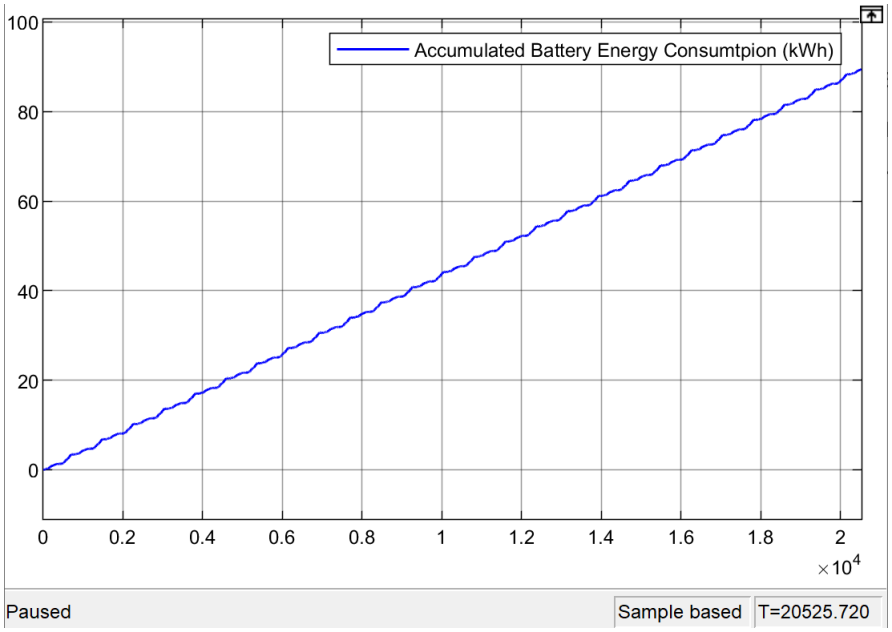

Figure 4-8 Figure 5 3 Total accumulated battery energy consumption result - Large BEV

The final accumulated battery energy consumption of the Large BEV under repeating extra-urban WLTP cycle with a simulation time of 20525 s and 405.7 km driving distance was 89.44 kWh with an overall energy efficiency of 220.3 Wh/km. Based on this result, the battery parameters developed as Table 4-5 shows.

Table 4-5 Parameter of the battery pack in the Large BEV

Open_Circuit_Cell_Voltage	3.75	V
Battery_Cell_Capacity_Max	3.105	Ah
Nubmer_of_Cells_in_Parallel_per_Module	4	-
Nubmer_of_Cells_in_Series_per_Module	1	-
Nubmer_of_Modules_in_Series	96	-
Nubmer_of_Modules_in_Parallel	20	-

The nominal cell voltage of the battery pack was 3.75 V, the cell capacity was 3.105 Ah, 4 cells were connected in parallel in each module, and the module capacity was 12.42 Ah. The battery pack had 11520 pieces of 18650 Lithium battery cells, there were 96 connected modules in series, and 20 modules connected in parallel. Therefore, the battery capacity of the Large BEV was 89.44 kWh, and the voltage was 360 V (248.44 Ah).

Also, the maximum power demand from the vehicle under a given duty cycle should have been considered to examine if the battery pack had a peak discharge power higher than the peak power demand. Figure 4-9 and Figure 4-10 presented the battery

power curve plot under WLTP urban and extra-urban duty cycles, the power demand was in the range from (-) 59 kW to (+) 63 kW (during regenerative braking scenarios, the power demand was a negative value).

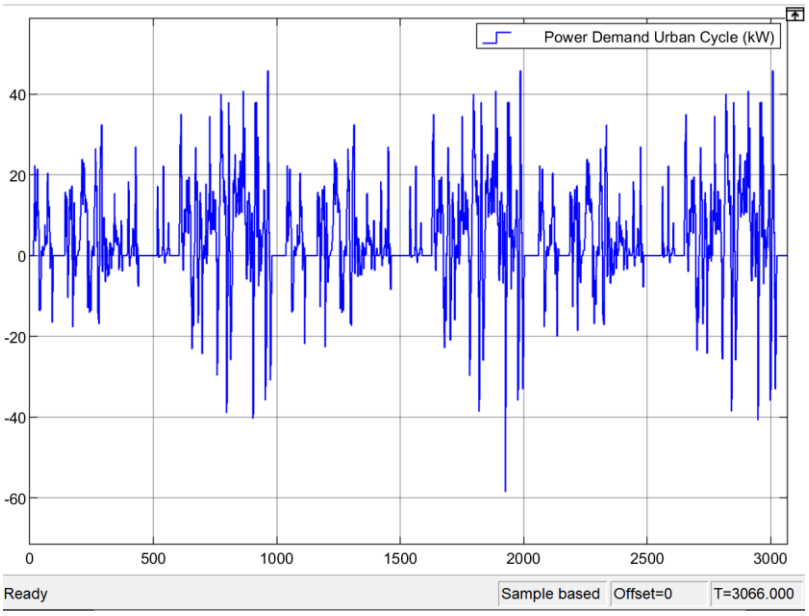

Figure 4-9 Large BEV power demand under urban duty cycle

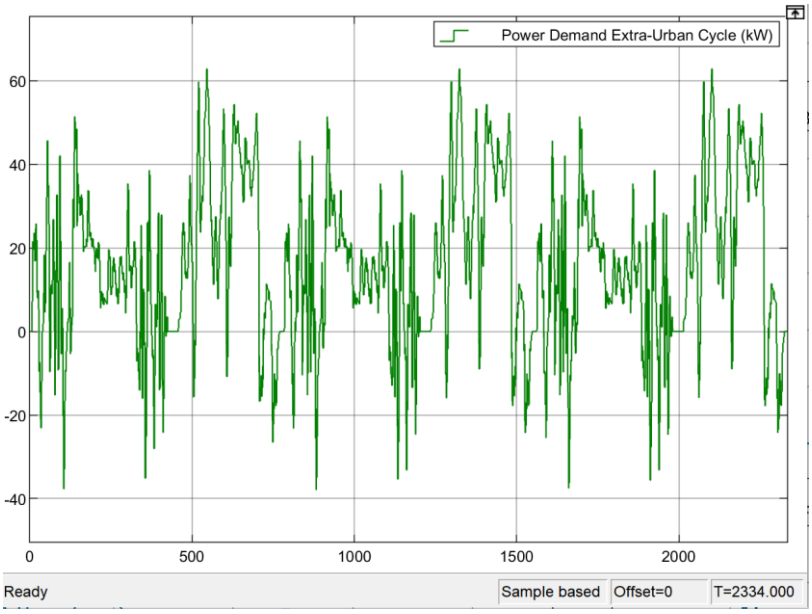

Figure 4-10 Large BEV power demand under extra urban duty cycle

The charge C-rate and discharge C-rate of this battery pack were set as 0.8 C and 5 C (Battery University, 2022), thus, through the calculations by 3-9, the maximum charge and discharge power of this battery pack was about (-) 71.5 kW and (+) 447.1 kW. Therefore, the maximum discharge power of the battery pack was higher than the peak power demand and the absolute value of maximum charge power was higher than the peak regenerative power. This means that the proposed battery pack for the

Large BEV can offer enough power for the BEV as well as maintain its State of Health (SoH).

To summarise, the vehicle powertrain & dynamics parameters of the Large BEV were referred to the current marketing data of the full-size BEVs in the UK and the battery pack parameters method considered vehicle range demand of the travel behaviour in the UK based on the average cross-city trip distances between London and main cities in England. The vehicle and battery parameters of the Large BEV are listed in Table 4-3 and Table 4-5.

4.3.3. FC Range Extender System Parameterisation

The range extender system parameterisation included two steps: the size of the FC stack and the hydrogen tank. The methodology of the FC stack considered the power demand of the vehicle under given duty cycles based on the results from the simulation model as well as the physical parameters (system weight as an input of model) referred to the market-ready FCEVs. In this method, the FC stack was supposed to offer enough power to fulfil the peak power demand of the vehicle in case the battery SoC was low and the FC range extender could power the vehicle alone. The methodology of defining hydrogen tank size involved simulating the hydrogen consumption while the FCRE was installed into the Eco-BEV and driven under an extra-urban long-distance journey scenario. The input parameters including the journey distance, duty cycle, and simulation time used here were the same as the battery size definition of Large BEV in Section 4.3.2. (Repeating extra-urban WLTP cycle with a simulation time of 20525s and 405.7 km driving distance).

The FC stack power was determined by the power demand of the Eco-BEV under both urban and extra-urban duty cycles (shown above in Figure 4-6 and Figure 4-7), the FC power should fulfil the peak battery power demand. The peak battery power demand under the WLTP urban cycle is about 32 kW and in extra-urban, the peak power demand is around 46 kW. Therefore, the power of the FC stack should be over 46 kW, the hypothesis of the rated FC power is set as 50 kW which can offer all the demands of the Eco-BEV even when the battery SoC is very low. In that case, the FC system is able to offer sufficient power to the vehicle at the same time charge the battery.

A fuel cell stack with a nominal output of 50 kW 625 V was selected, the parameters of this fuel cell stack are shown in Figure 4-11.

```
Fuel cell nominal parameters:
  Stack Power:
      -Nominal = 50000 W
      -Maximal = 120400 W
  Fuel Cell Resistance = 0.66404 ohms
  Nerst voltage of one cell [En] = 1.1342 V
  Nominal Utilization:
      -Hydrogen (H2)= 99.25 %
      -Oxidant  (O2)= 70.4 %
  Nominal Consumption:
      -Fuel = 501.8 slpm
      -Air  = 1194 slpm
  Exchange current [i0] = 0.91636 A
  Exchange coefficient [alpha] = 0.26402

Fuel cell signal variation parameters:
  Fuel composition [x_H2] = 99.95 %
  Oxidant composition [y_O2] = 21 %
  Fuel flow rate [FuelFr] at nominal Hydrogen utilization:
      -Nominal = 417.3 lpm
      -Maximum = 1460 lpm
  Air flow rate [AirFr] at nominal Oxidant utilization:
      -Nominal = 2100 lpm
      -Maximum = 7350 lpm
  System Temperature [T] = 338 Kelvin
  Fuel supply pressure [Pfuel] = 1.5 bar
  Air supply pressure [PAir] = 1 bar
```

Figure 4-11 Fuel Cell stack parameters (Matlab, 2019)

The nominal power of this FC stack is 50 kW, and the maximal power is 120.4 kW with 900 cells. There are two main reasons for selecting this FC stack. Firstly, the peak power demand of the Eco-BEV in this simulation is 46 kW, thus, the selected FC stack should have a power over 46 kW to provide enough power. At the same time, for considerations of the FC system lifespan, maintaining the output power of the fuel cell below its peak, particularly around the nominal power, can significantly extend the system's lifespan. Operating under lower power conditions reduces the thermal and mechanical stress on key components, such as the proton exchange membrane (PEM) and catalyst layers. Excessive stress at high power outputs accelerates degradation through chemical, thermal, and mechanical pathways, thereby shortening the lifespan of the PEM. This optimisation strategy helps ensure the durability and efficiency of the fuel cell system (Madhav et al., 2024). Secondly, considering the real-world power demands of the popular BEVs in the UK, such as those with power demands like the Nissan Leaf and VW e-Golf which have peak power of 110 kW and 100 kW (Evspecifications, 2023; Evspecifications, 2024). Therefore, the decision is based on the fuel cell's ability to meet both current and potential future needs with a nominal power of 50 kW and a peak power of 120.4 kW which is well-suited to handle higher power demands during periods of rapid acceleration or when driving at high speeds.

The polarization curve of this FC is presented in Figure 4-12.

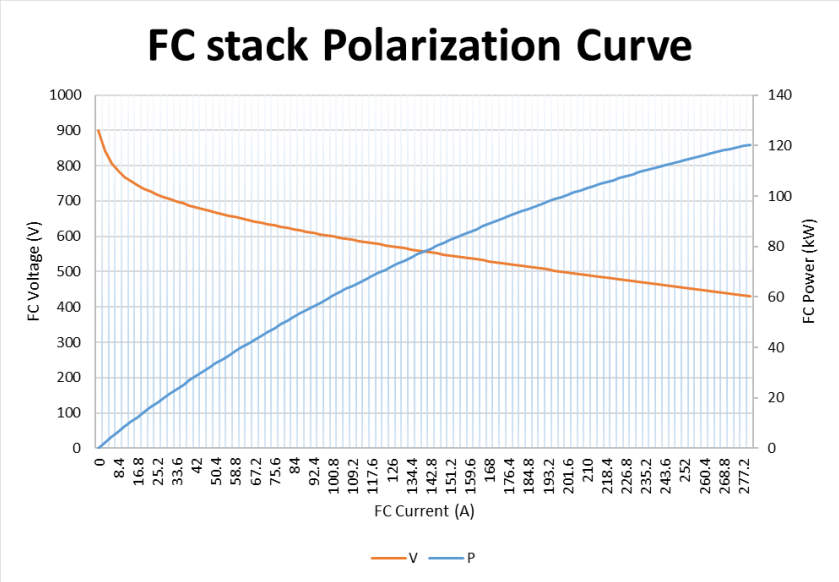

Figure 4-12 FC stack Polarization Curve (Matlab, 2019)

After the selection of the FC stack, the hydrogen tank capacity can be confirmed by inputting the parameters of the FC stack and the BEV to simulate the hydrogen consumption under the given duty cycle (Repeating extra-urban WLTP cycle with a simulation time of 20525s and 405.7 km driving distance), the output of hydrogen consumption was assumed as 90% of the total hydrogen tank capacity to avoid effects on energy consumption due to different driving behaviours leads the fluctuations on hydrogen consumption. This FC stack was connected to a DC-DC converter with a 97% efficiency in series and together connected in parallel to the vehicle's current bus.

In this simulation, an estimation of the FC range extender system weight was made as 300 kg (Toyota, 2021), which was added to the total weight of the vehicle. The EMS in this simulation regulated the battery SoC to remain around 40%, which means the FC system provides all the energy to get the total hydrogen gas consumption.

Through this simulation, the accumulated hydrogen gas consumption result is shown in Figure 4-13.

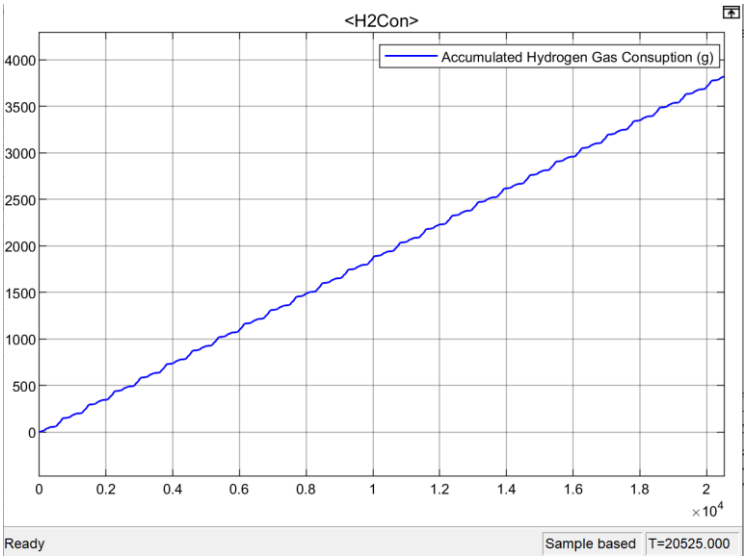

Figure 4-13 Accumulated hydrogen gas consumption (g) - hydrogen tank size definition simulation

The total hydrogen gas consumption was 3819 g where the overall FC system efficiency was 57.32%.

In this simulation, the battery SoC was regulated by the State-Machine control strategy to fluctuate slightly around 40% as Figure 4-14 shows (X-axis: battery SoC, Y-axis: simulation time).

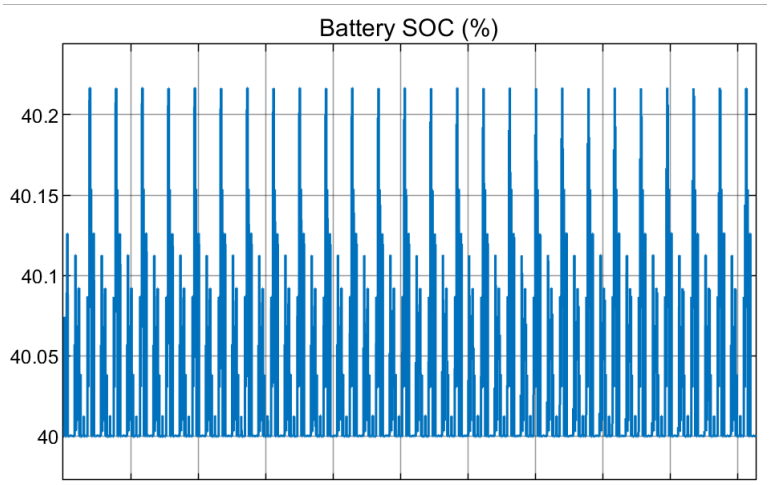

Figure 4-14 Battery SoC curve - hydrogen tank size definition simulation

However, the accumulated energy consumption from the battery was not zero at the end of this simulation due to the slight fluctuations in the battery SoC, the result of the total energy consumption of the battery was -251.3 Wh which means the battery was charged by the FC system for 251.3 Wh. Converting this energy consumption value with the FC system's overall efficiency (57.32%) and the nominal energy density of hydrogen gas (33.3 Wh/g), the equivalent hydrogen gas consumption of charging the battery was 13.16 g. Thus, the total hydrogen consumption in this simulation was

3805.84 ≈ 3806 g which is 90% of the target hydrogen tank capacity of this FC range extender. Therefore, the capacity of the hydrogen tank of this FC range extender should be 4229 g, it was set as 4.3 kg.

In conclusion, the parameters the proposed DHFCRE included an FC stack nominal power of 50 kW (625 V DC), a DC-DC converter with 97% efficiency and hydrogen tanks with a total capacity of 4.3 kg, the total weight of this FC range extender system was estimated as 300 kg.

4.4. Summary of Model Parameterisation

In this chapter, based on the analysis of existing scientific research, marketing information and transportation statistics published by the UK government, the key parameters of the components in the simulation model of the proposed “DHFCRE + Eco-BEV” powertrain concept and the competing powertrain of the full-size Large BEV were defined. The WLTP duty cycle is selected for the simulation and the development of EMS control strategies and the EPA duty cycle was used for EMS control system developments. The limitations of the duty cycle are summarised as follows:

A study has been conducted by the existing member in Coventry University Microcab Lab, using a real-world 3D duty cycle in a physical component-based Modelica/Dymola vehicle model to increase the result accuracy of more than 30% improvement compared to the result based on a 2D NEDC simulation in a simplified model (Apicella, 2019). In this project, the 2D WLTP duty cycle is used as the simulation duty cycle input, which is supposed to have a higher accuracy than the NEDC cycle. However, in this drive cycle, the road slope angle, the real-world wind speed, air temperature and air density changes are not considered. These may lead to changes in the vehicle’s rolling resistance and aerodynamic drag forces and the required power from the energy storage device will be changed to fulfil the increased power demand to move the vehicle based on the duty cycle requirements.

Chapter 5 Energy Management System

5.1. Introduction

According to the aims of this project, apart from the simulations for the performance evaluation of the proposed powertrain concept 'DHFCRE + Eco-BEV', the second aim of this project is to improve the performance of this powertrain concept including increasing associated vehicle functionality, overall energy efficiency and reduce cost. The implementation of scientific control strategies and algorithms for the Energy Management System (EMS) is one of the most effective methods to realise the improvements and optimisations for hybrid energy source vehicles (Kok, 2015; Ren, 2021). The methodology of this chapter includes following steps:

- Identify the functional requirements of the EMS for the proposed DHFCRE + Eco-BEV powertrain.
- Review the different types of EMS strategies and algorithms in the field of hybrid energy source vehicles.
- Develop the EMS algorithms based on the requirements and structure from literature.
- Test the EMS algorithms performance including battery management, energy distribution between battery pack and FC system, overall energy efficiency and fuel economy.
- Optimise the EMS by establishing a front-end program of selecting algorithms based on external information.

The main functional requirements of the EMS for the proposed DHFCRE is summarised as follows:

- Manage the energy flow in the DHFCRE + Eco-BEV powertrain combination system.
- Determine the timing and commands for main components such as charge/discharge of the battery, and the operation condition of the FC stack including idle, optimal power and full load.
- Monitor and regulate the key operating signals of the vehicle within the given constraints such as battery maximum charge power, FC output power, battery SoC condition, regenerative braking power, etc.
- Optimise the performance of the powertrain in terms of increasing energy efficiency and reducing fuel cost.

5.2. EMS Control Strategy Principles

For the multi-energy source vehicle applications, the EMS control strategies can be sorted into three types – Rule-Based (RB) control strategies, Optimisation-Based (OB) control strategies and Learning-Based (LB) control strategies (Sorlei et al., 2021; Ferahtia et al., 2023; Kok, 2015). This section will discuss the principles, advantages, shortages, requirements and application examples of the control strategies in these 3 types and determine the control strategies for the proposed 'DHFCRE + Eco-BEV' powertrain concept.

5.2.1. Rule-Based (RB) EMS

A rule-based strategy, in the context of energy management for hybrid and fuel cell electric vehicles, involves the utilisation of predefined rules or algorithms to direct the management of energy within the vehicle. These rules are established based on certain criteria or conditions related to the vehicle's operation, such as the state of charge (SoC) of the battery, vehicle speed, and power demand. The most widely used RB strategies include State-Machine control strategy, Proportional and Integral (PI) control strategy, Fuzzy Logic (FL) control strategy, etc. The features of the Rule-Based (RB) EMS can be summarised as follows (Sorlei et al., 2021; Ferahtia et al., 2023; Ren, 2021):

1) **Advantages**
   - Simplicity in implementation and operation with high adaptivity.
   - Requires minimal computational resources.
   - Effective in scenarios with predictable operating conditions.

2) Shortages
   - Potential suboptimal performance outside predefined conditions.
   - Performance significantly depends on the preset parameters and rules.

3) Implementation requirements
   - Can be implemented with basic vehicle parameters and driving cycles.
   - No need for a pre-trained model based on simulation or real-world experiments or extensive database.

4) Application examples
   - The State-Machine control strategy is used in the Toyota Prius hybrid vehicle and employs a distinctive energy management strategy through its Hybrid Synergy Drive (HSD) system. This system intricately balances the use of an electric motor and an internal combustion engine to optimize energy efficiency,

a critical aspect in reducing fuel consumption and emissions while maintaining satisfactory driving performance (Biddle, 2014).

- The Fuzzy Logic (FL) control strategy is used in an FCEV control system which increases the fuel economy and overall energy efficiency of the FCEV as well as optimises the battery SoC response which prolongs the battery lifespan (Ren, 2021).

5.2.2. Optimisation-Based (OB) EMS

The Optimisation-Based (OB) strategies involve the use of mathematical optimisation techniques to find the most efficient way to use energy sources. This approach can vary from static optimisation methods, which are based on predefined driving cycles, to dynamic methods that adjust in real-time based on current conditions, including global optimisation and real-time optimisations (Sorlei et al., 2021). There are several popular OB EMSs for hybrid vehicles: Dynamic Programming (DP) strategy, Pontryagin's minimum principle (PMP), equivalent consumption minimisation strategy (ECMS), external energy minimisation strategy (EEMS), etc. The features of the Optimisation-Based (OB) EMS can be summarised as follows (Ferahtia et al., 2023; Kok, 2015):

1) Advantages

- Potential for higher efficiency by finding optimal solutions within defined parameters.
- Flexibility in adjusting objectives based on desired outcomes in real-time, providing a flexible and adaptive approach to energy management.

2) Shortages

- High computational demand, possibly unsuitable for real-time applications.
- Significant dependency on accurate and comprehensive vehicle models.
- Real-time optimisation can be challenging to implement in vehicles due to latency issues.

3) Implementation requirements

- Requires detailed vehicle modelling and possibly a substantial database to inform the optimisation process.
- Understanding the vehicle's potential driving cycles is beneficial for predictive optimisation models.

4) Application examples

- An adaptive ECMS strategy was implemented in an FCEV city bus project in China, it increased the fuel economy and prolonged the lifespan of both the battery pack and FC stack. (Xu et al., 2009).
- Pontryagin's minimum principle (PMP) is used in an FCEV control system which reduces the hydrogen consumption of the FCEV at the same time extends the battery lifespan (Li et al., 2019).

5.2.3. Learning-Based (LB) EMS

Learning-based (LB) strategies in EMS leverage the power of Machine Learning (ML) and Artificial Intelligence (AI) to dynamically optimize the energy distribution between different power sources within a vehicle. Unlike rule-based or optimisation-based strategies that rely on predefined rules or mathematical models, learning-based approaches adapt and improve over time based on data (Reddy et al., 2019). The core mechanism involves collecting vast amounts of operational data from the vehicle, including driving patterns, speed, acceleration, battery State of Charge (SoC), and external conditions like terrain and weather. LB algorithms such as Reinforcement Learning (RL) and Neural Networks (NNs) can analyse internal and external data to identify patterns and make predictions on the most efficient energy usage for given conditions. The features of the Optimisation-based (OB) EMS can be summarised as follows: (Sorlei et al., 2021; Ferahtia et al., 2023; Kok, 2015)

1) **Advantages**

- LB strategies can be highly adaptable to the driver's behaviour, vehicle condition, and external environment, optimizing energy usage over time.
- LB strategies usually provide continuous improvements, as more data is collected, the system's performance can continuously improve, potentially uncovering new strategies for energy savings.

2) **Shortages**

- LB approaches, especially deep learning models, require substantial computational power, which can be a constraint in onboard vehicle systems.
- Significant amounts of diverse and high-quality data are needed to train the models effectively. This can be a barrier to entry early in the deployment.
- LB models, particularly deep learning models, can be complex and act as "black boxes," making it difficult to understand how decisions are made.

3) **Implementation requirements**

- Data collection and processing requirement: the target vehicles require sensors and data logging capabilities to collect the necessary operational data. Additionally, data preprocessing and feature selection are critical steps to ensure model accuracy.
- High-performance computational hardware is necessary to run these models in real-time. Alternatively, some processing can be offloaded to cloud-based systems, though this introduces latency and reliance on continuous connectivity.
- Initial model training requires a substantial dataset, often obtained from simulations or real-world driving data. Periodic updates and retraining with new data are necessary to maintain and improve system performance.

4) Application examples

- Tesla's electric vehicles leverage machine learning in various aspects of vehicle operation, including energy management. Tesla's approach to data collection and analysis allows for continuous updates and improvements to vehicle efficiency and battery management strategies (Tesla US, 2019).
- An LB energy management strategy based on the Markov Chain is implemented in the EMS of a hybrid vehicle with an ultra-capacitor and battery pack, it increases the energy efficiency of the vehicle and extends the range without oversizing the vehicle or sacrificing drivability (Kok, 2015).

5.2.4. EMS Principles Summary

In the context of advancing energy management strategies within the domain of hybrid and hydrogen fuel cell vehicles, the above review embodies a multifaceted approach aimed at elevating vehicle efficiency and sustainability. The findings can be summarised as follows: The mentioned three types of EMS have been widely used in multi-energy source vehicle applications and realised performance optimisations in different cases from both industrial and experimental perspectives. RB strategies are notable for their simplicity and reliability, providing a strong basis for initial tests in new powertrain concepts, especially when limited by computational resources. OB strategies, through mathematical models, lead to better efficiency but need more computing power or existing experimental results. LB strategies can offer qualified adaptability and continuous improvement but require high-performance databases or pre-trained models as well as advanced computing hardware.

This project focus leans towards harnessing RB and OB strategies as a starting point for evaluating the performance of the tested control logic on this novel powertrain concept of DHFCRE + Eco-BEV. Then using simplified LB strategies which require only basic computational resources, the LB strategy will be trained model by existing simulation results generated by RB and OB strategies instead of experimental data due to the limited resources. Since the cooperation between Coventry University and Microcab Ltd has terminated while this project is ongoing, real-world experiments are not available for the database generation and accumulation of experimental data. Also, the FCEV hardware of EMS and high-performance computational resources are limited. This approach allows for the exploration of EMS within manageable computational demands and without the necessity for large datasets or advanced modelling capabilities. Through the simulation results of the different strategies under different drive cycles and vehicle parameters, the advantages and shortcomings of the tested control strategies under certain conditions can be identified. This will be valuable for the further optimisations of the EMS for the DHFCRE with a range of supporting results from different simulations under different conditions. The key requirements of the EMS algorithms include maintaining the battery SoC, battery and FC power at a healthy level, and increasing the vehicle's energy efficiency or fuel economy performance.

After the establishment of the EMS algorithms in the Matlab/Simulink model, each EMS will be tested by undertaking a test simulation under a given duty cycle to evaluate the performance of different EMS in terms of the management result on battery SoC, battery and FC output powers, vehicle overall energy efficiency and fuel cost. The test procedure for SoC, battery power and FC power involves monitoring the SoC and power curves plotted from the simulation results to ensure they meet the specified constraints. The measurement of overall energy efficiency is the total accumulated energy consumption combining battery electricity and hydrogen fuel consumption in Wh/km. The fuel cost in the EMS testing simulation includes the electricity and hydrogen gas cost in GBP. The price of electricity and hydrogen gas was collected through online retailer information in Dec 2022, where the electricity price is £0.74 /kWh (E. ON, 2022), and the hydrogen gas price: is £12 /kg (AutoTrader, 2022).

The energy management strategies in this project are classified into three levels. The first level is the basic strategy which means the energy flows under the passive physical rules with a small number of external control instructions (State-Machine EMS based on rules and actions). The second level is the advanced control algorithms which have complex rules, equations and learnings to realise detailed control

instructions for the output parameters including the Fuzzy Logic as a special RB EMS, ECMS as an OB EMS and the ANN model as an LB EMS. The third level is the 'upgraded strategy', which provides further optimisations for the selected control algorithms by connecting the external information and conditions including the driver's essential preference (such as least time consumption (fewer charging times), lowest fuel cost, and highest vehicle overall energy efficiency), charging infrastructure availability. The EMS optimisation flow chart is shown in Figure 5-1.

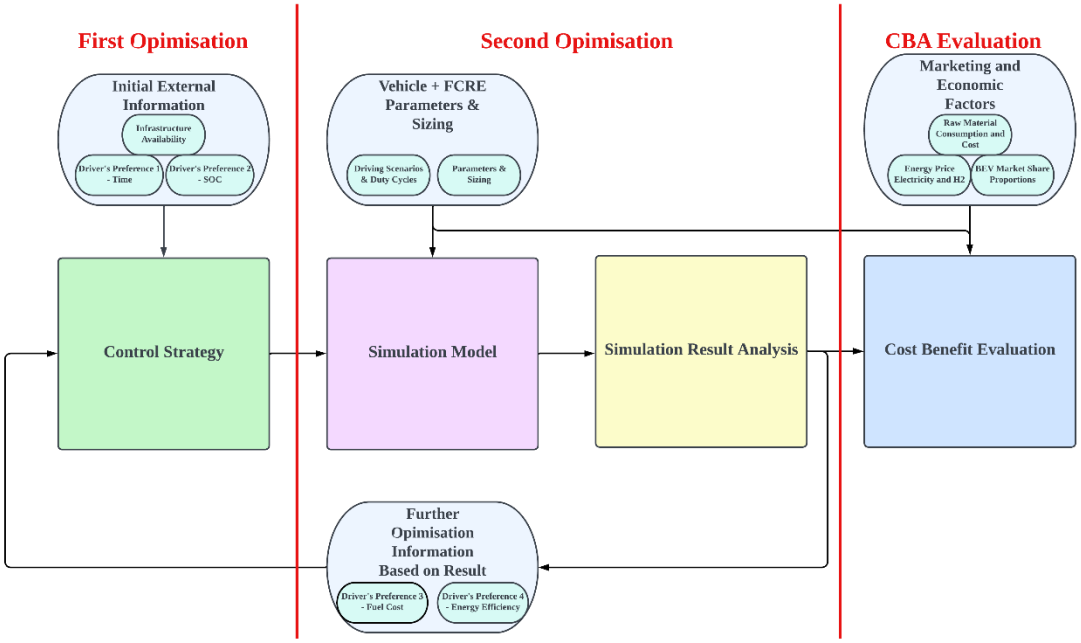

Figure 5-1 EMS optimisation flow chart

Apart from the initial external information, the performance of control strategies will be evaluated through simulation results under different driving scenarios including urban, extra-urban and mixed duty cycles. Through the result analysis, the superiorities of different control strategies in terms of overall vehicle energy efficiency and fuel economy will be highlighted which can provide further information for the EMS optimisation and provide more options to the BEV driver. Finally, by adding the marketing and economic factors, the Cost Benefit Analysis (CBA) from the macroscope perspective will be conducted to present the macro-economic and environmental impacts of the proposed DHFCRE system.

5.3. State-Machine EMS

5.3.1. State-Machine EMS Principles

The first RB strategy is the State-Machine control strategy based on the basic rules which offers control instructions while the inputs are under important changes. In this

model, the important changes in the inputs include (but are not limited to) – u(1) the vehicle required power ($> 0\ or\ \leq 0$), and u(2) the battery SoC (if the SoC is under the healthy level). This energy management strategy is developed in the state machine of the Matlab/Simulink platform as Figure 5-2 shows.

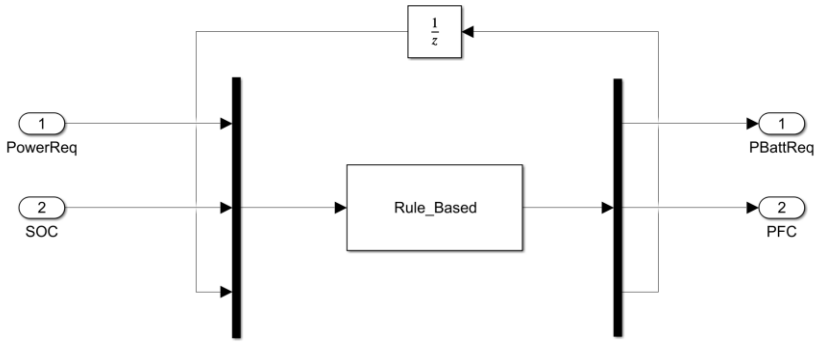

Figure 5-2 State-Machine control strategy illustration

5.3.2. Parameter Setup and Logic Description

In order to regulate the strategy to produce actions to outputs, the parameterisation of boundary values of the inputs and outputs will need to be set at the beginning of the development.

The input/output parameters were defined and listed below:

$\mathrm{u}(1)$ is the required power (kW)

$\mathrm{u}(2)$ is the state of charge (SoC) of the battery

Pfc is the FC power (kW)

$Pbatt$ is the battery power (kW)

The boundary values were listed below:

- Minimum SoC: $SOC_{min} = 10\%$
- Maximum SoC: $SOC_{max} = 90\%$
- Optimal SoC 1: $SOC_{opt1} = 70\%$
- Optimal SoC 2: $SOC_{opt2} = 40\%$
- Battery maximum charge power: $P_{batt\_char\_max} = -10\ kW$
- Maximum FC power: $Pfc_{max} = 50\ kW - \ the\ \max power\ of\ the\ FC$
- FC Idle power: $Pfc_{min} = 2\ kW - \ the\ \mathrm{idle}\ power\ of\ the\ FC$

- Optimal FC power: $Pfc_{opt} = 40\ kW -\ the\ \text{optimal}\ power\ of\ the\ FC$

The battery maximum charge power is determined by considering both the lower limit of the vehicle required power (- 33 kW) and the battery allowed maximum charging referring to Section 4.3.3 which is - 10 kW.

The considerations of the maximum and optimal power of FC includes the technical data of the Eco-BEV (referring to Section 4.3.1) and the technical data of the FC system (referring to Section 4.3.3). The range of required power of the Eco-BEV is from (-) 33 kW to (+) 46 kW, after adding the weight of the FCRE system the upper limit of required power increased to (+) 51 kW. The technical data of maximum output power of the FC system is about 120 kW and the optimal output power of the FC system is 50 kW. Therefore, the FC max power of 50 kW can fulfil all the required power of the vehicle at the same time ensure the FC system operating under its optimal working conditions.

The State-Machine algorithm were defined as the following state flows:

First stage: confirm the vehicle's drive mode based on the required power $u(1)$.

1) **Regenerative mode**: $u(1) \leq 0$

In the first mode, the required power of the vehicle is a negative value which means the re-generative motor supplies the power to charge the battery.

2) **Drive mode 1**: $u(1) \geq Pfc_{max}$

In the second mode, the required power of the vehicle is very high and its higher than the maximum power of the FC (> 50 kW)

3) **Drive mode 2**: $Pfc_{max} + P_{batt\_char\_max} \leq u(1) < Pfc_{max}$

In the third mode, the required power of the vehicle is in the range of 40 kW to 50 kW.

4) **Drive mode 3**: $Pfc_{opt} + P_{batt\_char\_max} \leq u(1)\ < Pfc_{max} + P_{batt\_char\_max}$

In the fourth mode, the required power of the vehicle is in the range of 30 kW to 40 kW.

5) **Drive mode 4**: $0 < u(1)\ < Pfc_{opt} + P_{batt\_char\_max}$

In the fifth mode, the required power of the vehicle is in the range of 0 to 30 kW.

2nd stage: regulate the values of outputs based on the battery SoC condition cases and preset control logics and rules

1) **Regenerative mode**: $u(1) \leq 0$ (when required power is lower than 0 kW)
   a) **Case 1**: $\mathrm{u}(2) \geq SOC_{max}$ (when battery SoC is over 90%)

In the **Case 1** of **Regenerative mode**, if the battery SoC is over the maximum SoC (**90%**), then

$$Pfc = 0 \text{ and } Pbatt = 0$$

This means in the regenerative mode, when the current battery SoC is greater or equal to 90%, the output power of the battery and FC are both **0**, at this condition, the **FC system** is turned **off** and the **regenerative motor** is turned **off**.

   b) **Case 2**: $\mathrm{u}(2) < SOC_{max}$ (when battery SoC is lower than 90%)

In the **Case 2 of Regenerative mode**, if the battery SoC is in the **lower** than the maximum SoC (**90%**), at the same time, the value of required power is **smaller** than $P_{batt\_char\_max} + Pfc_{min}$ (**-8 kW**), then

$$Pfc = Pfc_{min} \text{ and } Pbatt = P_{batt\_char\_max}$$

It means in the regenerative mode, when the current battery SoC is lower than 90% and the power demand is in the range from -8 kW to 0, the **FC system** is turned to **idle** mode and output power of FC is **2 kW** to prevent frequently turning on and off of the FC (protect the FC system and prolong its lifespan). The **regenerative motor** is turned **on** to charge the battery with its maximum charge power **(-) 10 kW**.

   c) **Case 3**: $\mathrm{u}(2) < SOC_{max}$ (when battery SoC is lower than 90%)

In the **Case 3 of Regenerative mode**, if the battery SoC is in the **lower** than the maximum SoC (**90%**), at the same time, the value of required power is **greater** than $u(1) > P_{batt\_char\_max} + Pfc_{min}$ (**-8 kW**), then

$$Pbatt = P_{batt\_char\_max} \; and \; Pfc = \; u(1) - Pbatt$$

It means in the regenerative mode, when the current battery SoC is lower than 90% and the power demand is lower than -8 kW. The **regenerative motor** is turned **on** to charge the battery with its maximum charge power **(-) 10 kW**. The **FC system** is turned on, and the output power of FC equals the **required power minus battery power**.

2) **Drive mode 1**: $u(1) \; \geq Pfc_{max}$ (when required power is higher than 50 kW)

In the **Drive mode 1**, the output power of FC and battery are fixed values with respectively:

$$Pfc = Pfc_{max} \text{ and } Pbatt = u(1) - Pfc_{max}$$

It means in **Drive mode 1,** when the power demand is over the maximum power of FC, the **FC system** works as the primary power source, its power output is the FC maximum power (**50 kW**) and the **battery pack** output power equals to **power demand minus FC maximum power**.

3) **Drive mode 2**: $Pfc_{max} + P_{batt\_char\_max} \leq -u(1) < Pfc_{max}$ (when required power in the range of 40 – 50 kW)
   a) **Case 1**: $u(2) \geq SOC_{max}$ (when battery SoC is over 90%)

In the **Case 1** of the **Drive mode 2**, if the battery SoC is over the maximum SoC (**90%**), then

$$Pfc = Pfc_{min} \; and \; Pbatt = u(1) - Pfc$$

It means in the **Drive mode 2**, when the current battery SoC is over or equal to 90%, the FC system is turned **idle** with an output power of **2 kW** and the **battery pack** works as the primary power source, its output power equals the **power demand minus FC power**.

   b) **Case 2**: $SOC_{opt2} \leq u(2) < SOC_{max}$ (when battery SoC is in the range of 40% – 90%)

In the **Case 2** of the **Drive mode 2**, if the battery SoC is in the range from the Optimal SoC 2 (**40%**) to the maximum SoC (**90%**), then

$$Pfc = Pfc_{min} \text{ and } Pbatt = u(1) - Pfc$$

It means in the **Drive mode 2**, when the current SoC is within the range of 40% - 90%, the **FC system** is turned **idle** with an output power of **2 kW** and the **battery pack** works as the primary power source, its output power equals the **power demand minus FC power**.

   c) **Case 3**: $SOC_{min} < u(2) < SOC_{opt2}$ (when battery SoC is in the range of 10% – 40%)

In the **Case 3** of the **Drive mode 2**, if the battery SoC is in the range from the Minimum SoC (**10%**) to the Optimal SoC 2 (**40%**), then

$$Pfc = Pfc_{opt} \; and \; Pbatt = u(1) - Pfc$$

It means in the **Drive mode 2**, when the battery SoC is within the range of 10% - 40%, the **FC system** is the primary power source, it is turned to its optimal output with an

output power of (**40 kW**) to supply the vehicle power demand as well as charge the battery. The **battery pack** charging power equals the **demanded power minus the FC power**.

d) **Case 4**: $u(2) \leq SOC_{min}$ (when battery SoC is lower than 10%)

In the **Case 4** of the **Drive mode 2**, if the battery SoC is lower than the minimum SoC (**10%**),

$$Pfc = Pfc_{max} \; and \; Pbatt = u(1) - Pfc_{max}$$

It means in the drive model, when the current SoC is lower than 10%, the **FC system** is the primary power source, it is turned to its maximum output with an output power of (**50 kW**) to supply the vehicle power demand as well as charge the battery. The **battery pack** charging power equals the **demanded power minus the FC power**.

4) **Drive mode 3**: $Pfc_{opt} + P_{batt\_char\_max} \leq \mathrm{u}(1) < Pfc_{max} + P_{batt\_char\_max}$ (when required power in the range of 30 – 40 kW)
   a) **Case 1**: $u(2) \geq SOC_{max}$ (when battery SoC is over 90%)

In the **Case 1** of the **Drive mode 3**, if the battery SoC is over the maximum SoC (**90%**), then

$$Pfc = Pfc_{min} \; and \; Pbatt = u(1) - Pfc$$

It means in the **Drive mode 3**, when the current battery SoC is over or equal to 90%, the FC system is turned **idle** with an output power of **2 kW** and the **battery pack** works as the primary power source, its output power equals the **power demand minus FC power**.

b) **Case 2**: $SOC_{opt2} \leq u(2) < SOC_{max}$ (when battery SoC is in the range of 40% – 90%)

In the **Case 2** of the **Drive mode 3**, if the battery SoC is in the range from the Optimal SoC 2 (**40%**) to the maximum SoC (**90%**), then

$$Pfc = Pfc_{min} \text{ and } Pbatt = \mathrm{u}(1) - Pfc$$

It means in the **Drive mode 3**, when the current SoC is within the range of 40% - 90%, the **FC system** is turned **idle** with an output power of **2 kW** and the **battery pack** works as the primary power source, its output power equals the **power demand minus FC power**.

c) **Case 3**: $SOC_{min} < u(2) < SOC_{opt2}$ (when battery SoC is in the range of 10% – 40%))

In the **Case 3** of the **Drive mode 3**, if the battery SoC is in the range from the Minimum SoC (**10%**) to the Optimal SoC 2 (**40%**), then

$$Pfc = Pfc_{opt} \; and \; Pbatt = u(1) - Pfc$$

It means in the **Drive mode 3**, when the battery SoC is within the range of 10% - 40%, the **FC system** is the primary power source, it is turned to its optimal output with an output power of (**40 kW**) to supply the vehicle power demand as well as charge the battery. The **battery pack** charging power equals the **required power minus the FC power**.

d) **Case 4**: $u(2) \leq SOC_{min}$ (when battery SoC is lower than 10%)

In the **Case 4** of the **Drive mode 3**, if the battery SoC is lower than the minimum SoC (**10%**), then

$$Pbatt = P_{batt\_char\_max} \; and \; Pfc = u(1) - Pbatt$$

It means in the **Drive mode 3**, when the battery SoC is within the range of 10% - 40%, the FC system is the primary power source and the **battery pack** is charged by its maximum charging power of (**-10 kW**). The output power of **FC system** equals to the **required power minus the battery power.**

5) **Drive mode 4**: $0 < u(1) < Pfc_{opt} + P_{batt\_char\_max}$ (when required power in the range of 0 – 30 kW)

a) **Case 1**: $u(2) \geq SOC_{max}$ (when battery SoC is over 90%)

In the **Case 1** of the **Drive mode 4**, if the battery SoC is over the maximum SoC (**90%**), then

$$Pfc = Pfc_{min} \; and \; Pbatt = u(1) - Pfc$$

It means in the **Drive mode 4**, when the current battery SoC is over or equal to 90%, the FC system is turned **idle** with an output power of **2 kW** and the **battery pack** works as the primary power source, its output power equals the **power demand minus FC power**.

b) **Case 2**: $SOC_{opt2} \leq u(2) < SOC_{max}$ (when battery SoC is in the range of 40% – 90%)

In the **Case 2** of the **Drive mode 4**, if the battery SoC is in the range from the Optimal SoC 2 (**40%**) to the maximum SoC (**90%**), then

$$Pfc = Pfc_{min} \text{ and } Pbatt = \text{u(1)} - Pfc$$

It means in the **Drive mode 4**, when the current SoC is within the range of 40% - 90%, the **FC system** is turned **idle** with an output power of **2 kW** and the **battery pack** works as the primary power source, its output power equals the **power demand minus FC power**.

c) **Case 3**: $u(2) \leq SOC_{opt2}$ (when the battery SoC is lower than 40%)

In the **Case 3** of the **Drive mode 4**, if the battery SoC is lower than the Optimal SoC 2 (**40%**), then

$$Pbatt = P_{batt\_char\_max} \; and \; Pfc = u(1) - Pbatt$$

It means in the **Drive mode 4**, when the current SoC is lower than 40%, the FC system is the primary power source and the **battery pack** is charged by its maximum charging power of (**-10 kW**). The output power of **FC system** equals to the **required power minus the battery power.**

The full Matlab code of this State-Machine algorithm is presented in Appendix 2.1.

5.3.3. State-Machine EMS Test

The test of this State-Machine control strategy focused on the battery SoC fluctuations to examine the performance of regulating the battery SoC during long-distance journeys while at the same time monitoring the battery and FC power. The method of this simulation was to use the parameters of the Eco-BEV and the range extender as input (mentioned in Section 4.3), the initial battery SoC is set as 95%, then selected the State-Machine control strategy in the EMS under the repeating WLTP extra-urban drive cycles. The length of per drive cycle was 15.412 km and the duration was 778 s, in this testing simulation, 13 times repeating of this WLTP extra-urban cycle was the duty cycle input, and the focusing output was the battery SoC curve.

- **Battery SoC plot**

The simulation result of the battery SoC plot is presented in Figure 5-3

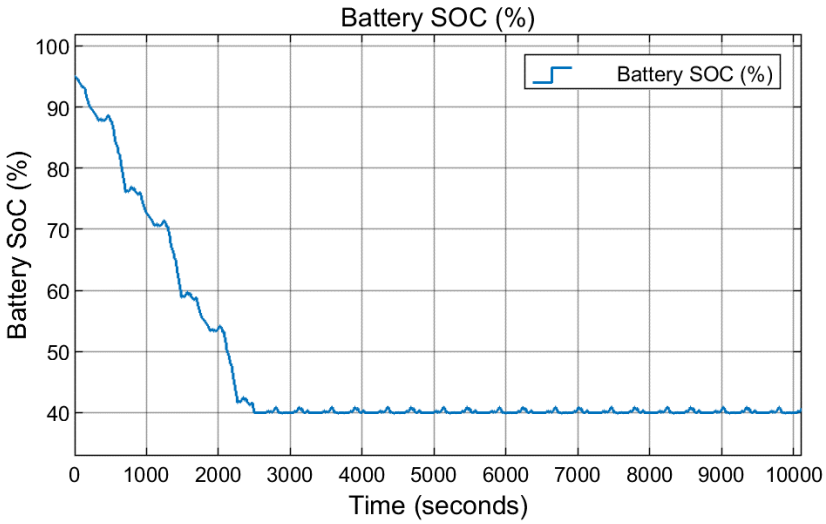

Figure 5-3 Battery SoC plot – State-Machine control strategy test

The battery SoC curve shows that under the control of the State-Machine strategy, the battery is the primary power source while the SoC is higher than 40%. When the SoC reach the lower limit of battery nominal SoC, the FC system supplies the main part of the energy to power the vehicle. The fluctuations of SoC near to 40% is due to the re-generative braking power charged to the battery pack during the decelerations. This State-Machine control strategy can maintain the battery SoC at around 40% to protect the battery and extend its lifespan.

- **Battery and FC power plot**

The simulation result of the battery and FC power plot is presented in Figure 5-4 the orange line is FC power and the blue line is battery power.

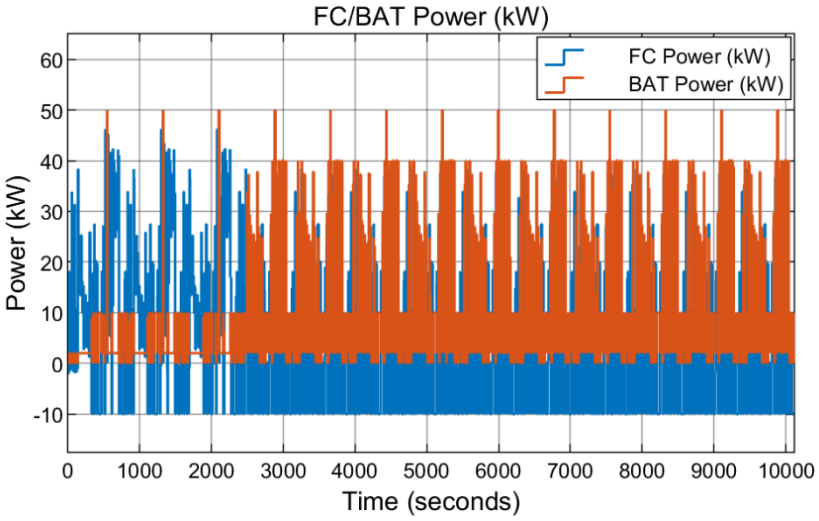

Figure 5-4 Plot of battery and FC power – State-Machine control strategy test

The battery and FC power plot graph proves that firstly, the battery power was regulated within the range of -10 kW to 46 kW. According to Section 4.3.2, the maximum charge and discharge power of the battery pack is -10 kW and 50 kW, thus, this range is within the safety range of the battery pack. For the FC stack, the output power fluctuated from 2 to 50 kW which is under the safety range of the FC output which means under the control of this algorithm, the FC stack is not turned off and on frequently, this would be useful to extend the lifespan for the FC stack (Nguyen et al., 2021).

- **Vehicle overall energy efficiency and fuel cost**

The results of overall energy efficiency and fuel cost from the State-Machine EMS test simulation were 298 Wh/km and £24.16, respectively.

5.4. Fuzzy Logic EMS

5.4.1. Fuzzy Logic Principles

Fuzzy Logic control constitutes a computerised digital control technology founded on fuzzy set theory, fuzzy linguistic variables, and Fuzzy Logic reasoning. It is recognised as a distinct type of Rule-Based (RB) control strategy (Sorlei et al., 2021). In 1965, scientist L.A. Zadeh established the foundations of fuzzy set theory in the United States (Zadeh, 1965). By 1973, he had delineated the concept of Fuzzy Logic control along with related theorems (Zadeh, 1973). Subsequently, in 1974, E.H. Mamdani in the United Kingdom developed the first fuzzy controller, which was premised on fuzzy control statements. He implemented this control strategy in the management of boilers and steam engines, achieving significant laboratory success (Mamdani, 1974). This pioneering endeavour signalled the inception of fuzzy controllers. Fuzzy Logic controllers have since become extensively utilised across various modern industries. The fuzzy control strategy is a kind of nonlinear control strategies, which belongs to the category of intelligent control. A major feature of fuzzy control is that it has both a systematic theory and a large number of practical applications (Johnson, 2022).

Compared with Boolean Logic which only allows the variable to be either Yes/1 or No/0, as Figure 5-5 shows that fuzzy Logic is a form of many-valued logic in which the truth value of a variable can be any real number between 0 and 1. It is used to deal with the concept of partial truth, where the truth value may be between completely true and completely false (Yes or No) (Novák, Perfilieva and Močkoř, 1999).

The Fuzzy Logic control strategy is widely used in the low-carbon vehicle area, especially for those that have more than one kind of power energy such as hybrid electric vehicles and hydrogen fuel cell electric vehicles. This part will introduce some representative applications of fuzzy controllers in these areas and the performance of the fuzzy controllers. (Ma et al., 2019).

Figure 5-5: Fuzzy Logic vs Boolean Logic (Chai, 2022)

The architecture of the Fuzzy Logic controller is usually designed in the following structure as Figure 5-6 shows.

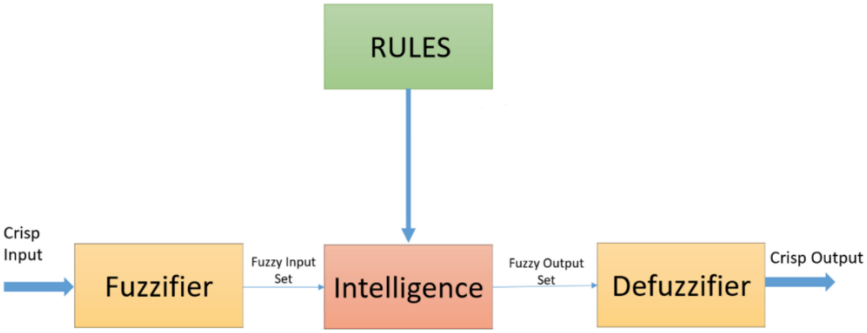

Figure 5-6 Architecture of Fuzzy Logic Controller (Johnson, 2022)

The working process of fuzzy controllers includes the following steps (Johnson, 2022)

- **Fuzzification:**

The initial step involves allocating the inputs to fuzzy sets with specified degrees of membership, which can range anywhere within the interval [0,1]. If the input is 0, it does not belong to the respective fuzzy set; conversely, an input of 1 signifies complete

membership within the set. Values between 0 and 1 reflect the degree of uncertainty regarding membership in the set. Fuzzy sets are typically characterised using linguistic descriptors, thereby facilitating reasoning about system inputs in a linguistically intuitive manner. A fuzzy set is commonly represented as either a triangular or trapezoidal curve, characterised by a rising slope, a peak where the value reaches 1 (the peak's width can be 0 or greater), followed by a declining slope.

- **Rules instalment:**

The second step is to install rules for the fuzzy controller. Fuzzy Logic handles member values in a way that mimics Boolean logic. For this, substitutions for the basic operators AND, OR, and NOT must be available. There are several ways to do this. A common alternative is called the Zadeh operator, where:

In Boolean logic:

AND(x,y)

OR(x,y)

NO(x)

In Fuzzy logic:

MIN(x,y)

MAX(x,y)

1 – x

For TRUE/1 and FALSE/0, the Boolean expressions have the same result as the Fuzzy expressions.

The IF/THEN rule is one of the most popular rules in fuzzy controllers. Using the above hot water boiler example, the rules can be set in the following format:

IF temperature IS cold THEN boiler_power is high

IF temperature IS warm THEN boiler_power is moderate

IF the temperature IS hot THEN boiler_power is low

Given a certain temperature, the fuzzy variable hot has a certain true value and is copied to the high variable. If the output variable appears in several THEN parts, the OR operator is used to combine the values of the individual IF parts.

- **Defuzzification:**

The last step is defuzzification, which outputs a crisp continuous variable from fuzzy values. One popular method of defuzzification is to cut the membership function area for a fuzzy value and combine the resulting curves using the OR operator. Then find the centre-of-weight of the area under the curve, the x position of this point is the final output. (Johnson, 2022).

5.4.2. Parameter Setup and Description

According to Section 3.4.2, the inputs of the energy management system are the total required power and battery SoC, and the outputs are the power of the FC system and battery. The first layer (Figure 5-7) of this Fuzzy Logic based control system to confirm the driving mode (driving or regenerative braking).

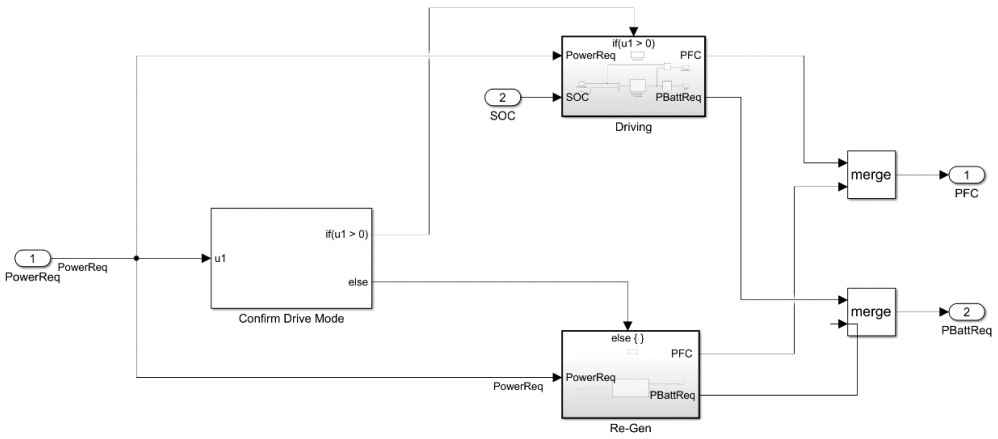

Figure 5-7 Fuzzy Logic control system structure – first layer

The second layer (Figure 5-8) of the Fuzzy Logic EMS is the fundamental function of the Fuzzy Logic algorithm.

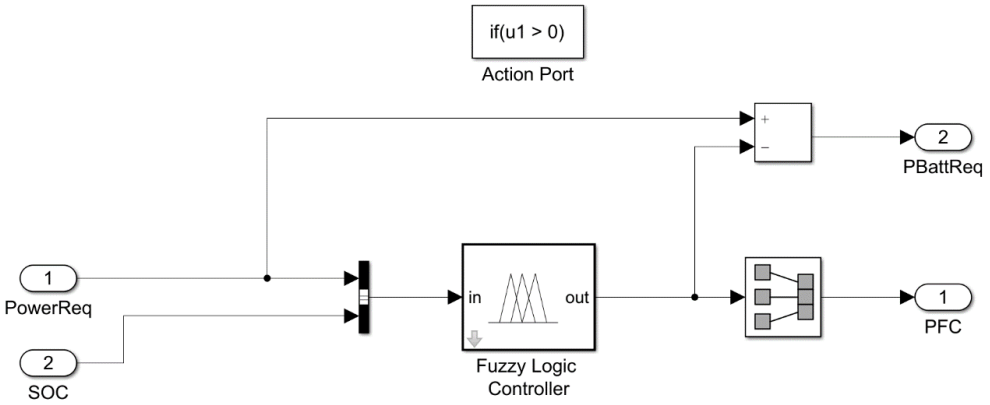

Figure 5-8 Fuzzy Logic control system structure – fundamental layer

The fuzzy controller will regulate the output value of the power of the FC system based on the fuzzy algorithm and the output battery power is calculated from the total required power minus FC power.

According to the discussions from Section 5.4.1 about the fuzzy logic principles and design methodology, the development processes of the Fuzzy Logic controller include 2 steps, with respectively membership function setup and rules development. As Figure 5-9 shows, that the fuzzy controller developed by using the Matlab Fuzzy Logic Designer includes 2 inputs, 1 output, 3 membership functions and 12 Mamdani style rules.

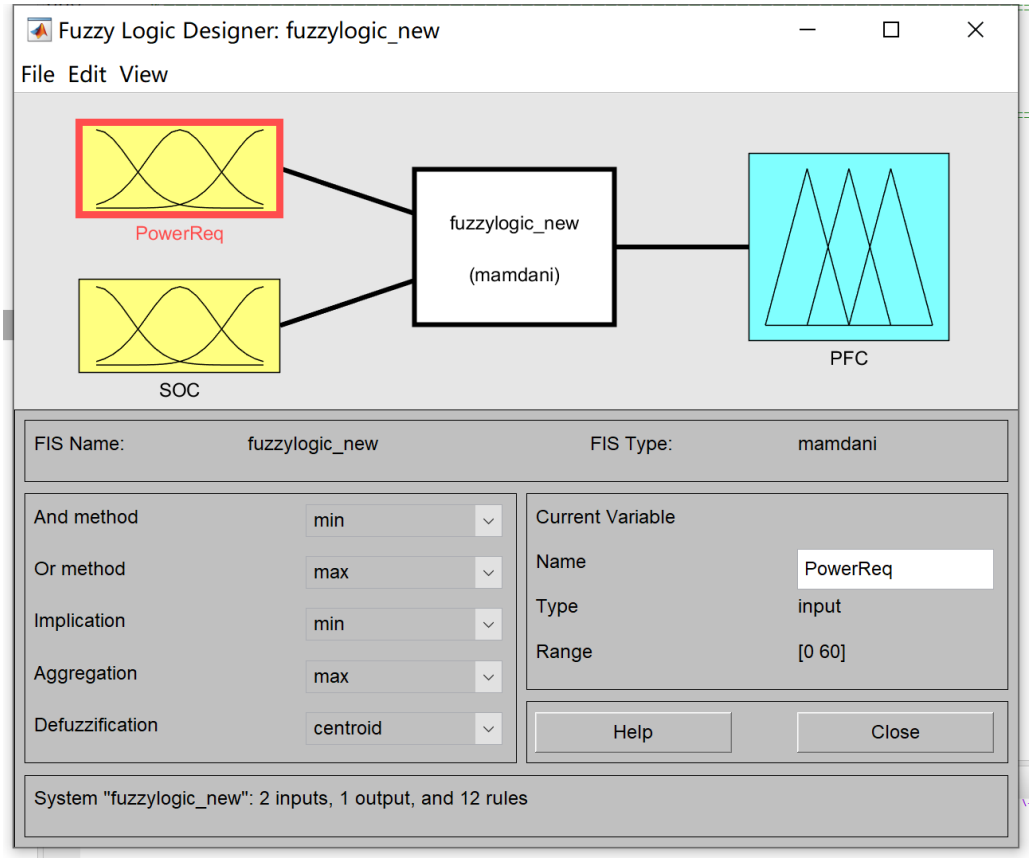

Figure 5-9 Fuzzy Logic controller structure in Matlab

There were 3 membership functions in this Fuzzy Logic controller (Figure 5-10),

- Input 1 – PowerReq – Total required power (kW)
- Input 2 – SoC – Battery SoC (%)
- Output – PFC – FC system power (kW)

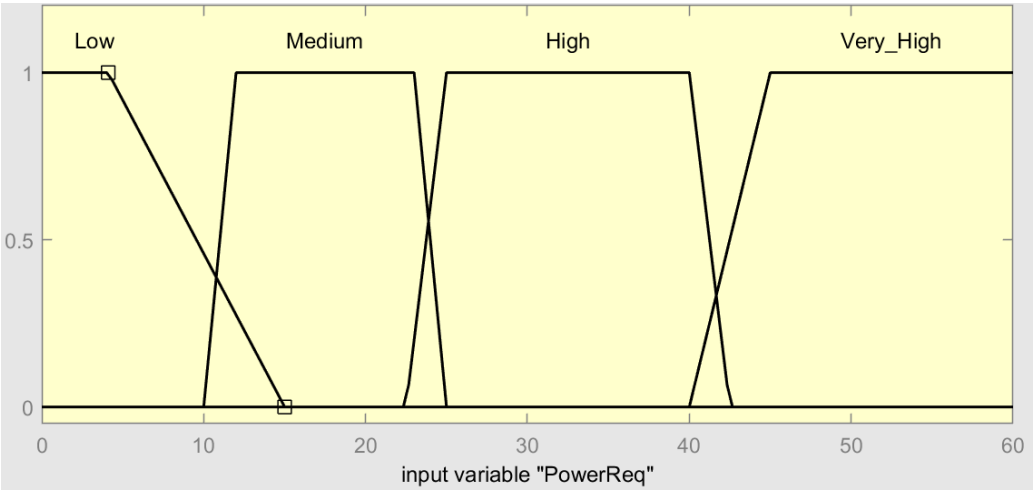

(a)

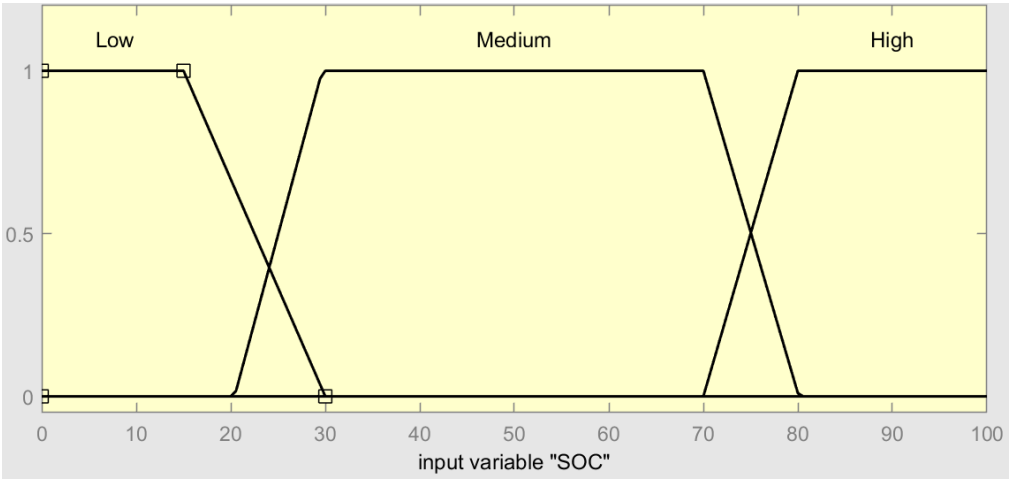

(b)

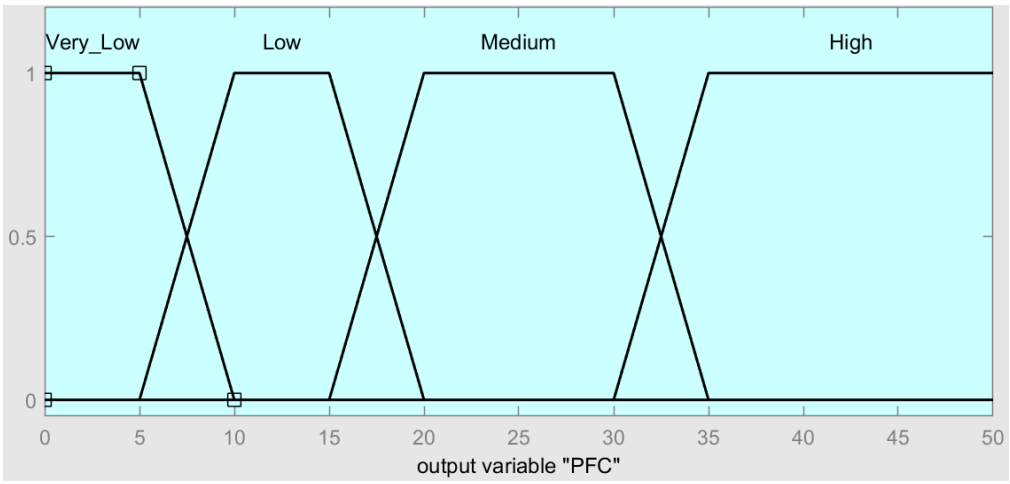

(c)

Figure 5-10 Membership functions of fuzzy controller

The Mamdani-style rules of this fuzzy controller are:

- If (PowerReq is Low) and (SoC is Low) then (PFC is High)
- If (PowerReq is Low) and (SoC is Medium) then (PFC is Low)
- If (PowerReq is Low) and (SoC is High) then (PFC is Very Low)
- If (PowerReq is Medium) and (SoC is Low) then (PFC is High)
- If (PowerReq is Medium) and (SoC is Medium) then (PFC is Medium)
- If (PowerReq is Medium) and (SoC is High) then (PFC is Very Low)
- If (PowerReq is High) and (SoC is Low) then (PFC is High)
- If (PowerReq is High) and (SoC is Medium) then (PFC is Medium)
- If (PowerReq is High) and (SoC is High) then (PFC is Very Low)
- If (PowerReq is Very High) and (SoC is Low) then (PFC is High)
- If (PowerReq is Very High) and (SoC is Medium) then (PFC is Medium)
- If (PowerReq is Very High) and (SoC is High) then (PFC is Very Low)

Regulated by the above membership functions and rules, the output of the FC system power surface graph is shown in Figure 5-11.

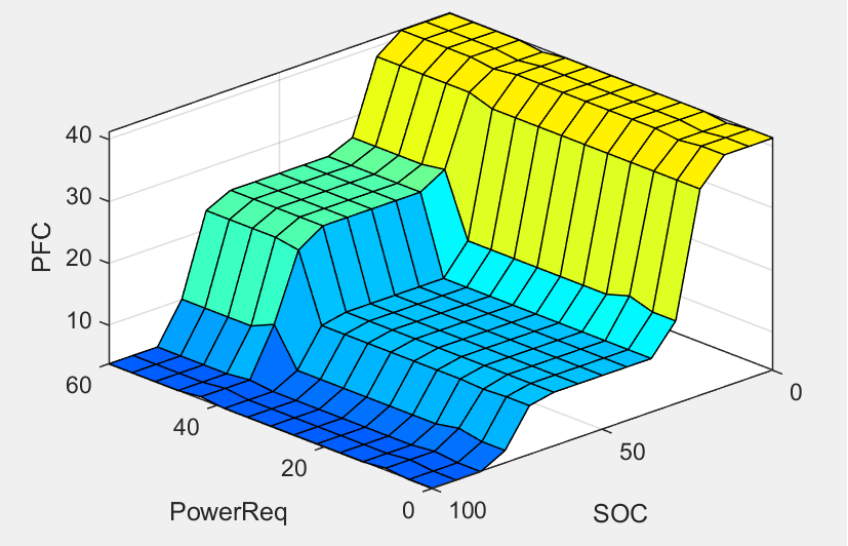

Figure 5-11 Fuzzy Logic output FC power surface graph

The settings of parameters, membership functions and rules involve the considerations of the range of inputs power required for different vehicles and duty cycles, battery nominal SoC with considerations on battery SoH, as well as the idling, nominal and maximum power of the FC system.

5.4.3. Fuzzy Logic EMS Test

Similar to the test on the State-Machine control strategy, the test of this Fuzzy Logic EMS algorithm also focused on the battery SoC curve to examine the performance of regulating the battery SoC during long-distance journeys. The method of this simulation was to use the parameters of the Eco-BEV and the range extender as input (mentioned in Section 4.3), the initial battery SoC was set as 95%, then select Fuzzy Logic controller in the EMS, under the repeating WLTP extra-urban drive cycles. The length of per drive cycle was 15.412 km and the duration was 778s, in this testing simulation, 13 times of repeating of this WLTP extra-urban cycle is the duty cycle input the focused outputs were the battery SoC and the battery/FC power plots.

- **Battery SoC plot**

The simulation result of the battery SoC plot is presented in Figure 5-12.

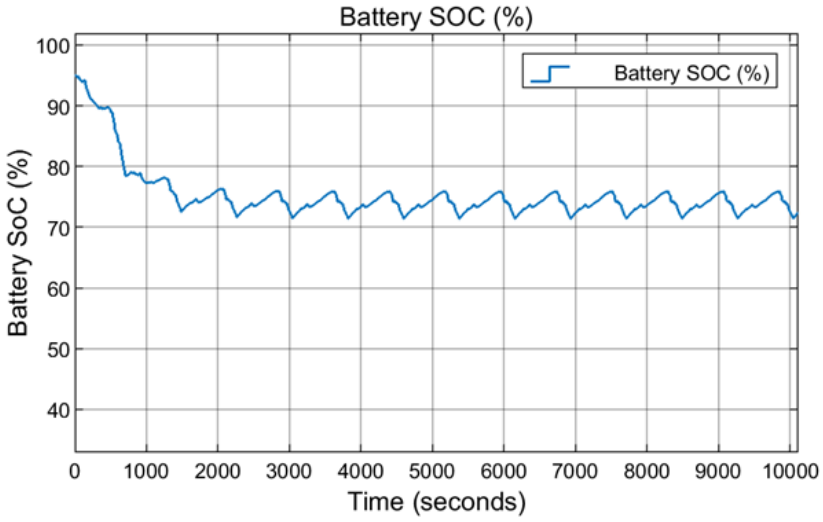

Figure 5-12 Battery SoC curve – Fuzzy Logic control strategy test

The battery SoC curve shows that under the control of this Fuzzy Logic controller, the battery was the primary power source while the SoC is higher than 80%. When the SoC reached the membership function 'medium' of battery SoC, the power from the FC system increased gradually from 'low' to 'medium' and supplies the main part of the energy to power the vehicle. This Fuzzy Logic control strategy can regulate the battery SoC to gradually fluctuate between 70% and 80% to protect the battery and extend its lifespan as well as keep the battery energy within a relevant-high level to fulfil the potential range demands for the remaining urban driving.

- **Battery and FC power plot**

The simulation result of the battery and FC power plot is presented in Figure 5-13 the orange line is FC power and the blue line is battery power.

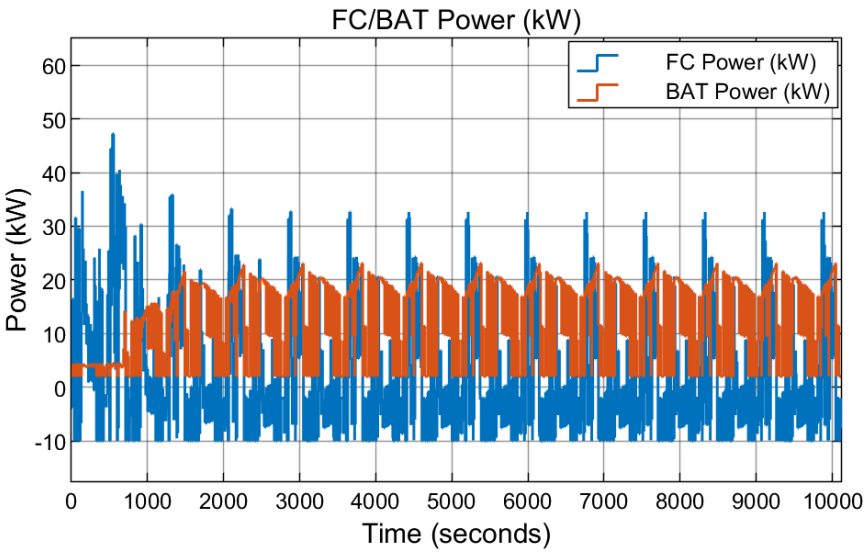

Figure 5-13 Plot of battery and FC power – Fuzzy Logic EMS test

The battery and FC power plot graph proves that firstly, the battery power was regulated within the range of -10 kW to 46 kW which is under the safety range of the battery pack. For the FC stack, the output power fluctuated from 2 to 25 kW which is under the safety range of the FC output power. Also, the FC power did not reach 0 which means during the whole simulation, the FC system was not turned off, this can extend the lifespan of the FC stack.

- **Vehicle overall energy efficiency and fuel cost**

The results of overall energy efficiency and fuel cost from the Fuzzy Logic EMS test simulation were 297.7 Wh/km and £22.58, respectively.

5.5. Equivalent Consumption Minimisation Strategy (ECMS)

5.5.1. ECMS Principles

The Equivalent Consumption Minimization Strategy (ECMS) is an optimisation-based energy management strategy first introduced by Paganelli in 1999. This strategy simplifies the global minimization issue into an instantaneous minimization problem that is solved at each moment, employing considerations based solely on the actual energy flow in the powertrain (Han et al., 2012; Sorlei et al., 2021). In the automotive sector, ECMS is extensively applied as Pontryagin's Minimum Principle (PMP) Energy Management System (EMS) for vehicles that utilise multiple energy sources, such as Hybrid Electric Vehicles (HEV) and Fuel Cell Electric Vehicles (FCEV) (Chen et al., 2021). ECMS is known for its computational efficiency, as it delivers instantaneous optimal control. Moreover, it has been demonstrated to reduce fuel consumption under specific conditions and offers a heuristic approach to solving the optimal control problem, thereby providing an effective solution to the HEV energy management challenge (Guzzella and Sciarretta, 2005).

In this project, the purpose of introducing the ECMS is to meet some special driver demands in real-world driving conditions with the consideration of the current high price of hydrogen gas. (AutoTrader, 2022). In this case, ECMS is developed to provide control actions to minimise the consumption of hydrogen energy.

5.5.2. Parameter Setup and Description

The ECMS controller in this model is developed by using the Matlab S-Function and the demonstration of the structure of the ECMS controller is shown in Figure 5-14.

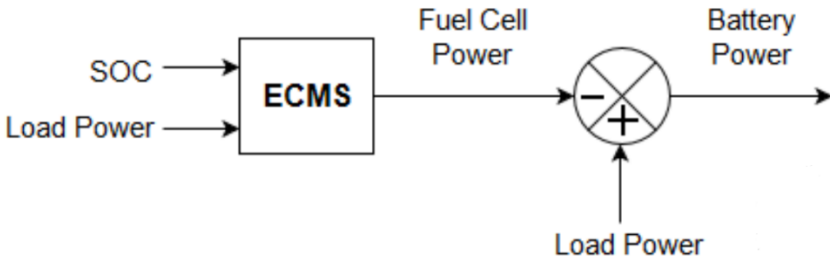

Figure 5-14 ECMS controller demonstration (Bassam et al., 2016)

The first layer (Figure 5-15) of this Matlab/Simulink-based ECMS controller regulates the minimum battery SoC as 10% to avoid the deep-discharge of the battery and affect the battery's SoH.

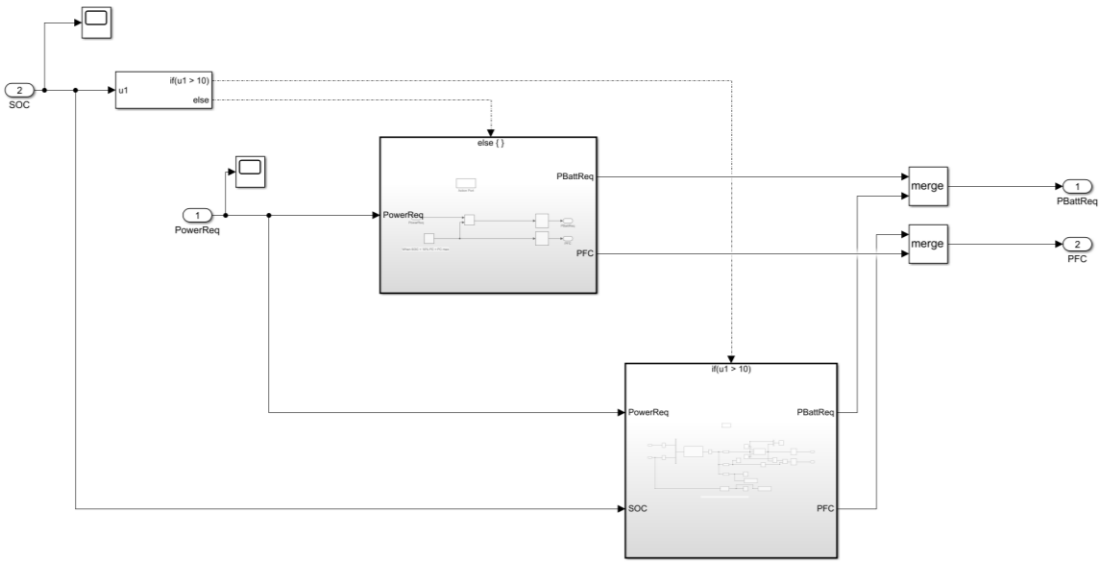

Figure 5-15 ECMS controller structure - first layer

The second layer (Figure 5-16) of the ECMS controller is the fundamental Matlab S-Function and relative calculations.

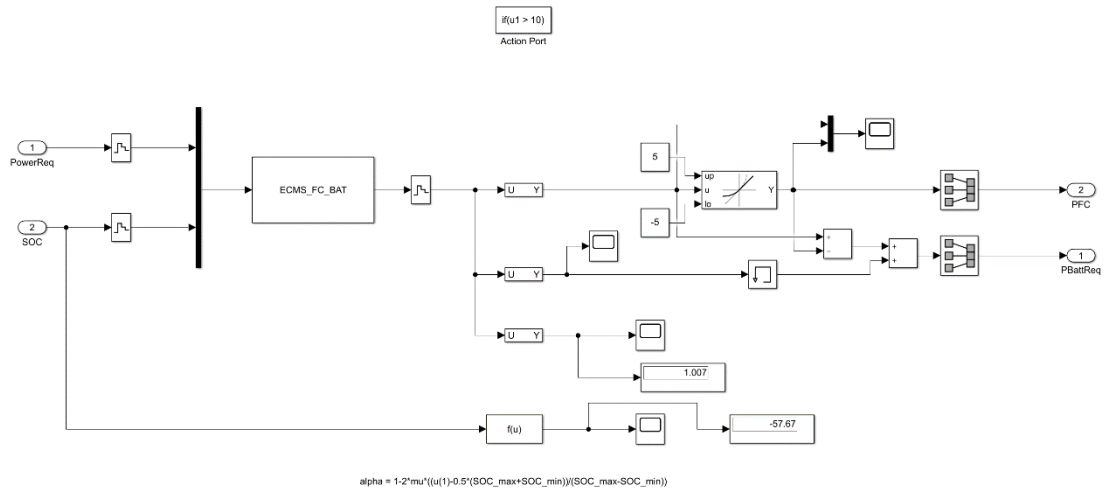

Figure 5-16 ECMS controller structure - fundamental layer

The design methodology of this Matlab S-Function based ECMS controller is to minimise the energy consumption and required power of the FC system with the consideration of battery SoC. The function was developed by using the 'fmincon' function of Matlab which is presented in Equation 5-1,

$$F_{ECMS} = min(J_{FC} + \beta J_{Batt}) \quad (5\text{-}1)$$

Where

J_{FC} is FC energy consumption in (Wh).

J_{Batt} is battery energy consumption (Wh).

β is the battery energy penalty coefficient

And

$$\begin{cases} J_{FC} = P_{FC} \cdot \Delta t \\ J_{Batt} = P_{Batt} \cdot \Delta t \end{cases} \quad (5\text{-}2)$$

Where

P_{FC} is the fuel cell output power (W)

P_{Batt} is the battery output power (W)

Δt is the sample time of the Matlab/Simulink model

This ECMS controller implemented the battery energy penalty coefficient (Equation 5-3) to balance the battery SoC. (Xu et al., 2009; Hafsi et al., 2022).

$$\beta = 1 - 2\mu \frac{[SOC - 0.5(SOC_{max} + SOC_{min})]}{SOC_{max} + SOC_{min}} \quad (5\text{-}3)$$

Where

μ is the constant to reflect the battery charge and discharge characteristics. (He & Yang, 2006; Hafsi et al., 2022).

SOC is the current battery state of charge.

SOC_{max} is the maximum battery state of charge (set as 90%).

SOC_{min} is the minimum battery state of charge(set as 10%)

The variable is defined as

$x = [P_{FC}, \beta, P_{Batt}]$

The boundary conditions of variables in the ECMS function are defined as (Hafsi et al., 2022).

$[P_{FC\_max} \leq P_{FC} \leq P_{FC\_min}]$

$[0 \leq \beta \leq 5]$

$[-P_{Batt\_max} \leq P_{Batt} \leq P_{Batt\_max}]$

The ECMS algorithm Matlab code is presented in the Appendix 2.2.

5.5.3. ECMS Control Algorithm Test

The test methodology of this ECMS control algorithm was to focus on the battery SoC curve to examine the performance of regulating the battery SoC during long-distance journeys at the same time monitoring if the battery and FC system output power are within the safety range. The method of this simulation was to use the parameters of the Eco-BEV and the range extender as input (mentioned in Section 4.3), the initial battery SoC was set as 95%, then select the ECMS control algorithm in the EMS under the repeating WLTP extra-urban drive cycles. The length of per drive cycle was 15.412 km and the duration was 778s, in this testing simulation, 13 times repeating of this WLTP extra-urban cycle is the duty cycle input, and the focusing output is the battery SoC curve.

- **Battery SoC plot**

The simulation result of the battery SoC plot is presented in Figure 5-17.

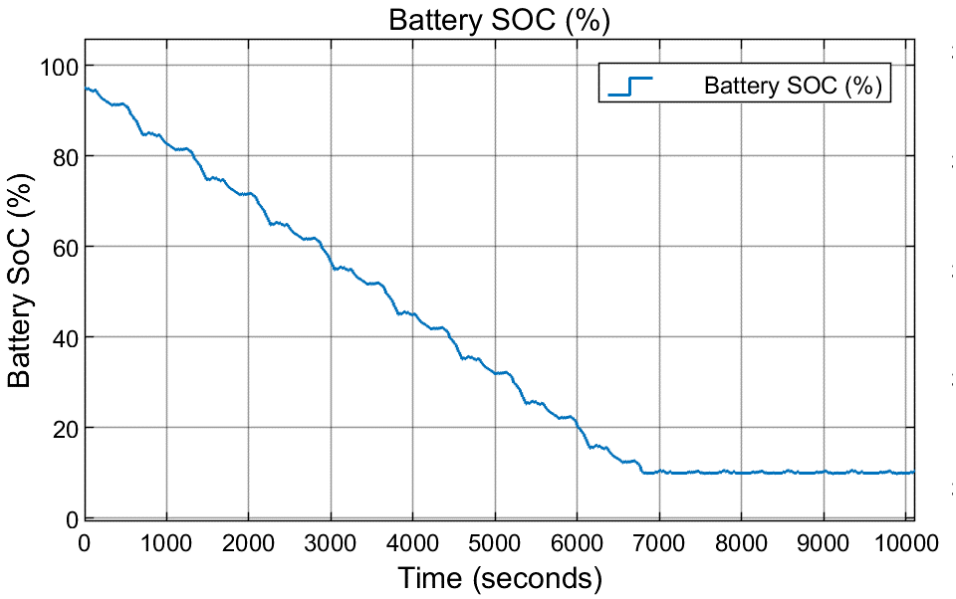

Figure 5-17 Battery SoC curve – ECMS control strategy test

The battery SoC curve shows that under the control of this ECMS controller, the battery was the primary power source while the SoC was higher than 10%. When the SoC reached the pre-set lowest limit of SoC at 10%, the fluctuation of SoC was very slight around 10%. The ECMS controller can minimise hydrogen fuel consumption by preferentially using energy from the battery pack. However, studies proved that the optimal SoC range of battery to protect its lifespan is about 20% to 80%, the over-charging and over-discharging should be avoided (Dini et al., 2024; Espedal et al., 2021; Huang, 2019). And this ECMS controller has risk to decrease the lifespan of the battery pack.

- **Battery and FC power plot**

The simulation result of the battery and FC power plot is presented in Figure 5-18 the orange line is FC power and the blue line is battery power.

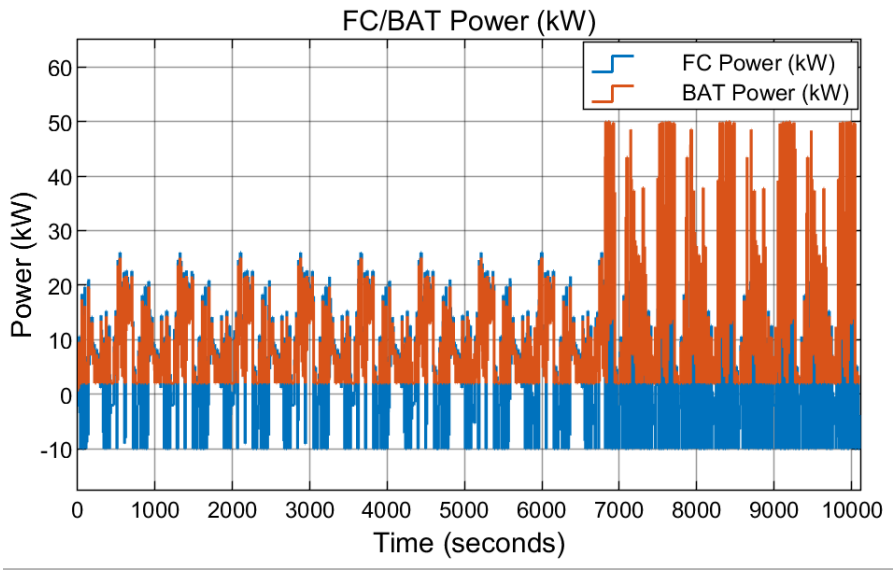

Figure 5-18 Plot of battery and FC power – ECMS EMS test

The battery and FC power plot graph proves that firstly, the battery power was regulated within the range of -10 kW to 30 kW which is under the safety range of the battery pack. For the FC stack, the output power fluctuated from 2 to 50 kW which is under the safety range of the FC output power. Also, the FC power did not reach 0 before the battery SoC was lower than the upper limit of 90%, which means during the rest of the simulation, the FC system is not turned off, this can extend the lifespan of the FC stack.

- **Vehicle overall energy efficiency and fuel cost**

The results of overall energy efficiency and fuel cost from the EMCS control algorithm test simulation were 273.3 Wh/km and £23.91, respectively.

5.6. Artificial Neural Network (ANN) EMS

5.6.1. ANN EMS Principles

The Artificial Neural Network (ANN) is a Learning-Based (LB) control strategy which is regarded as a pivotal facet of machine learning, designed to mimic the human brain's ability to learn from and interpret complex patterns. Since its conception, ANN has significantly influenced the landscape of research and development in Artificial Intelligence (AI) (Fogel et al., 1990). ANN comprise interconnected nodes and neurons, which are organised in layers: an input layer, one or more hidden layers, and an output layer. The efficacy of an ANN depends on the weight adjustments made during the training phase, where the network learns by adjusting these weights based on a given

feedback mechanism, commonly known as backpropagation (Janiesch et al., 2021). ANNs are versatile in their application, prominently featured in areas such as image and speech recognition, natural language processing, and predictive analytics, their ability to process large datasets and identify patterns makes them invaluable for complex decision-making processes (Thakur, 2021). In the automotive industry, ANNs are instrumental in advancing autonomous driving technologies, vehicle tracking, and predictive maintenance. For instance, Tesla employs neural networks for its Autopilot system, enhancing vehicle autonomy by processing vast amounts of data from vehicle sensors (Kumari & Bhat, 2021). Another application is predictive maintenance, where ANNs forecast potential vehicle malfunctions, thereby minimising downtime and maintenance costs (Xie et al., 2018). Also, ANNs can be utilised in the EMS of hybrid energy source vehicles to manage the energy flow of the vehicle (Sorlei et al., 2021).

Artificial Neural Networks (ANNs) operate based on a structure and functionality that closely mimic the biological neural networks of the human brain, Figure 5-19 shows the framework of an ANN model. Each neuron in an ANN receives inputs, which are then processed using weights that signify the importance of each input. These inputs are summed and passed through an activation function to determine whether the neuron will fire and to what extent.

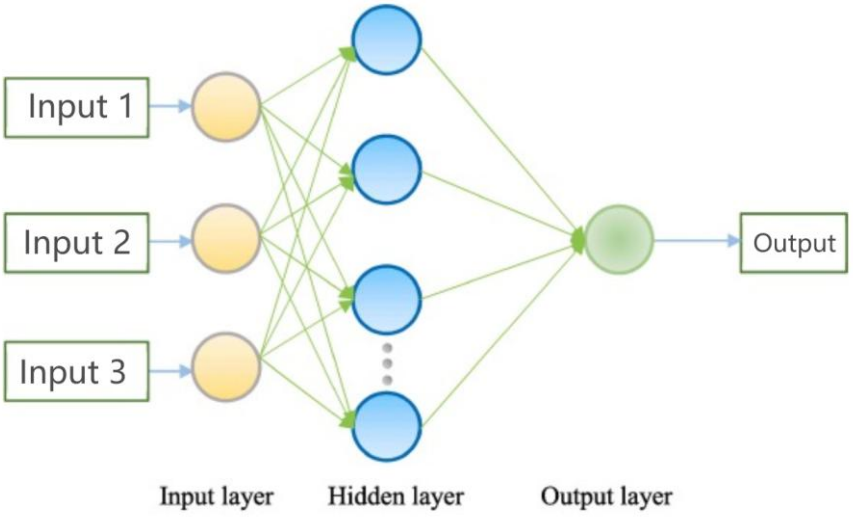

Figure 5-19 ANN model framework demonstration (Hafsi et al., 2022).

The structure of the ANN model involves several key components including (Millo et al., 2023):

- Input Layer: Receives the raw input data.

- Hidden Layers: Layers of neurons that apply weights to the inputs and pass them through activation functions to introduce non-linearities into the system, enabling the network to learn complex patterns.
- Output Layer: Produces the final output of the network.
- Weights and Biases: Parameters adjusted during training to minimise error.

5.6.2. Parameter Setup and Description

In this project, the most significant feature of ANN is that it can learn the output behaviour of the target parameter from the complex or invisible control algorithms. In the ideal condition, it can learn the control rules from a market-ready FCEV (such as Coventry University Microcab FCEV and Toyota Mirai FCEV) by analysing and learning from a large number of experimental data for the targeting input and output parameters, such as total power demand, battery SoC and output FC power. The performance of ANN depends on the design of the ANN structure design, the quality and scale of the experimental data, it can be trained to perform complex functions in various fields. However, due to the termination of Coventry University and Microcab, real-world experimental data is not available for training the ANN. An alternative method to train the ANN EMS is using the existing simulation results as the database for its learning (Hafsi et al., 2022; Sorlei et al., 2021). In this section, the simulation results of the proposed powertrain concept while using the Fuzzy Logic EMS under different duty cycles are used for training the ANN EMS. The reason for selecting Fuzzy Logic EMS results are twofold, firstly, compared with the test result of the Fuzzy Logic EMS, the State-Machine EMS has lower overall vehicle energy efficiency and higher fuel cost, and the training data should be selected from the best performance EMS. Secondly, even the ECMS algorithm has the highest overall energy efficiency, since it is a real-time optimisation function-based strategy, it calculates the minimised equivalent energy consumption for each sample time, which leads to a long simulation time. The data for training ANN requires a large scale of existing data under a large number of different duty cycles, using the ECMS algorithm to generate results for ANN training will consume longer time than Fuzzy Logic which will affect the efficiency of the project. Also, since ECMS is a real-time optimisation function-based strategy, the fluctuation range of the output parameter is much higher than the Fuzzy Logic, therefore, it is hard for the ANN model to build functions between inputs and outputs and will potentially affect the ANN EMS performance.

The ANN model is established in the Neural Network Toolbox of Matlab/Simulink, the inputs are set as two with respectively the power demand and the battery SoC, and

the output is the output power of the FC system. The structure of this ANN-based EMS is presented in Figure 5-20.

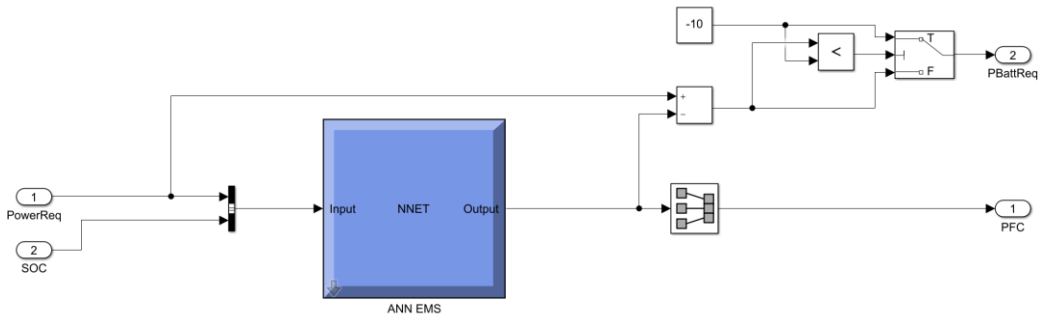

Figure 5-20 ANN-based EMS model structure in Matlab/Simulink

The main function of this ANN-based EMS is to calculate the output FC power through the trained functions related to the inputted power demand and battery SoC signals at the same time to regulate the battery charge power within the given constraint of battery maximum charge power.

The ANN EMS employed within this model is a two-layer feed-forward network, comprising sigmoid neurons in the hidden layer and linear neurons in the output layer. This configuration enables the network to adeptly fit multi-dimensional mapping problems, provided the data are consistent and the hidden layer contains a sufficient number of neurons. The preferred training method is the Levenberg-Marquardt backpropagation algorithm; however, should there be insufficient memory, the scaled conjugate gradient backpropagation method will be utilised instead (MathWorks, 2019).

The training data used for this ANN is generated from the simulation results of this model using Fuzzy Logic EMS under a number of different duty cycles including WLTP (urban and extra-urban), NEDC, EPA (FTP-72, FTP-75 and HWFET) and Japanese JC08 cycles. In total, 369065 sample results of the monitored parameters (power demand, SoC and FC power) are generated and utilised in the training for this ANN model. As Figure 5-21 shows, 70% of the data are used for training the ANN model and 15% are used for validation and testing.

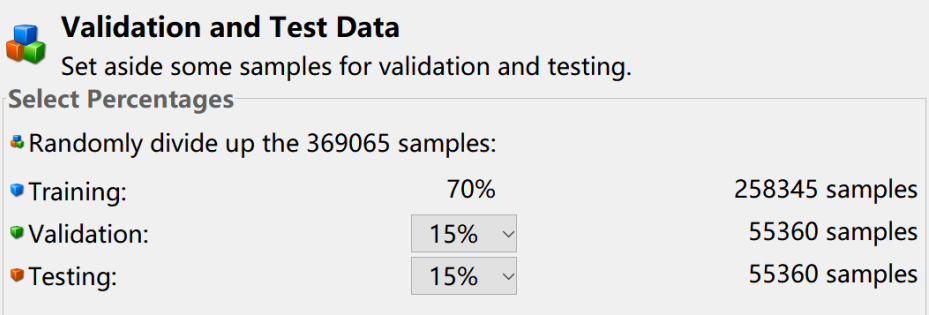

Figure 5-21 ANN training procedure.

The validation data here is used to measure network generalisation and to halt training when generalization stops improving. The testing data is for providing an independent measure of network performance during and after training (MathWorks, 2019). The structure of this ANN EMS model is presented in Figure 5-22.

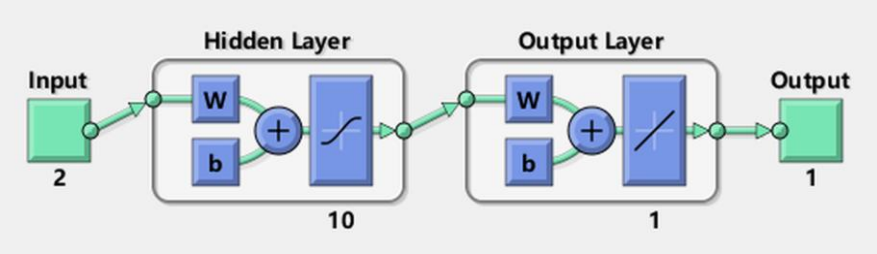

Figure 5-22 ANN EMS model structure

This ANN model has 2 inputs of power demand and battery SoC, 10 neurons in the hidden layer and 1 output layer with 1 output parameter of FC power.

This toolbox encompasses several training algorithms, including the Levenberg-Marquardt algorithm, Bayesian Regularisation, and the Scaled Conjugate Gradient method. The Levenberg Marquardt algorithm, whilst demanding greater memory, necessitates less time. Training ceases automatically when there is no further improvement in generalisation, as evidenced by a rise in the mean square error of the validation samples. Bayesian Regularisation, albeit time-intensive, is capable of achieving robust generalisation in challenging, diminutive, or noisy datasets. The training concludes based on adaptive weight minimisation (regularisation). The Scaled Conjugate Gradient method is less demanding in terms of memory. Training termination occurs automatically upon the deterioration of generalisation, signalled by an elevation in the mean square error of the validation samples (MathWorks, 2019). Since the scale of the training data prepared from the simulation is large, the Scaled Conjugate Gradient is selected.

The training results are presented in Figure 5-23 and Figure 5-24. Figure 5-23 illustrates the Mean Squared Error (MSE) performance of the neural network across epochs for training, validation, and test sets. Notably, the best validation performance was achieved at epoch 590 with an MSE of approximately 2.0534, as indicated by the dotted line. This suggests that the model was able to generalise in a relatively high since the validation error was low. The model did not overfit, as seen by the consistent decrease in error up to the 590th epoch, after which training was appropriately halted to prevent overfitting. The training and programming Matlab codes are presented in Appendix 2.3.

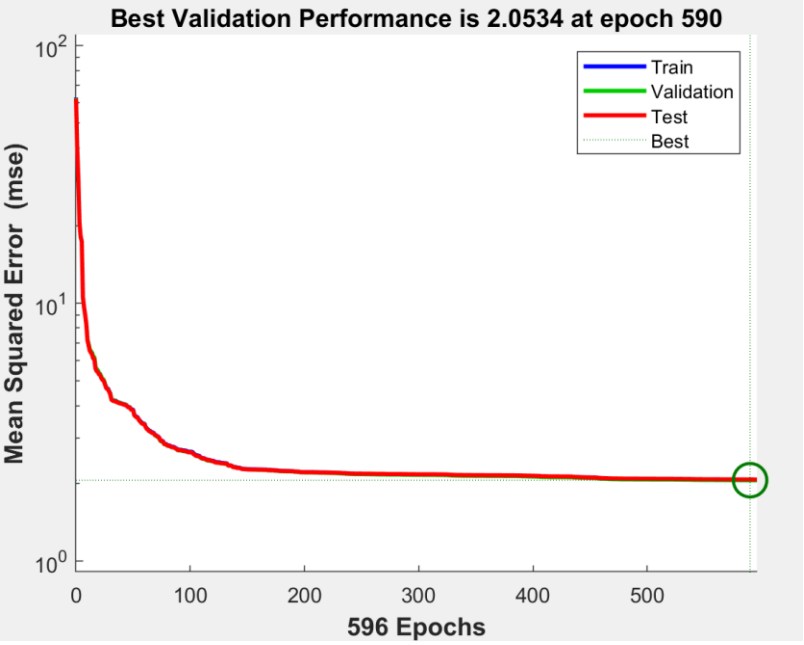

Figure 5-23 ANN model validation performance plot

Figure 5-24 shows an error histogram with 20 bins, which represents the distribution of the errors between the network outputs and the target values for training, validation, and test sets. The concentration of errors around the zero error line (orange line) suggests that the network predictions are fairly accurate.

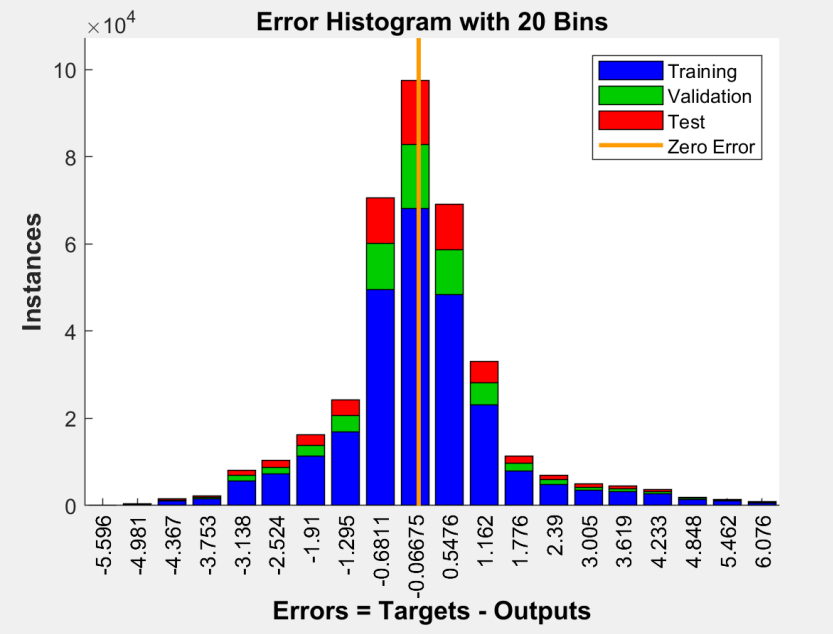

Figure 5-24 ANN EMS error histogram

In summary, the ANN appears to have been trained effectively, achieving a low mean squared error without signs of overfitting. The error distribution further implies that while the network is at a high accuracy level. This trained ANN EMS model was assessed by the same methodology as previous EMS strategies.

5.6.3. ANN EMS Test

The test methodology of this ANN-based control algorithm was to focus on the battery SoC curve to examine the performance of regulating the battery SoC during long-distance journeys at the same time monitoring if the battery and FC system output power are within the safety range. The method of this simulation was to use the parameters of the Eco-BEV and the range extender as input (mentioned in Section 4.3), the initial battery SoC was set as 95%, then select the ECMS control algorithm in the EMS under the repeating WLTP extra-urban drive cycles. The length of per drive cycle was 15.412 km and the duration was 778s, in this testing simulation, 13 times repeating of this WLTP extra-urban cycle was the duty cycle input, and the focusing output was the battery SoC curve.

- **Battery SoC plot**

The simulation result of the battery SoC plot is presented in Figure 5-25.

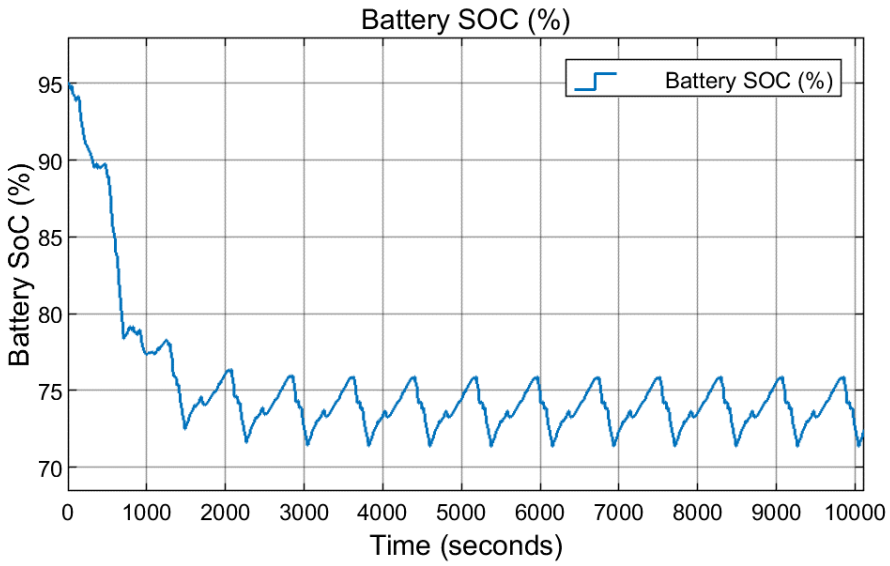

Figure 5-25 Battery SoC curve – ANN control strategy test

The battery SoC curve shows that under the control of this ANN EMS, the battery was the primary power source while the SoC was higher than 80%. Then, similar to the Fuzzy Logic EMS, the battery SoC fluctuated between 65% to 80% which means the FC system started to work as the primary power source to power the vehicle as well as charge the battery pack. After the whole driving cycle, the battery SoC remains at about 70%.

- **Battery and FC power plot**

The simulation result of the battery and FC power plot is presented in Figure 5-26, the orange line is FC power and the blue line is battery power.

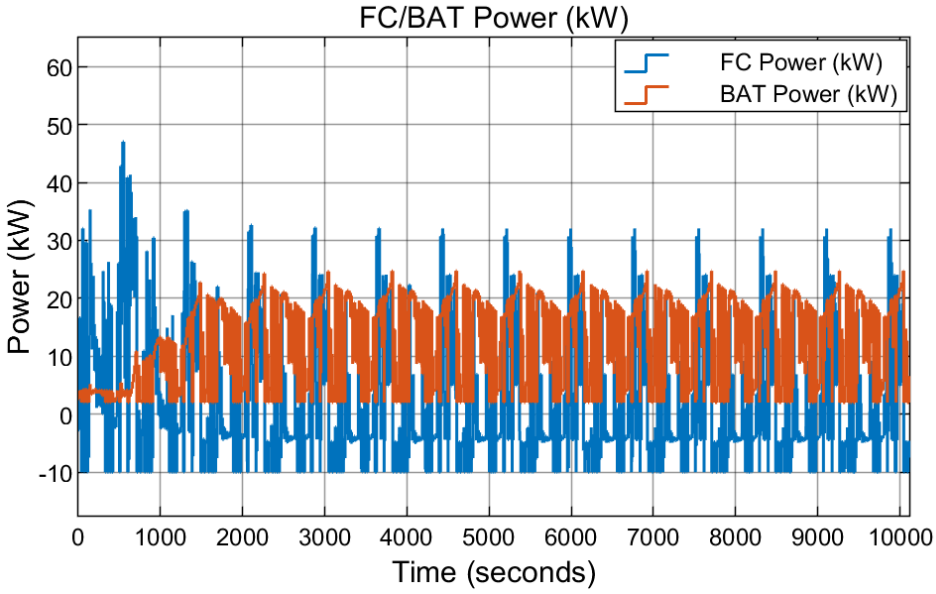

Figure 5-26 Plot of battery and FC power – ANN control strategy test

The battery and FC power plot graph proves that firstly, the battery power was regulated within the range of -10 kW to 46 kW which is under the safety range of the battery pack. For the FC stack, the output power fluctuated from 2 to 27 kW which is under the safety range of the FC output power. Also, the FC power did not reach 0 in the whole simulation, which means the FC system is not turned off, this can extend the lifespan of the FC stack.

- **Vehicle overall energy efficiency and fuel cost**

The results of overall energy efficiency and fuel cost from the ANN EMS test simulation were 297 Wh/km and £22.54, respectively.

5.7. EMS Optimisation with External Information

In accordance with the research objectives outlined in Section 1.3, the implementation of scientific EMS control algorithms is designed to protect the principal components of the power supply and to enhance the performance of the proposed novel powertrain concept termed "Eco-BEV + DHFCRE". This chapter detailed the development of four distinct scientific control algorithms for the EMS of the DHFCRE, each characterised by variations in battery SoC behaviour, fuel economy, and overall vehicle energy efficiency. Consequently, it is crucial to select the most suitable control algorithm, considering real-world conditions and user requirements. This necessitates the integration of the EMS algorithms with external data, including traffic conditions and driver preferences. To facilitate this integration, an optimisation of the EMS serves as a front-end program, enabling the selection of an optimal control algorithm that aligns with real-world conditions and meets driver specifications. As discussed in Section 5.2.4, the optimisation process of the EMS is structured in two distinct stages. The initial stage involves augmenting the EMS with external data, encompassing real-world traffic information the driver's preferences regarding time sensitivity for charging and the desired State of Charge (SoC) of the battery at the trip's conclusion. The subsequent stage of optimisation focuses on selecting the most effective EMS algorithm, aiming to achieve the best fuel economy and the highest overall vehicle energy efficiency. This selection is based on the simulation results derived from the four developed control algorithms.

The methodology for the first stage of optimisation of the EMS in this DHFCRE involves integrating external information with internal control algorithms to enhance the performance of the system. During this stage, after evaluating the characteristics of four control algorithms, drivers are given the option to select their preferred end-trip

battery State of Charge (SoC) level, thereby enabling them to specify the desired SoC at the conclusion of their journey. The second driver preference pertains to the charging command; this is applicable if the driver requires time-sensitive charging during the trip, facilitated by the public charging infrastructure. To implement this functionality, it is essential to incorporate external traffic data, including route planning and map information from the BEV's internal navigation system. The charging command is activated only when charging facilities are available and the driver is not pressed for time, thereby allowing the system to determine and inform the driver of the planned charging locations and times.

In the programming of this first stage of EMS optimisation, the above three external factors will be used to determine the selection of the internal control algorithms. According to the test result of these four EMS algorithms, the State-Machine control EMS regulates the SoC to slightly fluctuate around 40%, the Fuzzy Logic and ANN EMS can regulate the SoC to fluctuate between 70% and 80% and the ECMS algorithm can minimise the hydrogen gas consumption and regulate the SoC to slightly fluctuate around 10%.

The input of the external information in this first stage of EMS optimisation includes:

- **Driver's preference 1** – time sensitivity (if the driver wants to charge the car during the trip)

If the driver does not want to wait to charge the vehicle, the input is N.

Otherwise, if the driver would like to charge the vehicle during the trip, the input is Y.

- **Driver's preference 2** – End-trip battery SoC level (the remaining SoC after the trip)

If the driver would like to use as much energy as possible from the battery to reduce the running cost, the input is L. (low SoC around 10%).

If the driver would like to use the most energy from the battery to reduce the running cost as well as keep the battery SoC at a healthy level, the input is M. (medium SoC around 40%).

If the driver would like to keep the battery SoC at a high level to allow the vehicle to have a longer range after uninstalling the FC range extender as well as keep the SoC within a healthy range, the input is H (high SoC around 70% - 80%).

- **Charging infrastructure availability**

If there is a charging station within the remaining range of this BEV, the input is Y.

If there are no charging stations or the charging station is out of the remaining range of this BEV, the input is N.

The output of this control strategy is the selection of 4 control strategies (State-Machine, Fuzzy Logic, ECMS and ANN) and the charging command (Yes or No).

Therefore, the table of this first stage optimisation program with considerations of external information can be structured as following state flows shown in Table 5-1 and the upgraded EMS flow chart is shown in Figure 5-27.

Table 5-1 First stage EMS optimisation program state flow

External Information			Energy Management System Actions	
Time	**Charging infrastructure**	**Battery SoC**	**Control Strategy**	**Charging Command**
N	Y	L	ECMS	Y
N	Y	M	State-Machine	Y
N	Y	H	ANN	N
N	N	L	ECMS	N
N	N	M	State-Machine	N
N	N	H	ANN	N
Y	Y	L	ECMS	N
Y	Y	M	State-Machine	N
Y	Y	H	ANN	N
Y	N	L	ECMS	N
Y	N	M	State-Machine	N
Y	N	H	ANN	N

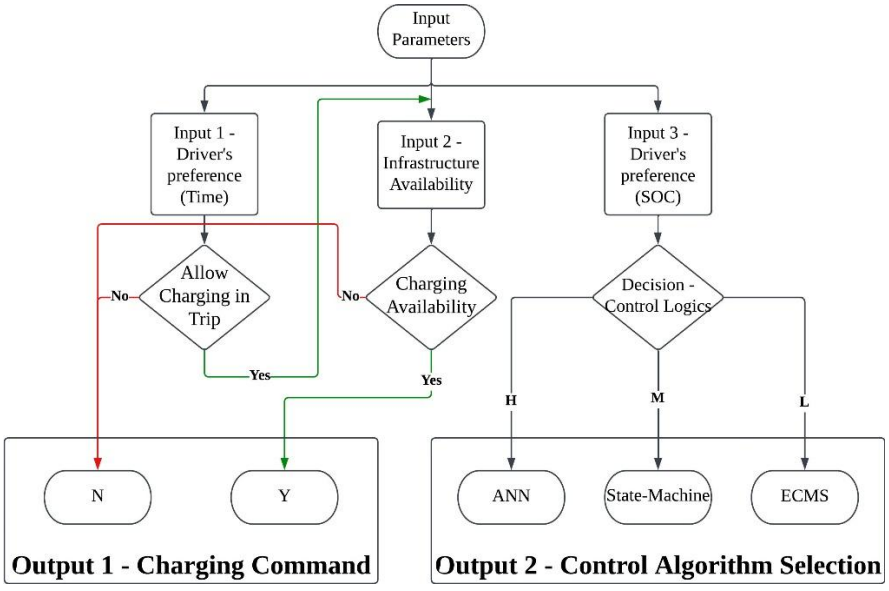

Figure 5-27 EMS front-end program flow chart

By adding this optimisation program, the external information and the driver's preference including the end-trip battery SoC level, time sensitivity and infrastructure availability are considered to select the most proper control logic in real-world journeys. It will be further optimised by using the simulation results of EMS algorithm performance under different types of driving scenarios in the following chapter.

In summary, this chapter developed four EMS control algorithms including State-Machine, Fuzzy Logic, ECMS and ANN. It also tested and evaluated the performance and characteristics of each EMS algorithm. With the help of these results, as well as introducing the external information including driver's preferences and infrastructure availability, a front-end program is added as the further optimisation for the EMS in the DHFCRE. The final optimisation of this front-end program will be accomplished by introducing the simulation results under different driving conditions of the EMS algorithm performance, these will be presented in the next chapter.

5.8. Summary of Energy Management System Development

This chapter firstly reviewed the principles and characteristics of the widely used EMS control strategies in the field of hybrid vehicle control applications. Then, based on the requirements of this novel powertrain concept of "DHFCRE + Eco-BEV", four control algorithms were developed and tested for the EMS, including State-Machine, Fuzzy Logic, ECMS and ANN models. Also, to further optimise the performance and functionality of the EMS, an optimisation method was proposed by developing a front-end program which enabled the connection between the DHFCRE and external information, such as BEV's VCU signals, traffic and navigation information, driver's preferences and the simulation results related to characteristics of EMS algorithms under certain driving conditions.

The limitations of the EMS development process are summarised as follows:

- **Learning-based ANN EMS algorithm database limitation**

According to the discussions in Section 5.6, a learning-based (LB) strategy of the Artificial Neural Network (ANN) model is developed for the EMS of the proposed DHFCRE. The ideal training method of the ANN model is to use the real-world experimental data of the market-ready FCEV products or the database of FCEV EMS testing data from research or manufacturing institutes. The ANN model can learn the control algorithms from these real-world data and use them to control the FCRE in the simulation model which is supposed to provide a higher level of performance. However,

in this project, due to the collaboration between Coventry University and Microcab Ltd ended while the project was ongoing, the real-world data for training the ANN is not available. The ANN is trained by the Fuzzy Logic EMS simulation results which have very similar control behaviours with the Fuzzy Logic EMS with only a slight improvement of the result.

- **BEV Application Programming Interface (API) requirements**

The EMS of this DHFCRE is developed to have the ability to manage the output power of the FC system and battery pack by analysing the input of total power demand and the battery SoC signals from the BEV internal Vehicle Control Unit (VCU). Also, the optimised EMS with the font-end program for the EMS algorithm requires the information from the BEV internal navigation system and the communication interface to allow the driver to select their preferences. Therefore, in real-world conditions, this will require the BEV to have Application Programming Interfaces (API) which allow the DHFCRE EMS system to intervene in the signal communication and control commands of the BEV. This will require the approval of the BEV manufacturers.

Chapter 6 Simulation Result and Analysis

6.1. Introduction

The main purpose of the modelling and simulation in this project is to first quantify and evaluate the performance of the proposed novel powertrain concept of “DHFCRE + Eco-BEV” compared to the competing full-size BEV in terms of key performance factors. Secondly, the simulation will assess the performance of different EMS control strategies under different driving scenarios to understand the superiorities of these strategies in terms of different vehicle performance perspectives such as fuel economy and overall energy efficiency.

The first step of the simulation is to establish the simulation scenarios based on the UK driving behaviours data published by the UK government and transform these data into driving cycle data inputs of the model. Also, the monitored output key performance

parameters will be identified which can comprehensively present the performance of different vehicle powertrains and control strategies. The second step is the simulation tests and result generations under the given driving scenarios, different powertrain types and control strategies, analysis of the results of monitored key performance parameters as well as identify the superiorities and shortcomings of different powertrain types and control strategies in different perspectives. The last step is to further optimise the EMS flow chart based on the upgraded EMS front-end program flow chart (Figure 5-27) through the simulation result analysis in terms of vehicle fuel economy and overall energy efficiency performance results of different control algorithms.

6.2. Simulation Scenarios and Parameters

6.2.1. Simulation Scenarios

As the discussion about the UK travel types and journey length mentioned in Section 4.3, according to the UK driving behaviours data published by the Department of Transport travels with a distance shorter than 50 miles (80 km) accounted for more than 97% of the total number of trips, and the length of the long-distance trips is set as longer than 100 miles (160 km). (GOV.UK, 2020). Therefore, in this chapter, the simulations were developed as 3 scenarios sorted by journey types and length as Table 6-1 shows,

- **Scenario 1** – Long distance highway journey (200 km), duty cycle used - WLTP extra-urban cycle
- **Scenario 2** – Medium distance mixed duty cycle (urban and extra-urban) journey (100 km)), duty cycle used - WLTP full cycle
- **Scenario 3** – Short distance urban journey (50 km) - WLTP urban cycle

The vehicle powertrain option wass set to 3 types, the Large BEV, Stand-alone Eco-BEV and Eco-BEV + FCRE (Eco-BEV with a Demountable Hydrogen Fuel Cell Range Extender installed). Also, in this FCRE, as Chapter 5 mentioned, four different control strategies (State-Machine, Fuzzy Logic, ECMS and ANN) were implemented to compare the performance of the control strategies under different scenarios and duty cycles. The parameters of the vehicles and FCRE in the simulations were based on the component parameterisation results from Chapter 4.3.

Table 6-1 Simulation Scenarios details

Scenario	Scenario 1	Scenario 2	Scenario 3

Journey Length	200 km	100 km	50 km
Duty cycle	Extra-Urban	Urban+Extra-Urban	Urban
Vehicle Powertrain	Large BEV	Large BEV	Large BEV
	Eco-BEV+FCRE (State-Machine)	Eco-BEV+FCRE (State-Machine)	Stand-alone Eco-BEV
			Eco-BEV+FCRE (State-Machine)
	Eco-BEV+FCRE (ECMS)	Eco-BEV+FCRE (ECMS)	Eco-BEV+FCRE (ECMS)
	Eco-BEV+FCRE (Fuzzy Logic)	Eco-BEV+FCRE (Fuzzy Logic)	Eco-BEV+FCRE (Fuzzy Logic)
	Eco-BEV+FCRE (ANN)	Eco-BEV+FCRE (ANN)	Eco-BEV+FCRE (ANN)

The simulation duration of Scenario 1 is 10096s (which is represented by13 times of repeating WLTP extra-urban cycles with a total distance of 200 km), Scenario 2 is 8115s (which represented by 4.3 times of repeating full WLTP cycles with a total distance of 100 km) and Scenario 3 is 6560s (which represented by 6.4 times of repeating WLTP urban cycles with a total distance of 50 km). The initial battery SoC is set as 95%.

In Scenario 1 and Scenario 2, the comparisons of the results of the monitored output parameters under the powertrain of Large BEV and Eco-BEV + FCRE (with different control strategies) will be presented. And in Scenario 3, the result of Eco-BEV without the FCRE will be presented and compared as well since the battery capacity of the Eco-BEV can offer enough range for only Scenario 3, in the other 2 scenarios, it will be charged by the FCRE.

6.2.2. Key Performance Parameters

According to the discussions in Section 4.1, the purpose of the simulations in this project is to evaluate the performance of this DHFCRE for the Eco-BEV in terms of the technical and cost under different scenarios and control strategies. In this chapter, 6 key output performance parameters of this simulation model are monitored and evaluated, including:

- **Speed trace plot – target and actual**

The vehicle speed trace plot (target and actual speed) will be presented first to monitor if the vehicle can reach the target speed as the required speed from the input duty cycle. If the vehicle cannot reach the target speed, it means that all the other results are invalid for the evaluation since the vehicle was not driving in the predefined configurations, the powertrain parameters must be modified first to make the vehicle reach all points of the duty cycle given speeds. When the actual speeds are the same with the duty cycle given values, the other technical results can be monitored.

- **Accumulated energy consumption**

The accumulated energy consumption result contains five outputs including

a. Accumulated battery energy consumption (kWh)
b. Accumulated hydrogen gas consumption (kg)
c. Hydrogen consumption rate (kg/100km)
d. Accumulated hydrogen equivalent energy consumption (Wh) which is calculated by using the nominal hydrogen gas energy density of 33.3 kWh/kg
e. Total accumulated energy consumption (kWh) (battery + hydrogen)

- **Vehicle overall energy efficiency**

The measurement of the conventional vehicles (diesel and petrol) is usually Miles per Gallon or Litres per 100 km, however, for the electric motor-powered zero tailpipe emission vehicles (ZTEV) including BEV and FCEV, the measurement of overall energy efficiency is usually Walt hour per kilometre (or kWh/100km) and Miles per Gallon Equivalent MPGe (US Gallon). (Aqua-Calc, 2022). Thus, the results of the vehicle's overall energy efficiency are selected as Wh/km and US MPGe.

- **Battery state of charge (SoC) curve**

As the previous discussion in the Chapter 5, one of the main purposes of the energy management system and control strategy is to regulate the battery SoC to ensure the battery is working at a healthy level to extend the battery lifespan. The plots of the battery SoC curve will be presented and discussed in Chapter 6.2.

- **Overall FC system efficiency**

According to the discussion in the FC system modelling part in Section 3.4, the efficiency of FC fluctuates with the output current (and power), thus, monitoring and comparing the FC system efficiency is another significant factor in evaluating the performance of the control strategies.

- **Fuel cost**

The last monitored parameter is the fuel cost for the whole journey, including the electricity and hydrogen gas cost in GBP. The price of electricity and hydrogen gas is collected online in Dec 2022, where the electricity price in the public charging station is £0.74 /kWh and for the off-peak home charger, the electricity price is £0.47 /kWh (E. ON, 2022), hydrogen gas price: £12 /kg (AutoTrader, 2022). For the long-distance and mid-range scenarios, since the Large BEV and Eco-BEV are required to use public charging stations during the trip, the electricity price of public charging stations (£0.74 /kWh) will be used for fuel cost calculations. For the short-urban scenario, both Large BEV and Eco-BEV can finish the whole duty cycle without charging, thus, they can be charged at home by using the off-peak electricity £0.47 /kWh which is more economical.

Comparisons of these above 6 parameters between different powertrains (Large BEV, Eco-BEV + FCRE and stand-alone Eco-BEV) will be presented and analysed in Section 6.2.

6.3. Simulation Results and Analysis

6.3.1. Simulation Result – Scenario 1 Long-Distance Highway Cycle

6.3.1.1. Speed Trace Plot – Targe and Actual

Figure 6-1 presents the vehicle speed plots of target velocity regulated by the duty cycle (in the solid blue curve) and actual velocity (red dotted curve) of the Large BEV and the Eco-BEV + FCRE with 4 different control strategies (State-Machine, Fuzzy Logic, ECMS and ANN). The speed curve shows that all of the vehicles in the simulation of Scenario 1 can reach the required speed of the duty cycle.

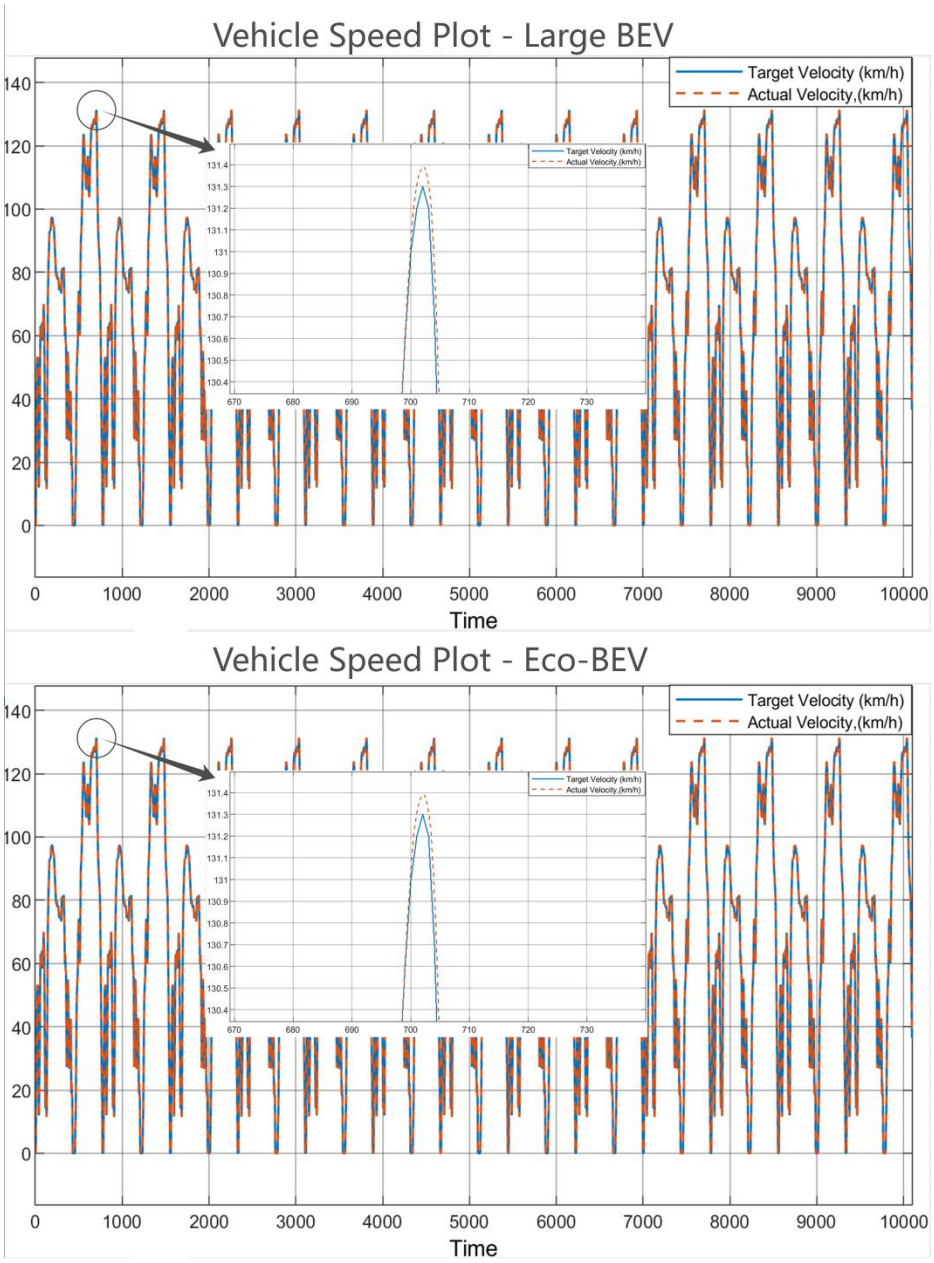

Figure 6-1 Vehicle speed plots – target and actual (km/h) – Scenario 1

As the enlarged plot presents, there are slight differences (about 0.1 km/h, 0.07%) at the peak speeds of the given driving conditions, the actual speed from the simulation feedback signal is slightly larger than the duty cycle target speed, this comes from the disturbances and noise in the simulation model such as changes in wind resistance or variations in road friction, which can cause minor fluctuations in speed. Since the scale of this noise is only 0.07%, it will not significantly affect the overall vehicle performance.

6.3.1.2. Vehicle Overall Energy Efficiency

Table 6-2 presents the simulation results of vehicle overall energy efficiency of the Large BEV and the Eco-BEV + FCRE with 4 different control strategies (State-Machine, Fuzzy Logic, ECMS and ANN) in Scenario 1.

Table 6-2 Vehicle overall energy efficiency results – Scenario 1

Parameter	Large BEV	Eco-BEV + FCRE (State-Machine)	Eco-BEV + FCRE (Fuzzy Logic)	Eco-BEV + FCRE (ECMS)	Eco-BEV + FCRE (ANN)
Vehicle Overall Efficiency (Wh/km)	220.40	298.00	297.70	*273.30*	297.00
Vehicle Overall Efficiency (MPGe)	95.02	70.28	70.35	*76.63*	70.52

In the 200 km extra-urban drive cycle, the overall energy efficiency (MPGe) result of the Large BEV is higher than the Eco-BEV + FCRE since the pure electric powertrain has a higher efficiency than the FC system. For the Eco-BEV + FCRE, in this scenario, the ECMS control strategy produce the highest overall vehicle energy efficiency.

6.3.1.3. Accumulated Energy Consumption

Table 6-3 presents the simulation results of vehicle overall energy efficiency of the Large BEV and the Eco-BEV + FCRE with 4 different control strategies (State-Machine, Fuzzy Logic, ECMS and ANN) in Scenario 1.

Table 6-3 Accumulated energy consumption results – Scenario 1

Parameter	Large BEV	Eco-BEV + FCRE (State-Machine)	Eco-BEV + FCRE (Fuzzy Logic)	Eco-BEV + FCRE (ECMS)	Eco-BEV + FCRE (ANN)
Accumulated energy consumption - battery (kWh)	44.15	6.99	2.88	10.93	2.89
H2 gas consumption (kg)	N/A	1.58	1.70	1.32	1.70
H2 gas consumption rate (kg/100km)	N/A	0.79	0.85	0.66	0.85

Equivalent H2 energy consumption (kWh)	N/A	52.68	56.74	43.82	56.61
Total Energy Consumption (kWh)	44.15	59.67	59.62	*54.75*	59.50

In this scenario, the total accumulated energy consumption result of the Large BEV is lower than the Eco-BEV + FCRE due to the higher efficiency of the pure BEV powertrain.

For the BEV + FCRE, the ECMS control strategy produces the lowest total overall energy consumption since it uses most energy from the battery and least from hydrogen gas which has higher efficiency.

6.3.1.4. Battery SoC Curve

Figure 6-2 presents the battery SoC plot results of the Large BEV and the Eco-BEV + FCRE with 4 different control strategies (State-Machine, Fuzzy Logic, ECMS and ANN) in Scenario 1.

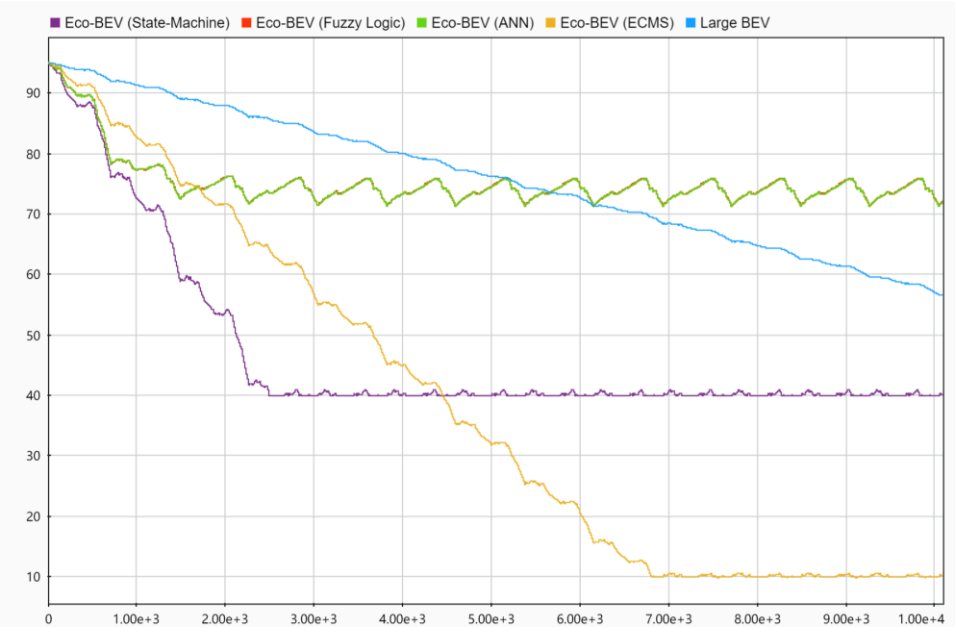

Figure 6-2 Battery SoC plots (X-axis: Time Y-axis: Battery SOC) – Scenario 1

Through the simulation,

- SoC of the Large BEV drops from 95% to 56%
- SoC of the Eco-BEV (State-Machine EMS) drops from 95% to 40%, then fluctuates slightly above 40% which is regulated by the control strategy.

- SoC of the Eco-BEV (Fuzzy Logic and ANN) drops from 95% to 70% and then fluctuates between 70% to 80% which is regulated by the control strategy.
- SoC of the Eco-BEV (ECMS) drops from 95% to 10%, then fluctuates slightly around 10% which is regulated by the control algorithm.
- The SoC of the 2 vehicles remained higher than 10% and avoided an deep-discharge on the battery to prolong the battery lifespan.

6.3.1.5. Overall FC System Efficiency

Table 6-4 shows the results of overall FC system efficiency of the Eco-BEV + FCRE with 4 different control strategies (State-Machine, Fuzzy Logic, ECMS and ANN) in Scenario 1.

Table 6-4 FC system efficiency results – Scenario 1

Parameter	Large BEV	Eco-BEV + FCRE (State-Machine)	Eco-BEV + FCRE (Fuzzy Logic)	Eco-BEV + FCRE (ECMS)	Eco-BEV + FCRE (ANN)
FC Stack efficiency	N/A	57.38%	60.37%	59.80%	*60.46%*

Under the extra-urban duty cycle of Scenario 1, the ANN control algorithm provided the highest overall FC system efficiency at 60.46%, the efficiency of the FC system using the ECMS is 59.8%, the State-Machine EMS is 57.38%, the Fuzzy Logic EMS is 60.37%.

6.3.1.6. Fuel Cost

Table 6-5 presents the simulation results of fuel cost of the Large BEV and the Eco-BEV + FCRE with 4 different control strategies (State-Machine, Fuzzy Logic, ECMS and ANN) in Scenario 1. The fuel price is Electricity Price: £0.74 /kWh, Hydrogen Gas Price: £12 /kg.

Table 6-5 Fuel cost results – Scenario 1

Parameter	Large BEV	Eco-BEV + FCRE (State-Machine)	Eco-BEV + FCRE (Fuzzy Logic)	Eco-BEV + FCRE (ECMS)	Eco-BEV + FCRE (ANN)
Fuel Cost (£)	32.78	24.16	22.58	23.91	*22.54*

The fuel cost of Scenario 1 with the 200 km extra-urban duty cycle for the Large BEV is £32.78 which is higher than the fuel cost of the proposed Eco-BEV + FCRE powertrain. For the Eco-BEV + FCRE with different control strategies, the ANN EMS

provided the lowest fuel cost at £22.54, the fuel cost of the vehicle using ECMS EMS is £23.91, the fuel cost of State-Machine EMS and Fuzzy Logic EMS are £24.16 £22.58.

6.3.2. Simulation Result – Scenario 2 Mid-Range Mixed Cycle

6.3.2.1. Speed Trace Plot – Targe and Actual

Figure 6-3 presents the vehicle speed plots of target velocity regulated by the duty cycle (in the solid blue curve) and actual velocity (red dotted curve) of the Large BEV and the Eco-BEV + FCRE with 4 different control strategies (State-Machine, Fuzzy Logic, ECMS and ANN). The speed curve shows that all of the vehicles in the simulation of Scenario 2 can reach the required speed of the duty cycle.

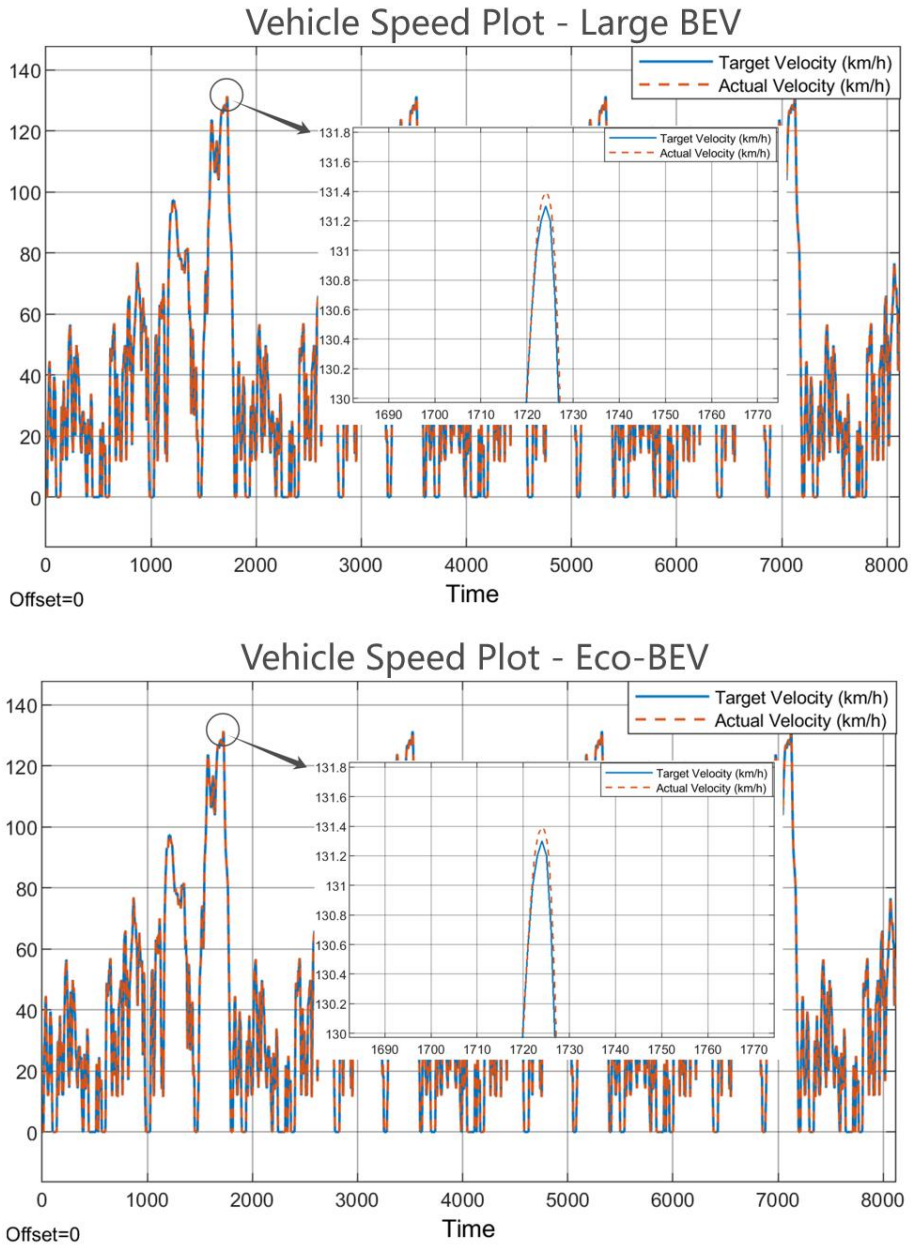

Figure 6-3 Vehicle speed plots – target and actual (km/h) – Scenario 2

Similar to Scenario 1, there are slight differences (about 0.1 km/h, 0.07%) at the peak speeds of the given driving conditions, the actual speed from the simulation feedback signal is slightly larger than the duty cycle target speed, this comes from the disturbances and noise in the simulation model such as changes in wind resistance or variations in road friction, which can cause minor fluctuations in speed. Since the scale of this noise is only 0.07%, it will not significantly affect the overall vehicle performance.

6.3.2.2. Vehicle Overall Energy Efficiency

Table 6-6 presents the simulation results of vehicle overall energy efficiency of the Large BEV and the Eco-BEV + FCRE with 4 different control strategies (State-Machine, Fuzzy Logic, ECMS and ANN) in Scenario 2.

Table 6-6 Vehicle overall energy efficiency results – Scenario 2

Parameter	Large BEV	Eco-BEV + FCRE (State-Machine)	Eco-BEV + FCRE (Fuzzy Logic)	Eco-BEV + FCRE (ECMS)	Eco-BEV + FCRE (ANN)
Vehicle Overall Efficiency (Wh/km)	199.60	229.00	249.40	*225.70*	248.80
Vehicle Overall Efficiency (MPGe)	104.93	91.46	83.97	*92.79*	84.18

In the 100 km urban & extra-urban mixed drive cycle, the overall energy efficiency (MPGe) result of the Large BEV is higher than the Eco-BEV + FCRE since the pure electric powertrain has a higher efficiency than the combined BEV + FC system. For the Eco-BEV + FCRE, in Scenario 2, the ECMS control strategy produce the highest overall vehicle energy efficiency.

6.3.2.3. Accumulated Energy Consumption

Table 6-7 presents the simulation results of vehicle overall energy efficiency of the Large BEV and the Eco-BEV + FCRE with 4 different control strategies (State-Machine, Fuzzy Logic, ECMS and ANN) in Scenario 2.

Table 6-7 Accumulated energy consumption results – Scenario 2

Parameter	Large BEV	Eco-BEV + FCRE (State-Machine)	Eco-BEV + FCRE (Fuzzy Logic)	Eco-BEV + FCRE (ECMS)	Eco-BEV + FCRE (ANN)
Accumulated energy consumption - battery (kWh)	19.16	6.69	2.13	5.80	2.13
H2 gas consumption (kg)	N/A	0.49	0.68	0.50	0.68
H2 gas consumption rate (kg/100km)	N/A	0.49	0.68	0.50	0.68
Equivalent H2 energy consumption (kWh)	N/A	16.21	22.81	16.78	22.76
Total Energy Consumption (kWh)	19.16	22.90	24.94	*22.57*	24.88

In this scenario, the total accumulated energy consumption result of the Large BEV is lower than the Eco-BEV + FCRE due to the higher efficiency of the pure BEV powertrain.

For the BEV + FCRE, the ECMS control strategy produces the lowest total overall energy consumption since it uses most energy from the battery and least from hydrogen gas which has higher efficiency.

6.3.2.4. Battery SoC Curve

Figure 6-4 presents the battery SoC plot results of the Large BEV and the Eco-BEV + FCRE with 4 different control strategies (State-Machine, Fuzzy Logic, ECMS and ANN) in Scenario 2.

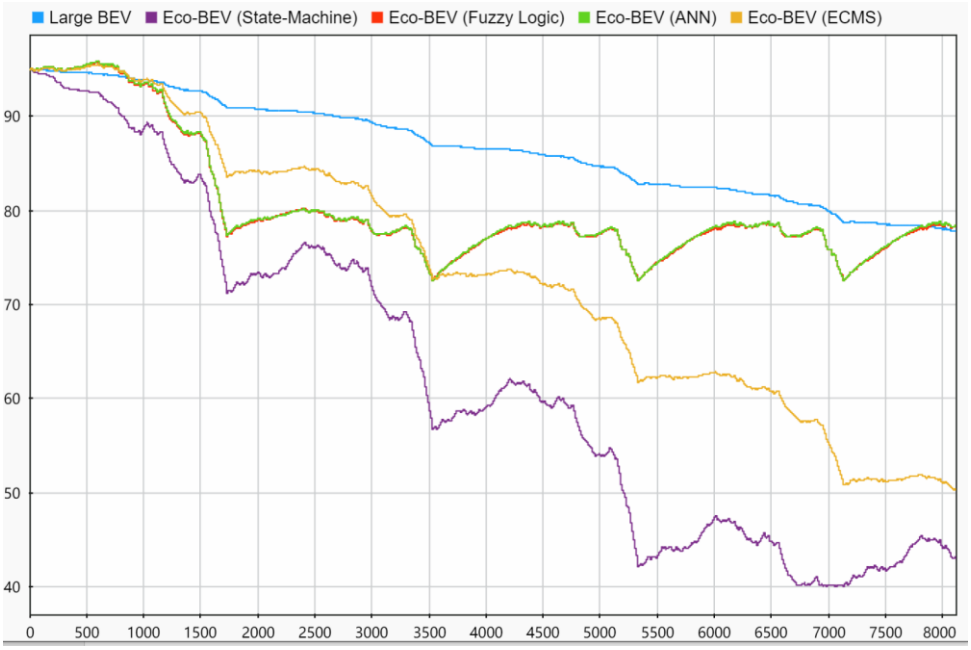

Figure 6-4 Battery SoC plots – Scenario 2

Through the simulation,

- SoC of the Large BEV drops from 95% to 77%
- SoC of the Eco-BEV (State-Machine EMS) drops from 95% to 40%, then fluctuates slightly between 40% and 50% which is regulated by the control strategy.
- SoC of the Eco-BEV (Fuzzy Logic) drops from 95% to 76% and then fluctuates between 70% to 80% which is regulated by the control strategy.
- SoC of the Eco-BEV (ECMS EMS) drops from 95% to 50%.
- SoC of the Eco-BEV (ANN) drops from 95% to 76.5% and then fluctuates between 70% to 80% which is regulated by the control strategy.
- The SoC of the 2 vehicles remained higher than 10% and avoided an deep-discharge on the battery to prolong the battery lifespan.

6.3.2.5. Overall FC System Efficiency

Table 6-8 shows the results of overall FC system efficiency of the Eco-BEV + FCRE with 4 different control strategies (State-Machine, Fuzzy Logic, ECMS and ANN) in Scenario 2.

Table 6-8 FC system efficiency results – Scenario 2

Parameter	Large BEV	Eco-BEV + FCRE (State-Machine)	Eco-BEV + FCRE (Fuzzy Logic)	Eco-BEV + FCRE (ECMS)	Eco-BEV + FCRE (ANN)
FC Stack efficiency	N/A	63.67%	63.46%	64.46%	63.67%

Under the mixed urban & extra-urban duty cycle of Scenario 2, the ECMS EMS provided the highest overall FC system efficiency at 64.46%, the efficiency of the FC system using the Fuzzy Logic EMS is 63.46% and for the State-Machine and ANN EMS are 63.67%.

6.3.2.6. Fuel Cost

Table 6-9 presents the simulation results of fuel cost of the Large BEV and the Eco-BEV + FCRE with 4 different control strategies (State-Machine, Fuzzy Logic, ECMS and ANN) in Scenario 2. The fuel price is Electricity Price: £0.74 /kWh, Hydrogen Gas Price: £12 /kg.

Table 6-9 Fuel cost results – Scenario 1

Parameter	Large BEV	Eco-BEV + FCRE (State-Machine)	Eco-BEV + FCRE (Fuzzy Logic)	Eco-BEV + FCRE (ECMS)	Eco-BEV + FCRE (ANN)
Fuel Cost (£)	14.22	10.81	9.80	10.35	9.78

The fuel cost of Scenario 2 with the 100 km urban & extra-urban duty cycle for the Large BEV is £14.22 which is higher than the fuel cost of the BEV + FCRE powertrain. For the Eco-BEV + FCRE with different control strategies, the ANN EMS provided the lowest fuel cost at £9.78, the fuel cost of the vehicle using ECMS EMS is £10.35, and the State-Machine EMS is the highest at £10.81, the fuel cost from Fuzzy Logic EMS is £9.8.

6.3.3. Simulation Result – Scenario 3 Short Urban Cycle

6.3.3.1. Speed Trace Plot – Targe and Actual

Figure 6-5 presents the vehicle speed plots of target velocity regulated by the duty cycle (in solid blue curve) and actual velocity (red dotted curve) of the Large BEV and the Eco-BEV + FCRE with 4 different control strategies (State-Machine, Fuzzy Logic

ANN and ECMS). The speed curve shows that all of the vehicles in the simulation of Scenario 3 can reach the required speed of the duty cycle.

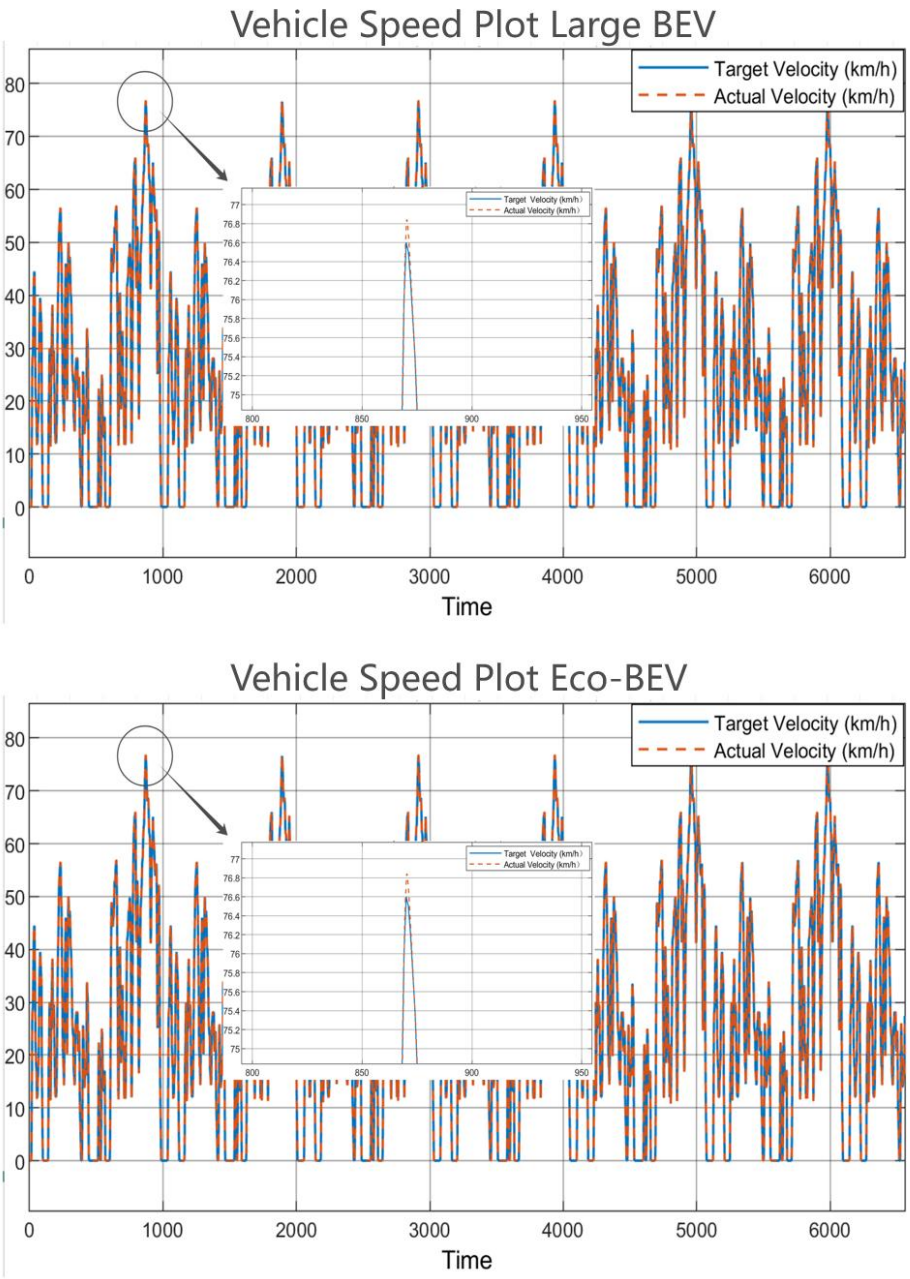

Figure 6-5 Vehicle speed plots – target and actual (km/h) – Scenario 3

Similar to Scenario 1 and 2, there are slight differences (about 0.2 km/h, 0.26%) at the peak speeds of the given driving conditions, the actual speed from the simulation feedback signal is slightly larger than the duty cycle target speed, this comes from the disturbances and noise in the simulation model such as changes in wind resistance or variations in road friction, which can cause minor fluctuations in speed. Since the scale of this noise is only 0.26%, it will not significantly affect the overall vehicle performance.

6.3.3.2. Vehicle Overall Energy Efficiency

Table 6-10 presents the simulation results of vehicle overall energy efficiency of the Large BEV, Eco-BEV and the Eco-BEV + FCRE with 4 different control strategies (State-Machine, Fuzzy Logic ANN and ECMS) in Scenario 3.

Table 6-10 Vehicle overall energy efficiency results – Scenario 3

Parameter	Large BEV	Eco-BEV + FCRE (State-Machine)	Eco-BEV + FCRE (Fuzzy Logic)	Eco-BEV + FCRE (ECMS)	Eco-BEV + FCRE (ANN)	Eco-BEV
Vehicle Overall Efficiency (Wh/km)	162.50	218.60	*184.20*	190.40	185.00	129.40
Vehicle Overall Efficiency (MPGe)	128.88	95.81	*113.70*	110.00	113.21	161.85

In the 50 km urban drive cycle, the overall energy efficiency (MPGe) result of the Large BEV is lower than the Eco-BEV due to the Large BEV having higher resistance (rolling and aerodynamic). Since the efficiency of the FC system is lower than the pure electric powertrain, the overall energy efficiency of the proposed powertrain Eco-BEV + FCRE is lower than the Large BEV and stand-alone Eco-BEV. For the EMS of Eco-BEV + FCRE, in this scenario, the Fuzzy Logic control strategy achieved the highest overall vehicle energy efficiency.

6.3.3.3. Accumulated Energy Consumption

Table 6-11 presents the simulation results of vehicle overall energy efficiency of the Large BEV, Eco-BEV and the Eco-BEV + FCRE with 4 different control strategies (State-Machine, Fuzzy Logic ANN and ECMS) in Scenario 3.

Table 6-11 Accumulated energy consumption results – Scenario 3

Parameter	Large BEV	Eco-BEV + FCRE (State-Machine)	Eco-BEV + FCRE (Fuzzy Logic)	Eco-BEV + FCRE (ECMS)	Eco-BEV + FCRE (ANN)	Eco-BEV
Accumulated energy consumption - battery (kWh)	8.11	0.64	1.14	0.80	1.07	6.45
H2 gas consumption (kg)	N/A	0.31	0.24	0.26	0.25	N/A
H2 gas consumption rate (kg/100km)	N/A	0.62	0.48	0.52	0.49	N/A
Equivalent H2 energy consumption (kWh)	N/A	10.27	8.05	8.70	8.16	N/A
Total Energy Consumption (kWh)	8.11	10.91	*9.19*	9.50	9.23	6.45

In this scenario, the total accumulated energy consumption result of the stand-alone Eco-BEV is the lowest since it has the same level of powertrain efficiency as the Large BEV but has lower weight and size which reduces the resistance and energy loss. Also, compared with the Eco-BEV + FCRE, the Eco-BEV has lower resistance (lower total vehicle weight) as well as higher powertrain efficiency than the FC system.

For the BEV + FCRE, the Fuzzy Logic control strategy produces the lowest total energy consumption since it uses most energy from the battery and least from hydrogen gas which has higher efficiency.

6.3.3.4. Battery SoC Curve

Figure 6-6 presents the battery SoC plot results of the Large BEV, the Eco-BEV + FCRE with 4 different control strategies (State-Machine, Fuzzy Logic, ECMS and ANN) and the Eco-BEV stand-alone without the range extender in Scenario 3.

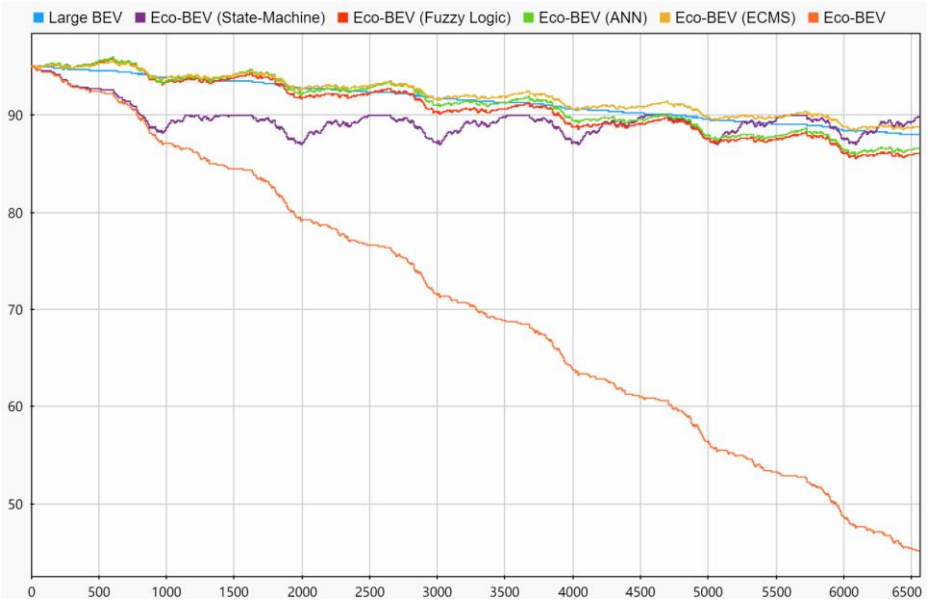

Figure 6-6 Battery SoC plots – Scenario 3

Through the simulation,

- SoC of the Large BEV drops from 95% to 88%
- SoC of the Eco-BEV (State-Machine EMS) drops from 95% to 89%.
- SoC of the Eco-BEV (Fuzzy Logic and ANN) slowly drops with fluctuations from 95% to 86% since the required power in the urban cycle is much lower than in the extra-urban cycle.
- SoC of the Eco-BEV (ECMS) drops from 95% to 90%.
- SoC of the Eco-BEV without range extender drops from 95% to 45%.
- The SoC of the 3 vehicles remained higher than 10% and avoided an deep-discharge on the battery to prolong the battery lifespan.

6.3.3.5. Overall FC System Efficiency

Table 6-12 shows the results of overall FC system efficiency of the Eco-BEV + FCRE with 4 different control strategies (State-Machine, Fuzzy Logic, ECMS and ANN) in Scenario 3.

Table 6-12 FC system efficiency results – Scenario 3

Parameter	Eco-BEV + FCRE (State-Machine)	Eco-BEV + FCRE (Fuzzy Logic)	Eco-BEV + FCRE (ECMS)	Eco-BEV + FCRE (ANN)
FC Stack efficiency	66.15%	*68.59%*	67.35%	68.63%

Under the urban duty cycle of Scenario 3, the ANN EMS provided the highest overall FC system efficiency at 68.63%, the efficiency of the FC system using the Fuzzy Logic EMS is 68.59%, the FC system efficiency of the State-Machine EMS and ECMS are 66.15% and 67.35%.

6.3.3.6. Fuel Cost

Table 6-13 presents the simulation results of fuel cost of the Large BEV, the Eco-BEV + FCRE with 4 different control strategies (State-Machine, Fuzzy Logic, ECMS and ANN) and the Eco-BEV without range extender in Scenario 3. The fuel price is Electricity Price: £0.47 /kWh (off-peak), Hydrogen Gas Price: £12 /kg.

Table 6-13 Fuel cost results – Scenario 3

Parameter	Large BEV	Eco-BEV + FCRE (State-Machine)	Eco-BEV + FCRE (Fuzzy Logic)	Eco-BEV + FCRE (ECMS)	Eco-BEV + FCRE (ANN)	Eco-BEV
Fuel Cost (£)	3.83	4.00	3.44	3.51	3.45	*3.05*

The fuel cost of Scenario 3 with the 50 km urban duty cycle for the Large BEV is £3.83 which is higher than the average fuel cost of the BEV + FCRE (£3.60) and Eco-BEV without range extender (£3.05). For the Eco-BEV + FCRE with different control strategies, the Fuzzy Logic EMS provided the lowest fuel cost at £3.44, the fuel cost of the vehicle using ECMS is £3.51, £3.44 for ANN and the State-Machine EMS is the highest at £4.00.

6.3.4. Simulation Result Analysis

This section will summarise the monitored results by scenarios to evaluate the performance of the FCRE with different control strategies from a macro perspective. Based on the analysis and discussion of the results, it will make some suggestions for using this FCRE in a proper method under different demands and conditions.

6.3.4.1. FCRE Performance in Long-Distance Extra-Urban Journeys

Since the target Eco-BEV is sized as a small/eco family vehicle with only 12.96 kWh battery capacity, in long-distance extra-urban journeys like the condition in Scenario 1, it will need help from the FCRE to avoid frequent charges and time consumption.

Determined by the control strategies, the FCRE offers distinctive characteristics on the power output as Table 6-14 shows. The performance of overall energy efficiency and fuel cost is conflicting under different control strategies.

Table 6-14 Simulation result summary – Scenario 1

Scenario 1 - 200 km extra-urban cycle - duration 10096s					
	Powertrain Types				
Result	**Large BEV**	**Eco-BEV + FCRE (State-Machine)**	**Eco-BEV + FCRE (Fuzzy Logic)**	**Eco-BEV + FCRE (ECMS)**	**Eco-BEV + FCRE (ANN)**
Speed plot (match duty cycle)	Y	Y	Y	Y	Y
Vehicle Overall Efficiency (Wh/km)	220.4	298	297.7	*273.3*	297
Vehicle Overall Efficiency (MPGe)	95.02	70.28	70.35	*76.63*	70.52
Accumulated energy consumption - battery (kWh)	44.15	6.99	2.88	10.93	2.89
H2 gas consumption (kg)	N/A	1.58	1.70	1.32	1.70
H2 gas consumption rate (kg/100km)	N/A	0.79	0.79	0.71	0.71
Equivalent H2 energy consumption (kWh)	N/A	52.68	56.74	43.82	56.61
Total Energy Consumption (kWh)	44.15	59.67	59.62	54.75	59.50
SOC Curve plot (higher than 10%)	Y	y	Y	Y	Y
FC Stack efficiency	N/A	57.38%	60.37%	59.80%	*60.46%*
Fuel Cost (£)	32.78	24.17	22.58	23.91	*22.54*

Firstly, compared with the Large BEV, in the long-distance extra-urban journeys, the Eco-BEV + FCRE has a lower average overall energy efficiency (72.68 MPGe) due to the energy loss in the FC system, which is about 23.5% lower than the Large BEV. However, from the fuel cost perspective, the Eco-BEV + FCRE with 4 control strategies has an average fuel cost of £23.48 which is 28.3% lower than the fuel cost of the Large BEV.

Secondly, for the overall energy efficiency of the Eco-BEV + FCRE, the ECMS EMS provide the highest overall energy efficiency at 76.63 MPGe which is 8.9% higher than the Fuzzy Logic EMS, 9% higher than the State-Machine EMS and 8.6% higher than the ANN EMS. The reason for this highest overall efficiency is that the energy efficiency

of the [battery – motor] powertrain combination is higher than the [FC – DC-DC – battery – motor] powertrain combination. Therefore, for the Eco-BEV + FCRE, the more energy used from the battery, the higher overall efficiency will be achieved.

Thirdly, for the fuel cost of the Eco-BEV + FCRE, the ANN EMS provide the lowest fuel cost at £22.54 which is 5.7% lower than ECMS EMS, 6.7% lower than State-Machine EMS and 0.2% lower than the Fuzzy Logic EMS. The reason for this result is that the ANN EMS provides the highest FC system efficiency at 60.46%. Also, the price of electricity and hydrogen gas affects the fuel cost, when the ratio of electricity price / hydrogen gas price rises, the control strategy which uses more hydrogen gas will achieve a lower fuel cost. On the contrary, when the hydrogen gas price drops, the control strategy which uses more hydrogen gas will achieve a lower fuel cost.

To conclude, in long-distance extra-urban journeys like the condition of Scenario 1. The overall energy efficiency of the Eco-BEV + FCRE is lower than the Large BEV due to the lower energy efficiency of the FC system compared with the pure BEV propulsion system. However, by implementing this FCRE to the Eco-BEV, the fuel cost can be reduced by about 28.4%. Also, for the different control strategies in the FCRE, the ECMS EMS provides the highest overall energy efficiency, but the ANN EMS achieves the lowest running cost. Therefore, during long-distance extra-urban journeys, if the driver prefers to choose a control strategy in the FCRE that provides the highest energy efficiency, the ECMS EMS should be selected. If the driver is more on the fuel cost, the ANN control strategy should be selected.

6.3.4.2. FCRE Performance in Mixed Urban & Extra-Urban Journeys

Since the target Eco-BEV is sized as a small/eco family vehicle with only 12.96 kWh battery capacity, which offers only about 80 km mixed urban and highway range, in trips with a distance around 100km with urban & extra-urban duty cycles like the condition in the Scenario 2, it will need the help from the FCRE to avoid frequently charges and time consumption.

Determined by the control strategies, the FCRE offers different characteristics on the power output as Table 6-15 shows. The performance of overall energy efficiency and fuel cost is conflicting under different control strategies.

Table 6-15 Simulation result summary – Scenario 2

Scenario 2 - 100 km urban & extra-urban cycle - duration 8115s					
	Powertrain				
Result	**Large BEV**	**Eco-BEV + FCRE (State-Machine)**	**Eco-BEV + FCRE (Fuzzy Logic)**	**Eco-BEV + FCRE (ECMS)**	**Eco-BEV + FCRE (ANN)**
Speed plot (match duty cycle)	Y	Y	Y	Y	Y
Vehicle Overall Efficiency (Wh/km)	199.6	229	249.4	*225.7*	248.8
Vehicle Overall Efficiency (MPGe)	104.93	91.46	83.97	*92.79*	84.18
Accumulated energy consumption - battery (kWh)	19.16	6.69	2.13	5.80	2.13
H2 gas consumption (kg)	N/A	0.49	0.68	0.50	0.68
H2 gas consumption rate (kg/100km)	N/A	0.49	0.68	0.50	0.68
Equivalent H2 energy consumption (kWh)	N/A	16.21	22.81	16.78	22.76
Total Energy Consumption (kWh)	19.16	22.90	24.94	22.57	24.88
SOC Curve plot (higher than 10%)	Y	Y	Y	Y	Y
FC Stack efficiency	N/A	63.67%	63.46%	*64.46%*	63.67%
Fuel Cost (£)	14.22	10.81	9.80	10.35	*9.78*

Firstly, compared with the Large BEV, in the mix of urban & extra-urban with around 100 km length journeys, the Eco-BEV + FCRE has a lower average overall energy efficiency (88.1 MPGe) due to the energy loss in the FC system, which is 16% lower than the Large BEV. However, compared with the result in Scenario 1 (23.5%), the difference in the overall efficiency is lower in the mix duty cycles. From the fuel cost perspective, the Eco-BEV + FCRE with 4 control strategies has an average fuel cost of £10.18 which is 28.4% lower than the fuel cost of the Large BEV.

Secondly, for the overall energy efficiency of the Eco-BEV + FCRE with different EMS algorithms, the ECMS EMS provide the highest overall energy efficiency at 92.79 MPGe which is 10.5% higher than the Fuzzy Logic EMS, 1.5% higher than the State-Machine EMS and 10.2 higher than the ANN EMS. The reason is that the energy efficiency of the [battery – motor] powertrain combination is higher than the [FC – DC-DC – battery – motor] powertrain combination. Therefore, for the Eco-BEV + FCRE, the more energy used from the battery the higher overall efficiency will be achieved.

Thirdly, for the fuel cost of the Eco-BEV + FCRE, the ANN EMS provide the lowest fuel cost at £9.78 which is 5.5% lower than ECMS EMS and 9.5% lower than State-Machine EMS and 0.2% higher than Fuzzy Logic EMS. The reason for this result is that the ANN EMS provides the second highest FC system efficiency at 63.67% and a better energy distribution ratio from battery and FC since the price of electricity and hydrogen gas affects the fuel cost when the ratio of electricity price / hydrogen gas price rises, the control strategy which used more hydrogen gas will achieve a lower fuel cost. On the contrary, when the hydrogen gas price drops, the control strategy which uses more hydrogen gas will achieve a lower fuel cost.

In summary, in the mixed urban & extra-urban journeys with a distance of around 100 km like the condition of Scenario 2. The overall energy efficiency of the Eco-BEV + FCRE is lower than the Large BEV due to the lower energy efficiency of the FC system compared with the pure BEV propulsion system. However, by implementing this FCRE to the Eco-BEV, the fuel cost can be reduced by about 28.4%. Also, for the different control strategies in the FCRE, the ECMS EMS provides the highest overall energy efficiency, but the ANN EMS achieves the lowest running cost. Therefore, during the l mixed urban & extra-urban journeys with a distance of around 100 km, if the driver prefers to choose a control strategy in the FCRE that provides the highest energy efficiency, the ECMS EMS should be selected. If the driver prefers to have the lowest fuel cost, the ANN control strategy should be selected.

6.3.4.3. FCRE Performance in Urban Journeys

Since the target Eco-BEV is sized as a small/eco family vehicle with 12.96 kWh battery capacity and about 50 km urban range, in the short-distance (lower than 50 km) urban journeys like the condition in Scenario 3, it can finish the whole journey without the help from the range extender and charging stations. However, in order to evaluate the performance of this DHFCRE under urban duty cycles, the simulation of the Eco-BEV + FCRE with 4 different control strategies is undertaken.

Determined by the control strategies, the FCRE offers different characteristics on the power output as Table 6-16 shows. The performance of overall energy efficiency and fuel cost is conflicting under different control strategies.

Table 6-16 Simulation result summary – Scenario 3

Scenario 3 - 50 km urban cycle - duration 6560s						
	Powertrain					
Result	**Large BEV**	**Eco-BEV + FCRE (State-Machine)**	**Eco-BEV + FCRE (Fuzzy Logic)**	**Eco-BEV + FCRE (ECMS)**	**Eco-BEV + FCRE (ANN)**	**Eco-BEV**
Speed plot (match duty cycle)	Y	Y	Y	Y	Y	Y
Vehicle Overall Efficiency (Wh/km)	162.5	218.6	*184.2*	190.4	185	129.4
Vehicle Overall Efficiency (MPGe)	128.88	95.81	*113.70*	110.00	113.21	161.85
Accumulated energy consumption - battery (kWh)	8.11	0.64	1.14	0.80	1.07	6.45
H2 gas consumption (kg)	N/A	0.31	0.24	0.26	0.25	N/A
H2 gas consumption rate (kg/100km)	N/A	0.62	0.48	0.52	0.49	N/A
Equivalent H2 energy consumption (kWh)	N/A	10.27	8.05	8.70	8.16	N/A
Total Energy Consumption (kWh)	8.11	10.91	9.19	9.50	9.23	6.45
SOC Curve plot (higher than 10%)	Y	Y	Y	Y	Y	Y
FC Stack efficiency	N/A	66.15%	68.59%	67.35%	*68.63%*	N/A
Running Cost (£)	3.83	4.00	*3.44*	3.51	3.45	3.05

Firstly, compared with the Large BEV and the Eco-BEV + FCRE in short-distance urban journeys, the Eco-BEV has the highest overall energy efficiency at 161.85 MPGe which is 25.6% higher than the Large BEV and 49.6% higher than the Eco-BEV + FCRE average (108.18 MPGe). The reason the stand-alone Eco-BEV has the highest overall energy efficiency is that compared with the Large BEV, it has a smaller size and weight which leads to lower rolling and aerodynamic resistance. Compared with the Eco-BEV + FCRE powertrain, the pure electric powertrain has a higher overall efficiency. Moreover, in the fuel cost perspective, the stand-alone Eco-BEV has the lowest fuel cost which is 15.3% lower than the average fuel cost of Eco-BEV + FCRE

with 4 control strategies (£3.60) and 20.4% lower than the Large BEV (£3.83). This proves that in the short-distance urban scenario, the most efficient and economical method is using the stand-alone Eco-BEV and charging it home by using off-peak electricity. The Eco-BEV owners do not need the FCRE during their everyday urban driving, since the range extender is designed as demountable, it can be used only for mid and long-distance journeys to avoid wasting time charging vehicles during the trip.

Secondly, in the short urban scenario, for the overall energy efficiency of the different EMS algorithms in the proposed powertrain of Eco-BEV + FCRE, the Fuzzy Logic EMS provides the highest overall energy efficiency at 113.7 MPGe which is 0.4% higher than the ANN EMS (113.21), 3.4 higher than ECMS (110.00) and 18.7% higher than the State-Machine EMS (95.81). The reason for this highest overall efficiency is that the energy efficiency of the [battery – motor] powertrain combination is higher than the [FC – DC-DC – battery – motor] powertrain combination. Therefore, for the Eco-BEV + FCRE, the more energy used from the battery the higher overall efficiency will be achieved.

Thirdly, for the fuel cost of the Eco-BEV + FCRE, the Fuzzy Logic EMS provide the lowest fuel cost at £3.44 which is 2.0% lower than ECMS (£3.51), 14.0% higher than State-Machine EMS (£4.00) and 0.3% higher than ANN EMS (£3.45). The reason for this result is related to the price comparison between the electricity and hydrogen gas, if the hydrogen gas price is transferred to the format of £/kWh, the price will be £0.36 / kWh, where the electricity price is £0.4721 per kWh (off-peak) and £0.7424 per kWh (public charging station) where the ratio of hydrogen price / electricity price is 76.3% and 48.5%. Thus, if the FC system's overall efficiency is higher than this ratio, the more hydrogen fuel used, the lower overall fuel price will be achieved, therefore, if the BEV is charged in the public charging station, the fuel cost will be higher than using the FCRE.

To conclude, in short-distance urban journeys like the condition of Scenario 1. The overall energy efficiency of the stand-alone Eco-BEV is higher than the Eco-BEV + FCRE and the Large BEV due to the lower energy loss on the internal powertrain and external aerodynamic and rolling resistance. The fuel cost of stand-alone Eco-BEV using home off-peak electricity is lower than the Large BEV and the Eco-BEV + FCRE. However, if the Eco-BEV is charged in the public charging station, the fuel cost will be higher than the Eco-BEV + FCRE powertrain concept. For different control strategies in the FCRE, the Fuzzy Logic EMS provides the highest overall energy efficiency and

lowest fuel cost. Therefore, during short-distance urban journeys, the Fuzzy Logic EMS should be selected.

6.4. EMS Further Optimisation with Simulation Results

According to the discussions in Section 5.2.4, the optimisation process of the EMS in the DHFCRE includes two stages, the first stage is implemented in Section 5.7 by introducing the external information on external infrastructure availability, driver's preferences of time sensitivity for charging and the end-trip SoC level. In the second stage of EMS optimisation, further information is added for the front-end program of EMS algorithm selections including driving scenarios, choice of best fuel economy or highest overall vehicle energy efficiency. Through the simulation and result analysis in Section 6.3, the performance and characteristics of the 4 developed control algorithms under different driving scenarios can be summarised as follows:

- **Long-distance highway scenario**

a. End-trip SoC level (low to high)

ECMS – 10%

State-Machine – about 40%

Fuzzy Logic and ANN – between 70% and 80%

b. Fuel economy (low to high)

ANN – £22.54

Fuzzy Logic – £22.58

ECMS – £23.91

State-Machine – £23.94

c. Overall TTW vehicle energy efficiency (high to low)

ECMS – 76.63 MPGe

State-Machine – 71.07 MPGe

ANN – 70.52 MPGe

Fuzzy Logic – 70.35 MPGe

- **Mid-distance mixed urban and extra-urban scenario**

a. End-trip SoC level (low to high)

State-Machine – about 40%

ECMS – about 50%

Fuzzy Logic and ANN – about 80%

b. Fuel economy (low to high)

ANN – £9.78

Fuzzy Logic – £9.80

ECMS – £10.35

State-Machine – £10.81

c. Overall TTW vehicle energy efficiency (high to low)

ECMS – 92.79 MPGe

State-Machine – 91.46 MPGe

Fuzzy Logic – 83.97 MPGe

ANN – 84.18 MPGe

- **Short-distance urban scenario**

Based on the simulation result of scenario 3 in section 6.3.3, in the short-distance (50 km) urban driving condition, the most efficient and economic powertrain is the stand-alone Eco-BEV which corroborated the idea of future BEV to be "tailored for usage" from the APC Roadmap. Adding the range extender in short-urban driving cycles will increase the fuel cost and affect the overall vehicle energy efficiency, therefore, it proved that the FCRE designed as a demountable device instead of directly fixed on with the BEV as a range-extended FCEV is a more efficient and economic powertrain hybridisation method. Therefore, this DHFCRE is suggested to be used only for mid and long-distance journeys when the range demand is longer than the range of stand-alone ECO-BEV to avoid frequently charging during the trip. However, to build a comprehensive front-end EMS algorithm selection program, the short-distance urban driving scenario is also considered. Based on the simulation result, if in special cases, the Eco-BEV driver is required to use the DHFCRE in the short-urban driving cycle, the Fuzzy Logic algorithm will be selected since it has the best fuel economy and highest overall vehicle energy efficiency in the short-urban driving cycle. The end-trip SoC level will remain as high (over 80%) and no need for charging the vehicle during the trip.

Based on the following results, the second stage EMS optimisation will add two more external information including the driving scenario information to identify the journey type from the BEV internal navigation system and the driver's preference on the choice of fuel economy or overall energy efficiency. The front-end control algorithm selection program is upgraded based on the first stage program presented in Section 5.7, the final flow chart of the EMS front-end program is presented in Figure 6-7.

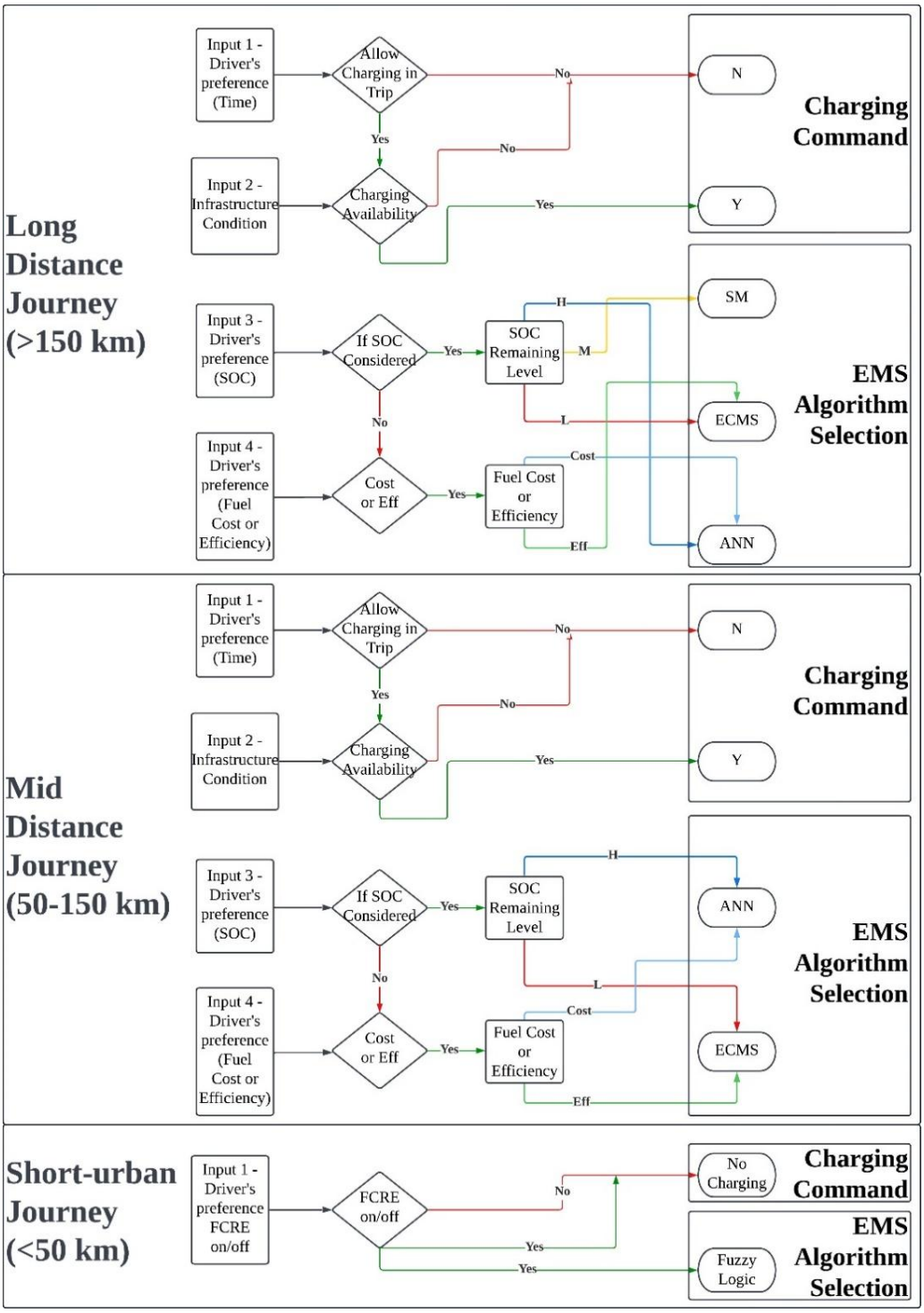

Figure 6-7 Final optimised EMS front-end program flow chart

Through the final optimised EMS front-end program control flow chart, while using this DHFCRE, the driver can select 5 preference commands including time sensitivity (determine if charge vehicle is during the journey), the infrastructure availability, end-trip battery SoC level, fuel economy or the environmental consideration of overall vehicle energy efficiency and the on/off selection for short-urban scenarios only. Therefore, the DHFCRE internal EMS is connected to the BEV and the driver to achieve a closed control loop from the demands of the driver and BEV internal information through the DHFCRE EMS to control the DHFCRE to work under the best situation of both battery electric powertrain and FC system and provide the most appropriate outputs.

6.5. Summary of Simulation Result and Analysis

This chapter firstly developed three driving scenarios for the simulations based on the EU WLTP duty cycle and the considerations of real-world driving conditions. Then, the key performance parameters of the results are identified to evaluate the performance of the proposed powertrain concept of “DHFCRE + Eco-BEV”.

The summary of the simulation result analysis and findings includes:

- **Fuel economy**

For fuel cost assessments, the "Eco-BEV + DHFCRE" powertrain configuration demonstrated a notable reduction in costs: 28.4% in the long-distance highway cycle, 28.3% in the mid-range mixed urban and extra-urban cycle, and 6% in the short-range urban cycle when compared with the larger, full-size BEV. This reduction in fuel costs was attributed to the increased resistances faced by the full-size BEV, which arose from a larger battery size designed to extend range, coupled with the comparative cost ratio between electricity and hydrogen gas. However, in the short-range urban cycle, the stand-alone Eco-BEV emerged as the most economical option, providing a fuel cost that was 15.3% lower than the Eco-BEV + DHFCRE configuration and 20.4% lower than that of the Large BEV.

- **Overall vehicle energy efficiency**

For the overall vehicle energy efficiency results, when compared with the target large full-size BEV, the proposed "Eco-BEV + DHFCRE" powertrain exhibited approximately 23.5% greater efficiency in the long-distance highway cycle, 16% in the mid-range mixed urban and extra-urban cycle, and a 16.1% improvement in the short-range urban cycle. Similarly, in line with the fuel cost findings, the stand-alone Eco-BEV

demonstrated the highest overall vehicle energy efficiency in the short-range urban cycle. The superior energy efficiency of the BEV is attributed to the [battery – motor] powertrain combination, which is more efficient than the [FC – DC-DC – battery – motor] powertrain combination, thus avoiding energy losses associated with the DC-DC converter and fuel cell stack.

- **Control algorithm characteristics and EMS further optimisations**

In the analysis of the performance and characteristics of scientific EMS control algorithms versus the rule-based State-Machine EMS, significant differences were observed. In both the long-distance highway cycle and the mid-range mixed urban and extra-urban cycle, the ANN EMS outperformed by achieving superior fuel economy, which was 6.7% and 9.5% lower than the State-Machine EMS respectively. The ECMS algorithm delivered the highest overall energy efficiency in these cycles, recording figures 9% and 1.5% higher than those of the State-Machine EMS.

In the short-range urban cycle, the Fuzzy Logic EMS demonstrated the lowest fuel cost alongside the highest overall energy efficiency. Following these findings regarding the control algorithm characteristics, a final optimisation was carried out on the EMS front-end program. This adjustment enabled the EMS to select the most suitable algorithm based on varying factors such as the driver's preferences, driving conditions, and external traffic information.

- **Result analysis summary and marketing model discussions**

Referring to the simulation results, the DHFCRE enhanced the functionality of the Eco-BEV by providing sufficient range and reducing fuel costs. However, this hybridisation of the powertrain led to a lower overall energy efficiency compared with the full-size large BEV across all driving scenarios. Notably, in short urban journeys, the stand-alone Eco-BEV displayed optimal performance in terms of both fuel economy and overall energy efficiency. Consequently, as suggested in this thesis, the range extender should be designed to be demountable rather than fixed, unlike in an FCEV.

Furthermore, statistics on UK driving behaviour indicate that long-distance trips account for only about 2% of journeys per year. Additionally, the cost of FC systems, such as FC stacks and hydrogen tanks, remains high due to limited production volumes. Therefore, the proposed business model for the DHFCRE advocates renting rather than purchasing. This approach offers several benefits:

Firstly, it enhances the functionality and cost-effectiveness for BEV owners. Secondly, it enables centralised refuelling of FC range extenders, which helps to mitigate infrastructure dependency and boost the utilisation rate of early-stage hydrogen stations. Moreover, the widespread adoption of the DHFCRE could hasten the transition from current BEVs to the ideal model envisaged by the APC roadmap, aiming to meet the 2050 goal of being “tailored for usage”. This allows consumers to choose their BEVs based solely on their personal needs, without concerns about range and size limitations. Finally, the popularisation of the DHFCRE could increase the production volume of hydrogen fuel cell systems, which is crucial for reducing the future costs of core components and enhancing vehicle customer understanding and acceptance.

The limitation of the simulation and result analysis mainly related to the duty cycle model. Referring to Section 6.2, the simulation scenarios are developed based on the WLTP urban and extra-urban duty cycles which are defined by the EU laws (Transport Policy, 2022) which lacked the results for other countries and regions.

.

Chapter 7 Cost Benefit Analysis

7.1. Introduction

According to the problem scopes discussed in Chapter 2, the most significant current issues which affect the speed of BEV popularisation are range anxiety, concern about the density of charging infrastructure, especially during long-distance journeys, the durability of the components in the vehicle (mostly about battery pack) and the Total Cost of Ownership (TCO) (World Economic Forum, 2021; National Grid Group, 2022; Nealefhima, 2023). The purpose of developing this Demountable Hydrogen Fuel Cell Range Extender (DHFCRE) is to reduce the impacts of the above issues of BEV and improve the performance of the Eco-BEVs.

In order to assess both the value and cost of adopting the novel hybridisation method that merges the Eco-BEV (in the most cost-effective size outlined in Section 4.3.1) with hydrogen fuel cell technology – specifically, the Demountable Hydrogen Fuel Cell Range Extender (DHFCRE) – a comprehensive Cost Benefit Analysis (CBA) is conducted. This analysis explores implications from both individual/household and broader national/societal perspectives. The CBA will account for economic factors as well as long-term environmental impacts, such as carbon emissions and consumption of relevant mineral resources.

In the field of CBA transportation solutions, the key factors include the short/long team costs for both individuals and the whole country, and the environmental impacts including carbon emission and energy consumption (MAXUS, 2023). The CBA from individual and household perspectives, accessing the Total Cost of Ownership (TCO) is an effective method to address the overall cost of a new vehicle (VTPI, 2016). The TCO for a ZTEV includes a number of factors such as vehicle purchasing price, vehicle tax, insurance cost, vehicle repairing and maintenance cost, running costs, depreciation value, etc (VTPI, 2016). From the societal and national perspective, the CBA of proposing a new ZTEV solution usually includes the economic considerations (manufacturing cost, fuel consumptions, etc.) and the environmental impact analysis (carbon emissions, energy efficiency, natural resources consumption) (M.J. Bradley & Associates, 2017).

In this chapter, the differences in economic and environmental impacts between two vehicle powertrain options – the Large BEV and the Eco-BEV (which utilises a rented FCRE for long-distance journeys in extra-urban areas) will be presented and discussed.

This analysis forms part of the CBA comparisons, aimed at evaluating the costs and benefits of the proposed “DHFCRE + Eco-BEV” concept in this thesis.

7.2. Individual/Household Perspective CBA

The total Cost of Ownership (TCO) is an effective financial tool to analyse the long-term cost and benefit for an individual or a household in purchase/leasing a family passenger vehicle product. (Transport & Environment, 2022). For family passenger vehicles, the TCO includes purchasing/leasing prices, running (fuel) costs, tax, maintenance costs, vehicle depreciation and insurance. (LetsTalkLeasing, 2020). In this thesis, the most significant aim of the individual/household CBA is to establish the economic comparison between the proposed concept “DHFCRE + Eco-BEV” and the full-size BEV. The economic comparison is linked to the simulation results presented in Chapter 6 including the core component size, fuel cost and overall energy efficiency of the two powertrain options. Thus, the economic comparison in this section will focus on the running cost and purchase cost based on the simulation results. An assumption is made that the costs of depreciation, tax, maintenance, and insurance are the same for the two powertrain options (the comprehensive TCO comparison method is discussed in the future works Section □). Thus, the TCO of the Large BEV includes the vehicle purchasing price and the running (fuel) cost. For Eco-BEV + renting range extender, the rent price of the DHFCRE and hydrogen fuel cost will be added to the total cost.

The TCO in this project can be calculated by Equation 7-1

$$TCO = P + C_r \quad (7\text{-}1)$$

Where,

P is the purchasing price of the vehicle. (Purchasing price fluctuates with time)

C_r is the running cost

The total lifetime running cost for the Eco-BEV + FCRE can be calculated by Equation 7-2, and the total lifetime fuel cost for a Large BEV can be calculated by Equation 7-3

$$C_{r1} = (P_o \times T_u \times L_u \times \eta_{u1} + \alpha_E \times P_p \times T_{ex} \times L_{ex} \times \eta_{ex1} + P_{rfc} \times T_{ex} + \alpha_{H2} \times P_{H2} \times T_{ex} \times L_{ex} \times \eta_{H2}) \times t_L \quad (7\text{-}2)$$

$$C_{r2} = (P_o \times T_u \times L_u \times \eta_{u2} + P_p \times T_{ex} \times L_{ex} \times \eta_{ex2}) \times t_L$$

(7-3)

Where

C_{r1} is the total running cost of the Eco-BEV + FCRE (£)

P_o is the Off-Peak electricity price (£/kWh)

T_u is the number of annual urban journeys per year based on the published data from the government

L_u is the Average urban journey length (km)

η_{u1} is the Average urban journey energy efficiency of the Eco-BEV + FCRE (kWh/km)

α_E is the Proportion of electricity energy used in the extra-urban journey of the Eco-BEV + FCRE (%)

P_p is the Peak electricity price (£/kWh)

T_{ex} is the Total annual extra-urban journey times

L_{ex} is the Average extra-urban journey length (km)

η_{ex1} is the Average extra-urban journey energy efficiency of the Eco-BEV + FCRE (kWh/km)

P_{rfc} is the Rent price of the FCRE (£ per time)

α_{H2} is the Proportion of hydrogen energy used in the extra-urban journey of the Eco-BEV + FCRE (%)

P_{H2} is the Price of the hydrogen gas fuel (£/kg)

η_{H2} is the Average extra-urban journey hydrogen energy efficiency of the FCRE (kg/km)

η_{u2} is the Average urban journey energy efficiency of the Large BEV (kWh/km)

η_{ex2} is the Average extra-urban journey energy efficiency of the Large BEV (kWh/km)

t_L is the Lifespan of the BEVs (years)

The purchasing price of vehicles may fluctuate with time since the cost of the main components is changing rapidly in recent years, such as the Lithium battery pack of the BEV and FC stack and hydrogen tank in the FC system (Watabe & Leaver, 2021).

The running cost, is pure electricity cost for the Large BEV, while for the Eco-BEV + FCRE, the renting price of FCRE and hydrogen gas cost will be added in.

The electricity price will include both the Peak and Off-Peak electricity prices. A hypothesis is made that, on one hand, the electricity consumed in urban journeys is considered as under the Off-Peak Price since household BEVs are usually charged at home overnight (during Off-Peak Hours), on the other hand, the electricity used in extra-urban (long-distance journeys) is considered as under the Peak Price since the BEVs will need to be charged in public charging stations in long-distance journeys.

The hydrogen gas price will also fluctuate with time due to the production method innovations and the growth of the hydrogen industry.

For the Eco-BEV + FCRE, as per the previous discussion in this chapter, the average extra-urban journey energy efficiency and the proportion of the energy used in extra-urban journeys for both electricity and hydrogen gas will be different under the different user preferences.

In the TCO analysis, all the parameters are set as fixed (based on the parameters defined in Section 4.3 and simulation results in Section 6.3) to present the comparisons of the costs between the 2 vehicles (Large BEV and Eco-BEV + FCRE).

The parameters are presented in Table 7-1.

Table 7-1 Parameters of the TCO analysis

Parameters		Eco-BEV	Large BEV
Vehicle Purchasing Price (£) (Carwow, 2022)		14000	35000
Vehicle Lifespan (Years) (National Grid Group, 2022)		15	15
Electricity Price (£) (E.ON Next, 2023)	Electricity price - Off-Peak (£)	0.4721	0.4721
	Electricity price - Peak (£)	0.7424	0.7424
Electricity Consumption Parameters (GOV.UK, 2022)	Total urban journeys (times/year)	946	946
	Average urban journey length (km)	8.88	8.88
	Average urban journey energy efficiency (kWh/km)	0.1294	0.1625
	Total extra-urban journeys (times/year)	7	7
	Average extra-urban journey length (km)	200	200
	Average extra-urban journey energy efficiency (kWh/km)	0.03	0.22
	Proportion of electricity used in extra-urban journey (%)	12.2%	100%
FC range extender rent price (£ per time)		30	
Hydrogen Gas Price (£/kg) (Autotrader, 2022)		12	
H2 Gas Consumption Parameters (GOV.UK, 2022)	FCRE total usage count per year	7	
	Average extra-urban journey length (km)	200	
	Average extra-urban journey H2 Gas energy efficiency (kg/km)	0.0076	
	Proportion of H2 Gas used in extra-urban journey (%)	87.8%	

Using the above parameters and Equation 7-1 to Equation 7-3, the annual urban/extra-urban running cost and lifetime running cost are calculated and presented in Figure 7-1 and Figure 7-2.

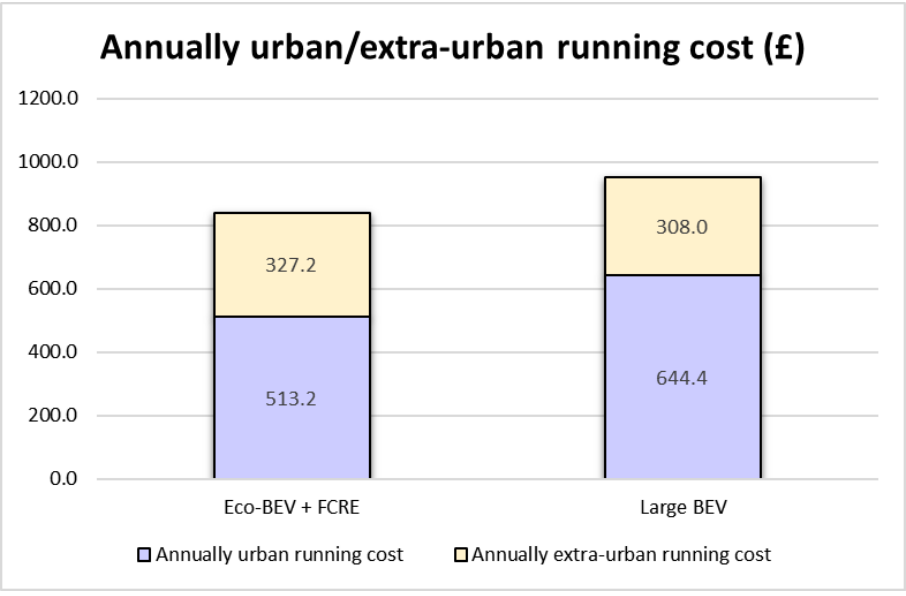

Figure 7-1 TCO analysis – Annually urban/extra-urban running cost (£)

The annual urban running costs for the Eco-BEV + FCRE and Large BEV are £513.2 and £644.4.

The annual extra-urban running costs for the Eco-BEV + FCRE and Large BEV are £327.2 and £308.

The annual total running costs for the Eco-BEV + FCRE and Large BEV are £840.4 and £952.4.

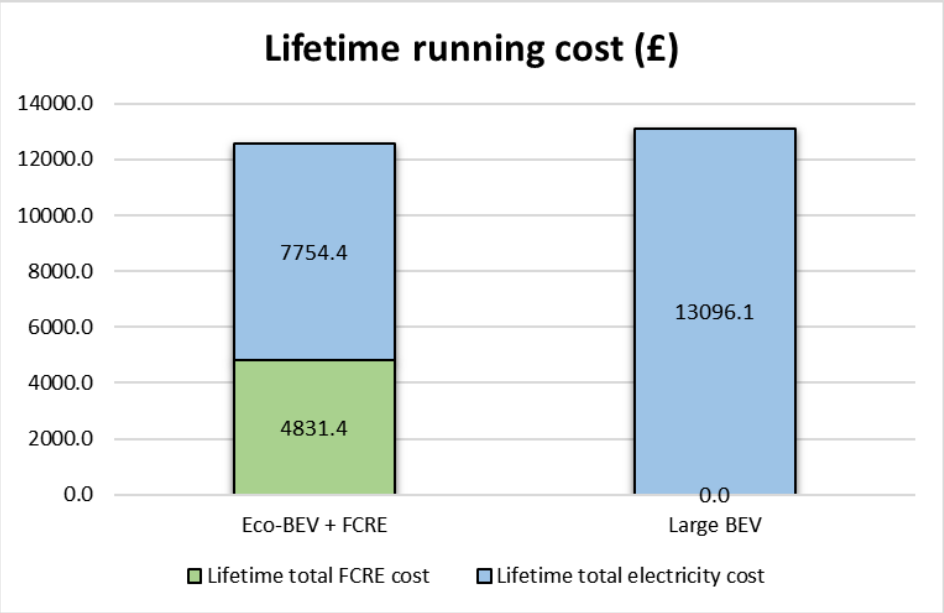

Figure 7-2 TCO analysis – Lifetime running cost (£)

The Lifetime total FCRE cost for Eco-BEV is £4831.4.

The Lifetime total electricity costs for the Eco-BEV + FCRE and Large BEV are £ 7754.4 and £13096.1.

The Lifetime total running costs for the Eco-BEV + FCRE and Large BEV are £12585.8 and £13096.1.

Therefore, the total cost of ownership can be calculated through 7-1 to (7-2)

(Figure 7-3)

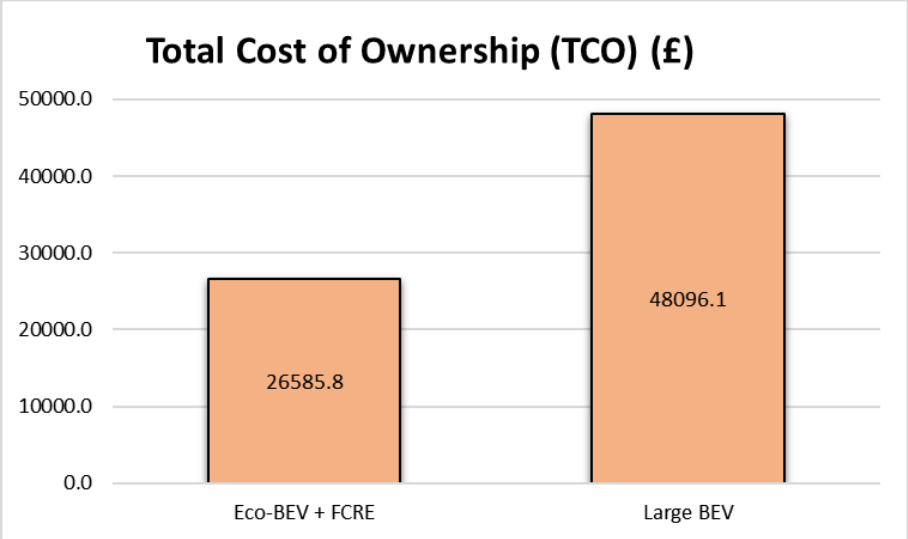

Figure 7-3 TCO analysis – Total Cost of Ownership (TCO) (£)

The Total Cost of Ownership (TCO) of the Eco-BEV + FCRE and Large BEV are £26585.8 and £48096.1.

In summary, the annual urban running cost for the Large BEV is 25.6% higher than the Eco-BEV due to the lower average energy efficiency caused by the higher weight and size which increase the rolling and aerodynamic resistances. However, the difference in the lifetime running cost of the 2 vehicles is smaller than the difference in the annual urban running cost, which is 5.9%. The reason for this smaller difference is that the total lifetime running cost of the Eco-BEV + FCRE includes the sum of the hydrogen fuel price and the assumed DHFCRE renting price and it is higher than the pure electricity cost. Finally, the most important benchmark – the TCO of Large BEV is about 79.2% higher than Eco-BEV + FCRE. There are 2 main sources of difference. Firstly, the purchasing price of Large BEV is more than doubled compared with Eco-BEV + FCRE. Secondly, the urban journey (the biggest proportion of journeys) running cost of a Large BEV is higher than Eco-BEV + FCRE due to the vehicle size. This means, for the household/individual, the total cost of ownership can be saved by 44.7% (£21510.4) if selecting Eco-BEV + FCRE – purchasing an economic size BEV and renting a DHFCRE for occasionally long-distance journeys only, rather than directly purchasing a large BEV.

7.3. National/Societal Perspective CBA

According to the APC Roadmap, the development direction of BEVs by 2050 is to realise ‘tailored for application’ (UK Automotive Council, 2017), which means people can make a decision to fulfil personal requirements while purchasing family cars like

in the current conventional vehicle market. However, limited by the performance of the current BEVs including range, charging infrastructure availability, charging speed and higher price compared with ICEVs in the same class, the market share proportion of small/eco size BEVs and large/luxury size BEVs shows a significant difference compared with the current conventional vehicles in the UK. For conventional vehicles, the percentage of small/eco-size vehicles (such as family hatchbacks) is around 57.2% and the percentage of large/luxury-size vehicles (such as saloons and SUVs) is about 42.8%. (Parkers, 2023). However, for the BEVs, the percentages are 31.4% and 68.6%. (Moveelectric, 2023). The reason for this difference in the market share proportion of small and large BEVs can be summarised by the following points.

1. The limited energy density of the battery pack in both volume and weight, the size of BEV is larger than ICEV to provide an equivalent range. The battery pack as the energy source component in the vehicle has significantly a lower energy density compared with fuel tanks in ICEV (34.2 MJ/L and 45.8 MJ/kg for gasoline) and FCEV (120 MJ/kg and 5.04 MJ/L @700 bar for Hydrogen). (RMI, 2019). While the current Lithium battery has an energy density of 0.66 MJ/kg and 1.66 MJ/L (University of Washington, 2020). Therefore, BEV manufacturers need to increase the vehicle size (or to first develop BEV versions for their large-size vehicles) to ensure enough range and interior space. Therefore, customers have to choose larger-size vehicles than ICEV to fulfil their range and space requirements.
2. Higher purchasing price compared with ICEVs. As per the light-duty vehicle sales data, (Parkers, 2023), the average price of best-selling BEVs is higher than ICEVs. And the prices of some BEV versions are higher than those ICEV vision of the same make. Therefore, the price of BEV is not affordable for all the current ICEV customers.
3. Charging issues, including charging speed and infrastructure availability. As per the discussions in Chapter xxx, the charging speed of BEV is lower than ICEV and FCEV, thus people will need more time cost while using the vehicle. Also, compared with the density of petrol stations, the number of public charging stations will still need significant growth. Therefore, compared with conventional vehicles, it is not enough convenient to have a BEV now. For the customers, the most feasible way to get the maximum convenience is to choose a large BEV with enough range to avoid frequently charging the vehicle.

Therefore, from the national/societal perspective, to solve this problem, the optimal proportion of 2 sizes of vehicles in the future should match the current values of conventional vehicles. This novel approach of DHFCRE is introduced to bridge the

above technical and economic gaps for the current BEVs to achieve the goal of 'tailored for usage' quicker in the future.

A CBA of this DHFCRE from the national/societal perspective will be undertaken which includes the consideration of long-term macroscopic cost and environmental impacts of the 2 vehicle types (Eco-BEV + Renting FCRE and Large BEV). This CBA mainly evaluates the total manufacturing cost of the main components in the 2 vehicle types, with the comparison between the current and optimal market share proportion of 2 sizes of vehicles and the impacts on the utilisation rate of infrastructure. The environmental evaluation will focus on the WTW carbon emission and the consumption of metal mineral resources in the 2 vehicle types.

Since this long-term macroscopic economic and environmental evaluation involves some future values of key parameters, some necessary predictions and hypotheses will be required in the calculations.

7.3.1. Manufacturing Cost

The long-term national/societal manufacturing cost of the 2 vehicle types is the first important benchmark to evaluate the cost and benefit of introducing this DHFCRE. In this project, the main difference between the 2 vehicle types is the energy source, where the only energy source of a Large BEV is the battery system, but a Large BEV has a battery pack and FC system working together in the occasionally long-distance journeys. Thus, the manufacturing cost comparisons in this CBA will only involve the cost of the battery system in 2 vehicles and the FC system in the DHFCRE.

The manufacturing cost of Eco-BEV + FCRE and 2 can be calculated by Equation 7-4 and Equation 7-5

$$C_{M1} = N_{EV} \times \alpha_1 \times (V_{B1} \times C_B + \alpha_{RE} \times V_{FC} \times C_{FC}) \quad (7\text{-}4)$$

$$C_{M2} = N_{EV} \times \alpha_2 \times V_{B2} \times C_B \quad (7\text{-}5)$$

Where,

C_{M1} is the manufacturing cost of Eco-BEV + FCRE (£).

N_{EV} is the total amount of BEV.

α_1 is the market share proportion of Eco-BEV + FCRE Eco-BEVs (%).

V_{B1} is the battery size in Eco-BEV + FCRE (kWh).

C_B is the battery cost (£/kWh).

α_{RE} is the coefficient of numbers of DHFCRE required for Eco-BEV.

V_{FC} is the size of the FC system (kW).

C_{FC} is the cost of the FC system (£/kW).

C_{M2} is the manufacturing cost of Large BEV (£).

α_2 is the market share proportion of Large BEV Large BEVs (%).

V_{B2} is the battery size in Large BEV (kWh).

Parameters settings:

1. N_{EV} – the total amount of BEV. In recent years, driven by the power of policy, the sales of BEVs have grown rapidly around the world. In the UK, the number of total registered BEVs (excluding hybrid vehicles) will be around 0.66 million by the end of 2022. (Zap-Map, 2023). This number will increase to 11 million by 2030, and over 30 million by 2040. (National Grid Group, 2020). The prediction by 2050 will be 37.4 million. (National Grid ESO, 2021).
2. V_{B1} & V_{B2} – the battery size of Eco-BEV + FCRE and 2. According to the vehicle and component parameterisation result in Chapter 4.3, the battery size of 2 vehicles is 12.96 kWh and 89.44 kWh.
3. C_B – the battery cost (£/kWh). By 2022, the average battery system cost in BEVs will be around £124/kWh (GreenCarReports, 2022). Researchers from the University of Münster suggest that the predicted price of a BEV battery system will be about £108/kWh by 2030, around £75/kWh by 2040 and about £58/kWh by 2050. (Mauler et al., 2021).
4. α_{RE} – the coefficient of numbers of DHFCRE required for Eco-BEVs. This demountable range extender is designed to fulfil the requirement of mostly long-distance journeys for small/eco-size vehicles. Therefore, the setting of this coefficient should consider the average times of long-distance journeys which is 7 times per year (based on the data from the UK Department of Transport) as TCO analysis mentioned above, thus the demand for DHFCRE is $\frac{7}{365}$ times per day. A hypothesis is made that the total amount of the DHFCRE is 3 times the demands to allow the time lost on the "Rent & Drop" process, centralised refuelling, and distribution process. The final coefficient is set as 0.0575.
5. V_{FC} – the size of the FC system (kW) is set as 50 kW.
6. C_{FC} – the cost of the FC system (£/kW). As per the data and predictions by NREL US, the system costs of hydrogen fuel cell systems are £128/kW by 2023, £107/kW

by 2030, £62/kW by 2040 and £45/kW by 2050. (NREL, 2021).

7. α_1 & α_2 – the market share proportion of small and large BEVs.

Figure 7-4 and Figure 7-5 present the comparison of the total manufacture cost of 2 types of vehicles by years while setting the market share proportion α as current values (31.4% small and 68.6% large) and the optimal values (57.2% and 42.8%).

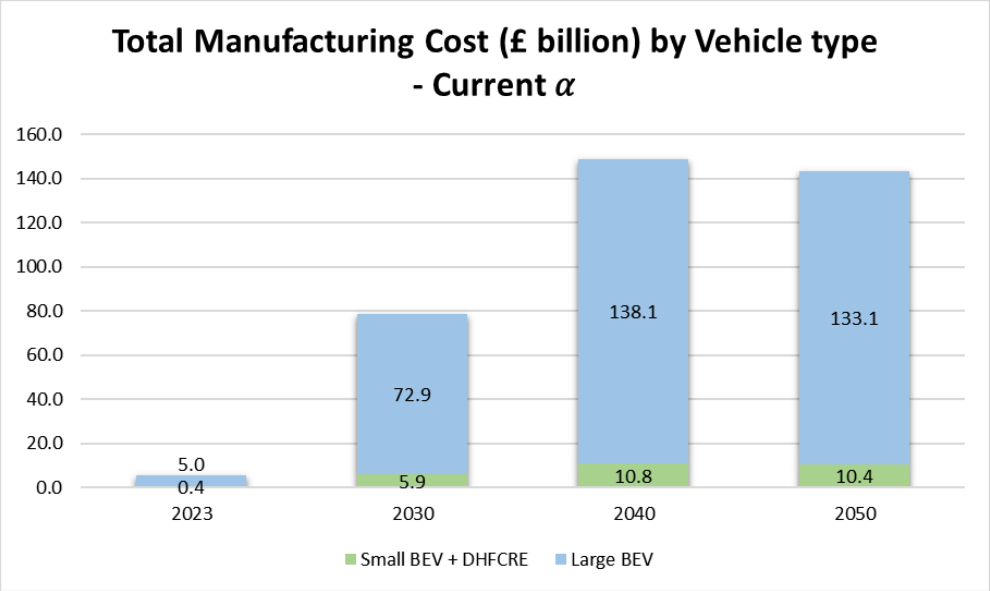

Figure 7-4 Total Manufacturing Cost (£ billion) by Vehicle type - Current α

When α – market share proportion of small and large BEVs are set as current values (31.4% small and 68.6% large),

The total manufacturing costs are:

£5.4 billion (£0.4 billion from Eco-BEV + FCRE and £5.0 billion from Large BEV) by 2023.

£78.8 billion (£5.9 billion from Eco-BEV + FCRE and £72.9 billion from Large BEV) by 2030,

£148.9 billion (£10.8 billion from Eco-BEV + FCRE and £138.1 billion from Large BEV) by 2040,

£143.5 billion (10.4 billion from Eco-BEV + FCRE and £133.1 billion from Large BEV) by 2050.

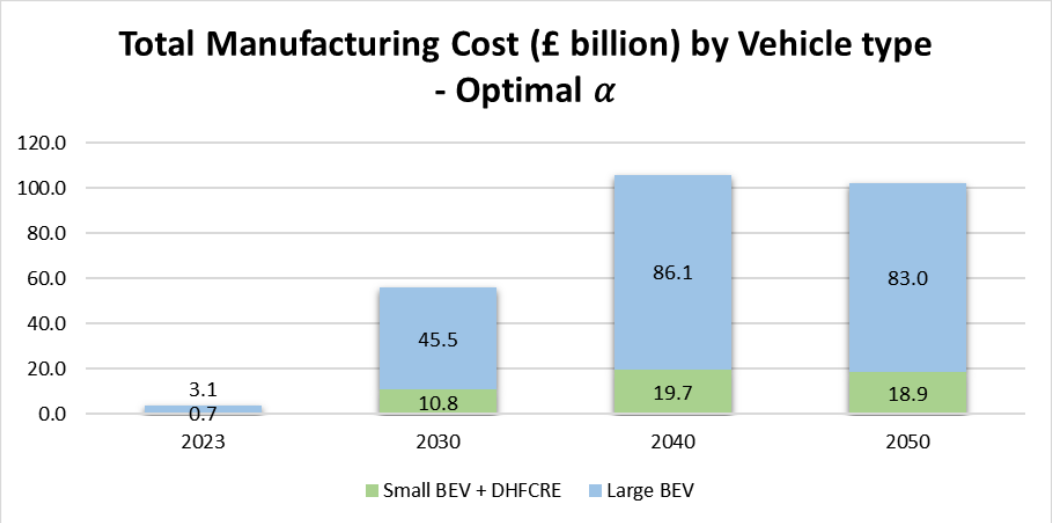

Figure 7-5 Total Manufacturing Cost (£ billion) by Vehicle type - Optimal α

When α – market share proportion of small and large BEVs are set as the optimal values (57.2% and 42.8%),

The total manufacturing costs are:

£3.8 billion (£0.7 billion from Eco-BEV + FCRE and £3.1 billion from Large BEV) by 2023,

£56.3 billion (£10.8 billion from Eco-BEV + FCRE and £45.5 billion from Large BEV) by 2030,

£105.8 billion (£19.7 billion from Eco-BEV + FCRE and £86.1 billion from Large BEV) by 2040,

£101.9 billion (£18.9 billion from Eco-BEV + FCRE and £83 billion from Large BEV) by 2050.

In summary, through the comparison of the above total manufacturing cost calculations, with the help of this DHFCRE, when the market share proportion of small and large BEVs are changed from the current value to the optimal values which are suggested by APC UK Roadmap to achieve the goal of BEV 'tailored for usage'. By introducing this DHFCRE, the total national/societal manufacturing cost will be reduced by about 28.6% by 2030, 28.9% by 2040, and 29% by 2050. Therefore, from the economic perspective, this DHFCRE could provide positive contributions to improve the current BEV performance in range and offer a flexible choice for the customer. It can partly bridge the gap between BEVs and ease the current conflict of range and cost for BEVs to allow customers to choose the most suitable vehicle size without over-concern on shortages of current BEVs). Finally, it helps to reduce the total long-term

national/societal manufacturing cost of Zero Tailpipe Emission Vehicle (ZTEV) by around 29% in the future.

7.3.2. Well-to-Wheel Carbon Emissions

In the automotive industry, the WTW carbon emission is one of the most important benchmarks to evaluate the environmental impact of a powertrain solution. For the ZTEV including pure BEV and FCEV, the TTW (Tank to Wheel) tailpipe emission is zero, therefore, the WTW carbon emission calculates only the WTT (Well to Tank) part. The WTT carbon emissions include carbon pollution from the production and distribution processes of the energy carriers (electricity and hydrogen gas in this project).

The total WTW carbon emissions of Eco-BEV + FCRE and Large BEV can be calculated by Equation 7-6 and Equation 7-7

$$M_{c1} = N_1 \times [(T_u \times L_u \times \eta_{u1} + \alpha_E \times T_{ex} \times L_{ex} \times \eta_{ex1}) \times \eta_{E-C} + (\alpha_{H2} \times T_{ex} \times L_{ex} \times \eta_{H2}) \times \eta_{H2-C}]$$

(7-6)

$$M_{c2} = N_2 \times (T_u \times L_u \times \eta_{u2} + T_{ex} \times L_{ex} \times \eta_{ex2}) \times \eta_{E-C}$$

(7-7)

Where

M_{c1} is the annual WTW total co_2 equivalent Emission per year (kg) of Eco-BEV + FCRE

N_1 is the total amount of the Eco-BEVs in Eco-BEV + FCRE

T_u is the Total annual urban journey times

L_u is the Average urban journey length (km)

η_{u1} is the Average urban journey energy efficiency of Eco-BEV (kWh/km)

α_E is the Proportion of electricity energy used in the extra-urban journey of Eco-BEV + FCRE (%)

T_{ex} is the Total annual extra-urban journey times

L_{ex} is the Average extra-urban journey length (km)

η_{ex1} is the Average extra-urban journey energy efficiency of Eco-BEV (kWh/km)

η_{E-C} is the WTT Production/Emission rate - Electricity/co_2 equivalent (kWh/kg)

α_{H2} is the Proportion of hydrogen energy used in the extra-urban journey of Eco-BEV + FCRE (%)

η_{H2} is the Average extra-urban journey hydrogen energy efficiency of the FCRE (kg/km)

η_{H2-C} is the WTT Production/Emission rate - H_2 Gas/co_2 equivalent (H_2-kg/co_{2e} -kg)

N_2 is the total amount of the Large BEV

M_{c2} is the annual WTW total co_2 equivalent Emission per year (kg) of Large BEV

η_{u2} is the Average urban journey energy efficiency of the Large BEV (kWh/km)

η_{ex2} is the Average extra-urban journey energy efficiency of the Large BEV Vehicle (kWh/km)

The parameter settings are presented in Table 7-2.

Table 7-2 Parameter settings of WTW carbon emission calculations

	Parameters	Current α $*^2$		Optimal α $*^3$	
		Small	**Large**	**Small**	**Large**
Electricity parameters	**Total vehicle amount by 2030** $*^1$	3454000	7546000	6292000	4708000
	Total urban journeys (times/year)	946	946	946	946
	Average urban journey length (km)	8.88	8.88	8.88	8.88
	Average urban journey energy efficiency (kWh/km)	0.1294	0.1625	0.1294	0.1625
	Total extra-urban journeys (times/year)	7	7	7	7
	Average extra-urban journey length (km)	200	200	200	200
	Average extra-urban journey energy efficiency (kWh/km)	0.165	0.22	0.165	0.22
	Proportion of electricity used in extra-urban journey (%)	12.2%	100.0%	12.2%	100.0%
	Production/Emission rate - Electricity/CO2 equivalent (kWh/kg) $*^4$	0.193	0.193	0.193	0.193
Hydrogen FC Parameters	**FCRE total usage count per year**	7	N/A	7	N/A
	Average extra-urban journey length (km)	200		200	
	Average extra-urban journey H2 Gas energy efficiency (kg/km)	0.0076		0.0076	
	Proportion of H2 Gas used in extra-urban journey (%)	87.8%		87.8%	
	Production/Emission rate - H2 Gas/CO2 equivalent (H2-kg/CO2-kg) $*^5$	5.55		5.55	

$*^1$ The Total vehicle amount by 2030 is calculated by using the predicted total BEV amount. (National Grid Group, 2020).

$*^{2-3}$ Same as the parameter settings in manufacturing cost calculations, Current α (31.4% small and 68.6% large), Optimal α (57.2% small and 42.8% large).

$*^4$ The WTT Production/Emission rate - Electricity/co_2 equivalent (kWh/kg) varies significantly while using different methods of power generation, therefore, the average WTT emission rate is used. (GOV.UK, 2018).

$*^5$ The WTT Production/Emission rate - H_2 Gas/ co_2 equivalent (H_2 -kg/ co_{2e} -kg) varies significantly while using different methods of hydrogen production and distribution, therefore, the average WTT emission rate is used. (Lee et al., 2018).

The result of the total annual WTW total co_2 equivalent emission per year is presented in Figure 7-6.

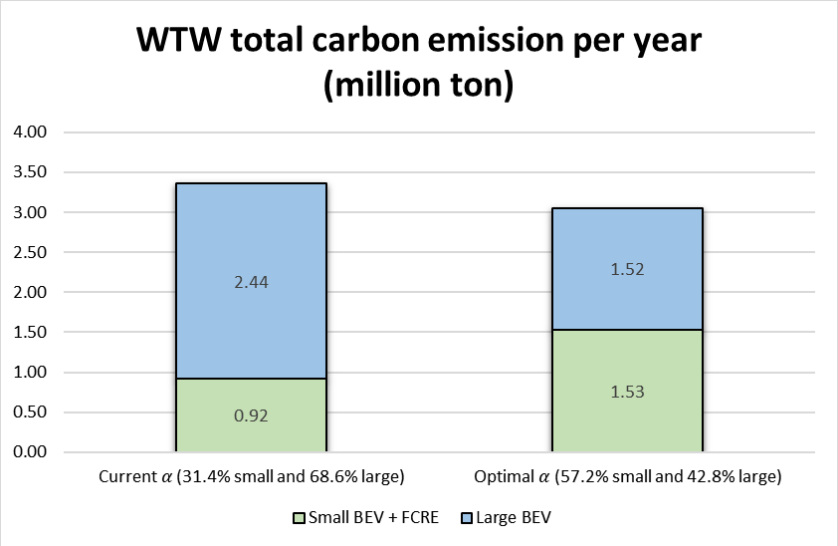

Figure 7-6 WTW total carbon emission per year (million tons)

For the current market share proportion of vehicles, the total annual carbon emissions of Eco-BEV + FCRE and Large BEV are 0.92 million and 2.44 million tons, 3.36 million tons in total.

For the optimal market share proportion of vehicles, the total annual carbon emissions of Eco-BEV + FCRE and Large BEV are 1.53 million and 1.52 million tons, 3.05 million tons in total.

Therefore, introducing this DHFCRE to allow BEV customers to purchase proper size BEVs can optimise the market share proportion of future BEVs to achieve the optimal rate. Then, the total carbon emissions can be reduced by about 9.1% which is about 0.31 million tons per year in the UK.

7.3.3. Raw Material Consumptions

As per the discussions in Chapter 2, the rapid growth and the large-scale target of the ZTEV market will significantly increase the demand for metal raw materials such as Lithium and Cobalt for batteries and platinum for fuel cell stack. However, the total reserves of these metal materials are fixed in the earth. Thus, the price of these materials will increase with the growth of the amount of new ZTEVs in the future.

This part will calculate the total consumptions of the metal materials for the Eco-BEV + FCRE and 2 by 2050 and will compare of results of different market share proportions α – Current α (31.4% small and 68.6% large), Optimal α (57.2% small and 42.8% large)

to evaluate the impact on raw material consumption of introducing this DHFCRE in the future automotive market.

The total material consumption of Lithium and Cobalt metal in the Eco-BEV + FCRE and the Large BEV can be calculated by Equation 7-8 and Equation 7-9

$$M_1 = \alpha_1 \times \ N_{EV} \times V_{B1} \times \mu \quad (7\text{-}8)$$

$$M_2 = \alpha_2 \times \ N_{EV} \times V_{B2} \times \mu \quad (7\text{-}9)$$

Where

M_1 is the total material consumption in Eco-BEV + FCRE (kg)

α_1 is the market share proportion of Eco-BEV + FCRE (%).

N_{EV} is the total amount of BEV.

V_{B1} is the battery size in Eco-BEV (kWh).

μ is the production transfer rate of metal material (kg/kWh)

M_2 is the total material consumption in Large BEV(kg)

α_2 is the market share proportion of Large BEV (%).

V_{B2} is the battery size in Large BEV (kWh).

The total material consumption of platinum metal in the FCRE can be calculated by Equation 7-10

$$M_{Pt} = \alpha_1 \times \ N_{EV} \times V_{FC} \times \alpha_{RE} \times \mu \quad (7\text{-}10)$$

Where

M_{Pt} is the total platinum metal consumption in FCRE (kg).

α_1 is the market share proportion of Eco-BEV + FCRE (%).

N_{EV} is the total amount of BEV.

V_{FC} is the size of the FC system (kW).

α_{RE} is the coefficient of numbers of DHFCRE required for Eco-BEV.

μ is the production transfer rate of metal material (kg/kW).

The parameter settings for the above equations are listed below (refer to section 7.2.1):

The total amount of BEV is 660000 in 2023, 11000000 by 2030, 30000000 by 2040, and 37400000 by 2050.

The Material consumption rate of Lithium is 0.16 (kg/kWh) (Battery University, 2022).

The Material consumption rate of Cobalt is 0.12 (kg/kWh) (Union of Concerned Scientists, 2022).

The coefficient of numbers of DHFCRE required is 0.0575.

FC System size is 50 (kW).

The Material consumption rate of Platinum is 0.00026 (kg/kWh). (HERAEUS PRECIOUS METALS, 2018).

Through the calculations on the raw material consumptions of the Eco-BEV + FCRE and BEV under the current and optimal market share proportion, it can be predicted that by introducing this FCRE for the Eco-BEV and achieving the optimal market share proportion for the future BEV market, the raw material consumption of battery including Lithium and Cobalt are significantly reduced. Due to the increase of FC system amount in the market, the platinum metal used in fuel cell catalysts will increase.

The calculation results of the raw materials consumption are listed in Table 7-3 and Figure 7-7 to Figure 7-9.

Table 7-3 Total national metal raw material consumption of Eco-BEV + FCRE and Large BEV

Raw Material Consumption		**2023**	**2030**	**2040**	**2050**	**Total Known Reserves***
Total material consumption (ton)	**Lithium (Current a)**	4580	76328	208166	259514	22000000
	Lithium (Optimal a)	2178	36299	98997	123416	
Total material consumption (ton)	**Cobalt (Current a)**	3435	57246	156124	194635	7600000
	Cobalt (Optimal a)	1633	27224	74247	92562	
Total material consumption (kg)	**Platinum (Current a)**	155	2583	7046	8784	69000000
	Platinum (Optimal a)	282	4706	12835	16001	

* Worldwide Total Known Reserves data from (Statista, 2022)

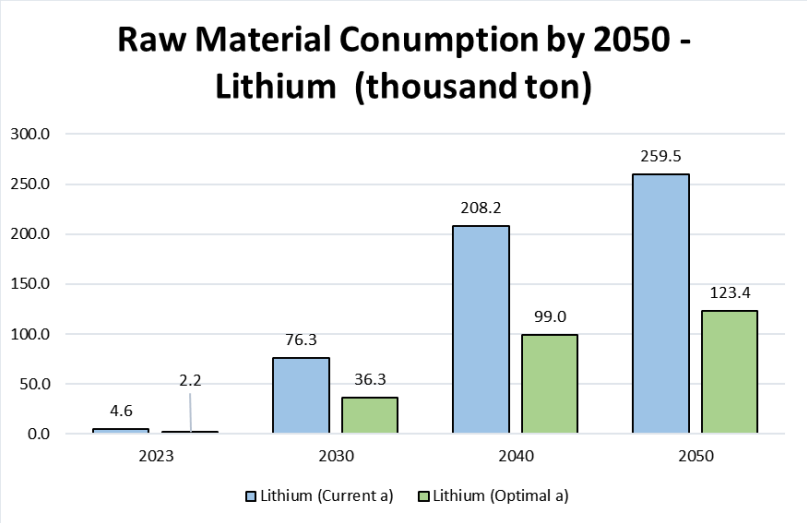

Figure 7-7 Raw material consumption by 2050 – Lithium (thousand tons)

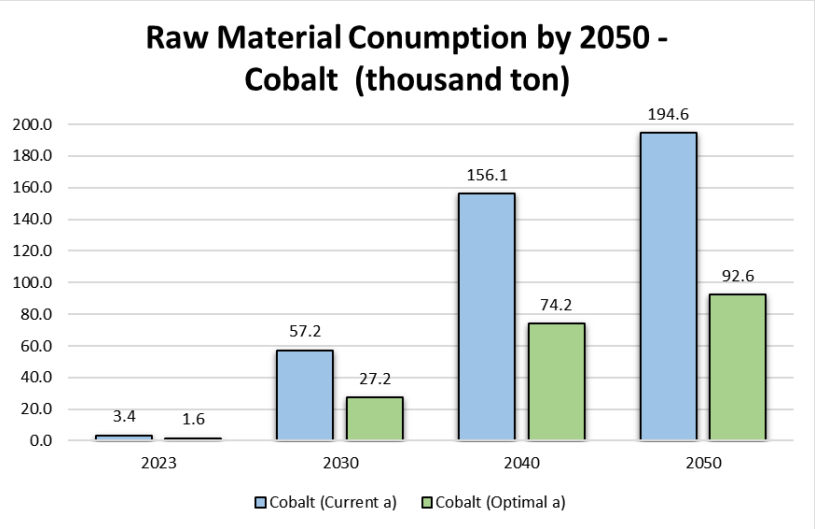

Figure 7-8 Raw material consumption by 2050 – Cobalt (thousand tons)

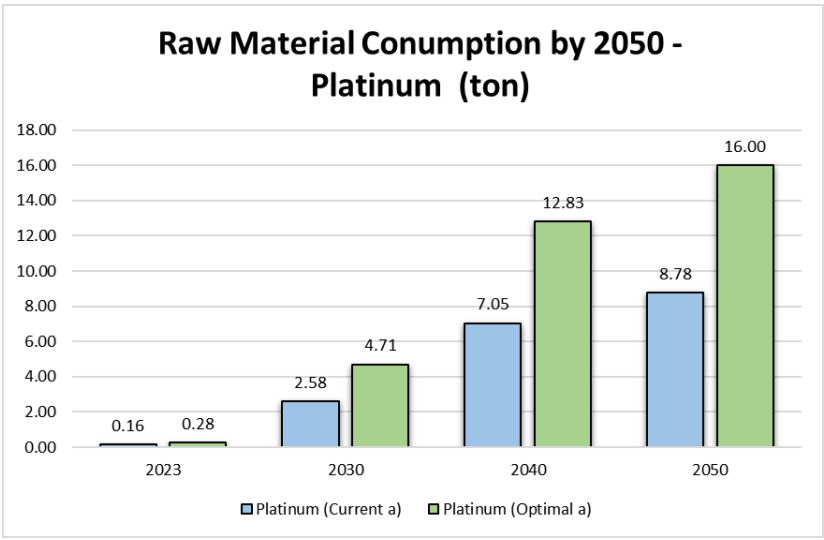

Figure 7-9 Raw material consumption by 2050 – Platinum (tons)

By introducing this FCRE to achieve the optimal BEV market share proportion by 2050, the consumption of Lithium metal material can be reduced by 52.4% (136098 tons) in the UK. While the total known reserves of Lithium metal are 22 million tons, this means that the UK BEV industry could save Lithium metal on vehicle batteries for the world for around 0.62% of the worldwide total reserve. For the Cobalt metal, by 2050, the total consumption of vehicle batteries in the UK will be reduced by 52.4% (102073 tons) which is 1.34% of the worldwide total reserve of Cobalt metal material. For the platinum metal, by 2050, the total consumption from the FC range extender will increase by 82.7% (7.2 tons) which is 0.01% of the worldwide total reserve.

7.4. Summary of Cost Benefit Analysis

Through the calculations and predictions in this CBA of introducing the demountable hydrogen fuel cell range extender (DHFCRE) for the Small/Eco-size BEVs, the result can be summarised as following points:

- **Individual/household perspective of cost**

Refer to the results of Section 7.1, from the perspective of individual/household cost on BEV, the total cost of ownership (TCO) (which only considered the purchase price and running cost) by choosing an Eco-BEV and renting FCRE for only long-distance journeys can reduce the 15-year TCO by 44.7% (about £21500) due to the benefit produced by this FCRE including the lower purchasing price and running cost. It avoids the energy waste in the Large BEV for the over-sized battery under short and mid-range journeys.

- **National/Societal perspective of cost**

From the national/societal manufacturing cost perspective of the BEV industry, by introducing this DHFCRE for the Eco-BEVs, the total national/societal manufacturing cost will be reduced by about 28.6% by 2030, 28.9% by 2040, and 29% by 2050. Therefore, from the economic perspective, this DHFCRE could provide positive contributions to improve the current BEV performance in range and offer a flexible choice for the customer. It can partly bridge the gap of BEVs and ease the current conflict of range and cost for BEVs to allow customers to choose the most suitable vehicle size without over-concern on shortages of current BEVs). Finally, it helps to reduce the total long-term national/societal manufacturing cost of ZTEV by around 29% in the future.

- **National/Societal perspective of environmental considerations**

From the national/societal environmental perspective of the future BEV industry, by introducing this DHFCRE for the Eco-BEVs, the total WTW carbon emissions and the metal raw material consumption can be reduced. This DHFCRE allows BEV customers to purchase proper size BEVs which can optimise the market share proportion of future BEVs. Then, the total carbon emissions can be reduced by about 9.1% which is about 0.31 million tons per year in the UK.

By introducing this FCRE to achieve the optimal BEV market share proportion by 2050, the consumption of Lithium metal material can be reduced by 52.4% in the UK which means that the UK BEV industry could save Lithium metal on vehicle batteries for the world around 0.62% of the worldwide total reserve. For Cobalt metal, by 2050, the total consumption of vehicle batteries in the UK will be reduced by 52.4% which is 1.34% of the worldwide total reserve of Cobalt metal material. For the platinum metal, by 2050, the total consumption from the FC range extender will increase by 82.7% however, it is only 0.01% of the worldwide total reserve.

The limitations of the CBA are summarised as follows:

- **Individual/household perspective CBA limitation**

As discussed in Section 7.2, in the calculations of the Total Cost of Ownership (TCO) for Large BEV and Eco-BEV + FCRE, only the vehicle purchasing price and running costs are compared. The cost of insurance, maintenance, repair, tax and depreciation are not considered since these parameters are not the key discussion points of this project.

- **Societal/national perspective CBA limitation**

For the societal CBA, a number of relevant parameters used prediction values such as the cost of Lithium battery, fuel cell stack and hydrogen tank will significantly fluctuate due to the change of product volume. Similarly, the carbon emission and raw material rates for the production of the battery pack and FC system may change related to future technological innovations.

Chapter 8 Conclusions and Future Works

8.1. Conclusions

Through the literature review on the investigation of BEV and FCEV technologies, the superiorities and drawbacks of them can be summarised as follows:

BEV has superiorities including high powertrain efficiency, fast-developing charging infrastructures, low fuel cost, fast-decreasing manufacturing cost due to increasing market volume, etc. But have shortages in energy density, range limit, charging speed, high cost (due to the mandatory larger size for longer range limited by the battery energy density), etc.

FCEV has superiorities including high energy density, fast refuelling speed, sufficient range, etc. But have limitations on high cost (both manufacturing and fuel cost due to market volume), limited infrastructure availability, lack of acceptance in public family vehicle customers, etc.

To leverage the advantages of the two technologies and to mitigate the limitations, a novel powertrain hybridisation method of “Eco-BEV + DHFCRE” was proposed. By popularising this demountable FC range extender under a “Rent & Drop” business model, it has potentials to magnify the superiorities of both technologies, such as fuel economy and higher energy consumption of BEV, the sufficient range and high energy density of FCEV. Also, it can deal with the problems of infrastructure dependency, and the high purchasing price due to expensive core components and the users can choose the most appropriate size of their BEVs without the “range anxiety” concerns.

To evaluate the performance of the proposed novel powertrain concept, simulation models of the proposed concept of “Eco-BEV + DHFCRE” and the full-size Large BEVs were developed based on the Matlab/Simulink platform. The simulation model was validated by the experimental test results from Coventry University Microcab Laboratory with an acceptable error level within the tolerance.

To protect the core components and optimise the performance of the proposed novel powertrain concept, scientific control algorithms were developed and tested for the EMS of the DHFCRE, including State-Machine, Fuzzy Logic, ECMS and ANN algorithms. Also, the EMS further optimisation framework was designed by developing a front-end program which connected the DHFCRE with the external information including the BEV’s VCU signals, traffic and navigation information, driver’s

preferences and the simulation results related to characteristics of EMS algorithms under certain driving conditions.

Based on analysis of published duty cycle data and the real-world driving conditions, the simulation scenarios are defined as follows based on the EU WLTP duty cycle:

Scenario 1 – Long-distance Highway cycle (200 km)

Scenario 2 – Mid-range mixed urban & extra-urban cycle (100 km)

Scenario 3 – Short-range urban cycle (50 km)

Through the simulation result analysis, the findings and contributions of this thesis can be summarised as follows:

- **Fuel economy**

For the fuel cost assessments, compared with the target large full-size BEV, the proposed powertrain of “Eco-BEV + DHFCRE” reduced 28.4% in the long-distance highway cycle, reduced 28.3% in the mid-range mixed urban & extra-urban cycle and reduced 6% in the short-range urban cycle. The reason for this fuel cost reduction includes the higher resistances of the full-size BEV due to the increased battery size to provide a longer range and the cost ratio between electricity and hydrogen gas. However, in the short-range urban cycle, the stand-alone Eco-BEV provides the lowest fuel cost which is 15.3% lower than the Eco-BEV + DHFCRE concept and 20.4% lower than the Large BEV.

- **Overall vehicle energy efficiency**

For the overall vehicle energy efficiency results, compared with the target large full-size BEV, the proposed powertrain of “Eco-BEV + DHFCRE” has an approximately 23.5% lower in the long-distance highway cycle, 16% lower in the mid-range mixed urban & extra-urban cycle and reduced 16.1% in the short-range urban cycle. Also, similar to the fuel cost results, in the short-range urban cycle, the stand-alone Eco-BEV provides the highest overall vehicle energy efficiency. The reason BEV has higher energy efficiency is that the energy efficiency of the [battery – motor] powertrain combination is higher than the [FC – DC-DC – battery – motor] powertrain combination which avoids the energy loss in the DC-DC and fuel cell stack.

- **Control algorithm characteristics and EMS further optimisations**

For the performance of and characteristics of the scientific EMS control algorithms compared with the rule-based State-Machine EMS, in the long-distance highway cycle

and mid-range mixed urban & extra-urban cycle, the ANN EMS has the best performance on the fuel economy which is 6.7% and 9.5% lower than the State-Machine EMS. The ECMS algorithm provided the highest overall energy efficiency in the long-distance highway cycle and mid-range mixed urban & extra-urban cycle which are 9% and 1.5 higher than the State-Machine EMS. In the short-range urban cycle, the Fuzzy Logic EMS has the lowest fuel cost and the highest overall energy efficiency. Based on these results of the control algorithm characteristics, a final optimisation was implemented for the EMS front-end program which enabled the EMS to select the most appropriate algorithm based on different driver's preferences, driving conditions and external traffic information.

- **Result analysis summary and marketing model discussions**

Referring to the simulation results, the proposed powertrain of DHFCRE increased the functionality of the Eco-BEV by offering sufficient range, at the same time reduced the fuel cost, but this powertrain hybridisation caused a lower overall energy efficiency compared with the full-size large BEV in all kinds of driving scenarios. However, in the short urban journeys, the stand-alone Eco-BEV had the best performance on both fuel economy and overall energy efficiency, this means as proposed in this thesis, the range extender should be designed into a demountable style instead of a fixed-on design like an FCEV. Also, the UK driving behaviour statistics proved that the frequency of long-distance trips was only about 2% per year. And the cost of FC systems (such as FC stack and hydrogen tanks) are very expensive now due to the low production volume. Hence, the ideal business model of this DHFCRE is renting rather than purchasing, this method has various advantages including:

Firstly, it can increase the vehicle functionality and cost-effectiveness for the BEV owners. Then, this allows the FC range extenders to be centralised refuelled which can avoid the infrastructure dependency and increase the utilisation rate of the early-stage hydrogen stations. Moreover, the popularisation of this DHFCRE can accelerate the transition of the current BEV to the ideal mode guided by the APC roadmap to realise the 2050 goal of being "tailored for usage", people can purchase their BEV by only considering their own demands without any concerns about the range and size conflicts. Finally, the popularisation of this DHFCRE can increase the production volume of the hydrogen fuel cell system which is important for the future cost reduction of core components as well as increase the understanding and acceptance of the vehicle customers.

An extensive Cost Benefit Analysis (CBA) of the proposed concept of “Eco-BEV + DHFCRE” is undertaken from both individual and societal perspectives with the considerations of both economic and environmental factors. The CBA results can be summarised as follows:

- **From the individual/household perspective**

The proposed concept of “Eco-BEV + DHFCRE” can reduce 5.9% of the vehicle's lifetime running cost and 79.2% of the Total Cost of Ownership (TCO) compared with the full-size large BEV.

- **From the societal/national perspective**

By popularising this DHFCRE, the market share proportion of the UK BEV market can be optimised, which means people can purchase their ideal size of BEV without concerns about the BEV range and size conflicts. It can reduce the total nationwide manufacturing cost by 29% before 2050. For the environmental considerations, it can reduce the national ZTEV Well to Wheel (WTW) carbon emissions by 9.1% and reduce 52.4% of raw metal material (Lithium and Cobalt) consumption for battery production.

To conclude, this thesis proposed a novel powertrain hybridisation concept of “Eco-BEV + DHFCRE”. Through simulation result analysis and CBA from both individual and societal perspectives with the considerations of both economic and environmental factors, evaluated and proved the performance of this powertrain concept. Also, to further optimise the performance of this DHFCRE, scientific control algorithms and pathways are developed and validated.

8.2. Limitations and Future Works

- **Modelling and validations**

The developed simulation model involves a number of look-up-table-based and simplified mathematical formula-based model components whose accuracy was lower than the physical models in theory. For future work, these models could be replaced by the physical models to realise the highest result accuracy.

The duty cycle model in this project is a 2D model which did not involve the road slope angle, the real-world wind speed, air temperature and air density changes. For future works, generating a 3D duty cycle and at the same time introducing these missed parameters can further improve the simulation result accuracy to present a simulation close to the real-world driving condition. Moreover, in order to evaluate the

performance of this concept in other regions, more duty cycles can be simulated such as Japan JC duty cycles for Asian driving conditions, and EPA cycles for North American conditions. The simulation results of control algorithms may defer the differences in the duty cycles.

Limited by the realistic difficulties mentioned in Section 3.5, the simulation model was validated by the experimental results from the Microcab dyno test instead of using the real-world tests and experiment based on the proposed powertrain concept of “DHFCRE + Eco-BEV”. For future works, the validations should focus on both the individual components and subsystems level and the overall vehicle performance level of the proposed concept, which could improve the accuracy of the model.

- **FCRE physical connection methods**

In this project, the physical connection of boot-based is used for the simulation parameterisations. However, the physical connection method should depend on the demand of the users since different connection style has various costs and benefits. The future works in this area can focus on the other two physical connection styles, further experiments are required to investigate the changes in rolling and aerodynamic resistance associated with relevant parameters. Such as some Computational Fluid Dynamics (CFD) aerodynamic simulations or experiments are required for the roof-rack-based style to confirm the changes in the vehicle's frontal area and the aerodynamic coefficient. For the trailer-based style, some simulations or experiments are required to confirm the extra rolling resistance from the trailer tyres and axles which will be added to the total vehicle rolling resistance

- **ANN algorithm and EMS signal communications**

The ideal training method of the ANN model is to use the real-world experimental data of the market-ready FCEV products or the database of FCEV EMS testing data from research or manufacturing institutes. However, due to realistic difficulties in this project, the ANN is trained by the Fuzzy Logic EMS simulation results which have very similar control behaviours with the Fuzzy Logic EMS with only a slight improvement of the result. For the future works, the real-world results and databased from research or manufacturing institutes can be used to further train the ANN EMS model to improve the performance of the EMS.

The EMS of this DHFCRE is developed to have the ability to manage the output power of the FC system and battery pack by analysing the input of total power demand and the battery SoC signals from the BEV internal Vehicle Control Unit (VCU). Therefore,

in real-world conditions, this will require the BEV to have Application Programming Interfaces (API) which allow the DHFCRE EMS system to intervene in the signal communication and control commands of the BEV. This will require the approval of the BEV manufacturers. For the future works, an extra program can be added with the artificial intelligence and machine learning models which empower the EMS to learn the complex real-world traffic conditions including traffic congestions and make predictions for the control strategy changes to further improve the efficiency and fuel economy for the EMS.

- **Cost Benefit Analysis**

In the CBA from Individual/household perspectives, calculations of the Total Cost of Ownership (TCO) for Large BEV and Eco-BEV + FCRE only compared the vehicle purchasing price and running costs. In the future works, the cost of insurance, maintenance, repair, tax and depreciation costs of both vehicle options should be discussed to establish a comprehensive comparison.

For the societal CBA, a number of relevant parameters used prediction values such as the cost of Lithium battery, fuel cell stack and hydrogen tank will significantly fluctuate due to the change of product volume. Similarly, the carbon emission and raw material rates for the production of the battery pack and FC system may change related to future technological innovations. The future work of the CBA should focus on the fast-updating parameters mentioned above and update the CBA result based on the latest values.

Reference

Aharon, I., Shmilovitz, D. and Kuperman, A. (2017) ‘Multimode power processing interface for fuel cell range extender in battery powered vehicle’, *Applied Energy*, 204, pp. 572–581. doi:10.1016/j.apenergy.2017.07.043.

Al-Alawi, B.M. and Bradley, T.H. (2013) ‘Total cost of ownership, payback, and consumer preference modeling of plug-in hybrid electric vehicles.’, *Applied Energy*, 103, pp. 488–506.

Apicella, M. (2019) *A multi-disciplinary approach to fuel cell vehicle modelling and simulation – a study to investigate and optimise overall electric vehicle and hydrogen fuel cell electric vehicle efficiency*. dissertation.

Autotrader (2023) *Hydrogen fuel call cars explained: Should I buy a hydrogen fuel cell car?*, *AutoTrader*. Available at: https://www.autotrader.co.uk/content/advice/hydrogen-fuel-cell-cars-overview (Accessed: 15 April 2023).

AVL (2019) *AVL CRUISETM*, *AVL*. Available at: https://www.avl.com/cruise (Accessed: 13 February 2019).

Ballard (2014) *FCgen® -1020ACS*, *FCgen1020 Spec Sheet*. Available at: https://www.ballard.com/about-ballard/publication_library/product-specification-sheets/fcgen1020-spec-sheet (Accessed: 09 April 2019).

Barros, V.R. and Field, C.B. (2015) *Climate change 2014*. Cambridge [u.a.]: Cambridge Univ. Pr.

Bassam, A.M. *et al.* (2016) ‘An improved energy management strategy for a hybrid fuel cell/battery passenger vessel’, *International Journal of Hydrogen Energy*, 41(47), pp. 22453–22464. doi:10.1016/j.ijhydene.2016.08.049.

Battery University (2018) *How to Prolong Lithium-based Batteries*, *Battery University*. Available at: https://batteryuniversity.com/learn/article/how_to_prolong_Lithium_based_batteries (Accessed: 01 January 2019).

Battery University (2021) *BU-107: Comparison table of secondary batteries*, *Battery University*. Available at: https://batteryuniversity.com/article/bu-107-comparison-table-of-secondary-batteries (Accessed: 04 March 2023).

Battery University (2022) *BU-205: Types of Lithium-ion*, *Battery University*. Available at: https://batteryuniversity.com/article/bu-205-types-of-Lithium-ion (Accessed: 22 April 2023).

Bayram, I.S. (2021) 'Impacts of electric vehicle charging under cold weather on Power Networks', *2021 56th International Universities Power Engineering Conference (UPEC)* [Preprint]. doi:10.1109/upec50034.2021.9548276.

Biddle, A. (2014) *Toyota car safety: Stability and control technologies*, *Toyota UK Magazine*. Available at: https://mag.toyota.co.uk/toyota-car-safety-stability-control-technologies/ (Accessed: 23 March 2023).

BMW (2019) *BMW i3 and i3s | New Vehicles | BMW UK*, *Bmw.co.uk*. Available at: https://www.bmw.co.uk/bmw-cars/bmw-i/2018-i3-and-i3s?gclid=Cj0KCQiArenfBRCoARIsAFc1FqforYlMbfaw-eV39IF4OF2A0fQ6X-dhPtKoXphBnmmUAunbUk9eF2QaAiNnEALw_wcB&gclsrc=aw.ds/ (Accessed: 07 January 2019).

Bodemann, C. (2004) 'The Successful Development Process with Matlab Simulink in the Framework of ESA's ATV Project', *55th International Astronautical Congress of the International Astronautical Federation, the International Academy of Astronautics, and the International Institute of Space Law* [Preprint]. doi:10.2514/6.iac-04-u.3.b.03.

Brennan, J.W. and Barder, T.E. (2016) *Battery Electric Vehicles vs. Internal Combustion Engine Vehicles*, *Arthur D Little*. Available at: http://www.adlittle.com/en/insights/viewpoints/battery-electric-vehicles-vs-internal-combustion-engine-vehicles (Accessed: 12 July 2018).

Bromaghim, G. *et al.* (2010) 1st edn, *Hydrogen and fuel cells: The U.S. market report*. 1st edn. Washington, DC: National Hydrogen Association.

Brooker, A. *et al.* (2015) 'FASTSim: A model to estimate vehicle efficiency, cost and performance', *SAE Technical Paper Series* [Preprint]. doi:10.4271/2015-01-0973.

Bubeck, S., Tomaschek, J. and Fahl, U. (2016) 'Perspectives of electric mobility: Total cost of ownership of electric vehicles in Germany', *Transport Policy*, 50, pp. 63–77.

Bundesregierung (2019) *Weitere Steuervorteile für Elektroautos*, *Startseite*. Available at: https://www.bundesregierung.de/Content/DE/Artikel/2016/05/2016-05-18-elektromobilitaet.html;jsessionid=4800885F4CF543C627A4132F978A0B08.s2t2 (Accessed: 11 June 2018).

Campanari, S., Manzolini, G. and Garcia de la Iglesia, F. (2009) 'Energy analysis of electric vehicles using batteries or fuel cells through well-to-wheel driving cycle simulations', *Journal of Power Sources*, 186(2), pp. 464–477. doi:10.1016/j.jpowsour.2008.09.115.

Cao, W., Zhang, J. and Li, H. (2020) 'Batteries with high theoretical energy densities', *Energy Storage Materials*, 26, pp. 46–55. doi:10.1016/j.ensm.2019.12.024.

CarEngineer (2020) *Vehicle inertia calculation tool*. Available at: https://www.car-engineer.com/vehicle-inertia-calculation-tool/ (Accessed: 13 June 2022).

CarMax (2023) *Electric car range: How much do you need?*, *CarMax*. Available at: https://www.carmax.com/articles/electric-car-range (Accessed: 05 January 2024).

Cassiano, D.R. *et al.* (2016) 'On-board monitoring and simulation of Flex Fuel Vehicles in Brazil', *Transportation Research Procedia*, 14, pp. 3129–3138. doi:10.1016/j.trpro.2016.05.253.

CEA (2016) *Technology roadmap for energy saving and new energy vehicles*. BEIJING: Beijing: China Machine Press.

Çeven, S., Albayrak, A. and Bayır, R. (2020) "Real-time range estimation in electric vehicles using Fuzzy Logic classifier," *Computers & Electrical Engineering*, 83, p. 106577. Available at: https://doi.org/10.1016/j.compeleceng.2020.106577.

Chai, W. (2022) *What is Fuzzy Logic? - Definition from SearchEnterpriseAI*, *SearchEnterpriseAI*. Available at: https://www.techtarget.com/searchenterpriseai/definition/fuzzy-logic#:~:text=Fuzzy%20logic%20is%20an%20approach,at%20Berkeley%20in%20the%201960s. (Accessed: 13 June 2022).

Chen, Z. *et al.* (2021) "A survey on key techniques and development perspectives of equivalent consumption minimisation strategy for hybrid electric vehicles," *Renewable and Sustainable Energy Reviews*, 151, p. 111607. Available at: https://doi.org/10.1016/j.rser.2021.111607.

Cioroianu, C.C. *et al.* (2017) 'Simulation of an electric vehicle model on the new WLTC test cycle using AVL Cruise Software', *IOP Conference Series: Materials Science and Engineering*, 252, p. 012060. doi:10.1088/1757-899x/252/1/012060.

Climate Action - European Commission (2017) *Proposal for post-2020 CO2 targets for cars and vans - Climate Action - European Commission*, *Climate Action - European Commission*. Available at: https://ec.europa.eu/clima/policies/transport/vehicles/proposal_en (Accessed: 22 March 2018).

CNN (2019) *These countries want to ban gas and diesel cars*, *CNNMoney*. Available at: https://money.cnn.com/2017/09/11/autos/countries-banning-diesel-gas-cars/index.html (Accessed: 10 September 2018).

Cobalt Institute (2022) *Cobalt market report 2021*, *Cobalt Institute*. Available at: https://www.Cobaltinstitute.org/wp-content/uploads/2022/05/FINAL_Cobalt-Market-Report-2021_Cobalt-Institute-1.pdf (Accessed: 04 March 2023).

Cornish, J. (2011) *Hydrogen Fueling Station Cost Reduction Study*, *Osti.gov*. Available at: https://www.osti.gov/servlets/purl/1120569 (Accessed: 16 July 2018).

Das, H.S., Tan, C.W. and Tatim, A.H.M. (2017) 'Fuel cell hybrid electric vehicles: A review on power conditioning units and topologies', *Renewable and Sustainable Energy Reviews*, 76, pp. 268–291.

Dassault Systèmes (2019) *Dymola - Dassault Systèmes®*, *3ds.com*. Available at: https://www.3ds.com/products-services/catia/products/dymola/ (Accessed: 02 March 2019).

De Almeida, S.C.A. and Kruczan, R. (2021) 'Effects of drivetrain hybridization on fuel economy, performance and costs of a fuel cell hybrid electric vehicle', *International Journal of Hydrogen Energy*, 46(79), pp. 39404–39414. doi:10.1016/j.ijhydene.2021.09.144.

Delos Reyes, J.R., Parsons, R.V. and Hoemsen, R. (2016) 'Winter happens: The effect of ambient temperature on the travel range of electric vehicles', *IEEE Transactions on Vehicular Technology*, 65(6), pp. 4016–4022. doi:10.1109/tvt.2016.2544178.

Deng, J. *et al.* (2020) 'Electric vehicles batteries: Requirements and challenges', *Joule*, 4(3), pp. 511–515. doi:10.1016/j.joule.2020.01.013.

Department for transport GOV UK (2018) *National Travel Survey:England 2017'*, *National Travel Survey*. Available at: https://assets.publishing.service.gov.uk/government/uploads/system/uploads/attachment_data/file/729521/national-travel-survey-2017.pdf (Accessed: 17 January 2019).

DieselNet (2022) *Emission Test Cycles: ECE 15 + EUDC / NEDC*, *Dieselnet.com*. Dieselnet.com. Available at: https://dieselnet.com/standards/cycles/ece_eudc.php (Accessed: 2022).

DriveElectric (2023) *Electric vehicle range - everything you need to know*, *DriveElectric*. Available at: https://www.drive-electric.co.uk/guides/general/electric-vehicle-range-everything-you-need-to-know/ (Accessed: 05 January 2024).

Du, C. *et al.* (2022) 'Optimization of Energy Management Strategy for fuel cell hybrid electric vehicles based on Dynamic Programming', *Energies*, 15(12), p. 4325. doi:10.3390/en15124325.

EAFO (2017) *Electric vehicle charging infrastructure | EAFO*, *Eafo.eu*. Available at: http://www.eafo.eu/electric-vehicle-charging-infrastructure (Accessed: 28 January 2018).

Edmondson, J. (2020) *High voltage hybrid cars, buses and trucks 2021-2041*, *IDTechEx Reports*. Available at: https://www.idtechex.com/en/research-report/full-hybrid-electric-vehicle-markets-2021-2041/788 (Accessed: 24 February 2023).

EERE (2019) *Hydrogen Production: Natural Gas Reforming*, *Energy.gov*. Available at: https://www.energy.gov/eere/fuelcells/hydrogen-production-natural-gas-reforming (Accessed: 09 January 2019).

EERE US (2023a) *Alternative fuels and advanced vehicles*, *Alternative Fuels Data Center: Alternative Fuels and Advanced Vehicles*. Available at: https://afdc.energy.gov/fuels/ (Accessed: 04 February 2024).

EERE US (2023b) *FOTW #1272, January 9, 2023: Electric Vehicle Battery Pack costs in 2022 are nearly 90% lower than in 2008, according to DOE estimates*, *Energy.gov*. Available at: https://www.energy.gov/eere/vehicles/articles/fotw-1272-january-9-2023-electric-vehicle-battery-pack-costs-2022-are-nearly (Accessed: 15 April 2023).

EESI (2017) *Comparing U.S. and Chinese Electric Vehicle Policies | Article | EESI*, *EESI*. Available at: http://www.eesi.org/articles/view/comparing-u.s.-and-chinese-electric-vehicle-policies (Accessed: 24 October 2017).

Elmer, T. *et al.* (2015) 'Fuel cell technology for domestic built environment applications: State of-the-art review'', *Renewable and Sustainable Energy Reviews*, 42, pp. 913–931.

EPA.GOV (2022) *Dynamometer Drive Schedules*. Environmental Protection Agency. Available at: https://www.epa.gov/vehicle-and-fuel-emissions-testing/dynamometer-drive-schedules (Accessed: 02 November, 2022).

EPA-US (2022) *Global Greenhouse Gas Overview*, *EPA*. Available at: https://www.epa.gov/ghgemissions/global-greenhouse-gas-overview (Accessed: 11 July 2024).

ETRAC (2017) *Ertrac - ERTRAC Roadmaps*, *Ertrac.org*. Available at: https://www.ertrac.org/index.php?page=ertrac-roadmap (Accessed: 02 July 2018).

Europa.EU (2014) *Lex - 02014L0094-20141117 - en - EUR-Lex*, *EUR*. Available at: https://eur-lex.europa.eu/legal-content/EN/TXT/?uri=CELEX%3A02014L0094-20141117 (Accessed: 05 January 2024).

European Commission (2017a) *EUROPA - Driving and parking patterns of European car drivers - a mobility survey | SETIS - European Commission*, *Setis.ec.europa.eu*. Available at: https://setis.ec.europa.eu/related-jrc-activities/jrc-setis-reports/driving-and-parking-patterns-of-european-car-drivers (Accessed: 20 July 2018).

European Commission (2017b) *Open Data Portal for the European Structural Investment Funds - European Commission | Socrata.*, *Socrata*. Available at: https://cohesiondata.ec.europa.eu/themes/7 (Accessed: 19 October 2017).

EV Magazine (2023) *Top 10: Best-selling evs in the UK*, *EV Magazine*. Available at: https://evmagazine.com/top10/top-10-best-selling-evs-in-the-uk (Accessed: 05 January 2024).

EvChargingMag (2023) *The top 10 Fastest Electric Vehicle Charging stations for 2023*, *EvChargingMag*. Available at: https://evchargingmag.com/the-top-10-fastest-electric-vehicle-charging-stations-for-2023 (Accessed: 15 April 2023).

EVspecifications (2022) *2012 Nissan Leaf SV - Specifications*, *EVSpecifications*. Available at: https://www.evspecifications.com/en/model/55b43 (Accessed: November 5, 2023).

EVspecifications (2022) *2012 Nissan Leaf SV - Specifications*, *EVSpecifications*. Available at: https://www.evspecifications.com/en/model/55b43 (Accessed: 05 November 2023).

Evspecifications (2023) *Tesla Specifications*, *Tesla electric car models, electric vehicles by years.* Available at: https://www.evspecifications.com/en/brand/b1e92 (Accessed: 30 April 2023).

Ev-volumes (2018) *EV-Volumes - The Electric Vehicle World Sales Database*, *Ev-volumes.com*. Available at: http://www.ev-volumes.com/country/total-world-plug-in-vehicle-volumes/ (Accessed: 17 February 2018).

Ferahtia, S. *et al.* (2023) 'Optimal Energy Management for Hydrogen Economy in a hybrid electric vehicle', *Sustainability*, 15(4), p. 3267. doi:10.3390/su15043267.

Fernández, R.Á., Cilleruelo, F.B. and Martínez, I.V. (2016) 'A new approach to battery powered electric vehicles: A hydrogen fuel-cell-based range extender system', *International Journal of Hydrogen Energy*, 41(8), pp. 4808–4819. doi:10.1016/j.ijhydene.2016.01.035.

Fogel, D.B., Fogel, L.J. and Porto, V.W. (1990) 'Evolving Neural Networks', *Biological Cybernetics*, 63(6), pp. 487–493. doi:10.1007/bf00199581.

Forbes (2017) *How Tesla's Battery Strategy Could Drive Strong Margins On Model 3*, *Forbes.com*. Available at: https://www.forbes.com/sites/greatspeculations/2017/08/18/how-teslas-battery-strategy-could-drive-strong-margins-on-model-3/#261aa2ee5cc9 (Accessed: 02 March 2018).

Franke, T., Rauh, N. and Krems, J.F. (2016) 'Individual differences in bev drivers' range stress during first encounter of a critical range situation', *Applied Ergonomics*, 57, pp. 28–35. doi:10.1016/j.apergo.2015.09.010.

Gagniuc, P.A. (2017) *Markov Chains* [Preprint]. doi:10.1002/9781119387596.

Gencoglu, M. and Ural, Z. (2009) 'Design of a PEM fuel cell system for residential application', *International Journal of Hydrogen Energy*, 34(12), pp. 5242–5248.

Geng, C., Jin, X. and Zhang, X. (2019) 'Simulation research on a novel control strategy for fuel cell extended-range vehicles', *International Journal of Hydrogen Energy*, 44(1), pp. 408–420. doi:10.1016/j.ijhydene.2018.04.038.

Global Energy Metals (2017) *Cobalt Demand*, *Global Energy Metals Corp.* Available at: https://www.globalenergymetals.com/Cobalt/Cobalt-demand/ (Accessed: 28 September 2018).

Google (2022) *Google Maps*. Google. Available at: https://www.google.com/maps (Accessed: December 1, 2023).

GOV UK (2023) *Vehicle licensing statistics: January to March 2023*, *GOV.UK*. Available at: https://www.gov.uk/government/statistics/vehicle-licensing-statistics-january-to-march-2023/vehicle-licensing-statistics-january-to-march-2023 (Accessed: 04 January 2024).

Grosjean, C. *et al.* (2012) 'Assessment of world Lithium resources and consequences of their geographic distribution on the expected development of the electric vehicle industry', *Renewable and Sustainable Energy Reviews*, 16(3), pp. 1735–1744.

Gu, X. *et al.* (2018) 'Developing pricing strategy to optimise total profits in an electric vehicle battery closed loop supply chain', *Journal of Cleaner Production*, 203, pp. 376–385.

Guzzella, L. and Sciarretta, A. (2005) "Vehicle Propulsion Systems." Available at: https://doi.org/10.1007/3-540-28853-8.

Hafsi, O. *et al.* (2022) 'Integration of hydrogen technology and energy management comparison for DC-microgrid including renewable energies and Energy Storage System', *Sustainable Energy Technologies and Assessments*, 52, p. 102121. doi:10.1016/j.seta.2022.102121.

Hagman, J. *et al.* (2016) 'Total cost of ownership and its potential implications for battery electric vehicle diffusion', *Research in Transportation Business & Management*, 18, pp. 11–17.

Han, J., Park, Youngjin and Park, Youn-sik (2012) 'A novel updating method of equivalent factor in ECMS for prolonging the lifetime of battery in fuel cell hybrid electric vehicle', *IFAC Proceedings Volumes*, 45(30), pp. 227–232. doi:10.3182/20121023-3-fr-4025.00059.

Hawley, D. (2023) *Fastest charging electric vehicles - J.D. Power and Associates*. Available at: https://www.jdpower.com/cars/shopping-guides/fastest-charging-electric-vehicles (Accessed: 26 November 2023).

He, B. and Yang, M. (2006) 'Optimisation-based energy management of series hybrid vehicles considering transient behaviour', *International Journal of Alternative Propulsion*, 1(1), p. 79. doi:10.1504/ijap.2006.010759.

Height, B. (2019) *Mesh Side Kit for Brenderup 1205s Trailers.*, *Tridenttowing.co.uk*. Available at: https://www.tridenttowing.co.uk/trailers-c1/trailer-options-accessories-c101/brenderup-trailers-options-and-accessories-c174/brenderup-1205s-trailer-complete-mesh-side-kit-450mm-height-p10676/s10676?utm_source=google&utm_medium=cpc&utm_term=brenderup-1205s-trailer-complete-mesh-side-kit-450mm-height-429658&utm_campaign=product%2Blisting%2Bads&gclid=CjwKCAjwm-fkBRBBEiwA966fZGs_5damjvAZZfNS8C3oOrRWXXSYmqwJCMw-kLKwSF6-IlXTocXo7hoCPOcQAvD_BwE (Accessed: 22 March 2019).

Hotset (2022) *What is a control algorithm? - hotset explained*, *hotset*. Available at: https://www.hotset.com/en/glossar/control-algorithm/ (Accessed: August 30, 2022).

Hunt, J. (2017) *Toyota Fuelling the Future*, *Climate Change Solutions*. Available at: http://www.climate-change-solutions.co.uk/wp-content/uploads/2017/03/JonHunttransportHFC2017.pdf/ (Accessed: 23 April 2018).

Hutchinson, T., Burgess, S. and Herrmann, G. (2014) 'Current hybrid-electric powertrain architectures: applying empirical design data to life cycle assessment and whole-life cost analysis', *Applied Energy*, 119, pp. 314–329.

Hydrogenbatteries.org (2023) *WHERE IS MY NEAREST HYDROGEN SERVICE STATION IN THE UK?*, *https://www.hydrogenbatteries.org/*. Available at: https://www.hydrogenbatteries.org/Where_Can_I_You_Buy_Filling_Up_With_Hydrogen_In_The_UK_Nearest_Service_Station.htm (Accessed: 15 April 2023).

Hypertextbook (2003) *Energy density of gasoline*, *Energy Density of Gasoline - The Physics Factbook*. Available at: https://hypertextbook.com/facts/2003/ArthurGolnik.shtml (Accessed: 15 April 2022).

Hypertextbook (2005) *Energy Density of Hydrogen - The Physics Factbook*, *Hypertextbook.com*. Available at: https://hypertextbook.com/facts/2005/MichelleFung.shtml (Accessed: 12 May 2017).

IEA (2022) *Executive summary – global fuel economy initiative 2021 – analysis*, *IEA*. Available at: https://www.iea.org/reports/global-fuel-economy-initiative-2021/executive-summary (Accessed: 15 April 2023).

IEA (2023a) *Trends in batteries – global EV outlook 2023 – analysis*, *IEA*. Available at: https://www.iea.org/reports/global-ev-outlook-2023/trends-in-batteries (Accessed: 04 January 2024).

IEA (2023b) *Trends in electric light-duty vehicles – global EV outlook 2023 – analysis*, *IEA*. Available at: https://www.iea.org/reports/global-ev-outlook-2023/trends-in-electric-light-duty-vehicles (Accessed: 30 January 2024).

IEA (2018) *Hydrogen Tracking Clean Energy Progress*, *Iea.org*. Available at: https://www.iea.org/tcep/energyintegration/hydrogen/ (Accessed: 22 January 2019).

Ieahev.org (2016) *Policies & Legislation, United States | IA-HEV*, *Ieahev.org*. Available at: http://www.ieahev.org/by-country/united-states-policy-and-legislation/ (Accessed: 01 October 2018).

InfoMine (2018) *5 Year Cobalt Prices and Price Charts*, *InfoMine*. Available at: http://www.infomine.com/investment/metal-prices/Cobalt/5-year/ (Accessed: 15 January 2019).

Intelligence, B. (2018) *Panasonic reduces Tesla's Cobalt consumption by 60% in 6 years ... | Benchmark Minerals*, *Benchmark Minerals*. Available at: https://www.benchmarkminerals.com/panasonic-reduces-teslas-Cobalt-consumption-by-60-in-6-years/ (Accessed: 28 December 2018).

International Energy Agency (2018) *Global EV Outlook 2018*. 1st edn. [S.l.]: International Energy Agency.

IOR Energy (2022) *List of common conversion factors (engineering conversion factors) ...*, *[Engineering Conversion Factors]*. Available at: https://web.archive.org/web/20100825042309/http:/www.ior.com.au/ecflist.html (Accessed: 04 March 2023).

Islameka, M. *et al.* (2023) 'Energy Management Systems for Battery Electric Vehicles', *Emerging Trends in Energy Storage Systems and Industrial Applications*, pp. 113–150. doi:10.1016/b978-0-323-90521-3.00006-5.

J.D.Power (2022) *Electric vehicle range testing: Understanding NEDC vs. WLTP vs. EPA*, *J.D. Power*. Available at: https://www.jdpower.com/cars/shopping-guides/electric-vehicle-range-testing-understanding-nedc-vs-wltp-vs-epa (Accessed: March 5, 2022).

Jaguemont, J., Boulon, L. and Dubé, Y. (2016) 'A comprehensive review of Lithium-ion batteries used in hybrid and electric vehicles at cold temperatures', *Applied Energy*, 164, pp. 99–114.

Janiesch, C., Zschech, P. and Heinrich, K. (2021) ‘Machine learning and deep learning’, *Electronic Markets*, 31(3), pp. 685–695. doi:10.1007/s12525-021-00475-2.

Jia, T., Wang, Y. and LI, Z. (2019) *The Research of Status of Hydrogen Energy Development*. TIANJIN: School of Auto and Transport Tianjin University of Technology and Education.

John Hayes CBE MP (2017) *£23 million boost for hydrogen-powered vehicles and infrastructure*, *GOV.UK*. Available at: https://www.gov.uk/government/news/23-million-boost-for-hydrogen-powered-vehicles-and-infrastructure (Accessed: 04 July 2018).

Johnson, D. (2022) *Fuzzy Logic Tutorial: What is, Architecture, Application, Example*, *Guru99*. Available at: https://www.guru99.com/what-is-fuzzy-logic.html (Accessed: 13 June 2022).

Kane, M. (2018) *Plug-In Electric Car Sales More Than Doubled In Germany In 2017*, *Inside EVs*. Available at: https://insideevs.com/plug-in-electric-car-sales-more-than-doubled-in-2017/ (Accessed: 02 January 2019).

Kate, P. *et al.* (2018) ‘Total cost of ownership and market share for hybrid and electric vehicles in the UK, US and Japan’, *Applied Energy*, 209, pp. 108–119.

Kato, Y. *et al.* (2016) *Energy Technology Roadmap of Japan*. New York: Springer.

Kok, T.A.H. (2015) *Development of a strategy for the management and control of multiple energy sources within series hybrid electric vehicles*. Sunderland: University of Sunderland.

Kumari, D. and Bhat, S. (2021) ‘Application of artificial intelligence in tesla- A case study’, *International Journal of Applied Engineering and Management Letter*s, pp. 205–218. doi:10.47992/ijaeml.2581.7000.0113.

Lagowski, K. (2017) *What You Should Know About Today’s Electric Car Batteries*, *FleetCarma*. Available at: https://www.fleetcarma.com/todays-electric-car-batteries/ (Accessed: 16 February 2018).

Li, C. *et al.* (2019) ‘Finite time thermodynamic optimization of an irreversible proton exchange membrane fuel cell for vehicle use’, *Processes*, 7(7), p. 419. doi:10.3390/pr7070419.

Li, L., Dababneh, F. and Zhao, J. (2019) ‘Cost-effective supply chain for electric vehicle battery remanufacturing’, *Applied Energy*, 226, pp. 277–286.

Li, R., Krishna Sinniah, G. and Li, X. (2022a) ‘The factors influencing resident’s intentions on E-bike Sharing usage in China’, *Sustainability*, 14(9), p. 5013. doi:10.3390/su14095013.

Li, X. *et al.* (2019) ‘Adaptive Energy Management Strategy for fuel cell/battery hybrid vehicles using Pontryagin’s minimal principle’, *Journal of Power Sources*, 440, p. 227105. doi:10.1016/j.jpowsour.2019.227105.

M.J. Bradley & Associates (2017) *Electric vehicle cost-benefit analysis*. Available at: https://www.nrdc.org/sites/default/files/electric-vehicle-cost-benefit-analysis_2017-09-27.pdf (Accessed: 01 February 2023).

Ma, K. *et al.* (2019) ‘Numerical Investigation on Fuzzy Logic Control Energy Management Strategy of Parallel Hybrid Electric Vehicle’, *Energy Procedia*, 158, pp. 2643–2648. doi:10.1016/j.egypro.2019.02.016.

Macquarie Research (2017) *Commodities Comment - The 2017 battery metal story might well be Cobalt*, *Macquarie Research*. Available at: https://www.metalicity.com.au/sites/metalicity.com.au/files/files/MacquarieCommoditiesComment%20Feb%202017.pdf (Accessed: 12 May 2018).

Mamdani, E.H. (1974) ‘Application of fuzzy algorithms for control of simple dynamic plant’, *Proceedings of the Institution of Electrical Engineers*, 121(12), p. 1585. doi:10.1049/piee.1974.0328.

Mathworks (2019) *AVL CRUISE*, *Mathworks.com*. Available at: https://www.mathworks.com/products/connections/product_detail/avl-cruise.html (Accessed: 13 February 2019).

Mathworks (2022) *Vehicle body 3DOF longitudinal*, *3DOF rigid vehicle body to calculate longitudinal, vertical, and pitch motion - Simulink*. Available at: https://www.mathworks.com/help/releases/R2019a/autoblks/ref/vehiclebody3doflongitudinal.html?container=jshelpbrowser (Accessed: June 2, 2022).

MathWorks (2019) *Matlab/Simulink Library - Fuel cell stack*, *Implement generic hydrogen fuel cell stack model - Simulink*. Available at: https://www.mathworks.com/help/releases/R2019a/physmod/sps/powersys/ref/fuelcellstack.html?container=jshelpbrowser (Accessed: September 2, 2019).

MAXUS (2023) *Cost-benefit analysis of electric vans in the UK*, *MAXUS Electric Vehicles and Vans*. Available at: https://saicmaxus.co.uk/cost-benefit-analysis-of-electric-vans-in-the-uk/ (Accessed: 01 January 2024).

McKinsey (2018) *Metals & Mining*, *McKinsey & Company*. Available at: https://www.mckinsey.com/industries/metals-and-mining/our-insights (Accessed: 16 January 2019).

Mekhilef, S., Saidur, R. and Safari, A. (2012) 'Comparative study of different fuel cell technologies', *Renewable and Sustainable Energy Reviews*, 16, pp. 981–989.

Microcab (2019) *Microcab H2EV*, *Microcab.co.uk*. Available at: http://www.microcab.co.uk/the-new-h2ev/ (Accessed: 08 October 2018).

Mikkelsen, K.B. (2010) 1st edn, *Design and evaluation of hybrid energy storage systems for electric powertrains*. 1st edn. Waterloo: University of Waterloo.

Millo, F. *et al.* (2023) 'Development of a neural network-based energy management system for a plug-in Hybrid Electric Vehicle', *Transportation Engineering*, 11, p. 100156. doi:10.1016/j.treng.2022.100156.

Ministry of Finance of the People's Republic of China (2017) *Notice on Adjusting the Financial Subsidy Policy for the Promotion and Application of New Energy Vehicles*, *Mof.gov.cn*. Available at: http://www.mof.gov.cn/gp/xxgkml/jjjss/201612/t20161230_2512230.html (Accessed: 09 August 2018).

Mobilityways (2022) *Cost of living and commuter trends – mobilityways*, *Mobilityways Cost of living and commuter trends Comments*. Available at: https://www.mobilityways.com/insights/cost-of-living-and-commuter-trends/ (Accessed: 05 May 2023).

Modelica (2018) *The Modelica Association — Modelica Association*, *Modelica.org*. Available at: https://www.modelica.org/ (Accessed: 01 March 2019).

Mohr, S.H., Mudd, G. and Giurco, D. (2012) 'Lithium Resources and Production: Critical Assessment and Global Projections', *Minerals*, 2(1), pp. 65–84.

Monticello, M. (2019) *Preparation and driving tips for safe towing*, *Consumer Reports*. Available at: https://www.consumerreports.org/car-safety/preparation-and-driving-tips-for-safe-towing/ (Accessed: 29 April 2023).

National Academies of Sciences, Engineering, and Medicine (2022) *Assessment of technologies for improving light-duty vehicle fuel economy?2025-2035*. Washington, D.C: National Academies Press.

National Grid (2017) *Electric dreams: The future for EVs | National Grid Group*, *Nationalgrid.com*. Available at: https://www.nationalgrid.com/group/case-studies/electric-dreams-future-evs (Accessed: 17 September 2018).

National Grid Group (2022) *What is ev charging anxiety – and is range anxiety a thing of the past?* Available at: https://www.nationalgrid.com/group/what-ev-charging-anxiety-and-range-anxiety-thing-past (Accessed: November 11, 2022).

Nealefhima (2023) *What are the biggest problems with electric cars?: Call us Today*, *Neale Fhima*. Available at: https://nealefhima.com/biggest-problems-electric-cars/ (Accessed: January 10, 2023).

Nguyen, H.L. *et al.* (2021) 'Review of the durability of polymer electrolyte membrane fuel cell in long-term operation: Main influencing parameters and testing protocols', *Energies*, 14(13), p. 4048. doi:10.3390/en14134048.

Ning, Q. *et al.* (2009) 'Modeling and Simulation for Fuel Cell-Battery Hybrid Electric Vehicle', *2009 International Conference on Computer Modeling and Simulation* [Preprint]. doi:10.1109/iccms.2009.62.

Nissan (2019) *Nissan LEAF - Top selling electric vehicule in Europe 2018 | Nissan*, *Nissan UK*. Available at: https://www.nissan.co.uk/vehicles/new-vehicles/leaf.html/ (Accessed: 10 January 2019).

Noori, M., Gardner, S. and Tatari, O. (2015) 'Electric vehicle cost, emissions, and water footprint in the United States: Development of a regional optimization model', *Energy*, 89, pp. 610–625.

Novák, V., Perfilieva, I. and Močkoř, J. (1999) "Mathematical Principles of Fuzzy Logic." Available at: https://doi.org/10.1007/978-1-4615-5217-8.

Novák, V., Perfilieva, I. and Močkoř, J. (1999) *Mathematical Principles of Fuzzy Logic* [Preprint]. doi:10.1007/978-1-4615-5217-8.

NREL (2019) *FASTSim: Future Automotive Systems Technology Simulator | Transportation Research | NREL*, *Nrel.gov*. Available at: https://www.nrel.gov/transportation/fastsim.html (Accessed: 03 March 2019).

Oil reserves (2018) *BP Global*. Available at: https://www.bp.com/en/global/corporate/energy-economics/statistical-review-of-world-energy/oil/oil-reserves.html (Accessed: 08 November 2017).

Oliveira, L. *et al.* (2015) 'Key issues of Lithium-ion batteries – from resource depletion to environmental performance indicators', *Journal of Cleaner Production*, 108, pp. 354–362.

Osborne, J. (2018) *Electric car forecast predicts 21% market share by 2035*, *Houston Chronicle*. Available at: https://www.chron.com/business/energy/article/Electric-car-forecast-predicts-21-market-share-11745799.php (Accessed: 02 February 2019).

Ottocar (2018) *Revealed! London's Top 5 Most Popular PCO Cars*, *PCO Blog | London's Most Popular Blog For PCO Drivers*. Available at: http://www.ottocar.co.uk/blog/londons-top-10-popular-pco-cars/ (Accessed: 25 December 2018).

Özel, F.M. *et al.* (2013) 'Development of a battery electric vehicle sector in north-West Europe: Challenges and strategies', *International Journal of Electric and Hybrid Vehicles*, 5(1), p. 1. doi:10.1504/ijehv.2013.053464.

Panasonic (2012) *NCR 18650*, *Engineering.tamu.edu*. Available at: https://engineering.tamu.edu/media/4247819/ds-battery-panasonic-18650ncr.pdf (Accessed: 11 November 2018).

Pawełczyk, M. and Szumska, E. (2018) 'Evaluation of the efficiency of hybrid drive applications in urban transport system on the example of a medium size city', *MATEC Web of Conferences*, 180, p. 03004. doi:10.1051/matecconf/201818003004.

Policies & Legislation, United States | IA-HEV (2016) *Ieahev.org*. Available at: http://www.ieahev.org/by-country/united-states-policy-and-legislation/ (Accessed: 18 January 2018).

Pollet, B., Staffell, I. and Shang, J. (2012) 'Current status of hybrid, battery and fuel cell electric vehicles: From electrochemistry to market prospects', *Electrochimica Acta*, 84, pp. 235–249.

Proposal for post-2020 CO2 targets for cars and vans - Climate Action - European Commission (2017) *Climate Action - European Commission*. Available at: https://ec.europa.eu/clima/policies/transport/vehicles/proposal_en (Accessed: 17 March 2018).

RCP (2016) "Every breath we take: the lifelong impact of air pollution." Available at: https://www.rcplondon.ac.uk/projects/outputs/every-breath-we-take-lifelong-impact-air-pollution (Accessed: 08 November 2017).

Reddy, N.P. *et al.* (2019) ‘An intelligent power and energy management system for fuel cell/Battery Hybrid Electric vehicle using reinforcement learning’, *2019 IEEE Transportation Electrification Conference and Expo (ITEC)* [Preprint]. doi:10.1109/itec.2019.8790451.

Ren, G., Ma, G. and Cong, N. (2015) ‘Review of electrical energy storage system for vehicular applications’, *Renewable and Sustainable Energy Reviews*, 41, pp. 225–236.

Ren, J. (2021) *Proton Exchange Membrane Fuel Cells (PEMFC) and Energy Storage System (ESS) passive hybridization for electric vehicles*, *Development and characterization of graphene-based microporous layers for proton exchange membrane fuel cells*. thesis. Available at: https://pureportal.coventry.ac.uk/en/studentTheses/proton-exchange-membrane-fuel-cells-pemfc-and-energy-storage-syst (Accessed: 2023).

RENAULT (2017) *250 miles (NEDC)* driving range*, *RENAULT*. Available at: https://www.renault.co.uk/vehicles/new-vehicles/zoe-250/driving range.html/ (Accessed: 19 September 2018).

Renault (2019) *ZOE | Electric | Renault UK*, *Renault*. Available at: https://www.renault.co.uk/vehicles/new-vehicles/zoe/motor.html (Accessed: 10 January 2019).

Rezazade, S. *et al.* (2018) ‘Investigation and comparison between PHEV and Shev for sedan vehicle based on advisor’, *2018 9th Annual Power Electronics, Drives Systems and Technologies Conference (PEDSTC)* [Preprint]. doi:10.1109/pedstc.2018.8343831.

Roth, M. (2015) ‘94th transportation research board annual meeting’, in *Lifetime costs, life cycle emissions, and consumer choice for conventional, hybrid, and electric vehicles*. Washington DC.

Ryan, D. *et al.* (2014) ‘European Electric Vehicle Congress’, in *Performance and energy efficiency testing of a lightweight FCEV Hybrid Vehicle*. Brussels.

Same, A. *et al.* (2010) ‘A study on optimization of hybrid drive train using Advanced Vehicle Simulator (advisor)’, *Journal of Power Sources*, 195(19), pp. 6954–6963. doi:10.1016/j.jpowsour.2010.03.057.

Satyapal, S. *et al.* (2007) 'The U.S. Department of Energy's National Hydrogen Storage Project: Progress towards meeting hydrogen-powered vehicle requirements', *Catalysis Today*, 120, pp. 246–256.

Senger, R.D., Merkle, M.A. and Nelson, D.J. (1998) 'Validation of advisor as a simulation tool for a series Hybrid Electric Vehicle', *SAE Technical Paper Series* [Preprint]. doi:10.4271/981133.

Shao, S., Pipattanasomporn, M. and Rahman, S. (2012) 'Grid Integration of Electric Vehicles and Demand Response With Customer Choice', *IEEE Transactions on Smart Grid*, 3(1), pp. 543–550. doi:10.1109/tsg.2011.2164949.

Sharaf, O.Z. and Orhan, M.F. (2014) 'An overview of fuel cell technology: fundamentals and applications', *Renewable and Sustainable Energy Reviews*, 32, pp. 810–853.

Shell UK (2023) *V-power fuel pump prices: Find a local station near you: Shell UK*, *Shell UK*. Available at: https://www.shell.co.uk/fuel-prices.html#vanity-aHR0cHM6Ly93d3cuc2hlbGwuY28udWsvbW90b3Jpc3QvZnVlbC1wcmljZXMuaHRtbA (Accessed: 15 April 2023).

Shi, X. *et al.* (2019) 'Battery electric vehicles: What is the minimum range required?', *Energy*, 166, pp. 352–358. doi:10.1016/j.energy.2018.10.056.

Shin, H.K. and Ha, S.K. (2023) 'A review on the cost analysis of hydrogen gas storage tanks for fuel cell vehicles', *Energies*, 16(13), p. 5233. doi:10.3390/en16135233.

Shu, H., Jiang, Y. and Gao, Y. (2010) *Model predictive control strategy of a medium hybrid electric vehicle*. Chongqing University. Available at: http://dx.doi.org/10.11835/j.issn.1000-582X.2010.01.007 (Accessed: August 19, 2023).

Sorlei, I.-S. *et al.* (2021) 'Fuel Cell Electric Vehicles—a brief review of current topologies and Energy Management Strategies', *Energies*, 14(1), p. 252. doi:10.3390/en14010252.

Statista (2023a) *China: Number of Shared Power Bank users 2025*, *Statista*. Available at: https://www.statista.com/statistics/1390237/china-number-of-shared-power-bank-users/ (Accessed: 15 October 2023).

Statista (2023b) *Cobalt reserves globally 2022*, *Reserves of Cobalt worldwide from 2010 to 2022*. Available at: https://www.statista.com/statistics/1058647/global-Cobalt-reserves/ (Accessed: 04 January 2024).

Statista (2023c) *Europe: Number of Electric Vehicle Charging stations 2022*, *Statista*. Available at: https://www.statista.com/statistics/955443/number-of-electric-vehicle-charging-stations-in-europe/ (Accessed: 15 November 2023).

Steward, D., Mayyas, A. and Mann, M. (2019) 'Economics and challenges of Li-ion battery recycling from end-of-life vehicles', *Procedia Manufacturing*, 33, pp. 272–279. doi:10.1016/j.promfg.2019.04.033.

TESLA (2019) *Model S | Tesla UK*, *Tesla.com*. Available at: https://www.tesla.com/en_GB/models/ (Accessed: 09 January 2019).

Tesla US (2019) *Microgrid Controller: Tesla Support*, *Tesla*. Available at: https://www.tesla.com/support/energy/tesla-software/microgrid-controller (Accessed: 24 February 2023).

Thakur, A. (2021) 'Fundamentals of Neural Networks', *International Journal for Research in Applied Science and Engineering Technology*, 9(VIII), pp. 407–426. doi:10.22214/ijraset.2021.37362.

The Department of Energy and Climate Change (DECC) (2012) *'Big fall' in UK petrol stations*, *BBC News*. Available at: http://www.bbc.co.uk/news/business-20791871/ (Accessed: 11 May 2017).

The Government of Japan (2016) *Tokyo Aims to Realize 'Hydrogen Society' by 2020 / JapanGov - The Government of Japan*, *JapanGov - The Government of Japan*. Available at: https://www.japan.go.jp/tomodachi/2016/spring2016/tokyo_realize_hydrogen_by_2020.html (Accessed: 17 August 2018).

Tiresize.com (2022) *Tyre size calculator*, *tiresize.com*. Available at: https://tiresize.com/tyre-size-calculator/ (Accessed: 01 November 2022).

TNS SOFRES (2014) *EP TENDER*, *Tbb.innoenergy.com*. Available at: https://tbb.innoenergy.com/wp-content/uploads/2015/11/EP-Tender.pdf (Accessed: 03 March 2018).

Torreglosa, J.P. *et al.* (2020) ‘Analyzing the improvements of energy management systems for hybrid electric vehicles using a systematic literature review: How far are these controls from rule-based controls used in commercial vehicles?’, *Applied*

Toyota (2021) *Under the skin of the new mirai*, *Toyota UK Magazine*. Available at: https://mag.toyota.co.uk/new-mirai-hydrogen-fuel-cell-electric-vehicle/ (Accessed: 02 February 2022).

Transport Policy (2022) *International: Light-duty: Worldwide harmonized light vehicles test procedure (WLTP)*, *Transportpolicy.net*. Available at: https://www.transportpolicy.net/standard/international-light-duty-worldwide-harmonized-light-vehicles-test-procedure-wltp/ (Accessed: August 22, 2022).

Tsakiris, A. (2023) *Analysis of hydrogen fuel cell and battery efficiency (presentation) – 27.02.2019*, *Copenhagen Centre on Energy Efficiency*. Available at: https://c2e2.unepccc.org/kms_object/analysis-of-hydrogen-fuel-cell-and-battery-efficiency-presentation-27-02-2019/ (Accessed: 15 April 2023).

Tycorun Batteries (2022) *18650 battery 4.2V vs 3.7V - comparison guide for 18650 with different voltages*, *18650 BATTERY 4.2V VS 3.7V - COMPARISON GUIDE FOR 18650 WITH DIFFERENT VOLTAGES*. Available at: https://www.tycorun.com/blogs/news/18650-battery-4-2v-vs-3-7v-comparison-guide-for-18650-with-different-voltages (Accessed: 24 April 2023).

UK Automotive Council (2017) *UK Passenger Vehicle Roadmap 2017*, *Automotivecouncil.co.uk*. Available at: https://www.automotivecouncil.co.uk/wp-content/uploads/sites/13/2017/09/Passenger-Car_.jpg (Accessed: 28 December 2017).

UK GOVERNMENT WEBSITE (2017) *Low-emission vehicles eligible for a plug-in grant*, *GOV.UK*. Available at: https://www.gov.uk/plug-in-car-van-grants (Accessed: 10 September 2018).

UNECE (2015) *Vehicle Regulations - Transport - UNECE*, *Unece.org*. Available at: http://www.unece.org/trans/main/welcwp29.html (Accessed: 10 June 2018).

UNECE (2018a) *Addenda to the 1958 Agreement (Regulations 101-120)*, *Unece.org*. Available at: http://www.unece.org/trans/main/wp29/wp29regs101-120.html (Accessed: 10 June 2018).

US Geological Survey (2017) *Global Cobalt reserves by country 2017* | *Statistic*, *Statista*. Available at: https://www.statista.com/statistics/264930/global-Cobalt-reserves/ (Accessed: 23 August 2018).

Vehicle Certification Agency UK (2023) *New Car Fuel Consumption & emission figures*, *Vehicle Certification Agency*. Available at: https://www.vehicle-certification-agency.gov.uk/fuel-consumption-co2/fuel-consumption-guide/zero-and-ultra-low-emission-vehicles-ulevs/#topic-title (Accessed: 04 December 2023).

Volkswagen (2019) *Electric & Hybrid Car Technology* | *Volkswagen UK*, *Volkswagen UK*. Available at: https://www.volkswagen.co.uk/electric-hybrid/ (Accessed: 12 January 2019).

VTPI (2016) *Transportation Cost and Benefit Analysis Techniques, Estimates and Implications [Second Edition]*, *Victoria Transport Institute - Transportation Cost and benefit analysis*. Available at: https://www.vtpi.org/tca/ (Accessed: 01 May 2022).

Wahono, B. *et al.* (2015) 'Analysis of range extender electric vehicle performance using vehicle simulator', *Energy Procedia*, 68, pp. 409–418. doi:10.1016/j.egypro.2015.03.272.

Wanitschke, A. and Hoffmann, S. (2020) 'Are Battery Electric Vehicles the future? an uncertainty comparison with hydrogen and combustion engines', *Environmental Innovation and Societal Transitions*, 35, pp. 509–523. doi:10.1016/j.eist.2019.03.003.

Waseem, M. *et al.* (2023) 'Fuel cell-based Hybrid Electric Vehicles: An integrated review of current status, key challenges, recommended policies, and future prospects', *Green Energy and Intelligent Transportation*, 2(6), p. 100121. doi:10.1016/j.geits.2023.100121.

Wipke, K. and Cuddy, M. (2015) *Using an Advanced Vehicle Simulator (ADVISOR) to Guide Hybrid Vehicle Propulsion System Development*, *Nrel.gov*. Available at: https://www.nrel.gov/docs/legosti/fy96/21615.pdf (Accessed: 18 February 2019).

Wipke, K. *et al.* (2013) *Advisor 2.0: A SecondGeneration Advanced Vehicle Simulator for Systems Analysis*, *NREL.GOV*. Available at: http://www.nrel.gov/docs/fy99osti/25928.pdf (Accessed: 15 February 2019).

World Economic Forum (2021) *4 reasons why electric cars haven't taken off yet*. Available at: https://www.weforum.org/agenda/2021/07/electric-cars-batteries-fossil-fuel/ (Accessed: 23 February 2022).

World Energy Council (2017a) *Average household electricity use around the world*, *shrinkthatfootprint.com*. Available at: http://shrinkthatfootprint.com/average-household-electricity-consumption (Accessed: 15 October 2017).

World Energy Council (2017b) *Shrinkthatfootprint.com*. Available at: http://shrinkthatfootprint.com/average-household-electricity-consumption (Accessed: 01 March 2018).

Wu, D. *et al.* (2019) 'Intelligent hydrogen fuel cell range extender for Battery Electric Vehicles', *World Electric Vehicle Journal*, 10(2), p. 29. doi:10.3390/wevj10020029.

Wu, G., Inderbitzin, A. and Bening, C. (2015) 'Total cost of ownership of electric vehicles compared to conventional vehicles: a probabilistic analysis and projection across market segments', *Energy Policy*, 80, pp. 196–214.

Xie, S. *et al.* (2018) 'An artificial neural network-enhanced energy management strategy for plug-in Hybrid Electric Vehicles', *Energy*, 163, pp. 837–848. doi:10.1016/j.energy.2018.08.139.

Xin Yao (1999) 'Evolving Artificial Neural Networks', *Proceedings of the IEEE*, 87(9), pp. 1423–1447. doi:10.1109/5.784219.

Xiong, R. and Shen, W. (2018) 'Battery management systems in electric vehicles', *Advanced Battery Management Technologies for Electric Vehicles*, pp. 231–248. doi:10.1002/9781119481652.ch8.

Xu, L. *et al.* (2009) "Adaptive supervisory control strategy of a fuel cell/battery-powered City Bus," *Journal of Power Sources*, 194(1), pp. 360–368. Available at: https://doi.org/10.1016/j.jpowsour.2009.04.074.

Yang, Y., Zhao, H. and Jiang, H. (2010) 'Drive train design and modeling of a parallel diesel hybrid electric bus based on AVL/Cruise', *World Electric Vehicle Journal*, 4(1), pp. 75–81. doi:10.3390/wevj4010075.

Zadeh, L.A. (1965) 'Fuzzy sets', *Information and Control*, 8(3), pp. 338–353. doi:10.1016/s0019-9958(65)90241-x.

Zadeh, L.A. (1973) 'Outline of a New Approach to the Analysis of Complex Systems and Decision Processes', *IEEE Transactions on Systems, Man, and Cybernetics*, SMC-3(1), pp. 28–44. doi:10.1109/tsmc.1973.5408575.

Zap-Map (2024) *How many charge points are there in the UK 2024*, *Zap-Map*. Available at: https://www.zap-map.com/statistics// (Accessed: 12 February 2024).

Zeng, T. *et al.* (2018) ‘Modelling and predicting energy consumption of a range extender fuel cell hybrid vehicle’, *Energy*, 165, pp. 187–197. doi:10.1016/j.energy.2018.09.086.

Zhang, G. *et al.* (2017) ‘Rapid restoration of electric vehicle battery performance while driving at Cold Temperatures’, *Journal of Power Sources*, 371, pp. 35–40. doi:10.1016/j.jpowsour.2017.10.029.

Zheng, Q. *et al.* (2018) “Equivalent Consumption Minimization Strategy Based on Dynamic Programming for Plug-in Hybrid Electric Vehicle,” *IFAC-PapersOnLine*, 51(31), pp. 612–617. Available at: https://doi.org/10.1016/j.ifacol.2018.10.146.

Zu, C.-X. and Li, H. (2011) ‘Thermodynamic analysis on energy densities of batteries’, *Energy & Environmental Science*, 4(8), p. 2614. doi:10.1039/c0ee00777c.

Appendices

Appendix 1 Motor Curves and Efficiency Maps

1.1. Motor Peak-Torque Curves

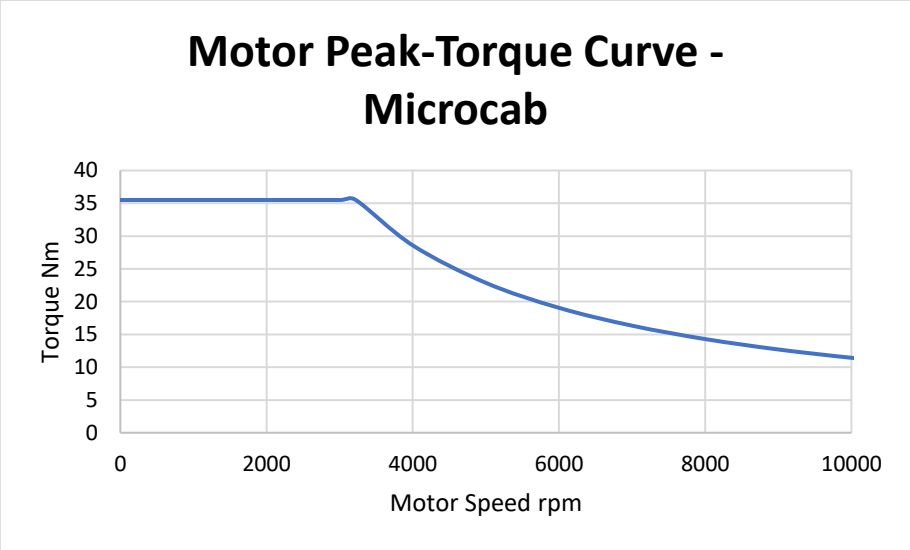

Figure 0-1: Electric Peak-Torque Curve Speed vs Torque – Microcab EV

Table 0-1: Electric Peak-Torque Curve data Speed vs Torque – Microcab EV

0	1000	2000	3000	3220	4000	5000	6000	7000	8000	9000	10000	11000	12000	13000
35.5	35.5	35.5	35.5	35.5	28.5775	22.862	19.05167	16.33	14.28875	12.70111	11.431	10.39182	9.525833	8.793077

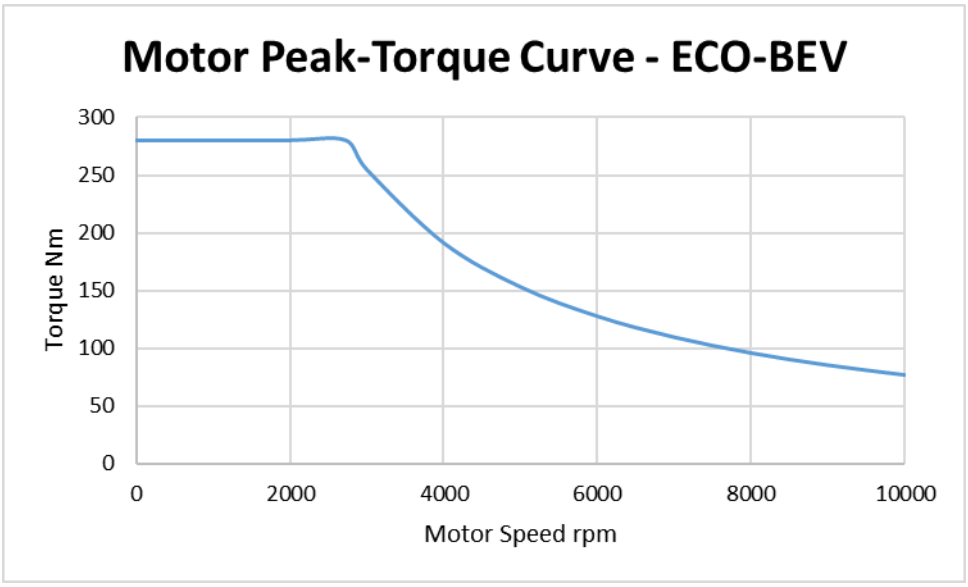

Figure 0-2: Electric Peak-Torque Curve Speed vs Torque – Eco-BEV

Table 0-2: Electric Peak-Torque Curve data Speed vs Torque – Eco-BEV

280	280	280	280	254.6479	190.9859	152.7887	127.324	109.1348	95.49297	84.88264	76.39437
0	1000	2000	2728.37	3000	4000	5000	6000	7000	8000	9000	10000

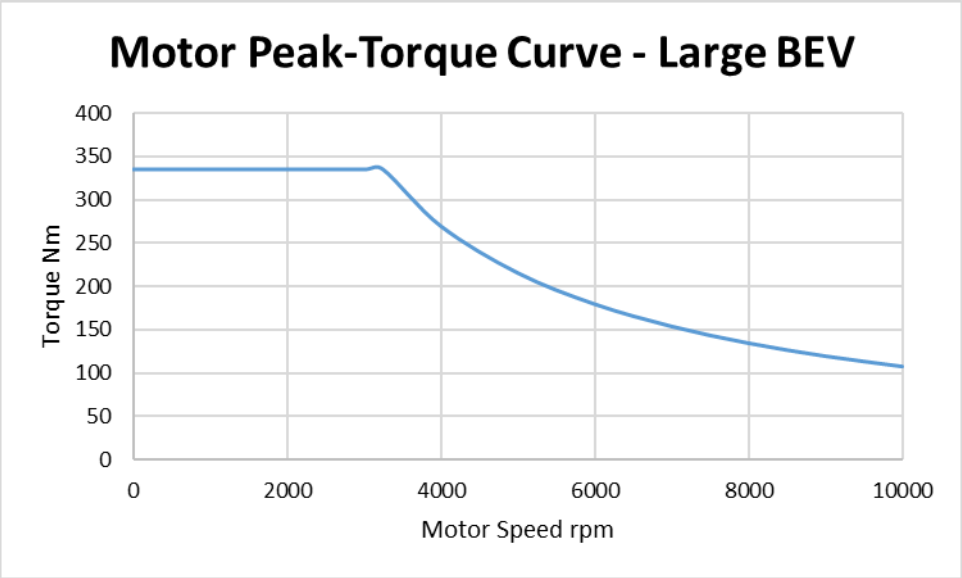

Figure 0-3: Electric Peak-Torque Curve Speed vs Torque – Large BEV

Table 0-3: Electric Peak-Torque Curve data Speed vs Torque – Large BEV

335	335	335	335	335	269.7676	215.8141	179.8451	154.1529	134.8838	119.8967	107.9071
0	1000	2000	3000	3250	4000	5000	6000	7000	8000	9000	10000

1.2. Motor Efficiency Maps

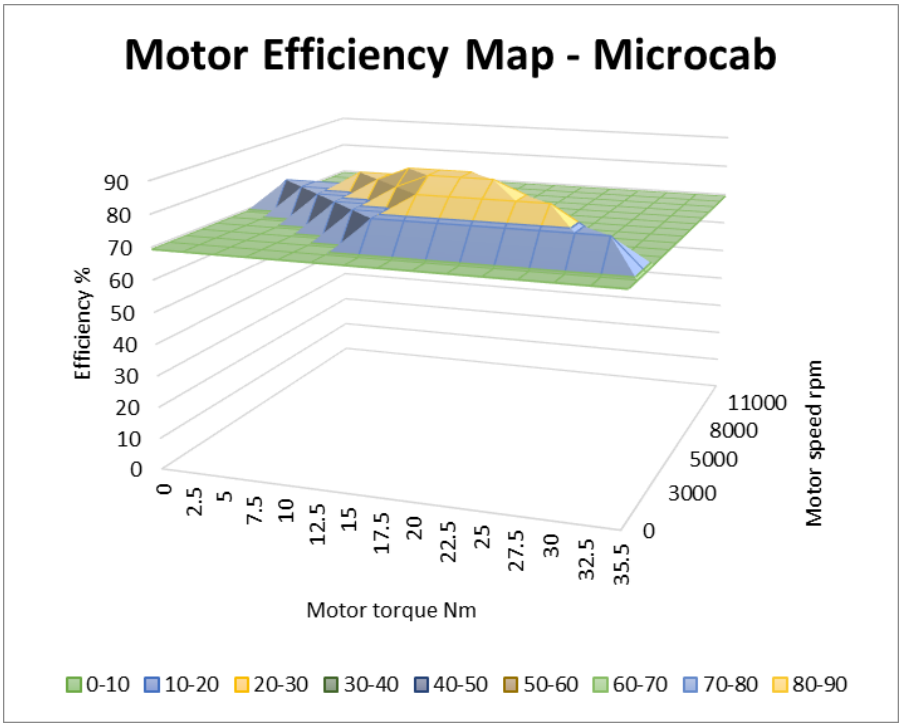

Figure 0-4: Electric motor efficiency map – Microcab EV

Table 0-4: Electric motor efficiency map data – Microcab EV

	0	2.5	5	7.5	10	12.5	15	17.5	20	22.5	25	27.5	30	32.5	35.5
0	69.3	69.3	69.3	69.3	69.3	69.3	69.3	69.3	69.3	69.3	69.3	69.3	69.3	69.3	69.3
1000	69.3	69.3	69.3	69.3	69.3	69.3	69.3	69.3	69.3	69.3	69.3	69.3	69.3	69.3	69.3
2000	69.3	69.3	69.3	69.3	69.3	69.3	79	79	79	79	79	79	79	79	69.3
3000	69.3	69.3	69.3	69.3	69.3	79	79	85	85	85	85	85	79	69.3	69.3
3220	69.3	69.3	69.3	69.3	79	79	85	89.1	89.1	89.1	85	79	69.3	69.3	69.3
4000	69.3	69.3	69.3	79	79	85	89.1	89.1	89.1	85	79	69.3	69.3	69.3	69.3
5000	69.3	69.3	79	79	85	85	85	85	85	79	69.3	69.3	69.3	69.3	69.3
6000	69.3	79	79	79	79	79	79	79	79	69.3	69.3	69.3	69.3	69.3	69.3
7000	69.3	69.3	69.3	69.3	69.3	69.3	69.3	69.3	69.3	69.3	69.3	69.3	69.3	69.3	69.3
8000	69.3	69.3	69.3	69.3	69.3	69.3	69.3	69.3	69.3	69.3	69.3	69.3	69.3	69.3	69.3
9000	69.3	69.3	69.3	69.3	69.3	69.3	69.3	69.3	69.3	69.3	69.3	69.3	69.3	69.3	69.3
10000	69.3	69.3	69.3	69.3	69.3	69.3	69.3	69.3	69.3	69.3	69.3	69.3	69.3	69.3	69.3
11000	69.3	69.3	69.3	69.3	69.3	69.3	69.3	69.3	69.3	69.3	69.3	69.3	69.3	69.3	69.3
12000	69.3	69.3	69.3	69.3	69.3	69.3	69.3	69.3	69.3	69.3	69.3	69.3	69.3	69.3	69.3
13000	69.3	69.3	69.3	69.3	69.3	69.3	69.3	69.3	69.3	69.3	69.3	69.3	69.3	69.3	69.3

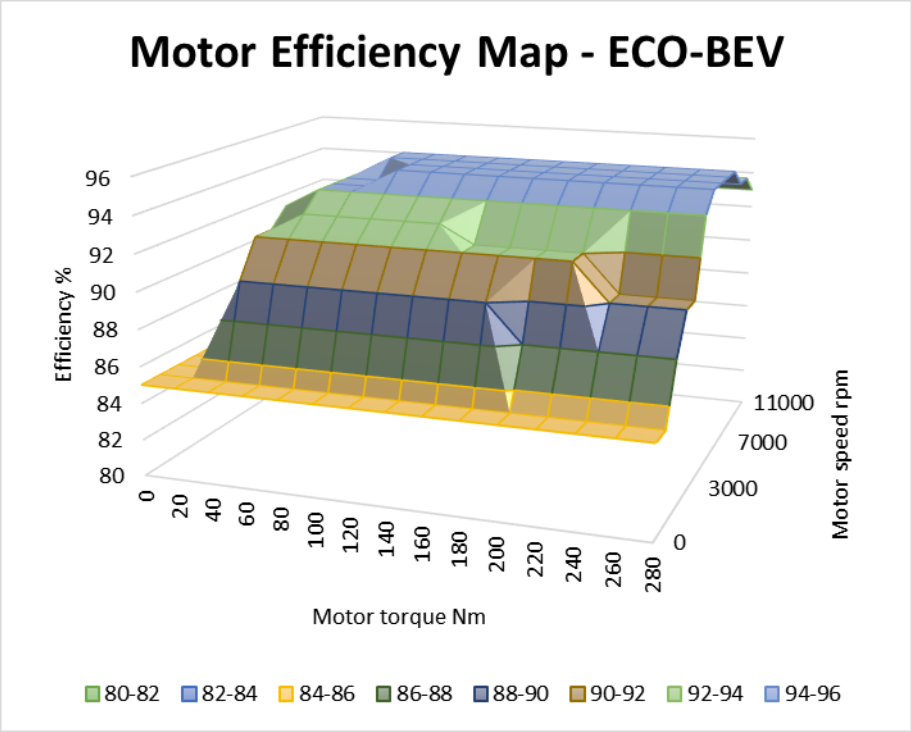

Figure 0-5: Electric motor efficiency map – Eco-BEV

Table 0-5: Electric motor efficiency map data – Eco-BEV

	0	20	40	60	80	100	120	140	160	180	200	220	240	260	280
0	85	85	85	85	85	85	85	85	85	85	85	85	85	85	85
1000	85	85	85	85	85	85	85	85	85	85	85	85	85	85	85
2000	85	85	90	90	90	90	90	90	90	90	88	88	88	88	88
2728.37	85	85	92	92	92	92	92	92	92	92	92	92	90	90	90
3000	85	85	92	93	93	93	93	93	92	92	92	92	90	90	90
4000	85	85	93	94	94	94	94	94	94	94	94	94	94	94	94
5000	85	85	93	94	94	95	95	95	95	95	95	95	95	95	95
6000	85	85	93	94	94	95	95	95	95	95	95	95	95	95	95
7000	85	85	93	94	95	95	95	95	95	95	95	95	95	95	95
8000	85	85	93	94	95	95	95	95	95	95	95	95	95	95	95
9000	85	85	93	94	94	94	94	94	94	94	94	94	94	94	94
10000	85	85	93	94	94	94	94	94	94	94	94	94	94	94	94
11000	85	85	90	92	93	93	93	93	93	93	93	93	93	93	93

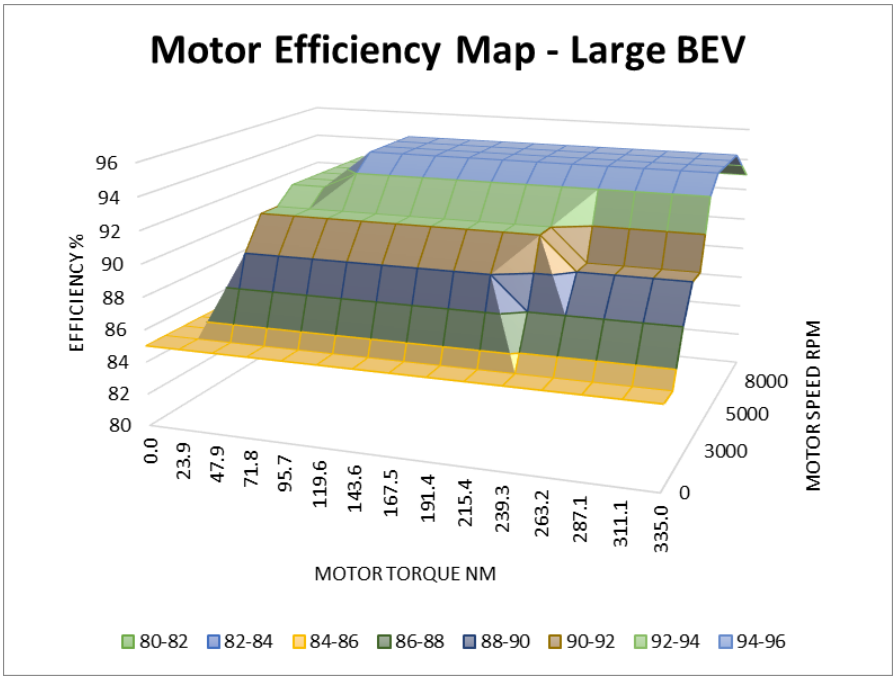

Figure 0-6: Electric motor efficiency map – Large BEV

Table 0-6: Electric motor efficiency map data – Large BEV

	0.0	23.9	47.9	71.8	95.7	119.6	143.6	167.5	191.4	215.4	239.3	263.2	287.1	311.1	335.0
0	85	85	85	85	85	85	85	85	85	85	85	85	85	85	85
1000	85	85	85	85	85	85	85	85	85	85	85	85	85	85	85
2000	85	85	90	90	90	90	90	90	90	90	88	88	88	88	88
3000	85	85	92	92	92	92	92	92	92	92	92	90	90	90	90
3250	85	85	92	92	92	92	92	92	92	92	92	90	90	90	90
4000	85	85	93	93	94	94	94	94	94	94	94	94	94	94	94
5000	85	85	93	93	95	95	95	95	95	95	95	95	95	95	95
6000	85	85	93	93	95	95	95	95	95	95	95	95	95	95	95
7000	85	85	93	93	95	95	95	95	95	95	95	95	95	95	95
8000	85	85	93	93	95	95	95	95	95	95	95	95	95	95	95
9000	85	85	93	93	94	94	94	94	94	94	94	94	94	94	94
10000	85	85	90	90	93	93	93	93	93	93	93	93	93	93	93

Appendix 2 EMS Control Algorithm Matlab Codes

2.1. State-Machine EMS Matlab Codes

```
function [sys,x0,str,ts,simStateCompliance] = StateMachContr(t,x,u,flag)

switch flag

  %%%%%%%%%%%%%%%%%%
  % Initialization %
  %%%%%%%%%%%%%%%%%%
  case 0
    [sys,x0,str,ts,simStateCompliance]=mdlInitializeSizes;

  %%%%%%%%%%%%%%%%
  % Derivatives %
  %%%%%%%%%%%%%%%%
  case 1
    sys=mdlDerivatives(t,x,u);

  %%%%%%%%%%
  % Update %
  %%%%%%%%%%
  case 2
    sys=mdlUpdate(t,x,u);

  %%%%%%%%%%
  % Outputs %
  %%%%%%%%%%
  case 3
    sys=mdlOutputs(t,x,u);

  %%%%%%%%%%%%%%%%%%%%%%%%
  % GetTimeOfNextVarHit %
  %%%%%%%%%%%%%%%%%%%%%%%%
  case 4
    sys=mdlGetTimeOfNextVarHit(t,x,u);

  %%%%%%%%%%%%%
  % Terminate %
  %%%%%%%%%%%%%
  case 9
    sys=mdlTerminate(t,x,u);

  %%%%%%%%%%%%%%%%%%%%
  % Unexpected flags %
  %%%%%%%%%%%%%%%%%%%%
  otherwise
    DAStudio.error('Simulink:blocks:unhandledFlag', num2str(flag));

end

function [sys,x0,str,ts,simStateCompliance]=mdlInitializeSizes

sizes = simsizes;

sizes.NumContStates  = 0;
sizes.NumDiscStates  = 0;
```

```
sizes.NumOutputs     = 3;
sizes.NumInputs      = 3;
sizes.DirFeedthrough = 1;
sizes.NumSampleTimes = 1;   % at least one sample time is needed

sys = simsizes(sizes);

str = [];

ts  = [-1 0];

simStateCompliance = 'UnknownSimState';

function sys=mdlDerivatives(t,x,u) %#ok<*INUSD>

sys = [];

function sys=mdlUpdate(t,x,u)

sys = [];

function sys=mdlOutputs(t,x,u)
%constants initialization
Pbatt_Char_Max=-10;
SOC_min=10; SOC_max=90;
SOC_normal1=70;
SOC_normal2=40;
Pfc_min=2; Pfc_max=50;
Pfc_opt=40;


if( u(1)<=0 )
    state=1;
end

if( u(1)>=Pfc_max )
    state=2;
end

if( u(1)<Pfc_max && u(1)>=Pfc_max+Pbatt_Char_Max)
    state=3;
end

if( u(1)<=Pfc_opt && u(1)>Pfc_opt+Pbatt_Char_Max)
    state=4;
end

if( u(1)<=Pfc_opt+Pbatt_Char_Max && u(1)>0)
    state=5;
end

%%%%%%   Regenerative mode   %%%%%
%state 1
if( state==1 && u(2)>SOC_max )
            Pfc=0;
            Pbatt=0;
end
%state 1
if( state==1 && u(2)<=SOC_max && u(2)>=SOC_min && u(1)<=-8)
```

```
            Pfc=0;
            Pbatt=-10;
end
if( state==1 && u(2)<=SOC_max && u(2)>=SOC_min && u(1)>-8)
            Pfc=u(1)+10;
            Pbatt=-10;
end
%state 1
if( state==1 && u(2)<SOC_min && u(1)<=-8)
            Pfc=0;
            Pbatt=-10;
end
if( state==1 && u(2)<SOC_min && u(1)>-8)
            Pfc=u(1)+10;
            Pbatt=-10;
end
%%%%%%        END          %%%%%%%

%%%%%%      Drive mode     %%%%%%%
%state 2 u1>= 50
if( state==2 )
            Pfc=Pfc_max;
            Pbatt=u(1)-Pfc;
end

%state 3 40 < u1 < 50
if( state==3 && u(2)>SOC_max )%1
            Pfc=Pfc_min;
            Pbatt=u(1)-Pfc_min;
end

if( state==3 && u(2)>=SOC_normal1 && u(2)<=SOC_max )%2
            Pfc=Pfc_min;
            Pbatt=u(1)-Pfc;
end
if( state==3 && u(2)>SOC_normal2 && u(2)<SOC_normal1)%3
            Pfc=Pfc_min;
            Pbatt=u(1)-Pfc;
end

if( state==3  && u(2)>=SOC_min && u(2)<=SOC_normal2)%4
            Pfc=Pfc_opt;
            Pbatt=u(1)-Pfc;
end

if( state==3  && u(2)>0 && u(2)<SOC_min)%5
            Pfc=Pfc_max;
            Pbatt=u(1)-Pfc;
end

%state 4 30 < u1 < 40
if( state==4 && u(2)>SOC_max )%1
            Pfc=Pfc_min;
            Pbatt=u(1)-Pfc_min;
end

if( state==4 && u(2)>=SOC_normal1 && u(2)<=SOC_max)%2
            Pfc=Pfc_min;
            Pbatt=u(1)-Pfc;
```

```
end
if( state==4 && u(2)<SOC_normal1 && u(2)>SOC_normal2)%3
            Pfc=Pfc_min;
            Pbatt=u(1)-Pfc;
end

if( state==4  && u(2)>=SOC_min && u(2)<=SOC_normal2)%4
            Pfc=Pfc_opt;
            Pbatt=u(1)-Pfc;
end

if( state==4  && u(2)>0 && u(2)<SOC_min)%5
            Pfc=u(1)-Pbatt;
            Pbatt=Pbatt_Char_Max;
end

%state 5 0 < u1 < 30
if( state==5 && u(2)>SOC_max )%1
            Pfc=Pfc_min;
            Pbatt=u(1)-Pfc_min;
end

if( state==5 && u(2)>SOC_normal1 && u(2)<=SOC_max )%2
            Pfc=Pfc_min;
            Pbatt=u(1)-Pfc;
end
if( state==5 && u(2)>SOC_normal2 && u(2)<SOC_normal1)%3
            Pfc=Pfc_min;
            Pbatt=u(1)-Pfc;
end

if( state==5  && u(2)<=SOC_normal2 && u(2)>0)%4
            Pbatt=Pbatt_Char_Max;
            Pfc=u(1)-Pbatt;
end

sys = [Pbatt Pfc state];

function sys=mdlGetTimeOfNextVarHit(t,x,u)

sampleTime = 1;    %  Example, set the next hit to be one second later.
sys = t + sampleTime;


function sys=mdlTerminate(t,x,u)

sys = [];
```

2.2. ECMS Matlab Codes

```
function [sys,x0,str,ts,simStateCompliance] = ECMS(t,x,u,flag)
switch flag

  %%%%%%%%%%%%%%%%%%
  % Initialization %
  %%%%%%%%%%%%%%%%%%
  case 0
    [sys,x0,str,ts,simStateCompliance]=mdlInitializeSizes;
```

```
  %%%%%%%%%%%%%%%%
  % Derivatives %
  %%%%%%%%%%%%%%%%
  case 1
    sys=mdlDerivatives(t,x,u);

  %%%%%%%%%%
  % Update %
  %%%%%%%%%%
  case 2
    sys=mdlUpdate(t,x,u);

  %%%%%%%%%%
  % Outputs %
  %%%%%%%%%%
  case 3
    sys=mdlOutputs(t,x,u);

  %%%%%%%%%%%%%%%%%%%%%%%%
  % GetTimeOfNextVarHit %
  %%%%%%%%%%%%%%%%%%%%%%%%
  case 4
    sys=mdlGetTimeOfNextVarHit(t,x,u);

  %%%%%%%%%%%%
  % Terminate %
  %%%%%%%%%%%%
  case 9
    sys=mdlTerminate(t,x,u);

  %%%%%%%%%%%%%%%%%%%%
  % Unexpected flags %
  %%%%%%%%%%%%%%%%%%%%
  otherwise
    DAStudio.error('Simulink:blocks:unhandledFlag', num2str(flag));

end

function [sys,x0,str,ts,simStateCompliance]=mdlInitializeSizes
%
sizes = simsizes;

sizes.NumContStates  = 0;
sizes.NumDiscStates  = 0;
sizes.NumOutputs     = 3;
sizes.NumInputs      = 2;
sizes.DirFeedthrough = 1;
sizes.NumSampleTimes = 1;   % at least one sample time is needed

sys = simsizes(sizes);

%
% initialize the initial conditions
%
x0  = [];

%
% str is always an empty matrix
```

```
%
str = [];

%
% initialize the array of sample times
%
ts  = [-1 0];

simStateCompliance = 'UnknownSimState';

function sys=mdlDerivatives(t,x,u) %#ok<*INUSD>

sys = [];

function sys=mdlUpdate(t,x,u)

sys = [];

function sys=mdlOutputs(t,x,u) %#ok<*INUSL>
%constants initialization
Pbatt_char=10000; Pbatt_max=45000;SOC_min=10; SOC_max=90;
Pfc_min=2000; Pfc_max=50000;

%define Matrix Aeq

Aeq=[0 1 0;1 0 1];

%define Matrix beq
mu=0.6;
beq=[1-mu*2*((u(2)-0.5*(SOC_max+SOC_min))/(SOC_max+SOC_min)); u(1)];%

%define boundary conditions
lb=[Pfc_min, 0, -Pbatt_char];
ub=[Pfc_max, 5, Pbatt_max];

%define initial conditions
%x0=[Pfc_min, 0, 0];
x0=[0, 1, 3000];%[Pfc, alpha, Pbatt]
options =
optimoptions('fmincon','Algorithm','sqp','Display','off','MaxFunctionEvaluat
ions',1000,'MaxIterations',100);
[y,fval] = fmincon(@ecmsfun,x0,[],[],Aeq,beq,lb,ub,[],options);

Pfc=y(1); alpha=y(2); Pbatt=y(3);

sys = [Pfc Pbatt alpha];


function sys=mdlGetTimeOfNextVarHit(t,x,u)

sampleTime = 1;
sys = t + sampleTime;

function sys=mdlTerminate(t,x,u)

sys = [];

function f = ecmsfun(x)
f = (x(1)/1000)+x(2)*x(3)/1000;
```

2.3. ANN Programming Matlab Codes

```
x = data_9';
t = data_10';

trainFcn = 'trainscg';  % Scaled conjugate gradient backpropagation.

% Create a Fitting Network
hiddenLayerSize = 10;
net = fitnet(hiddenLayerSize,trainFcn);

net.input.processFcns = {'removeconstantrows','mapminmax'};
net.output.processFcns = {'removeconstantrows','mapminmax'};

net.divideFcn = 'dividerand';  % Divide data randomly
net.divideMode = 'sample';  % Divide up every sample
net.divideParam.trainRatio = 70/100;
net.divideParam.valRatio = 15/100;
net.divideParam.testRatio = 15/100;

net.performFcn = 'mse';  % Mean Squared Error

net.plotFcns = {'plotperform','plottrainstate','ploterrhist', ...
    'plotregression', 'plotfit'};

% Train the Network
[net,tr] = train(net,x,t);

% Test the Network
y = net(x);
e = gsubtract(t,y);
performance = perform(net,t,y)

% Recalculate Training, Validation and Test Performance
trainTargets = t .* tr.trainMask{1};
valTargets = t .* tr.valMask{1};
testTargets = t .* tr.testMask{1};
trainPerformance = perform(net,trainTargets,y)
valPerformance = perform(net,valTargets,y)
testPerformance = perform(net,testTargets,y)

% View the Network
view(net)

if (false)
    genFunction(net,'myNeuralNetworkFunction');
    y = myNeuralNetworkFunction(x);
end
if (false)
    genFunction(net,'myNeuralNetworkFunction','MatrixOnly','yes');
    y = myNeuralNetworkFunction(x);
end
if (false)
    gensim(net);
end
```